# Synthesis of TGF-Beta inhibitors and compounds for spatiotemporal drug release

Daniel Byrom

# Synthesis of TGF-Beta inhibitors and compounds for spatiotemporal drug release

**Daniel Byrom**

Doctoral program: Química Orgànica

Thesis director: **Antoni Riera Escalé**

Facultat de Química

Departament de Química Orgànica

Universitat de Barcelona



UNIVERSITAT DE
BARCELONA

Memoria presentada por Daniel Byrom para optar al grado de doctor por la Universidad de Barcelona

Daniel Byrom

Revisada por

Dr. Antoni Riera Escalé

Barcelona, septiembre de 2018

# Preface

The following doctoral thesis is a summary of the work carried out during four years in the lab of Professor Antoni Riera at the Institute for Research in Biomedicine Barcelona (IRB Barcelona). The work has been done with the financial support of the "Ministerio de Economia y Competitividad (MINECO)" (projects CTQ2014-56361-P and CTQ2011-23620), the Generalitat de Catalunya (2009SGR 00901), and also the IRB Barcelona. I also acknowledge MINECO for a FPI fellowship, for which I am very grateful. Without these grants, this doctoral thesis would not have been possible.

This thesis is comprised of two main projects, both of which designed and performed in close collaboration with Dr. Eduard Batlle's group (IRB Barcelona). The first describes our efforts in the synthesis of a transforming growth factor beta (TGF-β) inhibitor LY2157299 at a large scale, and the results of its subsequent use in a biological setting in the group of Eduard Batlle. Due to the resultant limitations of LY2157299, we designed and synthesised a novel TGF-β inhibitor with the aim of overcoming said limitations.

The second main theme is the design, synthesis and preliminary application of a novel method to release a drug at a specific time and place within a model system – be in *in vitro* or *in vivo*. The drug which was released in our system was 4-hydroxytamoxifen, which we used to activate the Cre recombinase -a toolkit used to invoke genetic changes -both *in vitro* and *in vivo*.

The chemical experiments were carried out in the lab of and under the supervision of Professor Riera. The biological experiments were carried out by or supervised by Dr. Daniele Tauriello – a postdoctoral researcher in the lab of Dr. Eduard Batlle.

# Acknowledgments

In September 2010, I vividly remember setting off from London City airport on a one-way flight to Barcelona – the day after defending my masters thesis at Imperial College London. At that time, I didn't have a real plan of what the next few months would have in store. I thought that if it didn't work out then I could always catch a flight back and nothing would be lost. I started looking jobs just to make ends meet, but I always had the hope of starting a PhD in Chemistry.

On a lunch break from this as yet unfruitful job search, I got in contact with Prof. Antoni Riera to inquire about the possibility of a PhD in his lab. He invited me down to his office where we sat and chatted for about an hour about chemistry and my future plans. Fast forward another month or so and I started work in his lab as a lab technician – a position I held for two years and thoroughly enjoyed. During this time, I learnt a great deal in terms of chemistry, scale-up and perhaps got a little too comfortable with performing reactions that worked!

A couple of years later in 2012, I was awarded an FPI fellowship from the Ministerio de Economia y Competitividad (MINECO). This work was performed in the lab of and under the supervision of Toni. During the next four years Toni not only provided me with support, but also gave me the freedom to explore areas I found most interesting. For employing me as a lab technician, for allowing me to perform this PhD in his lab and for his unconditional help and support I would especially like to thank Toni.

Perhaps next instead of a thank you should be an apology to Dr. Xavier Verdaguer – I'm sure reading this thesis Xevi you won't see a single P-chiral phosphine as was the original plan!!

A huge thanks to Daniele Tauriello – from a scientific point of view he taught me everything I needed to know both in terms of theory and practical work regarding all the biology used in this thesis - it was a bit of a steep learning curve at first, but I got there in the end! Outside of the lab too for our evenings in a certain 'restaurant', and later to our favourite watering hole where inevitably we had long discussions about science.

Thanks too to the Institut de Recerca en Biomedicine de Barcelona (IRB Barcelona) for providing a multidisciplinary environment to work in, and for providing access to all facilities needed to perform this doctoral thesis.

After a total of six years, I'm sure you can imagine that I shared the lab many people – Nuria, Silvia, Héléa, Alex of the fountain, Agus, craM, Ana, Amparo, Joan…. the list goes on. All of them who without doubt made the lab a better place.

Special mentions to: Prof. Dr. Pablo Martin-Gago who provided lots of entertainment both in and out of the lab. Craig for being my flatmate/lab mate/project-mate for the last 2 years of the thesis. Sean, Peter, Alessandro, Marta and Alvaro for our evening adventures. Edgar for his help, support and Christmas dinners! Anna for our walks home together. Ernest for providing daily entertainment by sounding like he's just walked out of a Shakespeare novel. Petita for our photoshoots which she loved so much….

From the UB and CSIC, I would like to thank Anna Costa, Arnald Grabulosa, and Carme Fàbrega for putting up with my annual 'chapa'! Also, to Pere Romea for his double life as Professor and psychologist – I hope I'm not the only one he sees looking panicked.

Outside of the science world, I'd like to thank my Dad for his constant help, advice and support, my sisters Susie and Joanna for their visits and helping keep moral up when times get tough. To Coxy for coming at the drop of a hat and surviving our mystery tours of Barcelona. To Jim for our motorbike adventures around Catalunya, for being there when I needed him most and for generally having a laugh together. Also, to the most recent addition to the family – Heidi. Her little smile always seems to light up the room. Let's just hope she can keep quiet during the defence!

Last and certainly not least I'd like to thank the special someone in my life, Davia, for being patient with me when times weren't so easy, and for being by my side during the fun times.

So, without further ado, let see what I've been doing while in the lab shall we?!

This thesis is dedicated to my grandmother Bea

# List of abbreviations

4-hydroxytamoxifen (4-OHT)

4-methylumbelliferone (4-MU)

Acetic acid (AcOH)

Acetonitrile (MeCN)

Active pharmaceutical ingredient (API)

American Joint Cancer Committee (AJCC)

Aqueous (aq.)

Base (B)

Benzyl (Bn)

Catalyst (cat)

Causes recombination (Cre)

Circa (ca.)

Colon Cancer Stem Cells (CoCSCs)

Colorectal cancer (CRC)

Common-mediator SMAD (co-SMAD)

Cyclin-dependant kinase (CDK)

Cyclohexyl (Cy)

Degrees Celsius (°C)

Deoxyribonucleic acid (DNA)

Dess-Martin periodate (DMP)

Dibenzylideneacetone (dba)

Dichloromethane (DCM)

Dimethyl sulfoxide (DMSO)

Dimethylamino pyridine (DMAP)

Dimethylformamide (DMF)

Diphenylphosphoryl azide (DPPA)

Enhanced green fluorescent protein (eGFP)

Epidermal growth factor (EGF)

Epithelial-to-mesenchymal transition (EMT)

Equivalents (eq.)

Ethanol (EtOH)

Ethyl acetate (EtOAc)

Extracellular matrix (ECM)

GlaxoSmithKline (GSK)

Glutathione (GSH)

Gram (g)

Growth and differentiation factors (GDFs)

Half maximal inhibitory concentration (IC50)

High pressure liquid chromatography (HPLC)

High resolution mass spectroscopy (HRMS)

Intraperitoneal (IP)

Isopropanol (iPrOH)

Kilodaltons (kDa)

Latency associated peptide (LAP)

Latent TGF-β binding proteins (LTBPs)

Leaving group (LG)

Lithium diisopropyl amine (LDA)

Logarithmic acid dissociation constant (pKa)

Mass spectroscopy (MS)

Medium pressure liquid chromatography (MPLC)

Messenger RNA (mRNA)

Mesyl chloride (MsCl)

Meta (*m*)

Methanol (MeOH)

Methoxymethyl acetal (MOM)

Methyl vinyl ketone - (MVK)

Micromolar (μM)

Mitogen-activated protein (MAP)

Modified oestrogen receptor ($ER^{T2}$)

Mouse tumour organoids (MTO)

Murine sarcoma virus (MuSV)

Nanomolar (nM)

N-bromosuccinamide (NBS)

Nerve growth factor (NGF)

Nuclear magnetic resonance (NMR)

Nucleophilic aromatic substitution (SNAr)

Oestrogen receptor (ER)

Ortho (*o*)

Overnight (on)

Para (*p*)

PD-1 ligand 1 (PD1-L1)

Pharmacokinetics/pharmacodynamics (PKPD)

Phenyl (Ph)

Pivaloyl (Piv or PIV)

Programmed cell-death protein 1 (PD-1)

*p*-Toluenesulfonic acid (TsOH *or p*-TsOH)

Retention factor (rf)

Ribonucleic acid (RNA)

Room temperature (rt)

Sarcoma growth factors (SGFs)

Short-hairpin RNA (shRNA)

SMAD (small mother against decapentaplegic)

Small double-stranded interfering RNA (siRNA)

Small latent complex (SLP)

Small molecule inhibitor (SMI)

Starting material (SM)

Structure activity relationship (SAR)

Tertiary (tert)

Tertiary butyl ($^{t}Bu$)

Tetrahydrofuran (THF)

Tetrahydropyran (THP)

TGF-β receptors (TGFBR)

Thin-layer chromatography (TLC)

Transforming growth factor beta (TGF-β)

Transforming growth factor-alpha (TGF-α)

Triethylamine ($NEt_3$ or $Et_3N$)

Trimethylsilyl (TMS)

Ultra-high pressure liquid chromatography (UPLC)

X-Ray powder diffraction (XRPD)

# Contents

# 1. Introduction and objectives

# 1 Introduction and objectives

A colon cancer is composed of a host of different cell types, besides the mutated epithelial cells. The deceptively straight-forward approach of directly targeting these cancer cells has given patients significant benefits, yet ultimately fails treating advanced disease – the current therapy it is not effective for metastatic patients. Moreover, the drugs that have been the staple of clinical practice have not changed very much over the last 50 years. An alternative approach has emerged from the field that studies of the role of the non-epithelial component of a tumour, also called tumour microenvironment or stroma.[1] Stroma is the part of an organ or tissue which does not have a specific role *per se* – it acts as a connective and structural part of the organ, which also includes the blood vessels.

Examples of how the tumour microenvironment can have an impact on cancer include the formation of new blood vessels to sustain growth, cell-cell communication with stimulating growth factors in a perverted version of normal tissue development, and immune responses that could kill cancer cells.[2] This work builds on the recent finding that transforming growth factor beta (TGF-β) signalling between cancer cells and the (non-mutant) surrounding cells plays a key role in these processes. The TGF-β signalling pathway is involved in a variety of cellular processes in healthy cells and tissues such as cell growth, homeostasis, and immune response among others. In short, the TGF-β ligands bind to the TGF-β receptors (TGFBR) activating the transmembrane kinase, which in turn phosphorylates and activates SMAD (small mother against decapentaplegic) proteins. This results in transcription of a range of target genes.[3] This is depicted in Figure 1.1.

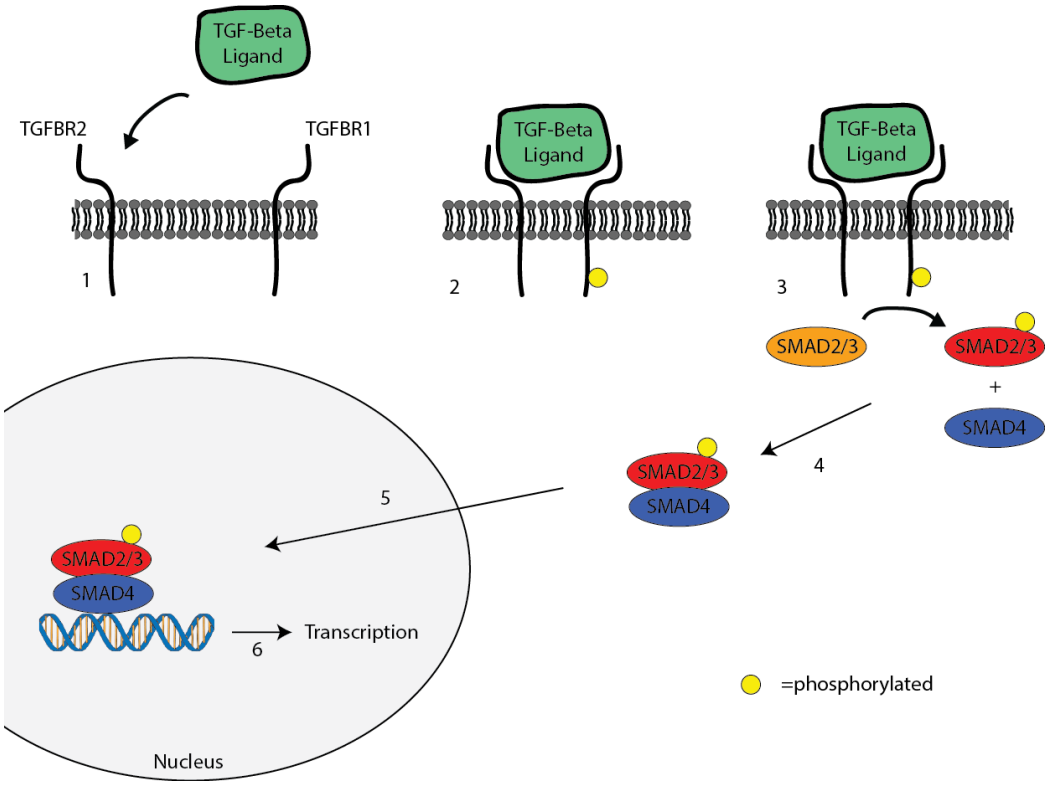


**Figure 1.1.** Overview of the TGF-β pathway. 1) TGF-β ligand binding to the receptor. 2) Dimerization of the receptors. 3) Activation of the kinase & SMAD phosphorylation. 4) SMAD dimerization. 5) SMAD complex transnucleation. 6) Gene transcription.

Various diseases such as cardiovascular disorders like atherosclerosis and cardiac fibrosis[4], diabetic nephropathy[5], multiple sclerosis[6] or cancer[7] are associated with aberrant levels of TGF-β and/or mutations in key components in the pathway.

In cancer, TGF-β has a dual, paradoxical role.[8,9] In early stage tumours, it mainly acts as a tumour suppressor. Therefore, advanced tumours frequently gain mutations in the pathway, abrogating the suppressive effects of TGF-β. Surprisingly, tumours mutated for the pathway that increase their production of the protein were found to have a worse prognosis. As it turns out, TGF-beta conditions the microenvironment to the tumour's advantage, inducing stromal fibroblasts to secrete cancer-promoting factors and possibly suppressing anti-cancer immunity.[10] This results in disease progression and metastatic initiation.

In the case of advanced tumours, inhibition of this pathway could effectively inhibit/block the cancers cells´ overall ability to suppress the immune system, increase proliferation, angiogenesis, among

other factors. Inhibition of the pathway is an important therapeutic target as it could stop advanced tumours in their tracks, and also prevent metastatic tumours from colonising new tissues.[11] In addition, as this type of therapy would impinge on the tumour microenvironment, the fact that this is mutationally stable could reduce the risk of acquired resistance.

To date, no TGF-β receptor-specific small molecule inhibitor (SMI) has reached the market. GlaxoSmithKline developed potent SMI's and they are used in *in vitro* studies, however they are not stable *in vivo*.[12,13],[14,15]

Eli Lilly & Company developed LY2157299 (**1-1**), also known as Galunisertib (Figure 1.2), which reached Phase II clinical trials for a variety of cancers.[16,17] The compound itself did not reach the market for reasons of which are currently unknown at the time of writing.

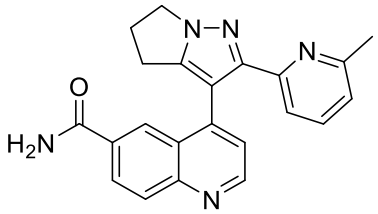


**1-1**

**Figure 1.2.** Galunisertib (LY2157299) – A TGF-β SMI developed by Eli Lilly & Co.

In collaboration with the group of Eduard Batlle (ICREA researcher and principal investigator in the oncology programme at IRB Barcelona) we decided to study the role TGF-β plays in tumour formation, proliferation, and especially metastasis initiation in colorectal cancer (CRC) - the latter being of high clinical relevance. Moreover, if the concept of inhibiting the TGF-β pathway to target the pro-metastatic tumour microenvironment can be shown to prevent metastatic initiation, it might also be a valuable tool to treat established metastases.

In order for us to be able to study the role TGF-β plays in CRC *in vivo*, we needed large quantities of the inhibitor LY2157299**, therefore the first objective of the doctoral thesis was to synthesise LY2157299 on a hundreds-of-grams scale.**

Although LY2157299 has a half-life of 8 hours in human, in mice the half-life is only 18 minutes which is relatively short.[17] This implies to study the effects of blocking TGF-β pathway in mice, treatment is needed twice daily via gavage at up to ten times higher doses than reported for human use.[16]

Furthermore, the gavage treatment itself is both time consuming and costly. Thus, it would be desirable to have a compound with a longer half-life which could result in an improved dosage regime, and also a better control of plasma concentration of the drug.

Moreover, the formulation described in the literature involves the use of a suspension which, if not homogeneous, could result in an erroneous dosage to each mouse. A soluble yet bioavailable inhibitor could overcome such limitations. Not only it would make the gavage formulation simpler, but it would also open doors to other methods of drug administration such as intravenous or intraperitoneal injection.

To achieve this goal, we planned to modify the skeleton of the LY2157299 in such a way that it still retained its activity, but also in its active form had a functional group which could act as a handle to enable us to modulate the physical properties of the molecule. We envisaged that such a handle would allow us to attach groups to the molecule, enabling us to modulate properties such as solubility or half-life, while also allowing the attachment of groups which could be cleaved at a time or place of our choosing – e.g. photo-labile groups. [18],[19]

In 2008 a structure activity relationship (SAR) study was published on the quinoline domain of the dihydropyrrolopyrazole series of inhibitors as shown in Table 1.1. Modification at position 2 was immediately ruled out due to the low $IC_{50}$ values. Positions 6 and 7 were of interest as they seemed to provide potent inhibitors, and entry 7e particularly stood out to us as Br is a bioisostere of hydroxyl group.[20] The hydroxyl group would give a handle to attach cleavable groups onto such as esters or PEGylated chains for example. This rationale led us to target compound **1-2** (Figure 1.3). To the best of our knowledge, hydroxyl group at position 6 had not been explored to date.

**Table 1.1.** Summary of the SAR of the compounds used by Li *et al*.[21]

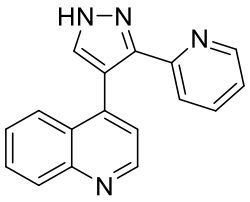

LY354947

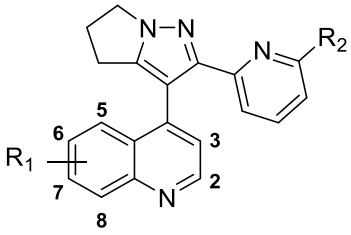

| Compounds | R1 | R2 | TGF-β R1 ic50 (μM) |
|---|---|---|---|
| **LY354947** | H | H | 0.059 ± 0.023 |
| **7b** | 2-Cl | H | 19.8 ± 0.2 |
| **7c** | 6,8-OMe | Me | 3.81 |
| **7d** | 8-F | Me | 0.928 ± 0.296 |
| **7e** | 6-Br | Me | 0.089 ± 0.022 |
| **7f** | 6-$OCF_3$ | Me | 0.141 ± 0.042 |
| **8** | 6-COOMe | Me | 0.526 |
| **9** | 6-$CONH(CH_2)N(CH_3)_3$ | Me | 0.193 |
| **10** | 2-OMe | H | >20 |
| **11** | 2-SEt | H | >20 |
| **12** | 2-$N(CH_2)_4$ | H | >20 |
| **13** | 7-OH | H | 0.16 |
| **14a** | 7-$O(CH_2)_3N(CH_2CH_2)_2NCH_3$ | H | 0.074 |
| **15** | 7-$O(CH_2)_2Cl$ | H | 0.044 |
| **15a** | 7-$O(CH_2)_2N(CH_3)_2$ | H | 0.024 ± 0.010 |
| **15b** | 7-$O(CH_2)_2N(CH_2CH_3)(CH_3)$ | H | 0.085 ± 0.041 |
| **15c** | 7-$O(CH_2)_2N(CH_2CH_2)_2NCH_3$ | H | 0.10 ± 0.071 |
| **15d** | 7-$O(CH_2)_2N(CH_2CH_2)_2O$ | H | 0.069 ± 0.031 |

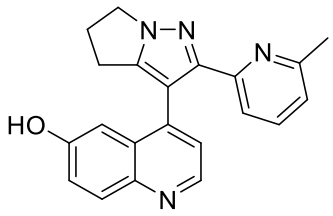

**1-2**

**Figure 1.3.** Target active compound for TGF-β inhibition.

Derivatisation of the phenol with groups cleavable by metabolism could help us modulate properties such as solubility and PKPD. We took inspiration from Irinotecan which needs to be metabolised into SN-38 to become active (Figure 1.3). The basic nitrogen of the piperidine tertiary amine can form salts, allowing for greater solubility in aqueous solutions, with the carbamate being able to be cleaved by metabolism *in vivo* via esterases in the body.[22] We proposed that modifying the newly designed TGF-β inhibitor with the same group as that of Irinotecan could allow us to have soluble variant **1-3** (Figure 1.4), which could potentially show improved PK/PD properties in mice.

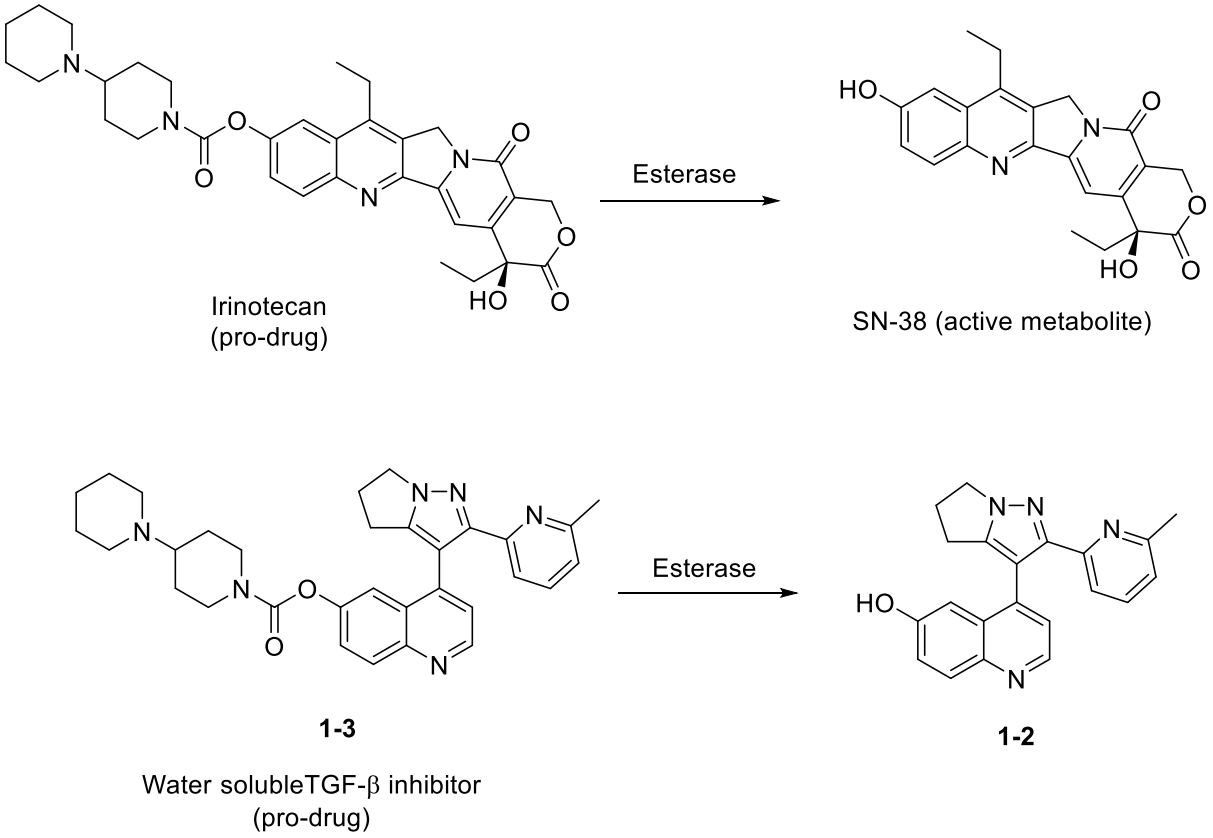


**Figure 1.4.** Formation of a water soluble TGF-β inhibitor.

These challenges bring us to our **second objective during the doctoral thesis: the design and synthesis of compound 1-2 and its derivatives as potential TGF-β inhibitors.**

In parallel to this work, we started a more ambitious project in collaboration with Dr Daniele Tauriello – a postdoctoral researcher in the group of Dr Eduard Batlle. This project was devoted to developing a new tool to study the communication between a cell and its environment.

The study of the effect that the suppression or activation of a gene in a given cell has on the neighbour cells would be of great importance to unravel the complex cellular interactions that underlie biological processes such as metastasis.

One of the most widely used methods to delete, activate or otherwise alter a gene is the Cre technology. Cre recombination is a technique commonly used in a biology laboratory both *in vivo* and *in vitro*. It is used to insert, or delete a gene at a specific point in a sequence of DNA, among others potential modifications.[23,24],[25] The ability to be able to turn off a gene at a particular moment (or location) can be essential to study a gene´s function, especially if a full knockout would be lethal. In this way, a gene or set of genes could be deleted during metastasis to determine their requirement/contribution to the process.

The Cre technology has two key components: 1) the Cre-recombinase – an enzyme which is able to cut the DNA at a specific sequence of base pairs and 2) the LoxP sites – which are the sites where the recombinase cuts.[26] When these sites are strategically placed around a target gene and in a specific directionality, this gene can be manipulated by the Cre technology as shown in Figure 1.5.

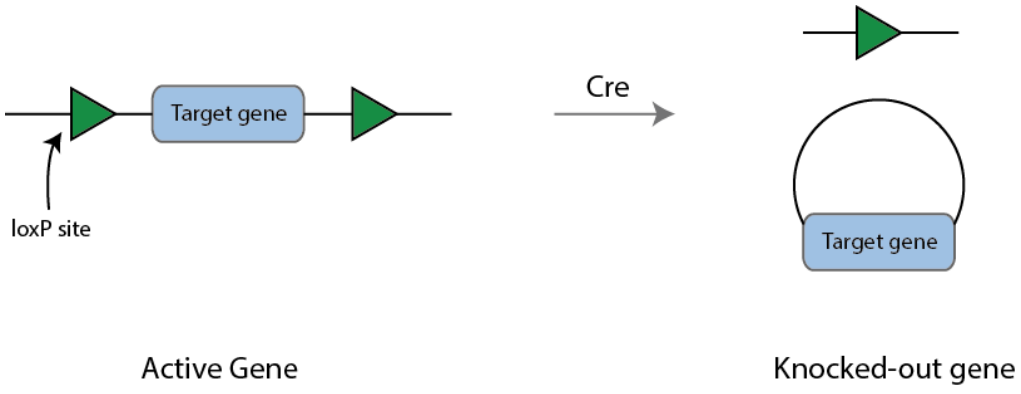


**Figure 1.5.** An example system of Cre system creating a gene knock out.

Activation of Cre can be achieved in a few ways, but the most convenient is the use of Cre bound to the oestrogen receptor – specifically the $ER^{T2}$ – a modified oestrogen receptor.[27] In practical terms, this works by having the active Cre enzyme bound to the oestrogen receptor which resides in the cytoplasm and therefore is not in contact with any genetic information (DNA). Induction of recombination is achieved by treating with a drug that binds to the oestrogen receptor. The most used is 4-hydroxytamoxifen (4-OHT, **1-5**) – the active metabolite of the known oncologic drug tamoxifen (**1-4**). Upon binding to the oestrogen receptor, transnucleation occurs bringing the Cre-$ER^{T2}$ complex into contact with the genetic information (DNA) and enabling said modifications to be performed around the LoxP sites.

It is important to remember that without 4-OHT, the Cre remains inactive and cannot perform any genetic changes. Therefore, if it were possible to liberate 4-OHT in a specific cell, we could reach our target of deleting or activating a gene in its direct environment. In practical terms, we would engineer the metastatic cancer cell to be the source of 4-OHT, thus targeting the stromal cells it interacts with. As there is already a wide range of mouse models with LoxP-flanked genes to pick from, we could assess the functional relevance of these genes in metastatic growth or initiation. Importantly this technology could be used to study other diseases.

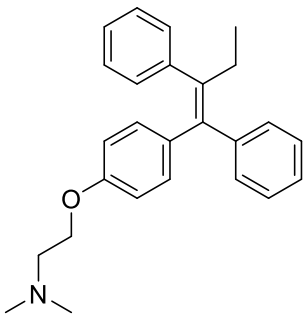


Tamoxifen **1-4**

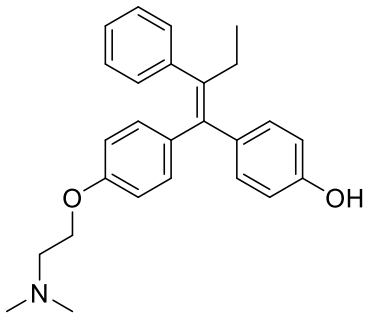


4-hydroxytamoxifen (4-OHT) **1-5**

**Figure 1.6.** Tamoxifen and its active metabolite 4-OHT.

The control of the release of an active compound both at the site as well as at the time is called spatio-temporal drug control. This can be triggered by a specific and usually external factor. Photo-switchable peptides are an example of these. Upon irradiation with a substrate-specific wavelength of light, the azo bond isomerises – typically from *trans* to *cis* – invoking a structural change to the peptide, thus modulating its activity.[28] As of yet, it is not possible to adopt this technique in the setting where individual cells are colonising an internal organ.

To use an analogy, a metastatic cell can be looked as a 'seed', whereas the organ it is trying to invade can be looked as the 'soil'. It is indeed this setting that emerging data suggest that the metastatic cancer cell most depends on a favourable soil.[29] To achieve this goal of charting the complex interactions, we aim to release 4-OHT in a specific place (cancer cell) in a temporally controllable fashion. To ensure specificity, we plan to use an exogenous (xeno) enzyme to liberate the drug in a permanent manner. To do so we plan to synthesise a prodrug which itself is inactive, but upon encountering an exogenous enzyme, it would split into the active 4-OHT plus the recognition part of the molecule. This is depicted schematically in Figure 1.7.

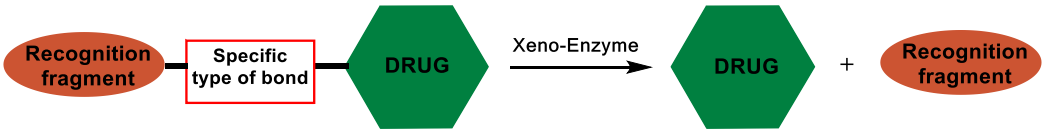


**Figure 1.7.** Release of a drug using a xeno-enzyme.

When looking for a method to activate the drug, Daniele Tauriello took inspiration from nature – in particular from lignin. Lignin is an aromatic biopolymer which is only able to be broken down by a few fungi and bacteria.[30,31] This stability led us to further consider its structure and degradation pathway. Masai *et al.* reported that enzymes LigE and LigF found in bacteria *Pseudomonas paucimobilis* SYK-6 were able to cleave the ether bond in the lignin degradation pathway (Figure 1.8) liberating Guaiacol.[32,33] LigF belongs to the glutathione-*S*-tranferase superfamily.[34] This superfamily of enzymes are able to conjugate glutathione (GSH) to a wide variety of potentially harmful agents to a cell. The structure of GSH is also shown below in Figure 1.8.

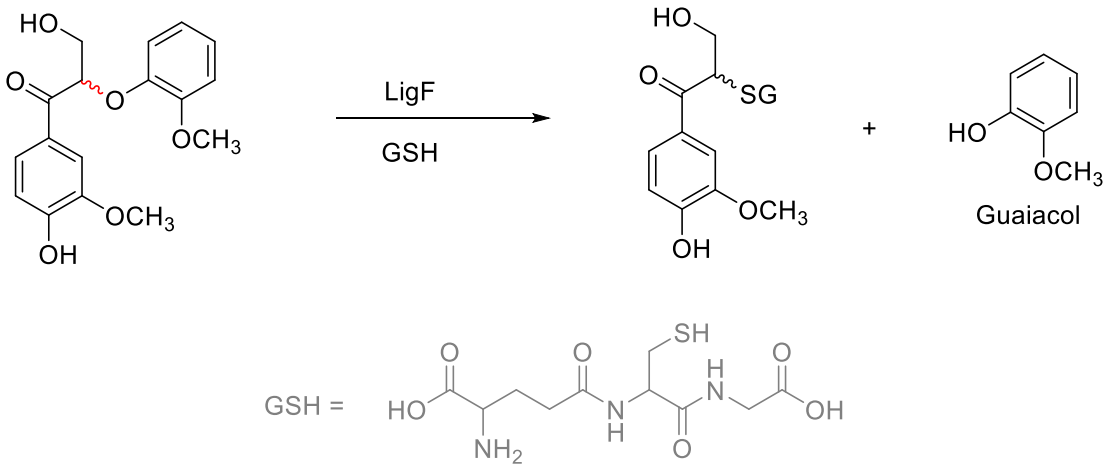


**Figure 1.8.** Beta etherase enzymactic activity in the lignin degradation pathway.

We proposed that the 4-OHT needed to activate the CRe-ER$^{T2}$, could be made into a stable compound *in vitro* and *in vivo* by linking it to the recognition fragment used by LigF – given that lignin cannot be broken down by humans. This new compound itself would be significantly different from 4-OHT, so we proposed that it would no longer be a substrate to the CRe-ER$^{T2}$. This is shown below in Figure 1.9. Since the work by Reiter *et al.* demonstrated that the hydroxy methyl chain alpha to the ketone was not necessary for the LigF activity,[35] we simplified our target molecule removing the hydroxymethyl group. We therefore designed compound **1-6**, which we named 'Guaymoxifen', as our first candidate molecule for spatiotemporal release of 4-OHT and consequent CRe activation.

If our collaborators in Batlle's group could encode LigF in a certain (cancer) cell, we would therefore trigger gene recombination in all surrounding cells that have Cre-ER$^{T2}$ and LoxP flanked genomic sites upon administration of Guaymoxifen. Provided the released 4-OHT does not spread sistemically, the only recombination would be local, ensuring specificity and decreasing potential toxicity. A further necessity was that the Guaymoxifen had itself to be unable to bind to the ER$^{T2}$ to avoid any unwanted recombination. We hypothesised that guaymoxifen would be metabolically stable and the metabolic machinery of the mammals would not be able to cleave the beta ether bond, and therefore no 4-OHT would be released.

Of note, if successful, a similar strategy could be used to deliver other drugs to effectively treat the tumour. Many of the currently used drugs (such as irinotecan) are highly effective cytotoxic agents yet fail to eradicate cancers due to a lack of specificity and high levels of toxicity. Levels high enough to kill cancer can also kill the patient; localised release is recognised as a powerful alternative and several efforts—using different (bio-)chemistry—have shown success.[36],[37]

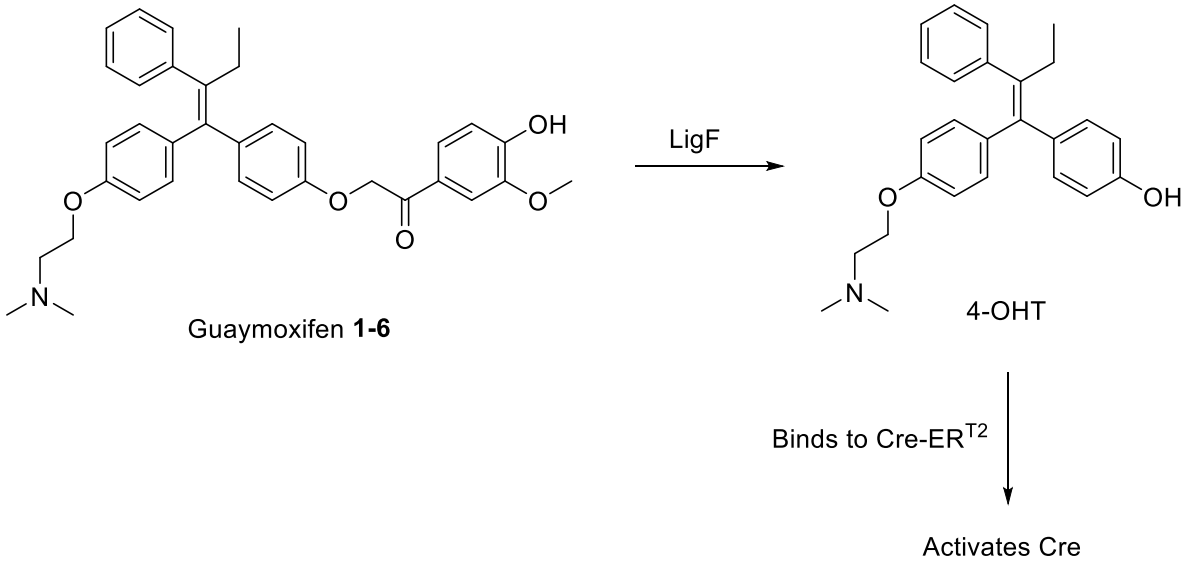


**Figure 1.9**. Target compound Guaymoxifen (**1-6**).

Before starting to synthesise our target compound, it was first necessary to explore the specificity of the LigF to the recognition fragment. We planned to modulate the groups on the phenyl ring of the recognition fragment, and using the same methodology used by Reiter *et al.* and Masai *el al.*, planned to check the ability of LigF to cleave the beta-keto ether bond by fluorescence as shown below in Figure 1.10.

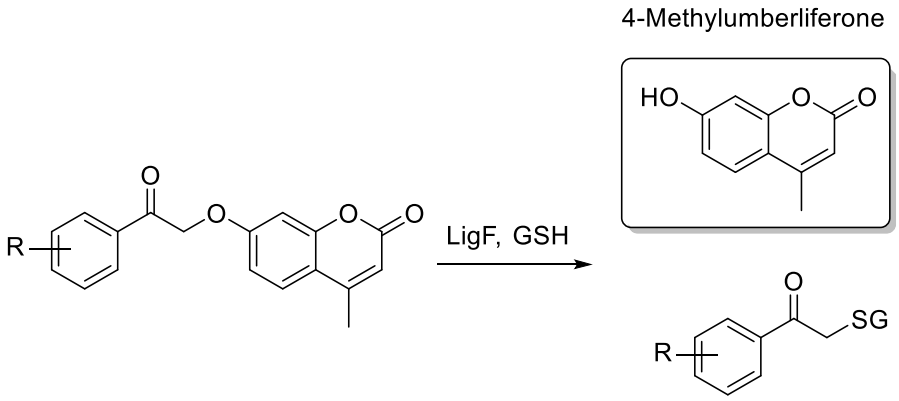


**Figure 1.10**. Testing the specificity of LigF for the recognition fragment by measuring the fluorescence of 4MU as it is produced.

This structural activity relationship will give us our final target compound, thus the **third objective for the doctoral thesis was the optimisation of the recognition fragment of our target compound to be cleaved by the exogenous enzyme LigF.**

After completing the third objective of the thesis by conducting a SAR of the recognition fragment, the final molecule had to be made and be submitted to biological testing. This is not a trivial exercise, as from the outset 4-OHT can exist as either the *cis* or the *trans* isomer as shown in Figure 1.11 below.

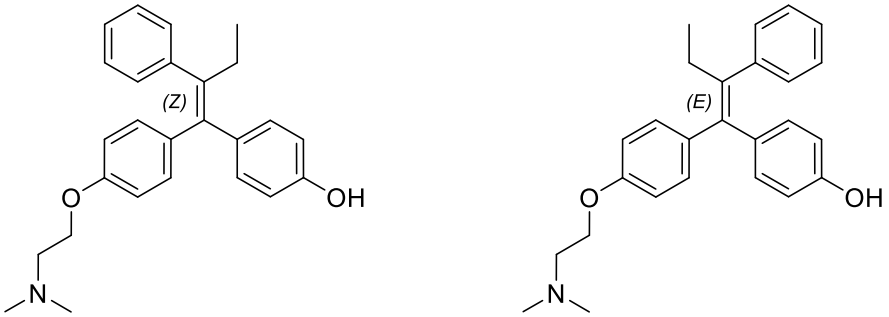


**Figure 1.11**. (*E*) and (*Z*) isomers of 4-hydroxytamoxifen.

The (*Z*)-4-hydroxytamoxifen has between 100-1000 times more affinity to the oestrogen receptor than the (*E*)-4-hydroxytamoxifen, therefore it would be important to synthesise specifically the isomer which upon bond cleavage by LigF would give the (*Z*)-4-OHT.[38] The first synthetic target for initial testing and proof of concept was a mixture of diastereomers of Guaymoxifen of sufficient quantity and purity to perform the initial biological assays.

The *E*/*Z* isomerisation is a factor which needs to be controlled. Furthermore, should the recognition fragment contain one or more chiral centres, this could add to the complexity of the synthesis of a single stereoisomer. With the target compound in hand, it should be submitted to biological testing to confirm the proof of concept of the molecule. If needed, further optimisation should be conducted on the final compound.

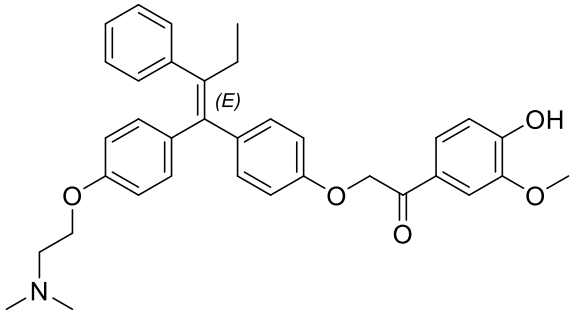


**Figure 1.12.** (*E*)-Guaymoxifen.

Therefore, the **fourth objective for the doctoral thesis was the synthesis and subsequent biological tests of our designed compound (*E*)-Guaymoxifen.**

## 1.1 References


[1] D. V. F. Tauriello, A. Calon, E. Lonardo, E. Batlle, *Mol. Oncol.* **2017**, *11*, 97–119.

[2] K. A. Rmali, M. C. A. Puntis, W. G. Jiang, *Colorectal Dis.* **2007**, *9*, 3–14.

[3] A. Weiss, L. Attisano, *Wiley Interdiscip. Rev. Dev. Biol.* **2013**, *2*, 47–63.

[4] M.-J. Goumans, P. Ten Dijke, *Cold Spring Harb. Perspect. Biol.* **2018**, *10*, a022210.

[5] S. Chen, B. Jim, F. N. Ziyadeh, *Semin. Nephrol.* **2003**, *23*, 532–543.

[6] A. Mirshafiey, M. Mohsenzadegan, *Neuropharmacology* **2009**, *56*, 929–36.

[7] G. C. Blobe, W. P. Schiemann, H. F. Lodish, *N. Engl. J. Med.* **2000**, *342*, 1350–1358.

[8] L. Yang, H. L. Moses, *Cancer Res.* **2008**, *68*, 9107–11.

[9] L. Kubiczkova, L. Sedlarikova, R. Hajek, S. Sevcikova, *J. Transl. Med.* **2012**, *10*, 183.

[10] A. Calon, E. Espinet, S. Palomo-Ponce, D. V. F. Tauriello, M. Iglesias, M. V. Céspedes, M. Sevillano, C. Nadal, P. Jung, X. H.-F. Zhang, et al., *Cancer Cell* **2012**, *22*, 571–584.

[11] E. C. Connolly, J. Freimuth, R. J. Akhurst, *Int. J. Biol. Sci.* **2012**, *8*, 964–78.

[12] J. F. Callahan, J. L. Burgess, J. A. Fornwald, L. M. Gaster, J. D. Harling, F. P. Harrington, J. Heer, C. Kwon, R. Lehr, A. Mathur, et al., *J. Med. Chem.* **2002**, *45*, 999–1001.

[13] G. J. Inman, F. J. Nicolás, J. F. Callahan, J. D. Harling, L. M. Gaster, A. D. Reith, N. J. Laping, C. S. Hill, *Mol. Pharmacol.* **2002**, *62*, 65–74.

[14] N. J. Laping, E. Grygielko, A. Mathur, S. Butter, J. Bomberger, C. Tweed, W. Martin, J. Fornwald, R. Lehr, J. Harling, et al., *Mol. Pharmacol.* **2002**, *62*, 58–64.

[15] S. DaCosta Byfield, C. Major, N. J. Laping, A. B. Roberts, *Mol. Pharmacol.* **2004**, *65*, 744–52.

[16] J. Rodon, M. A. Carducci, J. M. Sepulveda-Sánchez, A. Azaro, E. Calvo, J. Seoane, I. Braña, E. Sicart, I. Gueorguieva, A. L. Cleverly, et al., *Clin. Cancer Res.* **2015**, *21*, 553–60.

[17] S. Herbertz, J. S. Sawyer, A. J. Stauber, I. Gueorguieva, K. E. Driscoll, S. T. Estrem, A. L. Cleverly, D. Desaiah, S. C. Guba, K. A. Benhadji, et al., *Drug Des. Devel. Ther.* **2015**, *9*, 4479–99.

[18] W. Li, P. Zhan, E. De Clercq, H. Lou, X. Liu, *Prog. Polym. Sci.* **2013**, *38*, 421–444.

[19] C. G. Bochet, *J. Chem. Soc. Perkin Trans. 1* **2002**, 125–142.

[20] N. A. Meanwell, *J. Med. Chem.* **2011**, *54*, 2529–91.

[21] H.-Y. Li, W. T. McMillen, C. R. Heap, D. J. McCann, L. Yan, R. M. Campbell, S. R. Mundla, C.-H. R. King, E. a Dierks,

B. D. Anderson, et al., *J. Med. Chem.* **2008**, *51*, 2302–6.

[22] R. H. Mathijssen, R. J. van Alphen, J. Verweij, W. J. Loos, K. Nooter, G. Stoter, A. Sparreboom, *Clin. Cancer Res.* **2001**, *7*, 2182–94.

[23] J. Rossant, A. McMahon, *Genes Dev.* **1999**, *13*, 142–5.

[24] A. J. H. Smith, M. a De Sousa, B. Kwabi-Addo, A. Heppell-Parton, H. Impey, P. Rabbitts, *Nat. Genet.* **1995**, *9*, 376–385.

[25] R. Srinivasan, T.-Y. Lu, H. Chai, J. Xu, B. S. Huang, P. Golshani, G. Coppola, B. S. Khakh, *Neuron* **2016**, *92*, 1181–1195.

[26] A. Nagy, *Genesis* **2000**, *26*, 99–109.

[27] P. S. Hoppe, D. L. Coutu, T. Schroeder, *Nat. Cell Biol.* **2014**, *16*, 919–27.

[28] H. Janovjak, S. Szobota, C. Wyart, D. Trauner, E. Y. Isacoff, *Nat. Neurosci.* **2010**, *13*, 1027–32.

[29] F. Seretis, C. Seretis, H. Youssef, M. Chapman, *Anticancer Res.* **2014**, *34*, 2087–94.

[30] F. J. Ruiz-Dueñas, A. T. Martínez, *Microb. Biotechnol.* **2009**, *2*, 164–77.

[31] R. Vanholme, B. Demedts, K. Morreel, J. Ralph, W. Boerjan, *Plant Physiol.* **2010**, *153*, 895–905.

[32] E. Masai, Y. Katayama, S. Kubota, S. Kawai, M. Yamasaki, N. Morohoshi, *FEBS Lett.* **1993**, *323*, 135–40.

[33] E. Masai, A. Ichimura, Y. Sato, K. Miyauchi, Y. Katayama, M. Fukuda, *J. Bacteriol.* **2003**, *185*, 1768–75.

[34] L. F. Chasseaud, **1979**, pp. 175–274.

[35] J. Reiter, H. Strittmatter, L. O. Wiemann, D. Schieder, V. Sieber, *Green Chem.* **2013**, *15*, 1373.

[36] N. Oršolić, *Cancer Metastasis Rev.* **2012**, *31*, 173–94.

[37] M. R. Junttila, W. Mao, X. Wang, B.-E. Wang, T. Pham, J. Flygare, S.-F. Yu, S. Yee, D. Goldenberg, C. Fields, et al., *Sci. Transl. Med.* **2015**, *7*, 1–12.

[38] B. M. Ford, L. N. Franks, A. Radominska-Pandya, P. L. Prather, *PLoS One* **2016**, *11*, 1–23.

# 2. TGF-β Background

# 2 TGF-β Background

## 2.1 History of TGF-β

The discovery of the first growth factor - nerve growth factor (NGF) - was made by Montalcini and Cohen in 1952 and marked an important milestone in science history. The work was recognised by a Nobel prize and showed how polypeptides produced by cells can act as extracellular regulatory molecules for the surrounding cellular environment. Such finding opened the doors to a whole new branch of scientific research, which in the later years focused on how cells communicate and regulate their own growth and proliferation.[1]

During the late 1970's and the early 1980's, many new growth factors were being discovered, further elucidating the crucial role played by these polypeptides in regulating the life cycle of normal cells. However, little was still known about their involvement in the etiology of cancer. During those years, De Larco and Torado isolated and partially purified sarcoma growth factors (SGFs) from the supernatant of the murine sarcoma virus (MuSV)-transformed mouse 3T3 cells. When treated with these factors *in vitro*, normal fibroblast cells were able to overgrow in monolayer cultures and also form progressively growing colonies in soft agar – properties typically associated with a transformed malignant phenotype. Upon removal of these factors from the growth medium, the cells returned to their normal behaviour.[2]

A little under two years later in 1980, the same group went on to report that these polypeptides were not only found under the conditions showed in the aforementioned publication, but were also found in extracts from other cancer cell lines.[3] They named these newly discovered polypeptides *transforming growth factors* (TGFs) and went on to describe the concept of TGFs acting in an 'autocrine' manor in transformed cells, whereby a cell is producing/overexpressing a growth factor which acts upon and stimulates the external receptors of the cell itself.[4]

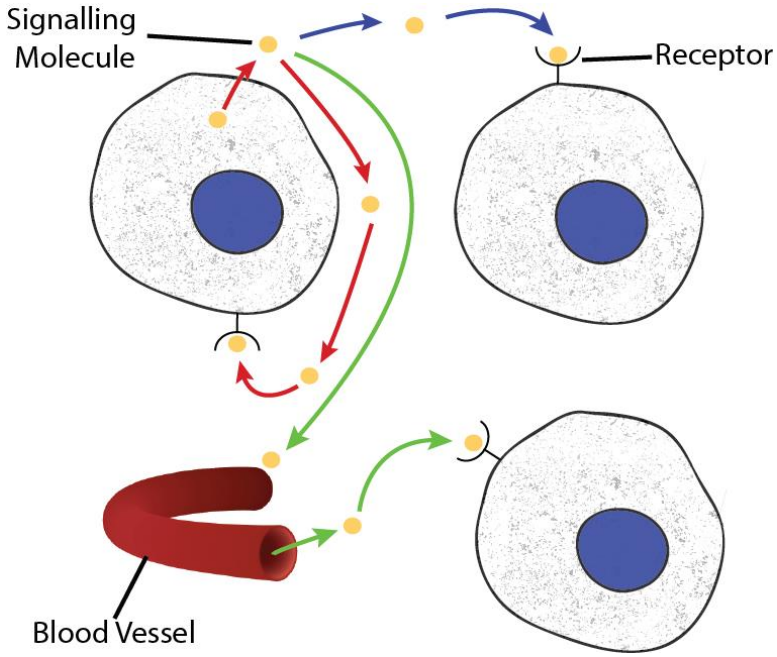


**Figure 2.1.** Types of Cell Signalling: Autocrine (red), Paracrine (blue), and Endocrine (green).

Using gel filtration, Roberts *et al*. then took the SGF extracts and purified them into two different fractions. Importantly, they noticed that both fractions were required to retain the transforming activity of the extract. If normal cells were treated with only one of the two purified fractions, the malignant phenotype was not observed and activity of the extract was lost.[5] This was the first indication that SGF could not be a single substance, but at least a mixture of two or more substances. The first fraction competed with epidermal growth factor (EGF) for receptor sites and itself did not induce large colony formation in soft agar.[6] It was named transforming growth factor-alpha (TGF-α). Just as TGF-α, the second fraction did not induce large colony formation in soft agar alone. However, unlike TGF-α, it did not compete with EGF. The second fraction when combined with EGF or TGF-α, enabled the cells to grow large colonies in soft agar. It was named TGF-β. Later on, TGFs were found to be present in other healthy tissues and organs around the body, and therefore it was then assumed that they were not cancer-specific factors, but that they played a functional role in normal healthy cells.[7]

R&D Systems®, using a method developed from Assoian[8], managed to produce homogeneous preparations of TGF-β, and from this point, many further advances in the understanding of TGF-β and its role in biologically functions were made. One notable discovery was that cells response to TGF-β

is context dependent. If certain cell lines are used, such as CCL-64, TGF-β was shown to act as a growth inhibitor contrary to the idea of what role TGF-β played until this point.[9]
It was from this point that the interest in TGF-β skyrocketed.

## 2.2 TGF-β ligands and receptors

After more than twenty-five years since the discovery of the first TGF-β ligand, it is now known that TGF-β is not a single polypeptide dimer, but a superfamily comprising of at least thirty ligands found not only in mammals, but also in frogs, fish, flies and worms, in different tissues and at any developmental stage. These can be split into two functional groups: the TGF-β-like group which includes the TGF-βs subfamily, activins, nodals and some growth and differentiation factors (GDFs), and the bone morphogenetic protein (BMP)-like group.[10]

### 2.2.1 TGF-β ligand synthesis

In mammalian tissues, the TGF-β subfamily is made up of three TGF-β isoforms, namely TGF-$\beta_1$, TGF-$\beta_2$, and TGF-$\beta_3$. The three ligands are either homodimeric or heterodimeric polypeptides, whose expression is controlled by distinct promoters.

TGF-β mRNAs are synthesised from genes coding for the different TGF-β isoforms in the nucleus of cells. Each mRNA is then translated into the corresponding precursor protein to give a pre-pro-TGF-β. Following the dimerisation of the pre-pro-TGF-β forms, the pre-pro tails are cleaved by proteases affording the mature TGF-β protein and the latency associated peptide (LAP), which keep interacting together to form what is known as the small latent complex (SLP). The SLPs are transported out of the cell into the extracellular matrix (ECM) where they first bind with latent TGF-β binding proteins (LTBPs), before being cleaved into the active dimer by ECM enzymes. This active TGF- β dimer is now capable of signalling in the TGF-β pathway.[11]

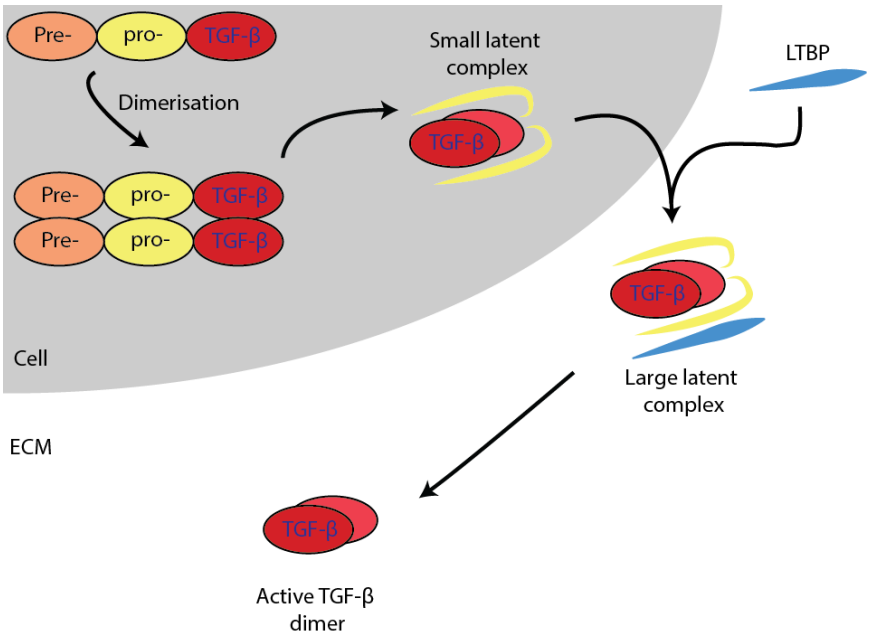


**Figure 2.2.** Synthesis of the active TGF-β dimer. Figure adapted from Kubiczkova, *et al*.[11]

### 2.2.2 TGF-β receptors and their activation

TGF-β receptors are part of a family of receptors, that binds to various members of the TGF-β superfamily of ligands. There are three types of TGF-β receptors (TGFBRs) and they play different roles in the signalling pathway.

TGFBR III, also known as betaglycan, is both the largest and the most abundant of the three receptors at 250-350 kDa and binds to several ligands of the TGF-β superfamily. Due to the lack of a kinase domain, it does not play a direct role in the signalling pathway - instead it retains the ligands in the ECM thus modulating their intracellular activity.[12]

On the other hand, receptor I (also known as activin receptor-like kinase 5 - ALK5) and receptor II are directly involved in signal transduction. Both are single pass serine/threonine kinases with receptor II weighing between 85 – 110 kDa and receptor I weighing between 65-70 kDa depending on the species in question.[13]

The binding of TGF-β dimers to the N-terminal extracellular domain of TGFBR II (1 in Figure 2.3) results in the recruitment of the type I receptor. This gives rise to a heterotetrameric complex consisting of a pair of each receptor (2 in Figure 2.3).

The TGFBR II can now phosphorylate the type I receptor, leading to a change in conformation and subsequent activation of the kinase domain of the latter (2 in Figure 2.3). The now active TGF-β-TGFBR complex is finally ready to mediate signal transduction.

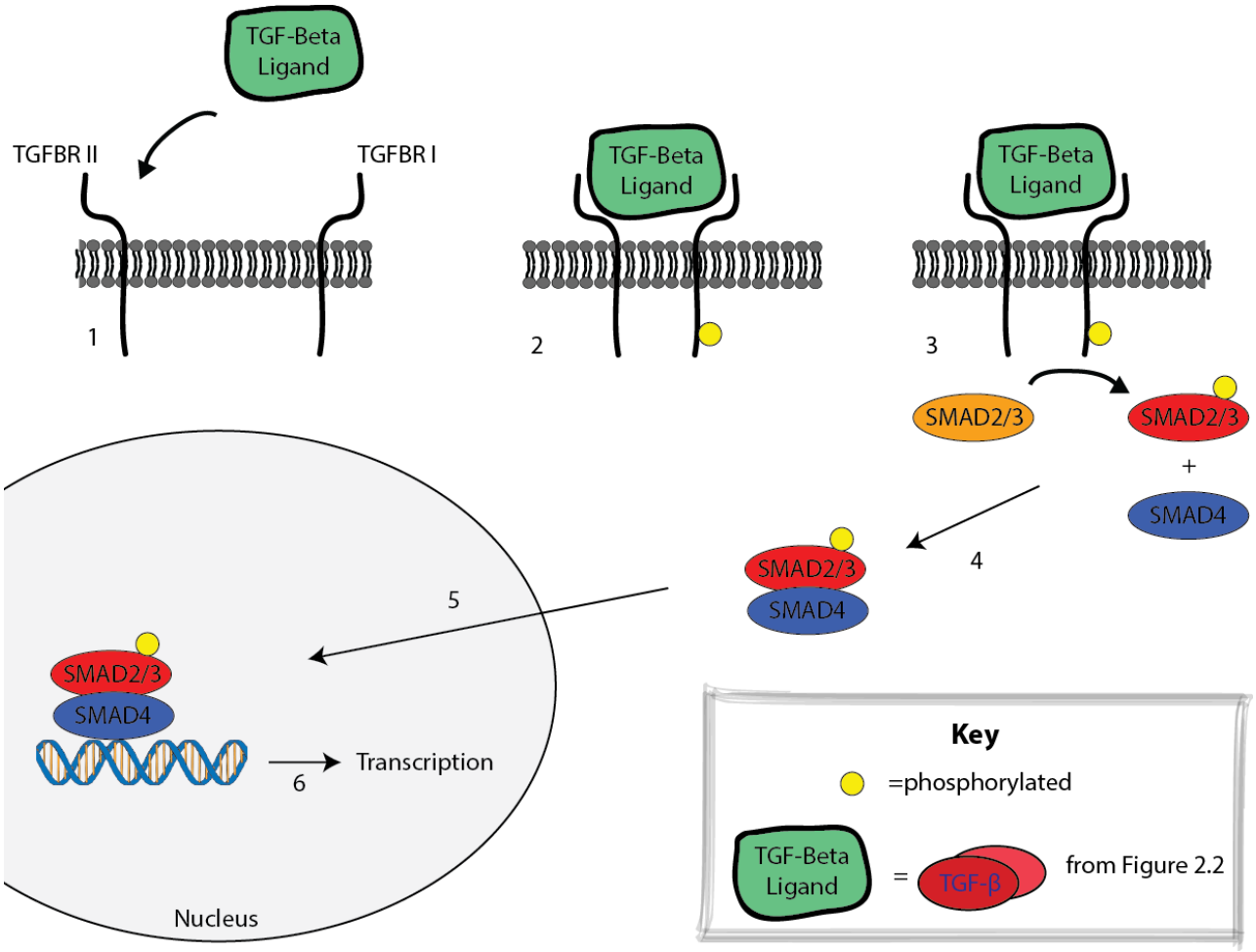


**Figure 2.3.** Canonical TGF-β signalling.

### 2.2.3 TGF-β signalling: The canonical SMAD pathway

TGF-β signalling pathway is initiated by the phosphorylation of TGFBR I (2 in Figure 2.3), which can then recognise and phosphorylate specific effector proteins. These proteins are a class of transcription factors known as receptor-regulated SMADs (R-SMADs). SMAD2 and SMAD3 are activated by the TGF- β subfamily as well as by activins and nodals ligands, while SMAD1, SMAD5 and SMAD8 by the BMP branch of the TGF-β superfamily of ligands.[14] Specifically regarding the TGF-β pathway, phosphorylation of SMAD2 and SMAD3 by TGFBR I yields the formation of a SMAD2/3 complex (3 in Figure 2.3), characterised by high affinity for the common-mediator SMAD (co-SMAD) SMAD4 (4 in Figure 2.3). This newly formed SMAD2/3-SMAD4 complex is then translocated into the nucleus where along with other co-factors, acts as a transcription factor and induces the transcription of TGF-β dependent genes (5 and 6 in Figure 2.3).[15]

## 2.3 Roles of TGF-β in healthy tissues

As previously mentioned, TGF-β is crucial to regulating cell growth, differentiation, and development in a wide range of biological systems. However, its role is also of fundamental importance when it comes to modulating immune responses during homoeostasis, infection and disease.

### 2.3.1 Regulation of the cell cycle and growth arrest

TGF-β is essential for the regulation of the cell cycle - the process proliferating cell growth. This cycle is made up of four phases as shown below in Figure 2.4.

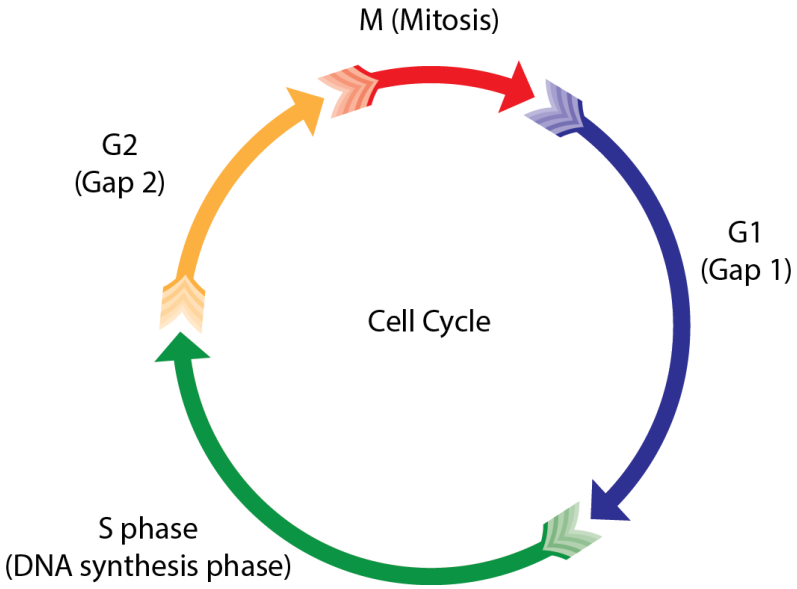


**Figure 2.4.** The cell cycle.

During the G1 phase, the cell prepares to copy its genome: RNA is transcribed, and proteins are synthesised. During the S phase, DNA is replicated, while the duplicated chromosomes are checked for errors in the following and last phase, G2, before the cell finally starts to divide (mitosis).

Two of the downstream proteins which are synthesised in the TGF-β pathway are p15 and p21. Levels of free cyclin-dependant kinase 4 (CDK4) are needed to increase for the cell to progress from G1 to S phase. p15 and p21 form complexes with CDK4, thus reducing the levels of free CDK4 in the cell. This reduction retains the cell in the G1 phase and therefore an overall pause in the cell cycle is observed.

In addition to this, TGF-β is also known to induce apoptosis in several cell types. This mechanism is not very well understood and is thought to go via a Daxx and/or a SMAD pathway.[16]

### 2.3.2 Immune modulation

As briefly mentioned before, TGF-β is also important in regulating the immune system. Mice which are TGFR I deficient survive only until approximately day 20 when they succumb to organ failure and death due to mixed inflammatory diseases and tissue necrosis. This suggests that TGF-β plays a crucial role in suppressing and controlling the immune system.[17] Similarly, SMAD3 deficient mice also die due to a malfunctioning immune system. Data show that deletion of the SMAD3 gene directly affects T-cell function and generally predisposes to leukemogenesis, thus implying that TGF-β plays an important role in regulating T-cell activation.[18]

### 2.3.3 Role of TGF-β in cancer and other diseases

It is hardly surprising that a pathway responsible for modulation of immune response, cell growth and mortality regulation could cause disease should this pathway fail in some way. In fact, mutations in some point(s) in TGF-β signalling pathway are involved in many diseases such as Loeys-Dietz syndrome, Marfan syndrome, hepatic fibrosis, left-right axis malformations, diabetes and cancer among others.[19–23] In cancer, a higher expression of TGF-β is usually correlated with the malignancy of the tumour, while disruptions of TGF-β immunosuppressive functions are often implicated in the pathogenesis of many autoimmune diseases.[24] [25]

### 2.3.4 Targeting TGF-β signalling in cancer

Nowadays, being diagnosed with cancer is not necessarily the death sentence it once was. Over the last two decades, general cancer-related deaths have dropped by 23%, and in specific cases such as uterine cancer, mortality rates have dropped 80% between 1930 and 2012.[26] Advances in diagnostics, changes in lifestyle and progress in treatments have all been factors in lowering the percentage of deaths per year attributed to cancer. All of this is despite an ageing population.

TGF-β's role in cancer is somewhat paradoxical; on one hand, we have the canonical TGF-β pathway acting as a growth inhibitor by stopping cells at G1 and causing apoptosis. In this instance, TGF-β is

acting as a tumour suppressor and is a major hurdle a malignant tumour must overcome in its attempt to progress to later stages. Nonetheless, tumours often manage to achieve this goal via mutations in the TGF-β receptors and/or in downstream components of the pathway.[27] The first consequence of such mutations is that pre-malignant and malignant cells start to divide more rapidly.

At this stage, tumours are advancing and escaping the control of TGF-β. Interestingly, these cells as well as the stromal cells within the tumour, increase their production of TGF-β. Such strategy works to the tumours advantage as the higher levels of TGF-β locally increases angiogenesis, cell mobility and interaction with the extracellular matrix while also reducing immune response.[28] All of these factors contribute in rendering the tumour more invasive and characterised by a generally more aggressive phenotype.[29]

Blocking the TGF-β pathway could reverse the effects that tumours have evolved to depend on in terms of their survival and proliferation resulting in disease.

Due to this paradoxical role, there were initial concerns as to the effectiveness of blocking the TGF-β pathway. Despite this, scientists developed various methods to block the pathway at various points, and then studied the biological response. Some of the employed approaches including the use of anti-ligand antisense oligonucleotides (ASOs)[30], antibodies[31], ligand-competitive peptides[32], and small molecule inhibitors (SMIs).

## 2.4 TGF-β small-molecule inhibitors

Small-molecule inhibitors (SMI) are of huge importance to the pharmaceutical industry. They can be produced cost-effectively on a large scale and have the great advantage of being taken orally -unlike peptide drugs, antibodies and ASOs. The crystal structure of TGFBR I bound in its inactive state to the known protein inhibitor FKBP12 shown by Huse *et al.* opened new opportunities to the design and synthesis of novel TGFBR I-specific inhibitors.[33]

Based on these findings, GlaxoSmithKline (GSK) started their own research program to find selective TGFBR I inhibitors. Through a high throughput screen, they identified a 1,5-naphthyridine aminothiazole derivative **2-1** as a potent inhibitor of TGFBR I.[34]

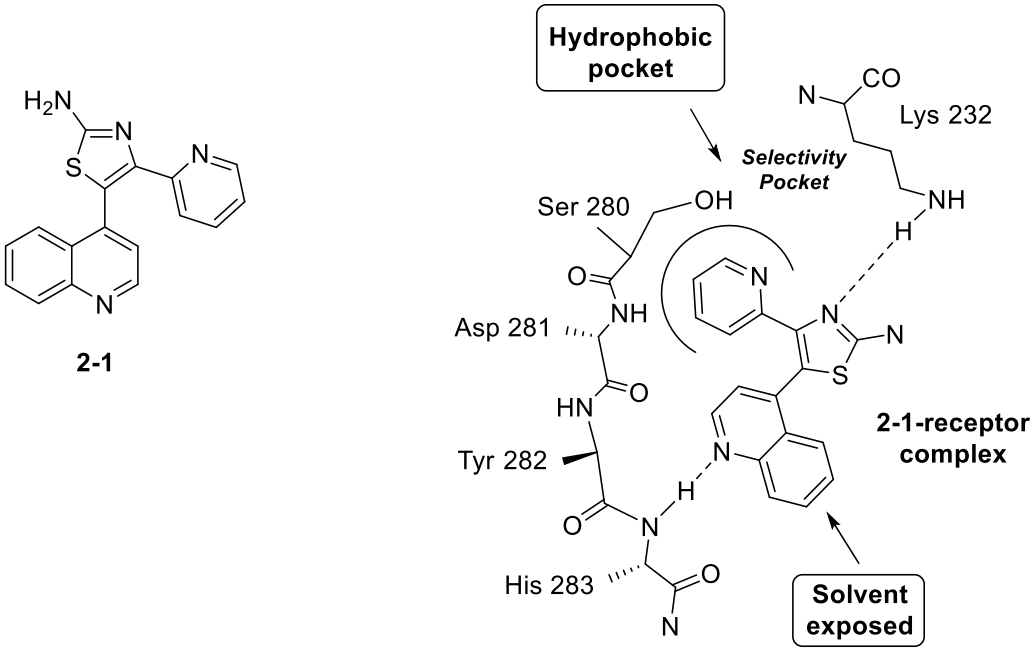


**Figure 2.5.** TGFBR I – **2-1** complex (adapted from Padua *et al.*) Unknown valences omitted for clarity.[29]

Importantly, **2-1** exhibited selectivity over p38 mitogen-activated protein (MAP) kinase with a reported $IC_{50}$ >16 µM when tested in the Sf9 assay versus an $IC_{50}$ of 6 nM when tested for ALK5 autophosphorylation inhibition. Based on the crystal structure of the ALK5-FKBP12 complex, the possibility that **2-1** selectivity came from the interaction between the substituted thiazole region of the molecule and the Lys-232 was discarded due to the fact that p38 MAP kinase shows an analogous region.[35]

Thanks to several SAR studies conducted over the three heterocyclic subunits, it was possible to shed light on the mode of inhibitor binding. One noteworthy finding was that the addition of a methyl in the 6 position of pyridine ring (alpha to the mono-substituted pyridine nitrogen) of **2-1**, resulted in a compound with similar binding properties to TGFBR I, but a six-fold increase in potency in the TGF-β cellular assay.

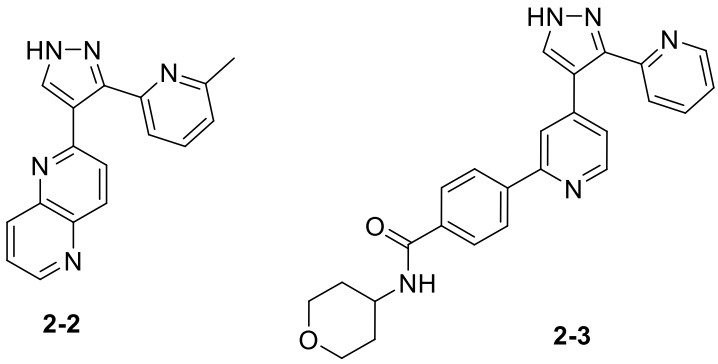


**Figure 2.6.** SMI TGF-β inhibitors developed by GSK.

Further optimisation of heterocyclic central core led to the pyrazole inhibitor **2-2**, which was tested for its selectivity against a panel of kinases and showed to have a greater $IC_{50}$ than 16 µM against all kinases tested. Finally, **2-2** was co-crystallised with ALK5 to confirm the hypothesised binding model. GSK went on in their research program now addressing their efforts in developing an orally active form of this lead compound and finally obtaining derivative **2-3**.[36]

Around the same time, Eli Lilly & Company began their own medicinal chemistry program for the search of ALK5 inhibitors. Through their high-throughput screen, they identified compound **2-4** as a 51 nM inhibitor in a cell-based assay.[37] Like with Gellibert *et al.*, a brief SAR analysis showed that replacement of the pyridyl group to a phenyl resulted in the loss of activity, while as before, the addition of a methyl at the 6 position of the pyridyl- group resulted in an increase in potency.

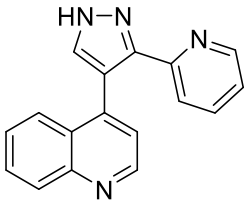


**Figure 2.7.** Lilly's TGF-β inhibitor high-throughput screen hit.

In 2007 during the continued SAR of the dihydropyrrolopyrazole series of TGFBR inhibitors, Eli Lilly & Company developed the orally bioavailable analogue **2-5**. [38]

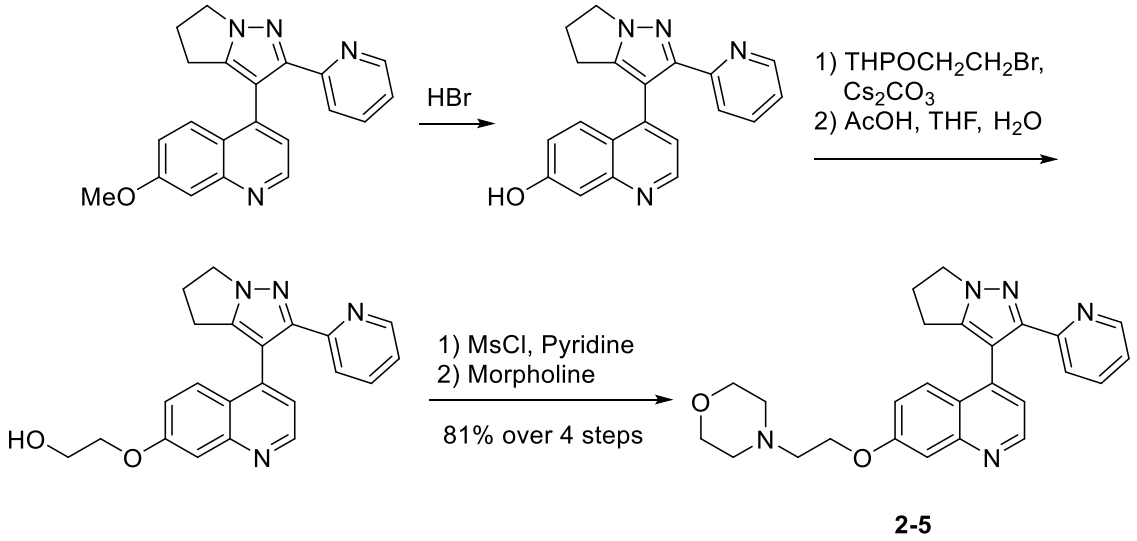


**Figure 2.8.** Synthesis of **2-5**.

Subsequent development of the aforementioned series, Eli Lilly & Company currently have **2-6** (LY2157299, also known publicly as Galunisertib) in clinical trials for various cancers such as glioblastoma, hepatocellular carcinoma, and pancreatic cancer.[39]

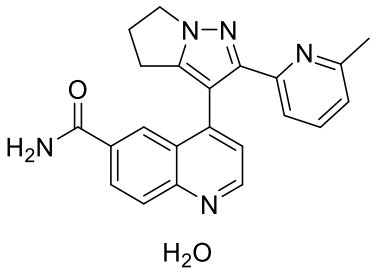


**Figure 2.9.** Structure of LY2157299 (Galunisertib).

One of the concerns with inhibiting the TGF-β pathway is that it plays a role in repairing damaged heart tissues. Inhibition of the pathway could potentially result in some severe and life threatening side effects for the patient.[40] This concern is not without precedent as damaged heart valves attributed to inhibition of the TGF- β pathway was what stopped GlaxoSmithKline's development of their ALK5 inhibitor program.[41]

With this in mind, Eli Lilly & Company went on to develop a dosing regimen with their inhibitor **2-6.**[42] The 28-day regimen consisted of 14 twice-daily doses, followed by 14 days without receiving any TGF-β inhibitor. This regimen was used in human clinical trials with the patients being closely monitored for heart damage by various techniques including 2D echocardiography and blood biomarkers. Upon testing inhibitor **2-6**, they noticed damage to the heart valves in a human clinincal trial in only one patient out of seventy nine. No other major medically relevant toxicity was developed by the patients, and this supported the use of **2-6** in further clinical trials. [43]

## 2.5 References


[1] L. Aloe, *Trends Cell Biol.* **2004**, *14*, 395–399.

[2] J. E. de Larco, G. J. Todaro, *Proc. Natl. Acad. Sci. U. S. A.* **1978**, *75*, 4001–5.

[3] A. B. Roberts, L. C. Lamb, D. L. Newton, M. B. Sporn, J. E. De Larco, G. J. Todaro, *Proc. Natl. Acad. Sci. U. S. A.* **1980**, *77*, 3494–8.

[4] M. B. Sporn, G. J. Todaro, *N. Engl. J. Med.* **1980**, *303*, 878–80.

[5] A. B. Roberts, M. A. Anzano, L. C. Lamb, J. M. Smith, M. B. Sporn, *Proc. Natl. Acad. Sci. U. S. A.* **1981**, *78*, 5339–43.

[6] M. a Anzano, A. B. Roberts, C. a Meyers, A. Komoriya, L. C. Lamb, J. M. Smith, M. B. Sporn, *Cancer Res.* **1982**, *42*, 4776–8.

[7] A. B. Roberts, C. A. Frolik, M. A. Anzano, M. B. Sporn, *Fed. Proc.* **1983**, *42*, 2621–6.

[8] R. K. Assoian, A. Komoriya, C. A. Meyers, D. M. Miller, M. B. Sporn, *J. Biol. Chem.* **1983**, *258*, 7155–60.

[9] R. Tucker, G. Shipley, H. Moses, R. Holley, *Science (80-. ).* **1984**, *226*, 705–707.

[10] A. Weiss, L. Attisano, *Wiley Interdiscip. Rev. Dev. Biol.* **2013**, *2*, 47–63.

[11] L. Kubiczkova, L. Sedlarikova, R. Hajek, S. Sevcikova, *J. Transl. Med.* **2012**, *10*, 183.

[12] J. L. Andres, *J. Cell Biol.* **1989**, *109*, 3137–3145.

[13] J. Massagué, *Cell* **1992**, *69*, 1067–70.

[14] K. Miyazono, *Cytokine Growth Factor Rev.* **2000**, *11*, 15–22.

[15] Y. Shi, J. Massagué, *Cell* **2003**, *113*, 685–700.

[16] K. Y. Lee, S. Bae, *J. Biochem. Mol. Biol.* **2002**, *35*, 47–53.

[17] M. M. Shull, I. Ormsby, A. B. Kier, S. Pawlowski, R. J. Diebold, M. Yin, R. Allen, C. Sidman, G. Proetzel, D. Calvin, *Nature* **1992**, *359*, 693–9.

[18] X. Yang, J. J. Letterio, R. J. Lechleider, L. Chen, R. Hayman, H. Gu, a B. Roberts, C. Deng, *EMBO J.* **1999**, *18*, 1280–91.

[19] E. M. Gallo, D. C. Loch, J. P. Habashi, J. F. Calderon, Y. Chen, D. Bedja, C. van Erp, E. E. Gerber, S. J. Parker, K. Sauls, et al., *J. Clin. Invest.* **2014**, *124*, 448–60.

[20] P. Matt, F. Schoenhoff, J. Habashi, T. Holm, C. Van Erp, D. Loch, O. D. Carlson, B. F. Griswold, Q. Fu, J. De Backer, et al., *Circulation* **2009**, *120*, 526–32.

[21] S. Dooley, P. ten Dijke, *Cell Tissue Res.* **2012**, *347*, 245–256.

[22] Y. Chen, E. Mironova, L. L. Whitaker, L. Edwards, H. J. Yost, A. F. Ramsdell, *Dev. Biol.* **2004**, *268*, 280–294.

[23] S. Chen, B. Jim, F. N. Ziyadeh, *Semin. Nephrol.* **2003**, *23*, 532–543.

[24] K. a Harradine, R. J. Akhurst, *Ann. Med.* **2006**, *38*, 403–14.

[25] J. Massagué, S. W. Blain, R. S. Lo, *Cell* **2000**, *103*, 295–309.

[26] R. L. Siegel, K. D. Miller, A. Jemal, *CA. Cancer J. Clin.* **2016**, *66*, 7–30.

[27] J. Massagué, *Cell* **2008**, *134*, 215–30.

[28] G. C. Blobe, W. P. Schiemann, H. F. Lodish, *N. Engl. J. Med.* **2000**, *342*, 1350–1358.

[29] D. Padua, J. Massagué, *Cell Res.* **2009**, *19*, 89–102.

[30] U. Bogdahn, P. Hau, G. Stockhammer, N. K. Venkataramana, A. K. Mahapatra, A. Suri, A. Balasubramaniam, S. Nair, V. Oliushine, V. Parfenov, et al., *Neuro. Oncol.* **2011**, *13*, 132–142.

[31] J.-S. Nam, M. Terabe, M. Mamura, M.-J. Kang, H. Chae, C. Stuelten, E. Kohn, B. Tang, H. Sabzevari, M. R. Anver, et al., *Cancer Res.* **2008**, *68*, 3835–43.

[32] N. Hermida, B. López, A. González, J. Dotor, J. J. Lasarte, P. Sarobe, F. Borrás-Cuesta, J. Díez, *Cardiovasc. Res.* **2009**, *81*, 601–9.

[33] M. Huse, Y. G. Chen, J. Massagué, J. Kuriyan, *Cell* **1999**, *96*, 425–36.

[34] F. Gellibert, J. Woolven, M.-H. Fouchet, N. Mathews, H. Goodland, V. Lovegrove, A. Laroze, V.-L. Nguyen, S. Sautet, R. Wang, et al., *J. Med. Chem.* **2004**, *47*, 4494–506.

[35] J. C. Lee, S. Kassis, S. Kumar, A. Badger, J. L. Adams, *Pharmacol. Ther.* **1999**, *82*, 389–97.

[36] F. L. de Oliveira, T. C. Araújo-Jorge, E. M. de Souza, G. M. de Oliveira, W. M. Degrave, J.-J. Feige, S. Bailly, M. C. Waghabi, *PLoS Negl. Trop. Dis.* **2012**, *6*, e1696.

[37] J. S. Sawyer, B. D. Anderson, D. W. Beight, R. M. Campbell, M. L. Jones, D. K. Herron, J. W. Lampe, J. R. McCowan, W. T. McMillen, N. Mort, et al., *J. Med. Chem.* **2003**, *46*, 3953–3956.

[38] H.-Y. Li, W. T. McMillen, C. R. Heap, D. J. McCann, L. Yan, R. M. Campbell, S. R. Mundla, C.-H. R. King, E. a Dierks, B. D. Anderson, et al., *J. Med. Chem.* **2008**, *51*, 2302–6.

[39] 'Lilly Oncology Pipeline', can be found under http://www.lillyoncologypipeline.com/tgfbr1-kinase-inhibitor.aspx, **2016**.

[40] M. Dobaczewski, W. Chen, N. G. Frangogiannis, *J. Mol. Cell. Cardiol.* **2011**, *51*, 600–6.

[41] S. Robinson, R. Pool, R. Giffin, *Qualifying Biomarkers*, **2008**.

[42] I. Gueorguieva, A. L. Cleverly, A. Stauber, N. Sada Pillay, J. A. Rodon, C. P. Miles, J. M. Yingling, M. M. Lahn, *Br. J. Clin. Pharmacol.* **2014**, *77*, 796–807.

[43] R. J. Kovacs, G. Maldonado, A. Azaro, M. S. Fernández, F. L. Romero, J. M. Sepulveda-Sánchez, M. Corretti, M. Carducci, M. Dolan, I. Gueorguieva, et al., *Cardiovasc. Toxicol.* **2015**, *15*, 309–23.

# Chapter 3

# Synthesis of TGF-β inhibitors

# 3. Synthesis of TGF-β inhibitors

## 3.1 Synthesis of Galunisertib (LY2157299)

The transforming growth factor beta receptor 1 (TGFBR I) specific inhibitor LY2157299 (**3-1**), also known by its non-proprietary name Galunisertib, was needed by the group of Dr. Eduard Batlle in their ongoing investigation in understanding the roles of transforming growth factor beta (TGF-β) in colorectal cancer progression. We synthesisized LY2157299 in a multigram scale following the synthesis developed by Eli Lilly & Company, abeit with small modifications. This is outlined in Scheme 3.1. [1]

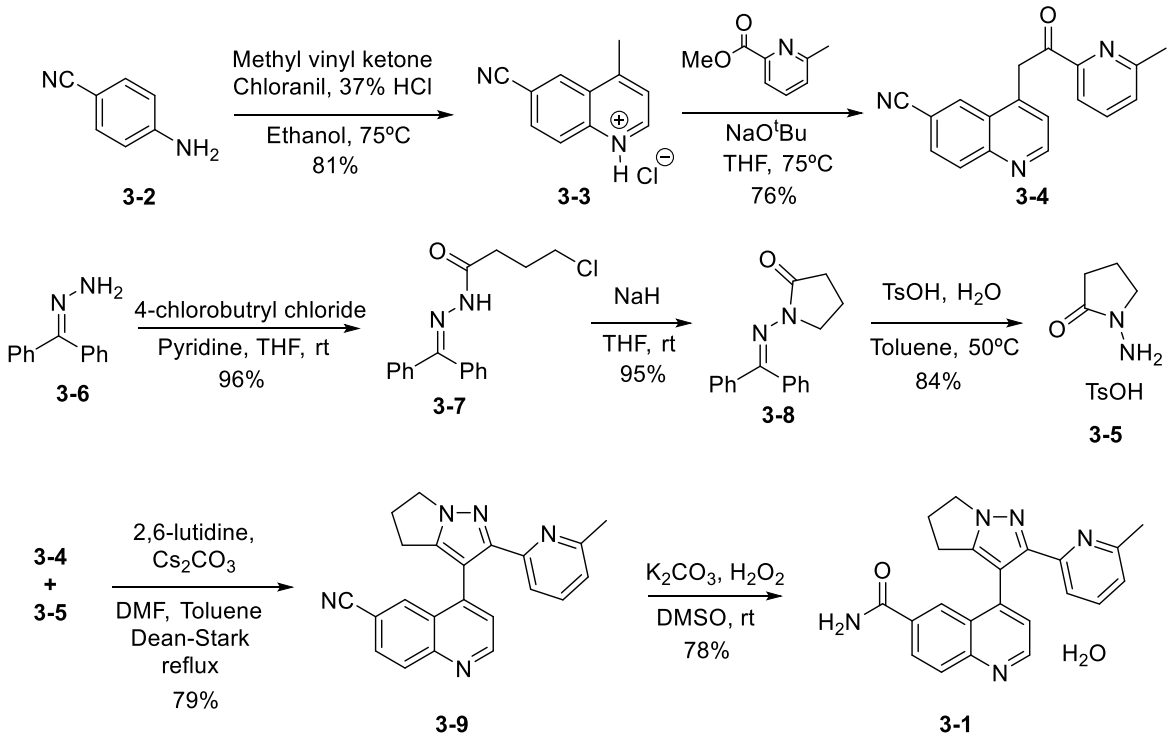


**Scheme 3.1.** Synthesis of LY2157299 (**3-1**).

The first step of the synthesis is the Doebner-Miller reaction between the 4-aminobenzonitrile **3-2** and methyl vinyl ketone, giving quinoline **3-3** as the hydrochloride salt. This reaction was performed several times, the largest being on a 300 g scale affording the product as a light brown solid in 81% yield.

A reasonable mechanism for this reaction is shown in Scheme 3.2. The aza-Michael addition of aniline **3-2** to the methyl vinyl ketone affords the enolate intermediate **3-2.1**. A proton is then transferred from the protonated amine to the enolate yielding intermediate **3-2.2**, which in turn is

attacked by the aromatic ring giving the Wheland intermediate **3-2.3** which rearomatizes to alcohol **3-2.4**. Then, the alcohol is dehydrated to give intermediate **3-2.5**. The dihydroquinoline **3-2.5** can be easily transformed into **3-2.6** via oxidation with chloranil (tetrachloro-1,4-benzoquinone). Quinoline **3-2.6** was separated from the reaction mixture as the HCl salt (**3-3**) via the addition of THF, thus making the mixture more apolar - precipitating the salt while keeping any remaining chloranil and its reduced form in solution.

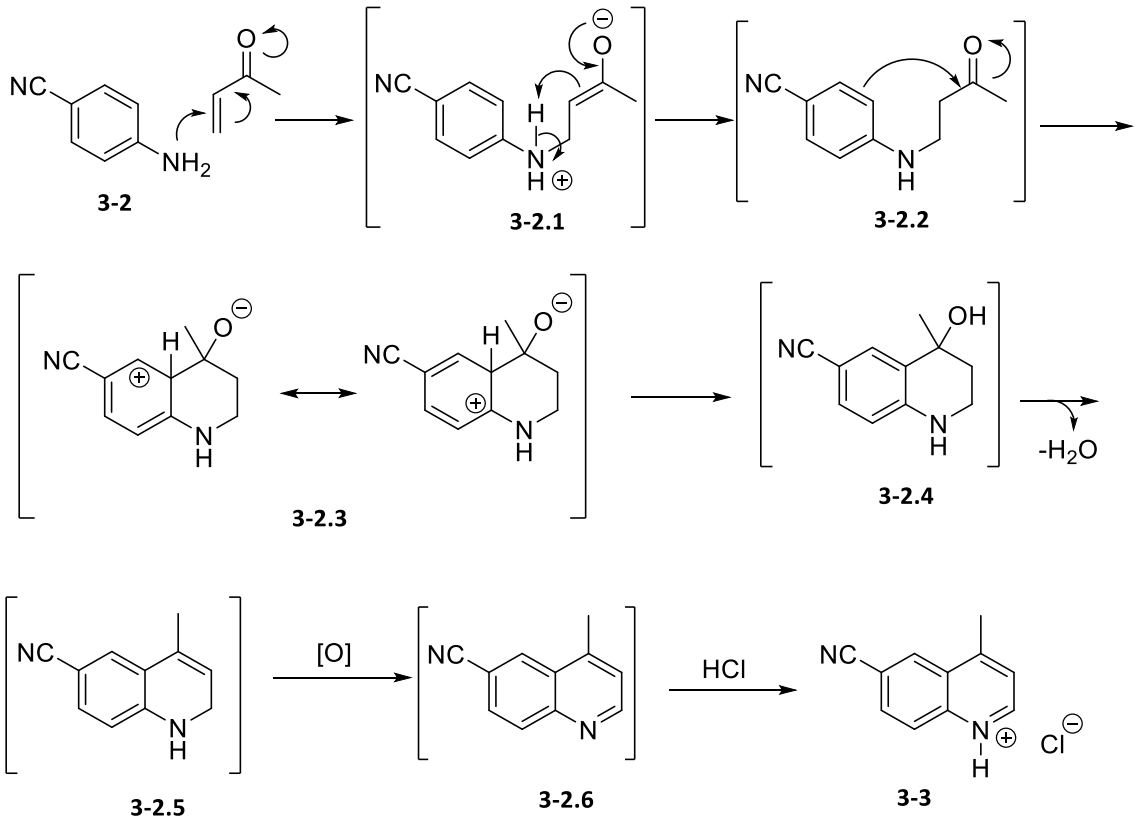


**Scheme 3.2.** Postulated mechanism of the Doebner-Miller reaction.

The second step of the synthesis was the acylation of quinolone **3-3** with methyl 6-methylpicolinate. Deprotonation of the methyl group of **3-3** was facilitated by the fact that the cyano-group on the quinoline ring withdraws electron density, thus increasing the acidity of the methyl group. The anion then could attack the ester of the methyl 6-methylpicolinate, and afforded compound **3-4**. A further equivalent of base was required as the $CH_2$ of the product of the reaction (**3-4**) is even more acidic than the $CH_3$ of the starting material. The extra equivalent of base forms enolate (**3-3.2**) which, interestingly, also acts as protection group for the product (**3-4**), stopping a possible nucleophilic attack at the newly formed carbonyl group. Working on a ca. 200 g scale,

compound **3-4** could be obtained in 76% yield as a brown solid following crystallisation from methanol.

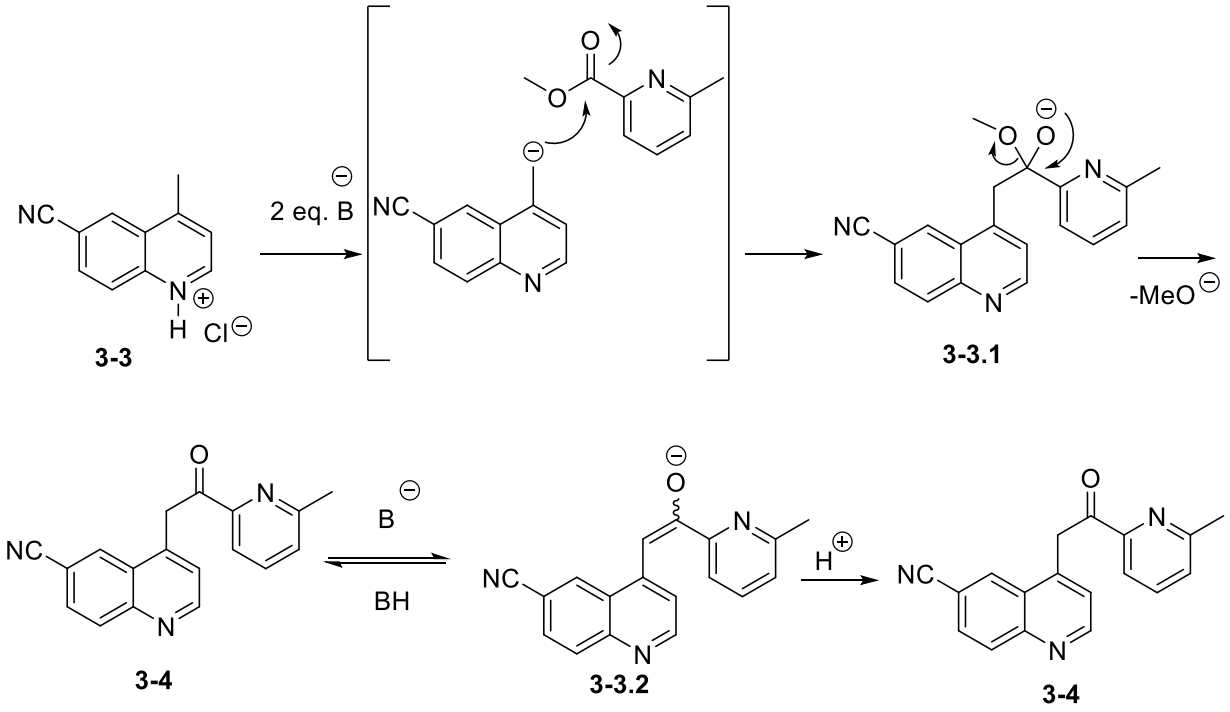


**Scheme 3.3.** Mechanism of the transformation of **3-3** to **3-4**. A base is depicted as 'B'.

As shown in Scheme 3.1, the 1-aminopyrrolidin-2-one (**3-5**) necessary for the next step was synthesised as its tosylate salt. Using methodology described by Taylor *et al.* benzophenone hydrazone **3-6** was reacted with 4-chlorobutryl chloride to give **3-7**, which following cyclisation with NaH, gave protected hydrazone **3-8** in a near quantitative yield.[2] Acidic hydrolysis of hydrazone **3-8** liberated the target compound **3-5** as its tosylate salt in 84% yield.[1] In this way, ca. 80 g of reagent per batch could be obtained with relative ease.

Ketone **3-4** and tosylate salt **3-5** were then combined and treated with 2,6-lutidine and $Cs_2CO_3$ under Dean-Stark conditions to afford compound **3-9** in 79% yield. The mechanism of this reaction involved the dehydration of **3-4**, forming the hydrazone intermediate **3-4.1** as shown in Scheme 3.4. This intermediate could be deprotonated *in situ* using $Cs_2CO_3$ forming the anion **3-4.2** which then attacks the carbonyl and cyclises to give **3-4.3**. Final dehydration under Dean-Stark conditions afforded **3-9** as a brown solid.

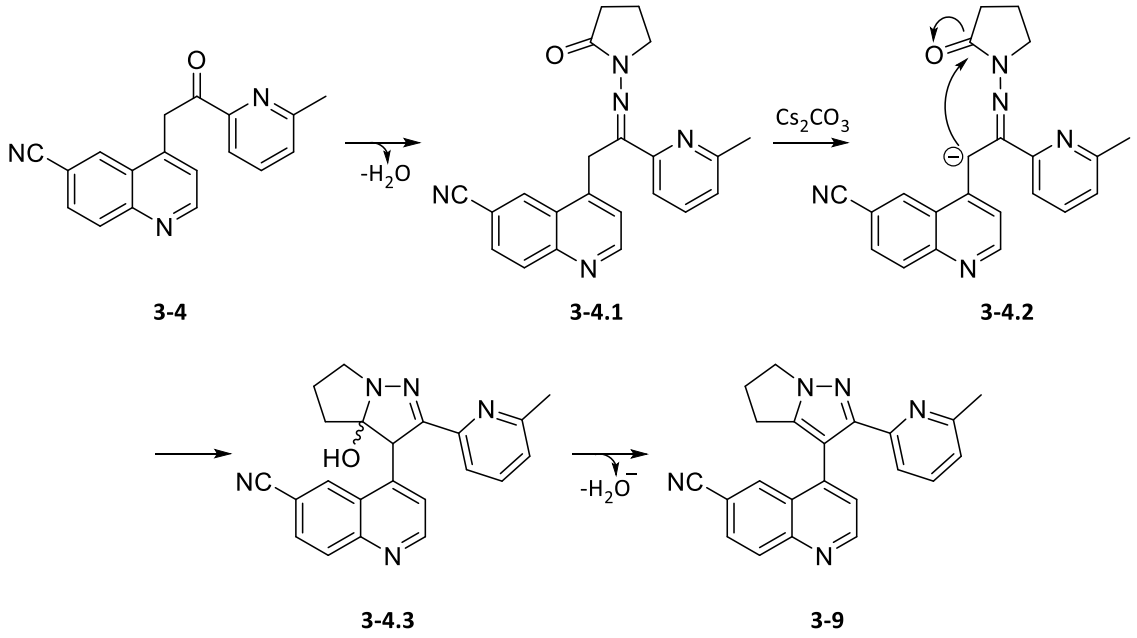


**Scheme 3.4.** Proposed mechanism for the synthesis of **3-9** from ketone **3-4**.

One noteworthy change we made to the synthesis was that we changed the base from $K_2CO_3$, as described by Eli Lilly & Co. in their patent, to $Cs_2CO_3$.[3] During some of the preparations of **3-9** from **3-4**, it was observed that the reaction ceased to progress from intermediate **3-4.1** to **3-9** after a certain point when followed by both TLC and $^1H$ NMR. Addition of more $K_2CO_3$ did not result in an increase in the conversion of **3-4.1** to **3-9** by NMR. We also investigated the addition of more DMF on the assumption that there was not enough $K_2CO_3$ in solution. This also did not influence the conversion by proton NMR.

$Cs_2CO_3$ was chosen as we thought it could perhaps solve problem should the problem be solubility of the $K_2CO_3$ in the organic solvents, as $Cs_2CO_3$ is more soluble in organic solvents than $K_2CO_3$. Also if the problem was concerned with the strength of base, cesium carbonate is a slightly stronger base and also displays the 'cesium effect'.[4] Thankfully this change to the procedure was sufficient for us never to see the reaction stop after partial conversion of **3-4.1** to **3-9**, therefore greatly improving the reproducibility of the reaction.

The last step of the synthesis was the transformation from **3-9** to **3-1.** This was achieved via base-catalysed hydrolysis of the nitrile with hydrogen peroxide. Following crystallisation from acetone-water, monohydrate **3-1** was afforded with 78% yield.

Up to a 5 g scale following the aforementioned protocol, the final product could be used 'as is' *in vivo*. However, when scaling up to tens and hundreds of grams, the crystallisation occurred at a slower rate which in turn gave larger crystals of monohydrate **3-1**. In theory this was good in terms of a purification method as a slower cooling should give rise to larger crystals, which in turn should be purer. However, these larger crystals proved to cause difficulties with regards to solubility when preparing the *in vivo* formulation. In order to make an amorphous compound which should overcome the solubility issues we were facing with the crystals, we considered ways employed in the pharmaceutical industry to change the solid form of an active pharmaceutical ingredient (API).

Techniques commonly employed to form an amorphous compound include; mechanical grinding, supercritical fluids, spray-drying, and order of addition of the anti-solvent amongst others.[5] This is summarised below in Figure 3.1.

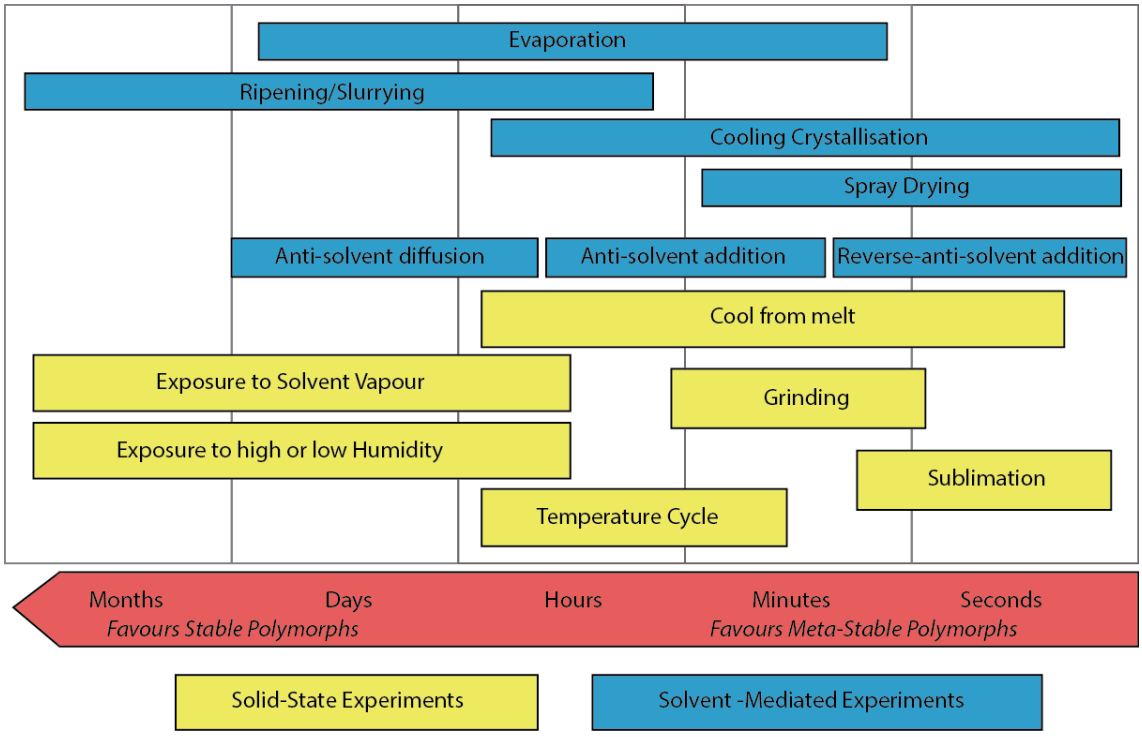


**Figure 3.1.** Methodologies Employed to Form Different Polymorphs and their stabilities. Adapted from Llinàs *et. al.*[6]

Firstly, we analysed our product (with the larger crystals) using X-Ray powder diffraction (XRPD) as shown in Figure 3.2. The measurement was performed at Enantia S.L by Joan Farran using their in-house diffractometer.

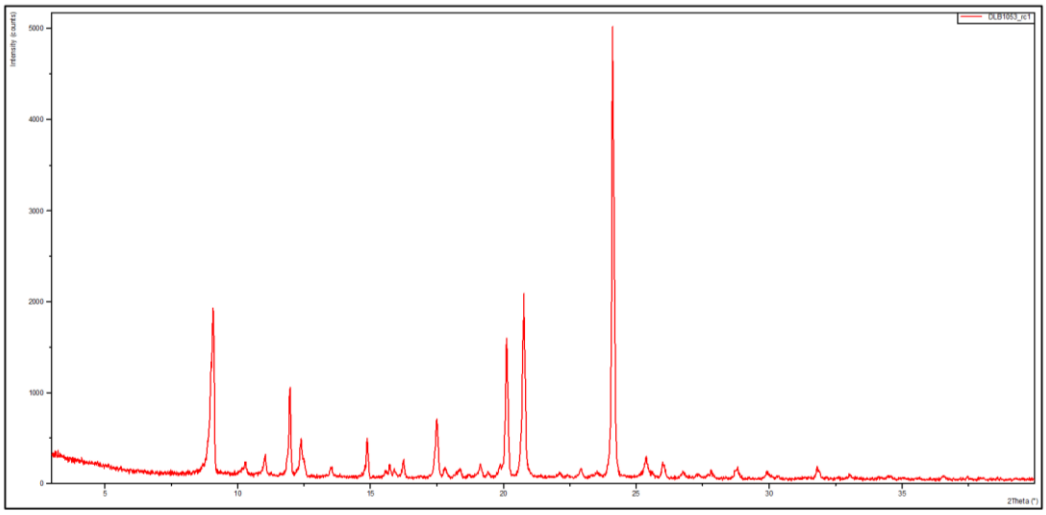

**Figure 3.2.** Powder X-ray diffraction of **3-1.**

We tried to obtain an amorphous solid by several procedures, including fast cooling and grinding the solid with a pestle and mortar. In the end, we opted for the reverse-anti-solvent addition method due to it being a more scalable process, and it also gave a solid with the desired properties.

After optimisation following various solubility tests, the monohydrate **3-1** was dissolved in the minimum amount of 6:4 ethanol:acetonitrile at reflux. This mixture was then added quickly with vigorous stirring to an ice-cold ice/water mixture, rapidly forming a white precipitate. Although a fine powder was obtained, X-ray powder diffraction (Figure 3.3 below) did not show a marked improvement in amorphicity; however, the dramatically reduced the particle size strongly facilitated making the *in vivo* formulation of monohydrate **3-1**.

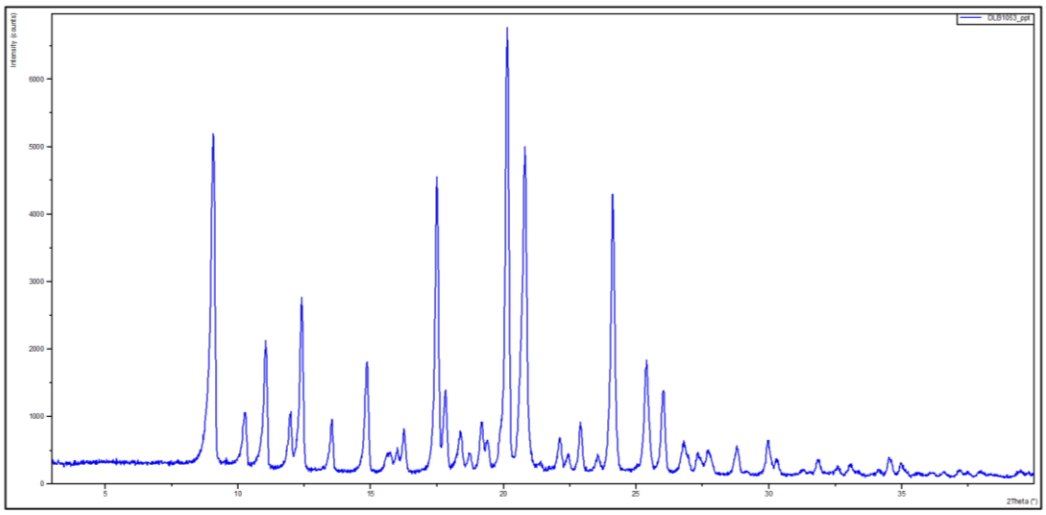

**Figure 3.3.** Powder X-ray diffraction of **3-1** after a fast precipitation in water.

This specific solid form of **3-1** was used by the Batlle lab both *in vitro* and *in vivo* in various batches ranging from 5 g to 100 g + were used over a four-year period. Differences in relative intensities of the peaks were attributed to preferential orientation of the crystals, and not that of a different polymorphic form being present.

## 3.2 Biological results of the use of Galunisertib (LY2157299, 3-1)

Eduard Batlle's group, using the TFG-β inhibitor **3-1** with which we provided them with, investigated the effects that TGF-β has on colorectal cancer, specifically the role it plays in disease progression and metastasis.

### 3.2.1 Dependency of Colorectal Cancer on a TGF-β-Driven Program in Stromal Cells for Metastasis Initiation (Cancer Cell, 2012)

Eduard Batlle's group, using the TFG-β inhibitor **3-1** with which we provided them with, investigated the effects that TGF-β has on colorectal cancer, specifically the role it plays in disease progression and metastasis.

Colorectal cancers (CRCs) originate in the intestinal epithelium as premalignant regions known as adenomas due to mutations in the WNT pathway (for example APC) . As time progresses, a proportion of these adenomas gain additional genetic mutations (for example KRAS, SMAD4) and gradually progress into malignant tumours. Clinically, the standard of care for CRCs is usually surgery to remove the primary tumour(s), however depending on the stage and aggressiveness of the CRC, patients relapse and form metastatic tumours, often in liver or lungs.[7] Mutational inactivation of the TGF-β pathway starts at the adenoma stage and affect 40%-50% of all CRCs. Although these transformed cells do not respond to the ligand, they themselves increase their production of TGF-β. We then investigated why CRCs would overexpress a protein to which they were unresponsive.

A case study of a cohort of 345 patients who had been treated in three separate hospitals where the information was publicly available was then analysed. Patients classified by the American Joint Cancer Committee (AJCC) staging standard (see paragraph 3.2.2 for more details) as being in stage I (which has a very good prognosis) were found to have low levels of TGF-β, whereas already metastatic patients (stage IV) had higher levels. As this staging system is not a robust method to predict the likelihood of relapse on an individual basis, the Batlle group asked if levels of TGF-β in the tumour could be a more reliable indicator of the probability of CRC relapse.

Patients were separated into different categories depending on the level of TGF-β expression in the tumour cells; high, medium or low. During 10 years of follow-up, patients' time to reoccurrence was compared to the level of TGF-β present in the CRC. It was found that low levels of TGF-β was an indication of high probability of a patient remaining disease free, however this probability dropped if the TGF-β levels in primary tumour samples was higher, as shown in Figure 3.4.

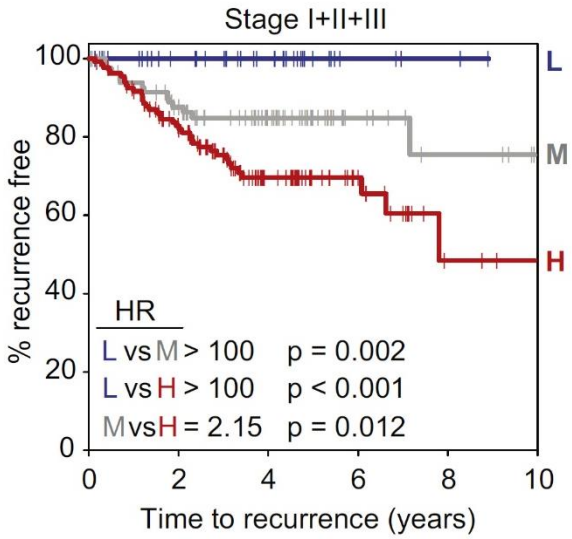


**Figure 3.4.** levels of TGF-β vs time to recurrence (L – Low; M – Medium; H – High).

Seeing that TGF-β levels in CRCs are a robust predictor of disease relapse, the Batlle group went on to investigate if TGF-β plays a role in tumour initiation. CRC cell lines which were unresponsive to TGF-β were genetically modified to secrete TGF-β1, and then implanted into immunocompromised mice. With respect to the control cells, the cells secreting TGF-β could form a colony at a dramatically increased rate with respect to the control cells not secreting TGF-β (Figure 3.5).

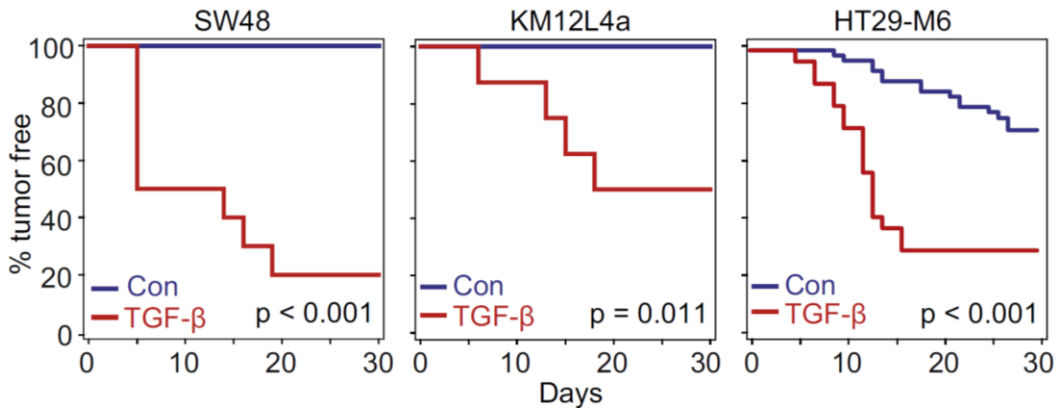


**Figure 3.5**. Tumour progression with cells excreting TGF-β (red) vs the corresponding control (blue).

In a more elaborate experiment, KM12L4a cells (Con or TGF-β) were implanted at the primary site of mice, to then measure the effect of TGF-β secretion on both tumour growth and spreading to the liver. In the case of both the control and the TGF-β secreting variant, the implanted cells could form aggressive colon tumours with no significant difference between one another. Interestingly however, two thirds of the mice implanted with the control cells were free of metastatic tumours. On the other hand, ten out of eleven of the mice implanted with the cells secreting TGF-β were found to have metastasis in the liver and/or the lung.

One explanation for the paradox that a protein to which the cancer cells are blind can help tumour formation and metastasis, is that the protein has an effect on the non-tumour cells in the environment, or stroma. Supporting this possibility, tumoral stroma cells were observed to be positive for a staining for phosphorylated SMAD2, a sign of activation of the TGF-β pathway (Figure 3.6, left).

This led the Batlle group to see if inhibition of TGF-β signalling in the stroma could stop the formation of metastatic tumours *in vivo*. Colon Cancer Stem Cells (CoCSCs) were isolated from the primary tumour of a patient with stage IV CRC. They were shown to be unresponsive to TGF-β as they contained mutations in the TGFBR2, and did not change their growth or behaviour when treated with TGF-β or with a TGF-β inhibitor. Furthermore, when these cells were injected into immunodeficient mice the tumour islands themselves were negative for pSMAD2, unlike the stroma (Figure 3.6, left). (see Chapter 2 Figure 2.3 for the TGF-Beta pathway involving pSMADs). When the mice were treated with the TGFBR I inhibitor Galunisertib (**3-1**), TGF-β signalling (visualized by pSMAD2 staining) was no longert observed in stromal tissues (Figure 3.6, right),

indicating the the inhibitor works in vivo and acts on the stroma.when the mice were treated with the TGFBR I inhibitor Galunisertib (**3-1**).

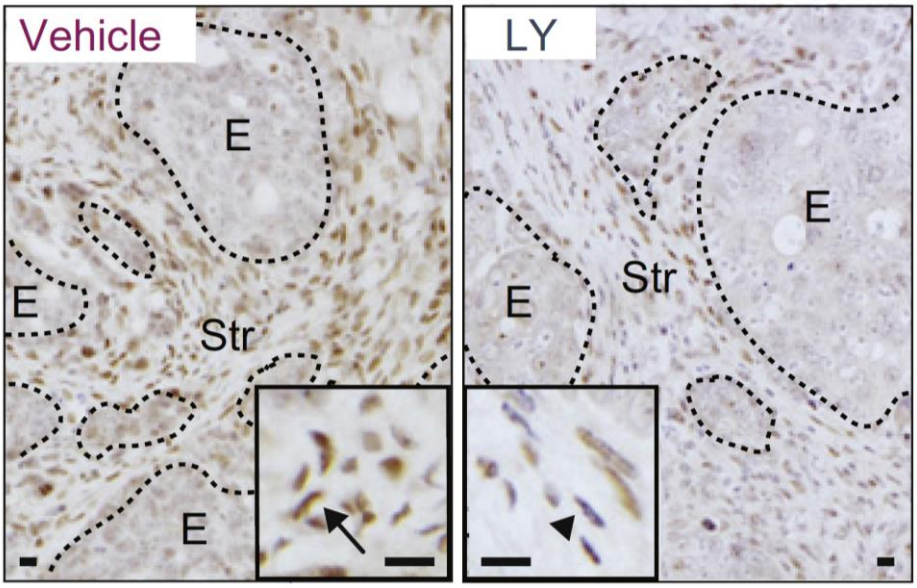


**Figure 3.6.** Sections of fixed tumour material, stained with antibodies for phosphorylated pSMAD2 stain. Treatment with **3-1** is indicated with 'LY'.

Importantly, mice treated with **3-1** were more resistant to formation of tumours when CoCSCs were injected subcutaneously (Figure 3.7) and had reduced amounts of liver metastasis when the CoCSCs were inoculated via the spleen.

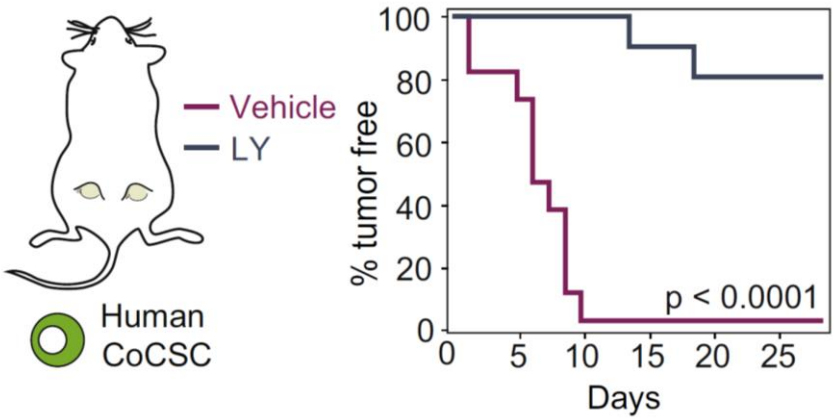


**Figure 3.7.** Percentage of mice tumour free both with (LY) and without (vehicle) treatment with **3-1** vs time.

Overall this indicates that inhibition of TGF-β in the tumour microenvironment prevents CRCs to form metastases. These results were published in Cancer Cell in 2012.[8]

It is worth noting that this paper has received already more than 400 citations (Google Scholar, July 2018).

### 3.2.2 Stromal gene expression defines poor-prognosis subtypes in colorectal cancer (Nature Genetics, 2015)

Patients who develop cancer (including CRC) typically have their tumours graded by the American Joint Committee on Cancer (AJCC) system. Staging from I to IV is given once an initially analysis has been performed on the tumour using the **TNM** classification of malignant tumours. This classifies tumours based upon 3 main factors. **T** describes the primary tumours size and whether or not it has invaded the nearby tissue. **N** describes the extent to which the cancer has extended to the lymph nodes, and finally **M** describes the distant metastasis. Dependant on the results from the TMN classification system, a patient is given the appropriate staging.

As staging describes tumour burden and the extent of spreading, it generally correlates with prognosis. For stages I and IV, this is very clear. Most patients who are classified as having an AJCC stage I tumours typically can have their tumour removed, and following appropriate treatment, have a very high probability of long-term disease-free survival. On the other hand, patients who are classified as having IV cancer, which is given when the tumour has spread to distant organs, have a dismally low disease-free survival rate. However, approximately 40 – 50% of CRC patients who are diagnosed with a stage II or stage III disease develop recurrent cancer during the course of their treatment, meaning that for stage II and stage III patients, the AJCC system is a poor predictor of the outcome of the disease: patients are frequently either under-treated or over-treated.

In an attempt to address these shortcomings, the field has been studying the expression patterns of genes associated with CRC relapse, with the purpose of identifying patient subtypes with differential prognosis. In 2012, the group of Eduard Batlle showed that high expression of (especially mesenchymal) TGF-beta target genes predict poor outcome.[8] Although other reports also pointed to these mesenchymal genes, it was not entirely clear whether those are genes

expressed in the mesenchymal compartment: the tumour stroma. In contrast, other labs proposed the idea that these poor prognosis genes may be expressed in cancer cells undergoing epithelial-to-mesenchymal transition (EMT). From this effort, groups had speculated that tumour aggressiveness could be related to the elevated expression of mesenchymal genes, and that these genes might be the result of an epithelial-to-mesenchymal transition (EMT), already associated to invasive behaviour in cancer.

However, in this paper the Batlle group showed that elevated expression of mesenchymal genes associated with poor prognosis in CRC samples is mainly contributed by tumour-associated stromal cells as opposed to the epithelial (or EMT-like) tumour cells. This was demonstrated by separating epithelial cells from the stromal cells, and profiling them separately. Figure 3.8 shows that genes that predict prognosis (Hazard ratio larger than 1) are expressed more strongly (represented on the y axis in normalized z-score) in stroma rather than epithelium, especially in tumour stroma.

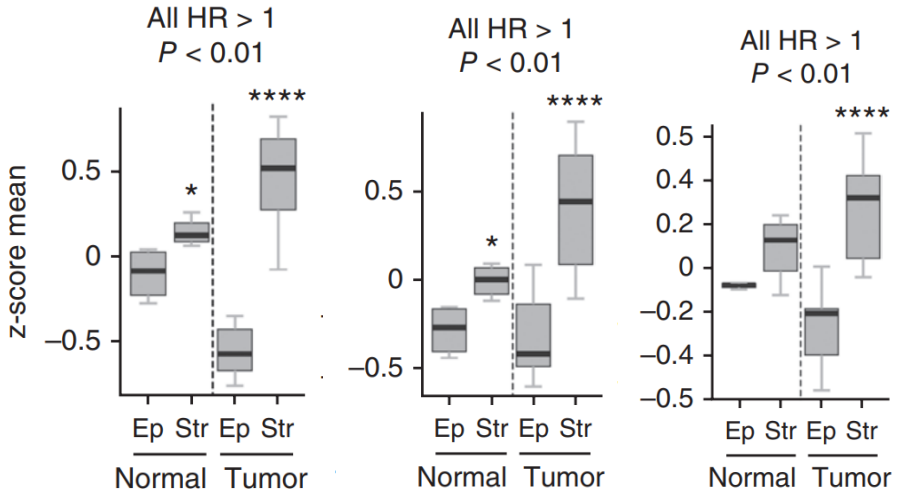


**Figure 3.8.** Mean expression (z score) of genes that predict relapse (gray) in the three studies in laser capture–microdissected (LCM) tumour epithelial (Ep) and stromal (Str) compartments or stroma and epithelial cells from normal colonic mucosa. *HR: hazard ratio; P: P-value.*

When looking specifically at TGF-β signalling in the CRC subtypes, they saw that this was one of the processes which was enriched in the subtype with worst prognosis.[9]

Analysis of TGF-β signalling in epithelial tumour cells was performed by taking primary CRC samples, and growing isolated epithelial cells as three-dimensional organoid cultures. This was needed as virtually all CRC lines available have lost their response to TGF-β due to inactivating mutations in components in the TGF-β pathway.

Patient-derived organoids (PDO) from four of the eight primary CRC tumours were responsive to TGF-β (PDO2, PDO3, PDO4 and PDO6), which resulted in a cytostasis upon treatment with TGF-β; these responsive organoids fail to grow. This response could be blocked when treating the cultures with **3-1** (named 'LY' in the Figure 3.9)

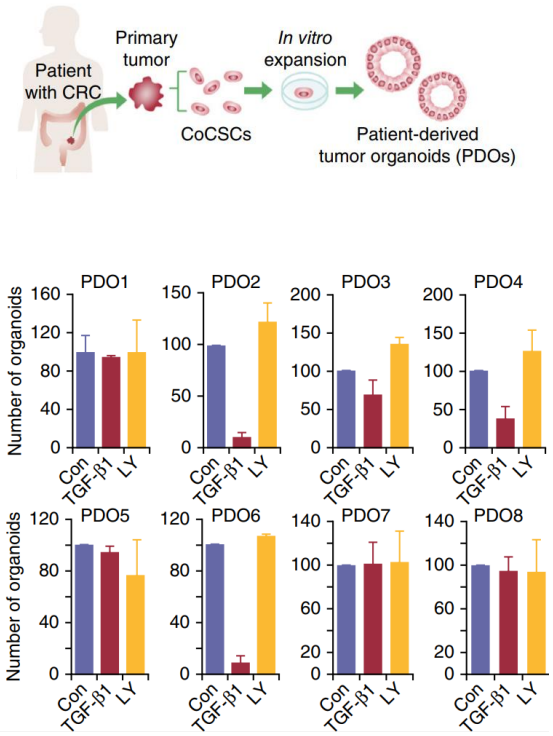


**Figure 3.9.** Tumour organoid formation capacity in the presence or absence of recombinant TGF-β1 protein (5 ng/ml) or LY2157299 TGF-βRI inhibitor (LY; 1 μM).

The remaining PDOs were completely insensitive to TGF-β. When these PDOs were interrogated for metastasis forming capacity, two of the TGF-β -unresponsive organoids, namely PDO1 and PDO7, were able to form metastatic tumours in mice. This was achieved by injecting the cells via the spleen of immunodeficient mice. Both of these PDOs express high levels of TGF-β. When parallel experiments were ran by injecting the same two organoids, however this time treating the mice with **3-1**, significantly fewer metastasis were formed during the experiment.

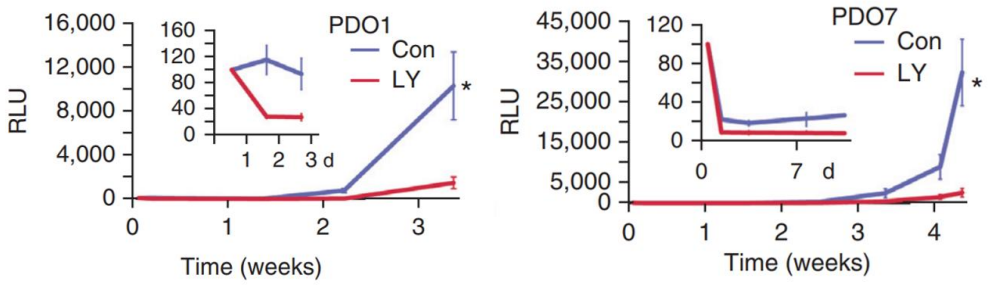


**Figure 3.10.** Normalized bioluminescence (RLU) over time from mice with intrasplenic inoculation with cells from PDO1 or PDO7 and treated with **3-1** (LY; PDO1, n = 5 mice; PDO7, n = 6 mice) or with vehicle (Con; PDO1, n = 5 mice; PDO7, n = 6 mice).

As the organoids themselves are not responsive to the effects of TGF-β (Figure 3.9), it was concluded that this reduced metastatic capacity caused by treatment with **3-1** can only be attributed to the inhibition of TGF-β signalling in the tumour microenvironment. The observation that **3-1** did not boost xenograft growth even in TGF-β–responsive tumour organoids indicates that the use of this inhibitor may be safe for a wide range of patients with CRC.

In conclusion: mesenchymal gene expression, especially TGF-β target genes expressed by stromal cells, defines the recently described poor prognosis CRC subtypes. Functionally, TGF-β expression in stromal cells promotes liver metastasis and may be therapeutically targeted by treatment with compounds like **3-1**.

These results were published in Nature Genetics in 2015. [10]

As of July 2018, the publication has been cited more than 300 times (Google Scholar).

### 3.2.3 TGF-β drives immune evasion in genetically reconstituted colon cancer metastasis (Nature, 2018)

Building on work from the from the two previous publications on TGF-β in the journals Cancer Cell and Nature Genetics, the Batlle group wanted to further investigate the role that TGF-β plays in CRC, and also to further translate the inhibition of TGF-β for patients with advanced CRC to the clinic. This is of additional interest, as TGF-β has been described as an immune suppressor, so that its inhibition might reactivate the immune system to attack the cancer cells.

To study the role of TGF-β and the immune system in CRC metastasis, a human-like, sophisticated mouse model system was lacking; therefore, Tauriello *et al*. set out to generate one. Progression of colorectal cancer generally coincides with genetic alterations in four pathways, namely WNT, EGFR, p53 and TGFβ. In order to study the combination of these mutations—and potentially generate a model for aggressive CRC, the Batlle group create a small library of mouse models via a breading programme with mice bearing conditional alleles in homologues of four key mutations found in CRC: $Apc^{fl/fl}$, $Kras^{LSL\text{-}G12D}$, $Tgfbr2^{fl/fl}$ and $Trp53^{fl/fl}$ (designated A, K, T and P, respectively). These mutations can be triggered in intestinal stem cells by treating adult mice with tamoxifen, which activates the $CreER^{T2}$ gene recombination enzyme that is genetically fused to the Lgr5 intestinal stem cell gene (designated L). The eight mouse strains which were made are shown below in Figure 3.11.


**Figure 3.11**. Combination of alleles used to generate mouse model.

Ninety percent of mice which contained all mutations (LAKTP) displayed invasive carcinomas, more than fifty percent of which breached all intestinal layers. These tumours were pathologically comparable to human tumours, and approximately forty percent of these resulted in metastases either locally or to the liver and lung. Mice bearing three of the mutations (LAKT, LATP and LAKP), while developing similarly invasive cancers, did not present with metastases. Mice with fewer mutations developed much less aggressive tumours. As measured by phospho-SMAD staining, tumours in compound-mutant (LAKTP) mice displayed high TGF-β activity in the tumour stroma, very similar to what is observed in patients with poor-prognosis. Furthermore, advanced cancers in both mice and human contain a reduced number of patrolling T lymphocytes, a sign that the immune system is less active—yet another parameter associated to poor prognosis. After taking the primary tumours from the mice, expanding them in three-dimensional culture and reinjecting the resulting mouse tumour organoids (MTO) into the caecum wall of mice, thirty-two percent of mice went on to develop AJCC T3-4 tumours, with forty percent of these successfully spreading to the liver, giving rise to a metastatic disease.

Treating mice with **3-1** eleven days after transplantation of LAKPT MTOs resulted in reduction of primary tumour size and a reduced extent of local cancer spreading (carcinomatosis), and moreover strongly blocked the appearance of distant (liver) metastases. Following immunohistology, a reduction in the number of pSMAD3 was observed – consistent with TGF-β inhibition. In experiments where MTOs were directly transplanted into the liver (to model metastatic initiation), treatment with **3-1** also resulted in drastically decreased metastatic burden, effectively curing a large population of the mice as can be seen below in Figure 3.12.

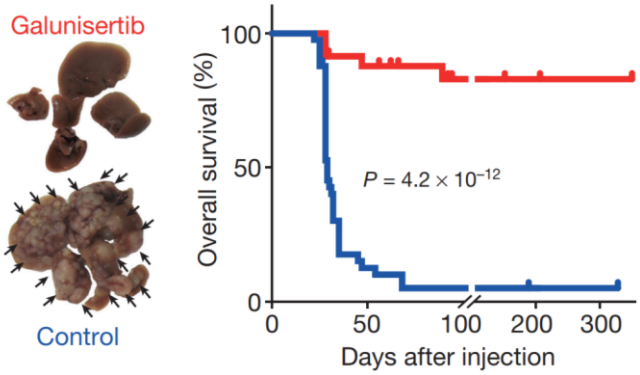


**Figure 3.12.** Survival vs time in mice with (red) and without (blue) treatment of **3-1**.

Flow-cytometry on livers which were colonised for 7-10 days by MTOs showed that there was increased recruitment of T lymphocytes following treatment with **3-1**, and that these immune cells were more active compared to control conditions. In addition, when these experiments were repeated in mice that miss this type of immune cells, the compound had no therapeutic effect. Tauriello *et al.* hypothesised that if a specific (adapted) immune response was responsible for tumour rejection, the mice may be immunized against these cancer cells.

To test this, mice which survived the initial exposure to MTOs and had treatment with **3-1,** were then rechallenged with the same MTOs: these reinjected tumour cells indeed failed to form tumours in mice previously cured of MTOs, but grew well in naïve mice. It is important to note that these mice did not receive any **3-1** during the rechallenge. They concluded that increased TGF-β levels in the tumour microenvironment limit adaptive immune responses by both limiting tumour infiltration (patrolling) and $T_H1$- effector type activation of T lymphocytes.

Finally, to assess the effectiveness of TGF-β inhibition in already formed metastases, **3-1** was given to mice on day fourteen after implantation, to better approach a potential clinical setting. This treating regime resulted in a reduction in tumour numbers, indicating some response. Interestingly, an increase in immune cells was indeed found in the area. However, treatment resulted in few complete remissions.

These **3-1** activated T-cells exhibited marked surface expression of programmed cell-death protein 1 (PD-1), and the authors found that the metastases progressively recruited PD-1 ligand 1 (PD1-L1) as they grew. The interaction between PD-1 and PD-L1 has been described as a potent immunosuppressive mechanism in cancer, and its inhibition using antibodies has been associated to strong responses in the clinic. However, it remains a challenge to predict when these treatments work, or if not: why they fail—as is the case for about 95% of patients with metastatic CRC.

Mirroring this failure in the clinic, treatment of the mice with PD-L1 checkpoint inhibitors did not have a significant effect on the tumours. However, combination therapy with **3-1** resulted in a pronounced immune response. This resulted in eradication of most metastases and prolonged progression-free survival for over a year after treatment was stopped: mice were cured of very aggressive, established liver metastases.

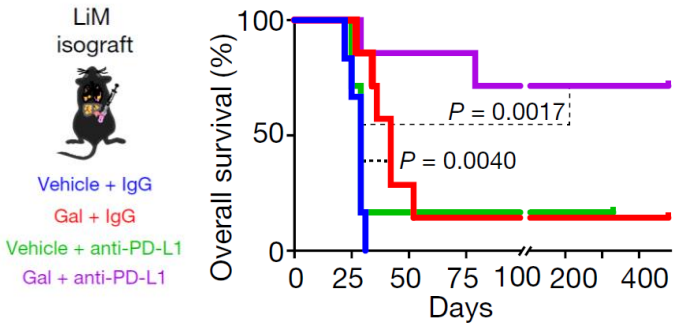


**Figure 3.13.** Treatment from day 14 of established liver metastases. (**3-1** = Gal)

Conclusion: Enabling immune infiltration and activation using TGF-β inhibitors is sufficient to confer susceptibility to anti-PD-1–PD-L1 checkpoint-based therapies, a strategy that may have broad applications for treatment of cancers that grow in a TGF-β -rich environment. These results strongly suggest that inhibition of TGF-β signalling could be promising as immunotherapy for patients with MSS, stroma-rich CRCs and a poor prognosis.

These results were published in Nature in 2018.[11]

## 3.3 Design and synthesis of a new TGF-β inhibitor

### 3.3.1 Design of compound 3-10 (HOLY)

During the use of **3-1** in Batlle's lab, it was noticed that some the positive controls were not positive in some of the experiments as they should have been. They hypothesised that both the dosing and the frequency of the **3-1** had to be increased as to make sure that TGF-β was being completely inhibited. Lahn *et al.* described how although the half-life in human is 8 hours, the half-life in different mammals varies. In particular, the half-life of LY2157299 was found to be only 20 minutes in mouse models – further increasing the complexity of studying TGF-β in mouse models.[12]

To look for a way to overcome these shortcomings of **3-1**, we sought to design a new TGF-β inhibitor which would be able to be administered easily, for example via an intraperitoneal (IP) injection, or also with the possibility of constant infusion using an osmotic pump.

The new molecule needed to have a 'handle' in which we could attach a wide variety of groups to, enabling us to tune both the PKPD properties and the physical properties. After derivatisation, the now prodrug would be metabolised releasing the active compound over a period. The handle could also be used to attach a chromophore, or even a photolabile fragment among other possibilities.

Prodrugs are drugs which have been modified from the parental compound to modulate properties such as solubility and (absorption, distribution, metabolism, excretion and toxicity (ADMET). Some of these properties can be modified also by other techniques, for example by solid form selection, as a certain polymorph could show a different solubility profile compared to another. Formulation is another way in which to overcome solubility and ADMET problems, however scientists are now turning to prodrugs as a way to improve the aforementioned drawbacks. Prodrugs are transformed into the API following cleavage of a carefully designed fragment attached to the API. This can be done by a variety of enzymes. This topic has recently been extensively reviewed by Rautio *et al.*[13]

In 2008, Li *et. al.* published a structure activity relationship (SAR) study on the quinoline domain of the dihydropyrrolopyrazole series of inhibitors as shown in the table below.[14]

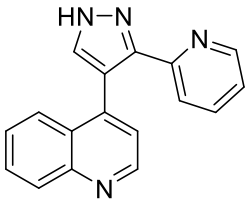

LY354947

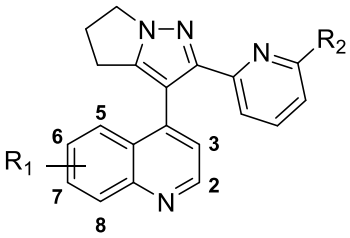

| Compounds | R1 | R2 | TGF-β R1 ic50 (μM) |
|---|---|---|---|
| **LY354947** | H | H | 0.059 ± 0.023 |
| **7b** | 2-Cl | H | 19.8 ± 0.2 |
| **7c** | 6,8-OMe | Me | 3.81 |
| **7d** | 8-F | Me | 0.928 ± 0.296 |
| **7e** | 6-Br | Me | 0.089 ± 0.022 |
| **7f** | 6-$OCF_3$ | Me | 0.141 ± 0.042 |
| **8** | 6-COOMe | Me | 0.526 |
| **9** | 6-$CONH(CH_2)N(CH_3)_3$ | Me | 0.193 |
| **10** | 2-OMe | H | >20 |
| **11** | 2-SEt | H | >20 |
| **12** | 2-$N(CH_2)_4$ | H | >20 |
| **13** | 7-OH | H | 0.16 |
| **14a** | 7-$O(CH_2)_3N(CH_2CH_2)_2NCH_3$ | H | 0.074 |
| **15** | 7-$O(CH_2)_2Cl$ | H | 0.044 |
| **15a** | 7-$O(CH_2)_2N(CH_3)_2$ | H | 0.024 ± 0.010 |
| **15b** | 7-$O(CH_2)_2N(CH_2CH_3)(CH_3)$ | H | 0.085 ± 0.041 |
| **15c** | 7-$O(CH_2)_2N(CH_2CH_2)_2NCH_3$ | H | 0.10 ± 0.071 |
| **15d** | 7-$O(CH_2)_2N(CH_2CH_2)_2O$ | H | 0.069 ± 0.031 |

**Table 3.1.** Kinase IC50 values of various inhibitors. Taken from Li *et. al.*[14]

From this study, what was apparent was that the substitution on the 2-position (highlighted in green) had a negative impact on the $IC_{50}$ value when changed for anything but a hydrogen atom. Derivatisation at the 7-position (highlighted in blue) produced some potent inhibitors. Entry 13 was of particularly interest as it would give a handle (7-OH) from which we could derivatise. However the 7-OH compound was clearly less potent ($IC_{50}$, 160 nM) than compound **3-1** (51 nM).[15]

On the other hand, modification at the 6-position (highlighted in yellow) appeared to be a promising starting point. Entry 7e (6-Br) particularly stood out as its $IC_{50}$ was nearly half that of entry 13, and although itself would not provide us with a handle for further modification, it is a bioisostere of the 6-hydroxy variant which, interestingly, had not been explored.[16] A direct comparison between entries 7e and 13, however, could not be made as they differ in their $R_2$ substituents.

Therefore, based on the above considerations we decided to synthesize previously unknown compound with a hydroxyl group at the 6-position that we called HOLY (**3-10**).

### 3.3.2 Retrosynthetic analysis of HOLY (3-10)

Following a synthetic scheme like that used in the synthesis of **3-1**, compound **3-10** had to be synthetized from a *p*-aniline with a masked or protected phenol in para-position. To this end we can consider the following options:

a) *p*-Methoxyaniline. The methoxy group would be hydrolysed at the end of the synthesis.
b) *p*-Nitroaniline. The nitro group would be reduced to the amine. Then the amine, via diazonium salt would be transformed into the phenol at the end of the synthesis.
c) *p*-Cyanoaniline. This approach would take advantage of the already developed synthesis of **3-1**. Then the amide would be transformed into the amine via Curtius or Hoffman rearrangement. The final steps of the synthesis would be the same of approach b): conversion of the amine into a phenol via diazonium salt.
d) *p*-Fluoroaniline. The last step would be the aromatic substitution of the fluoro.
e) *p*-Bromoaniline. The last step would be the conversion of the bromo into the phenol. This can be done by a number of methods such as palladium catalysed via boronate or copper catalysed.

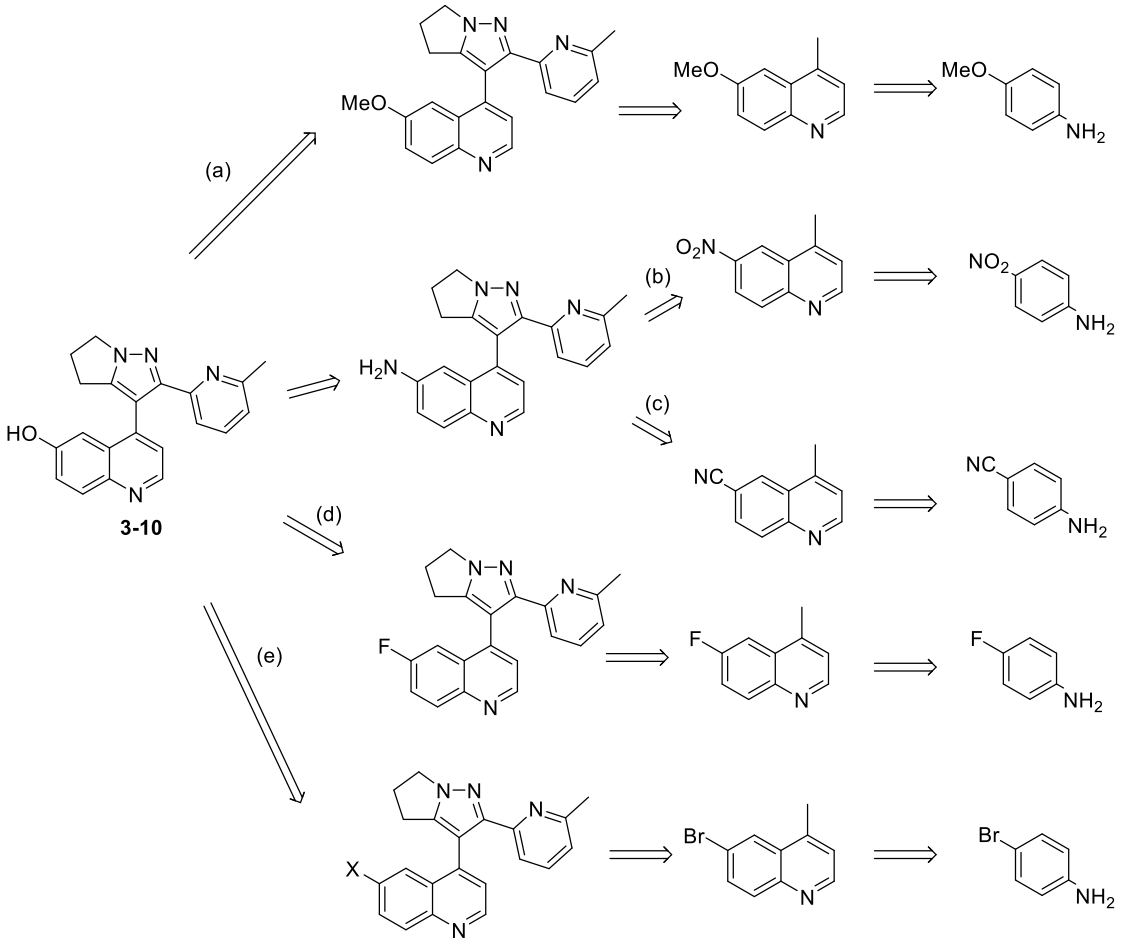


**Scheme 3.5.** Retrosynthetic analysis of HOLY (**3-10**).

## 3.3.3 Synthesis of HOLY (3-10) from *p*-methoxyaniline (route a)

In the first attempt to make **3-10**, we envisioned that it could be synthesised by starting from a protected phenol from the start of the synthesis, followed by deprotecting the phenol protecting group at the final step. We chose to protect the phenol as a methyl ether as this protecting group was thought to be able to be robust enough to withstand all the reaction conditions, and having the advantage that the methyl protected 4-hydroxyaniline (*p*-anisidine) was commercially available.

As shown in the Table 3.2, the first step was to make the 6-methoxy-4-methylquoline (**3-12**) via the Doebner-Miller reaction. The first step in the synthesis of **3-1** also used the Doebner-Miller reaction, however in that case the aniline was *para* to an electron withdrawing substituent whereas in the case of **3-12**, the *para* substituent is electron donating. This has two major implications in the quinoline synthesis; the first being that aniline **3-2** is less nucleophilic than aniline **3-11**: the *para*

cyano group is removing electron density from the nitrogen loan pair, whereas the *para* methoxy of **3-11** is pushing electron density onto the nitrogen. The concern was that **3-11** would be more likely to polyalkylate with respect to **3-2**. However, this was not observed during any of the attempts to form **3-12**.

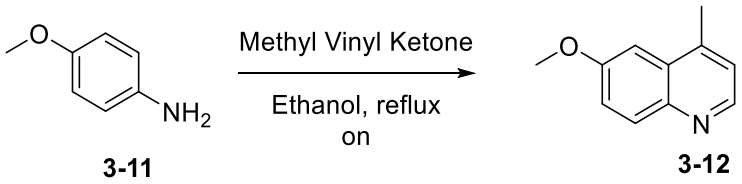


**3-11** **3-12**

| Entry | Conditions | Yield (%) |
|---|---|---|
| 1 | Chloranil | 0 |
| 2 | 2.5 eq. $FeCl_3$ | 41 |
| 3 | 2.5 eq $FeCl_3$, 0.2 eq $ZnCl_2$ | 39 |

**Table 3.2.** Summary of Doebner-Miller reaction of *p*-methoxyaniline and methyl vinyl ketone.

When using the same conditions used to make **3-3**, only the aza-Michael addition product was observed by $^1H$ NMR. As shown in Table 3.2, $FeCl_3$ was needed as a Lewis acid catalyst to activate the ketone towards attack by the aromatic ring. Entry 3 shows that in our hands and contrary to Cambell *et al.*, catalytic amounts of Lewis acid $ZnCl_2$ were not necessary for the reaction to occur.[17]

The low reactivity of the acetylation can be rationalised when taking into account the mechanism postulated in Scheme 3.2. The electrophilic aromatic substitution from **3-2.1** to **3-2.2** is the key step. Both **3-2** and **3-11** have *ortho* directing aniline groups which is what is needed for the electrophilic attack to the carbonyl in the quinoline synthesis. With respect to the cyano in **3-2**, it is a *meta* director – complementary to the aniline. However, the methoxy in **3-11** is a *ortho/para* director which is non-complementary to the aniline. This gives an explanation as to why stronger conditions were needed in the synthesis of **3-12**, and is depicted below in Scheme 3.6.

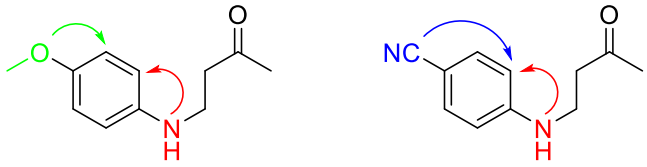


**Scheme 3.6**. Comparison between the para substituents of **3-12** and **3-3**.

From a mechanistic point of view and as shown in Scheme 3.6, the reaction involves an azo-Michael attack by the aniline to the methyl vinyl ketone forming intermediate *a*. The next step involves a Friedel-Crafts type attack by the aromatic ring to the carbonyl group forming intermediate *b*.

Although the reaction proceeds, both the oxygen and the protonated aniline in intermediate *a* deactivate the position alpha to the aniline. Even though the equilibrium will lay heavily towards the protonated aniline, the acid and the aniline are in rapid exchange with one another. The free base intermediate *a.1* has the aniline to now direct towards the *ortho* position yielding the intermediate *b*.

The position of the equilibrium between *a* and *a.1* could perhaps be shifted slightly in favour of the un-protonated form if a less electron donating group was present para to the aniline – with a less electron donating substituent, the aniline lone-pair would have a higher interaction with the ring pi-system and be less basic.

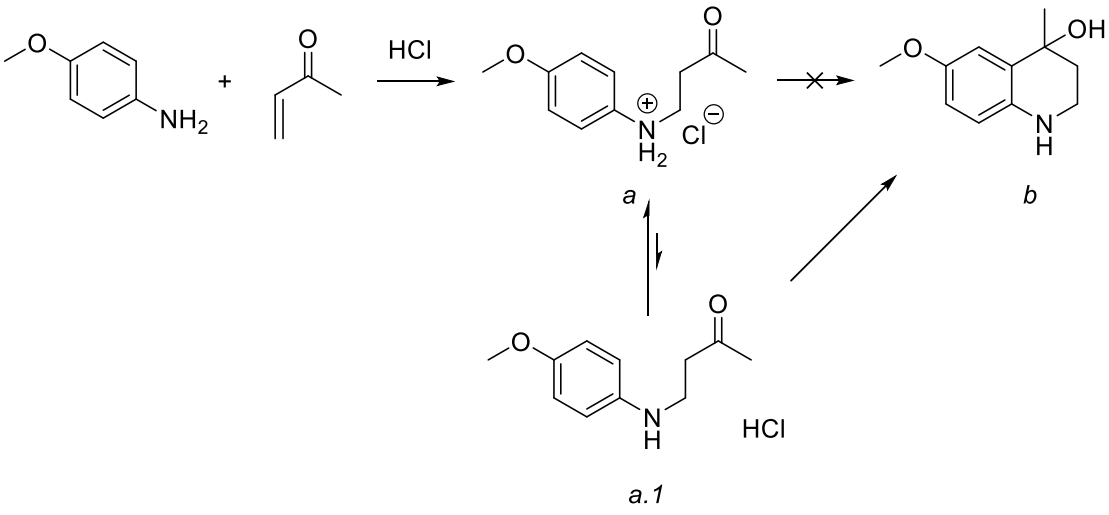


**Scheme 3.7.** Formation of intermediate *b*.

Subsequent dehydration followed by oxidation gave rise to what appeared to be **3-12** by TLC. However, the product could not be purified as easily as in the cyano case - the hydrochloride salt did not precipitate directly upon the addition of THF. Instead the reaction had to be cooled to room temperature and quenched with $NaOH_{(aq)}$. This reaction was exothermic and generated a relatively large quantity of what was presumed to be iron salts. These salts were very fine, and upon filtration through celite, frequently blocked the filtration equipment. The filtrate was then diluted with EtOAc and brine, the organic phase separated, the solvent removed, and the residue purified by column chromatography. Although we obtained **3-12** in low yields, we could obtain sufficient material to proceed to the next step.

The second step of the synthesis was the acylation of **3-12** with methyl 6-methylpicolinate (Scheme 3.8). Unfortunately, $NaO^tBu$ was not sufficiently basic for the reaction to proceed as happened in the synthesis of **3-4**. Upon addition of $NaO^tBu$ (pKa of conjugate acid is 17) to the starting material in THF at room temperature, no colour change was observed in the reaction mixture. This colour change is distinctive of the anion formed from the deprotonation of the methyl group which is conjugated with the quinoline ring. Furthermore, no change by TLC was observed after leaving the reaction overnight, and no change was observed by $^1H$ NMR of the crude reaction mixture after being left overnight.

A stronger base was needed, so instead LDA (pKa of conjugate acid is 36) was used which was strong enough to deprotonate the proton on the methyl group of **3-12**. This lead to the formation of a deep green solution, and after addition of the methyl ester, afforded **3-13** in a moderate yield. It is worth noting that a significant amount (ca. 20% by TLC) of an unidentified highly coloured red by product was formed under these reaction conditions. This by-product was neither isolated, nor were the conditions optimised to minimise its appearance.

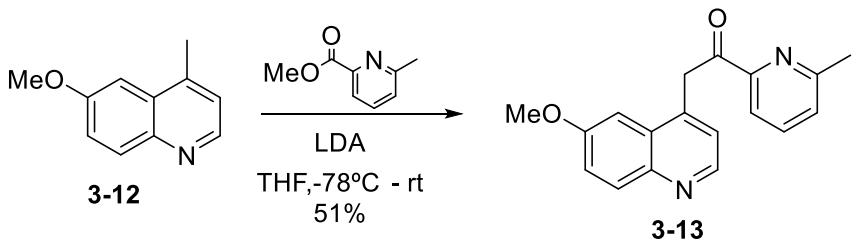


**Scheme 3.8.** Synthesis of **3-13**.

With compound **3-13** now in hand, its transformation into the methyl-protected target **3-14** compound via hydrazone formation and subsequent cyclisation was analogous to the synthesis of **3-1,** as shown below in Scheme 3.9. Gratifyingly, the methyl group was removed from the phenol ether by refluxing **3-14** in HBr in AcOH for two days to yield a sufficient amount of pure **3-10** whose activity was then tested for activity *in vitro*. A noteworthy point is that although the conditions appear to be harsh, there were no by-products observed and the reaction went 'spot to spot' by TLC.

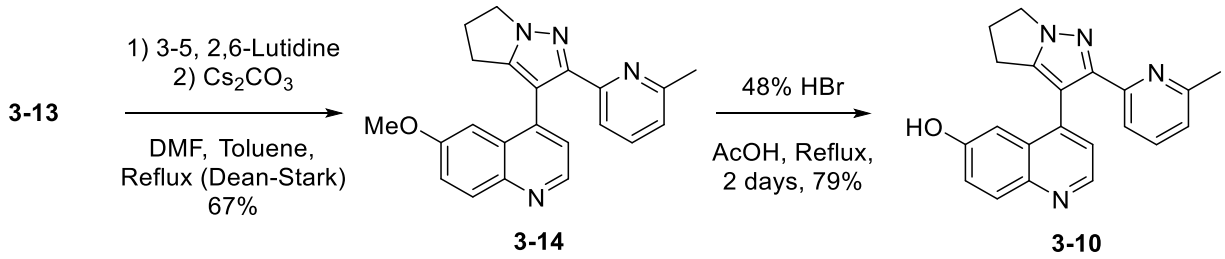


**Scheme 3.9.** Transformation of **3-13** into **3-10**.

As described in Chapter 3.5; the promising results from the *in vitro* tests prompted us to look for a more scalable and practical synthesis – one which could produce multi-gram scale quantities of **3-10** for use of it or its derivatives by the Batlle group.

Although we reached the final product, the first two steps of the reaction were of concern for scale up. The first step involved more than 2.5 eq of $FeCl_3$, which forms lots of iron species upon quenching with NaOH, and would be nearly impossible to filter at scale. The second step produced a deep red unidentified by-product dependant on the reaction. These aforementioned hurdles led us to search for a more practical, reproducible and scalable synthesis of **3-10**.

## 3.3.4 Synthesis of 3-10 from *p*-nitroaniline or *p*-cyanoaniline (routes b and c)

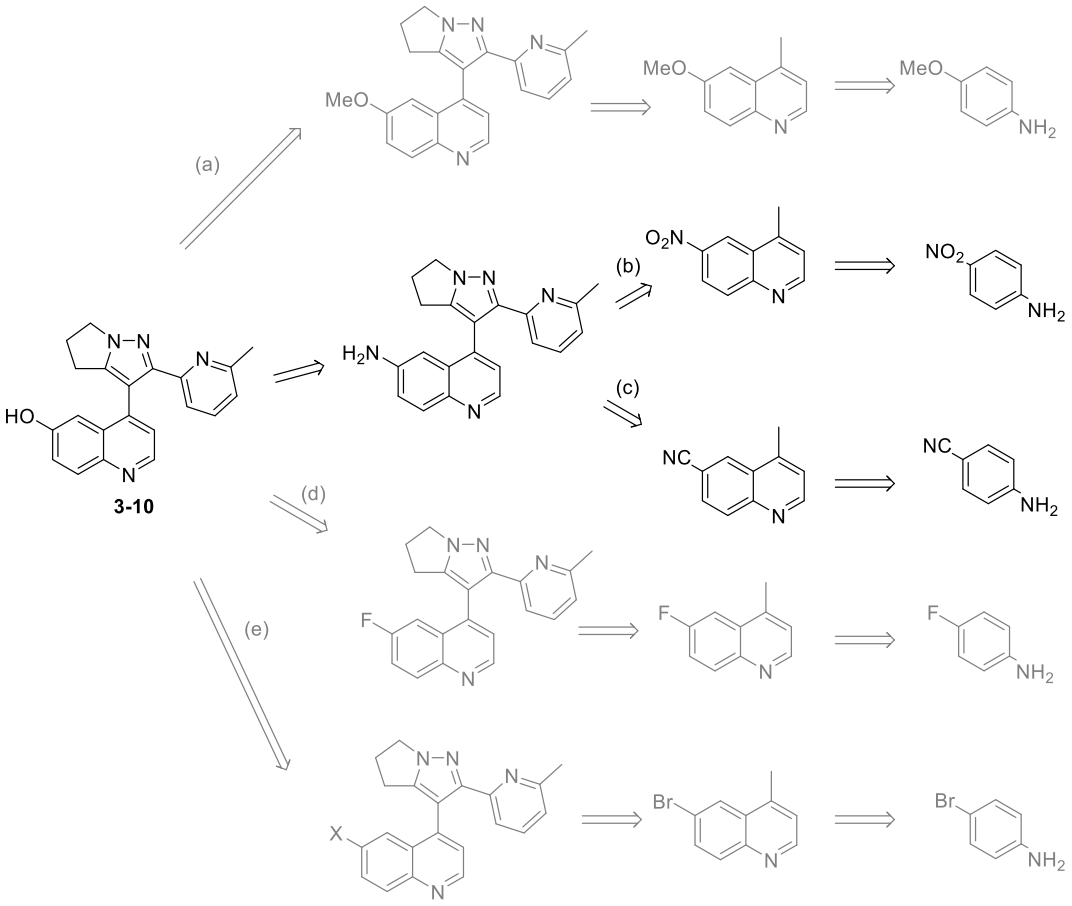


**Scheme 3.10**. Overview of routes b and c.

As explained in the development of route a, the electro-withdrawing groups on the aniline helped the formation of the quinoline. Therefore on paper, the *p*-nitroaniline appeared to be an excellent candidate as starting material. The nitro aniline serves as both an electro-withdrawing group as well as a protecting group for the proposed synthesis. It can then be reduced to the corresponding aniline, followed by functional group conversion to the phenol via the diazonium salt catalysed by copper (Scheme 3.11).

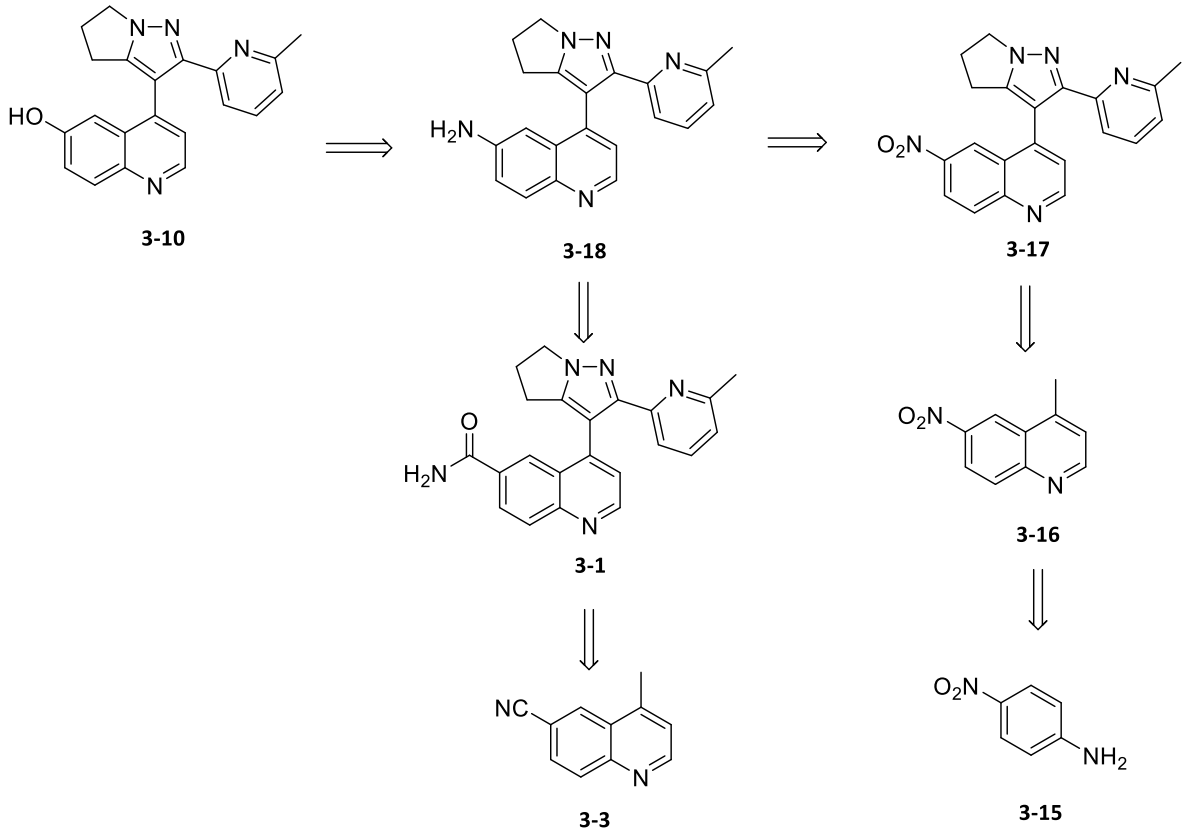


**Scheme 3.11.** Retrosynthetic analysis of compound **3-10** from *p*-nitroaniline or *p*-cyanoaniline.

However, since at that time in the lab we had surplus **3-1**, we attempted to transform it directly into the compound **3-18** via the Curtius rearrangement.

The first step, the acidic hydrolysis of the amide took place uneventfully. The zwitterion **3-19** could be isolated in good purity by precipitation at pH 5 (Scheme 3.12).

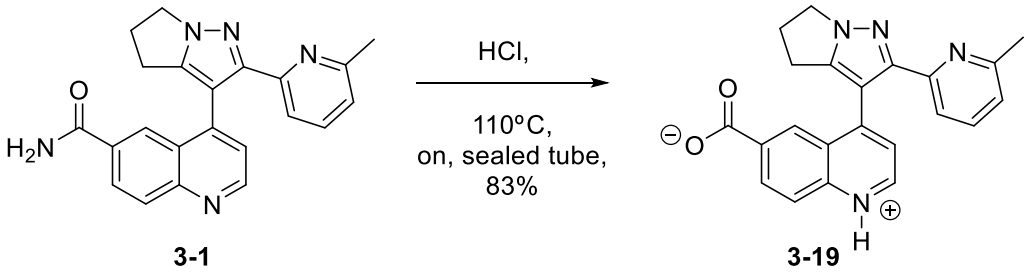


**Scheme 3.12**. Hydrolysis of amide **3-1**.

The acid had then to be converted into the aniline **3-18**. We planned to use the Curtius rearrangement so **3-18** was converted into the acyl azide **3-19.1** by treatment with diphenylphosphoryl azide (DPPA) and heated. Surprisingly, the main reaction product was the urea **3-20** (Scheme 3.13) as confirmed by mass spectrometry.

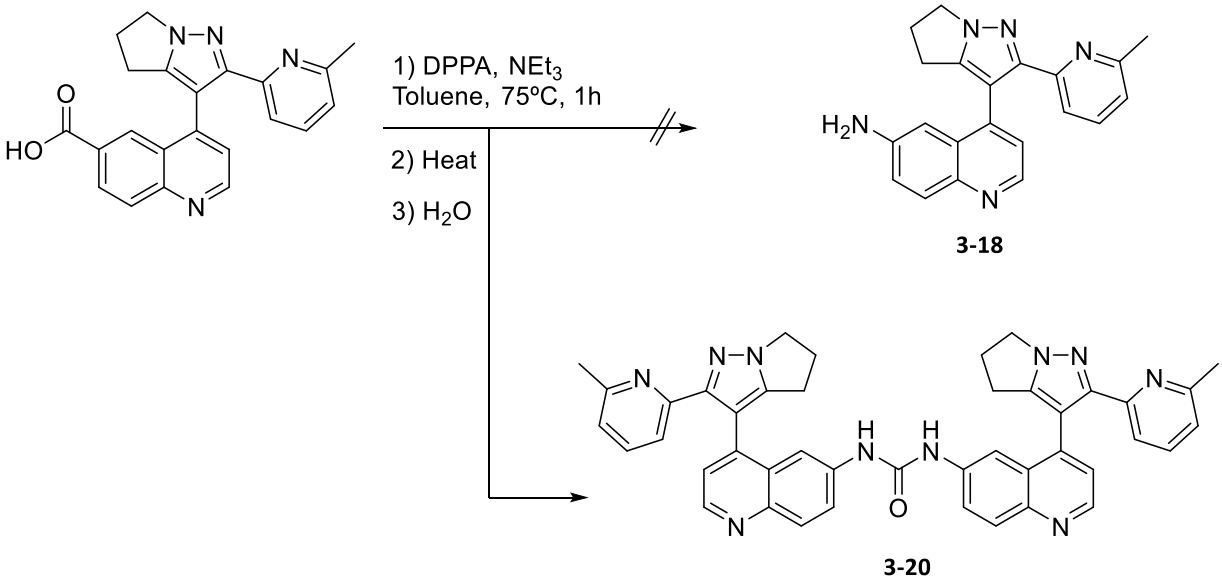


**Scheme 3.13.** formation of urea compound **3-20**.

This unexpected product can be rationalised according to the mechanism outlined in Scheme 3.14 The initially formed acyl azide **3-19.1** underwent the Curtius rearrangement affording isocyanate **3-19.2**. Quenching the isocyanate with water produces the desired aniline **3-18** after decarboxylation of the carbamic acid **3-19.3**. In this case, however, the reaction between isocyanate **3-19.2** and the desired aniline **3-18** takes place very easily affording the undesired urea compound **3-20.**

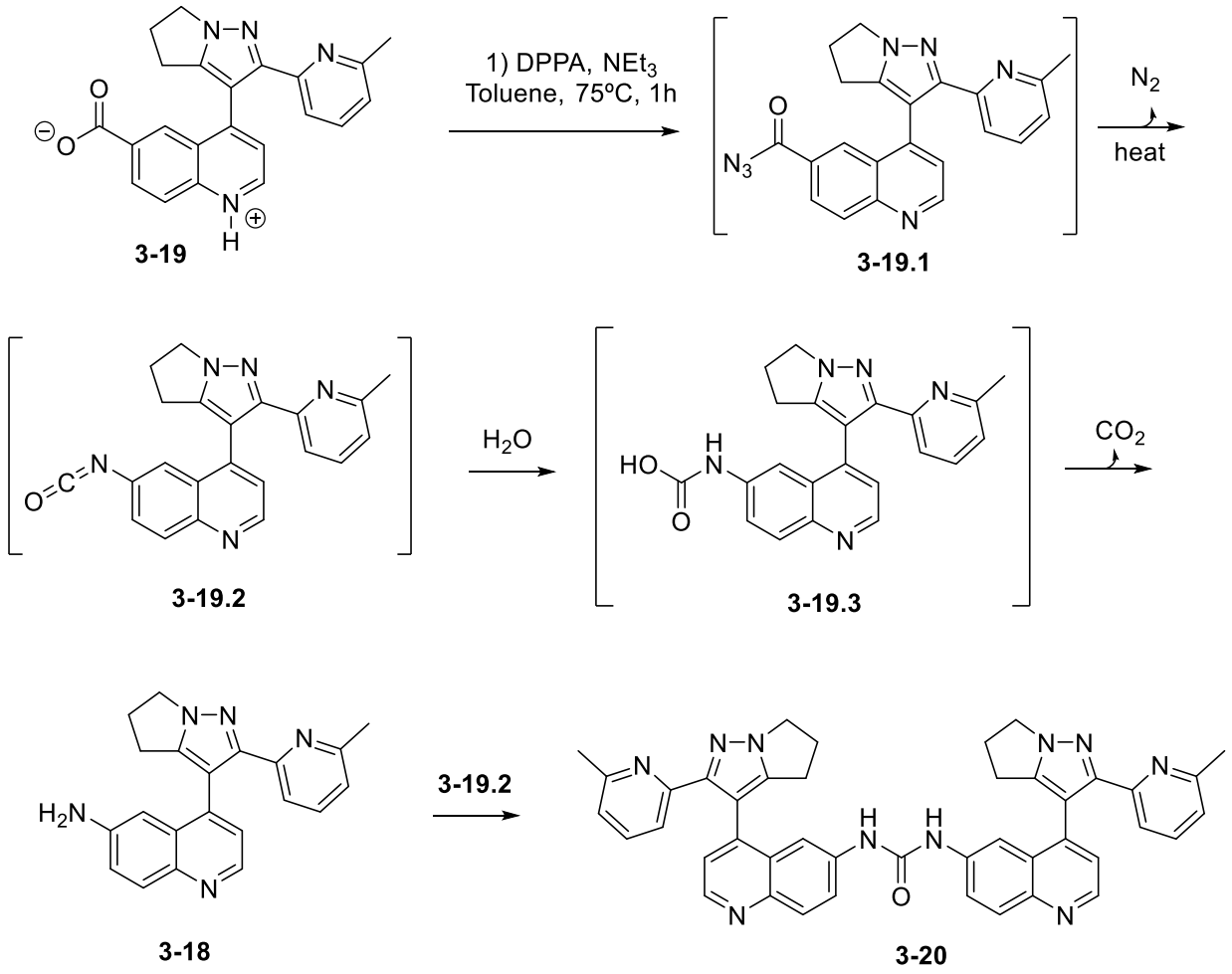


**Scheme 3.14**. Postulated reaction mechanism forming **3-20**.

To suppress this side reaction, we postulated that instead of attacking the isocyanate with water, it could be attacked with *tert*-butanol to give the BOC protected aniline **3-21** which would not be able to attack any additional isocyanate in solution. This strategy allowed us to access **3-21** in a good yield (Scheme 3.15).

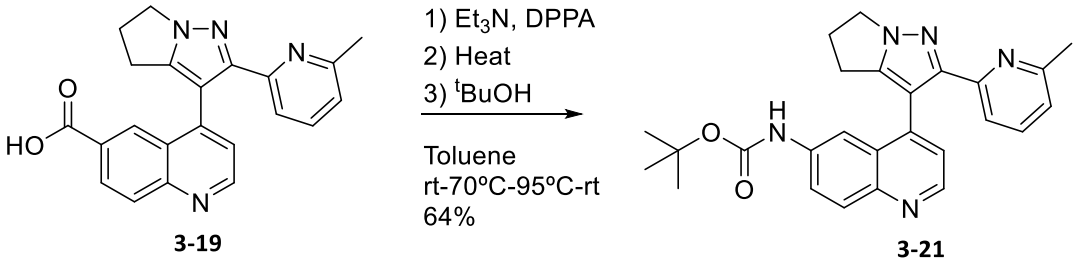


**Scheme 3.15.** Transformation of **3-19** to **3-21**.

Next we explored the conversion of the **3-21** into the corresponding phenol via the Sandmeyer reaction following a procedure reported in the literature.[18] As acidic conditions are required to form the diazonium salt, the BOC protected amine was first dissolved in acid at room temperature. The reaction was left until all the BOC had been deprotected by TLC. Upon deprotection of the BOC, the reaction mixture was cooled to 0ºC and treated with $NaNO_2$ to form the diazonium salt. $Cu_2O$ was then added under various conditions summarised in the Table 3.3.

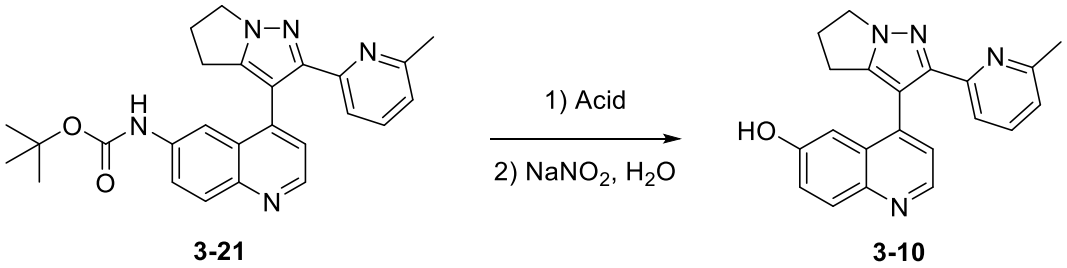


| Entry | Acid | Temperature (ºC) | Product | Notes |
|---|---|---|---|---|
| **1** | HCl (3M) | 0-rt-80 | **3-22**, **3-23**, and **3-24** | |
| **2** | HCl (3M) | 0-rt-80 | **3-22**, **3-23**, and **3-24** | 2 eq of $NaNO_2$ |
| **3** | $H_2SO_4$ | 0-rt o/n | **3-24** + complex mixture | |
| **4** | $H_2SO_4$ | 0-80 | **3-24** + complex mixture | diazonium salt added to water at 80 degrees |
| **5** | $H_2SO_4$ | 0-rt o/n | **3-24** + complex mixture | |
| **6** | $H_2SO_4$ | 0-rt o/n | complex mixture | urea added, 40 eq of $Cu(II)NO_3$ |

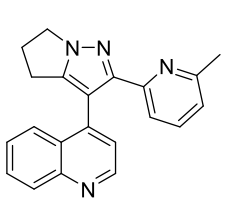

**3-22**

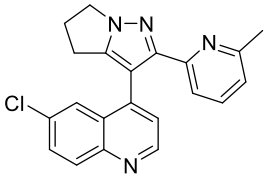

**3-23**

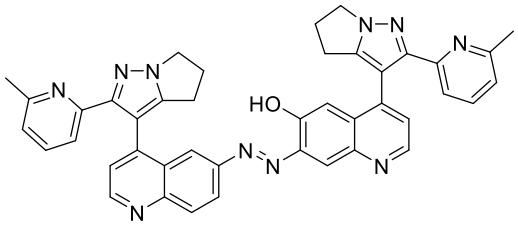

**3-24**

**Table 3.3.** Attempts at the formation of **3-10** from **3-21**.

By both TLC and by $^{1}$H NMR, no traceable amounts of the desired compound **3-10** were seen. Compound **3-24** was presumed to be the regioisomer as drawn, due the fact that the phenol acts as an *ortho/para* director in diazo coupling. As the *para* position is blocked, it is likely to go in the *ortho* position (5 or 7 on the quinoline ring). We proposed the 7-position due to the steric hindrance in the 5 position, however this was not investigated in any depth.

With not a trace of the phenol been seen by this point, it became apparent that this route should be abandoned.

## 3.3.5 Synthesis of 3-10 from *p*-fluoroaniline (route d)

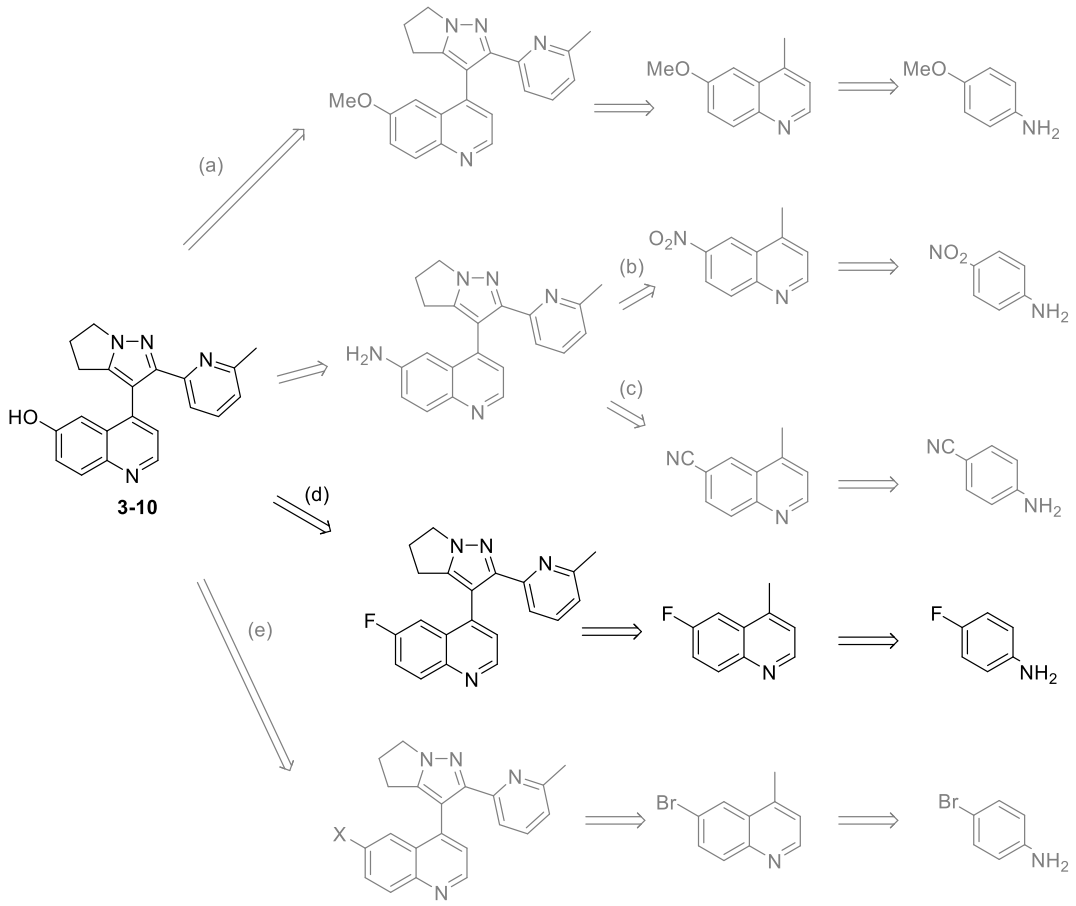


**Scheme 3.16**. Proposed synthesis of **3-10** from 4-fluoroaniline.

We then went on to investigate if an oxygenated fragment could be introduced via a nucleophilic aromatic substitution reaction ($S_NAr$) (route d). A typical $S_NAr$ involves the substitution of a halogen atom on an electron deficient aromatic ring with a nucleophile. Fluorine is the most reactive in an $S_NAr$ due to the it being the most electronegative halogen, facilitating the attack of a nucleophile to the electropositive carbon it is attached to. We synthesised compound **3-26** using the same methodology as was used to make **3-3** (Scheme 3.17).

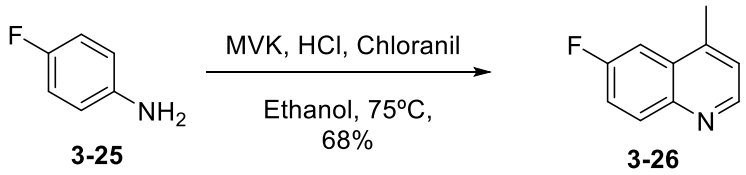


**Scheme 3.17**. Formation of quinoline **3-26** from aniline **3-25**.

Numerous attempts to substitute the fluorine to form an ether or a phenol failed, as summarised in Table 3.4. Unfortunately, we were not able to substitute the fluorine atom of **3-26** using $S_NAr$. We then went on to look at other alternatives using transition metal catalysis.

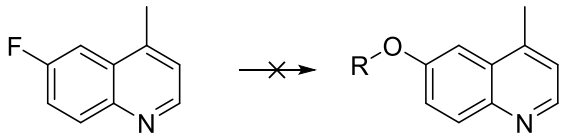


**3-26**

| Reagent | Solvent | Temp | Time | Yield (%) | R |
|---|---|---|---|---|---|
| NaOMe | MeOH | reflux | 3 days | 0 | Me |
| KO$^t$Bu | DMF | 150 $^o$C | 3 days | 0 | $^t$Bu |
| KOH | DMSO | 150 $^o$C | 3 days | 0 | H |
| KOH | Water | reflux | 3 days | 0 | H |
| NaO$^t$Bu | DMF | 150 $^o$C | o/n | 0 | $^t$Bu |
| $^i$PrOH/NaH | DMF | 150 $^o$C | o/n | 0 | $^i$Pr |
| NaOMe | DMF | 150 $^o$C | o/n | 0 | Me |

**Table 3.4**. $S_NAr$ attempts of compound **3-26**.

## 3.3.6 Synthesis of 3-10 from *p*-bromoaniline (route e)

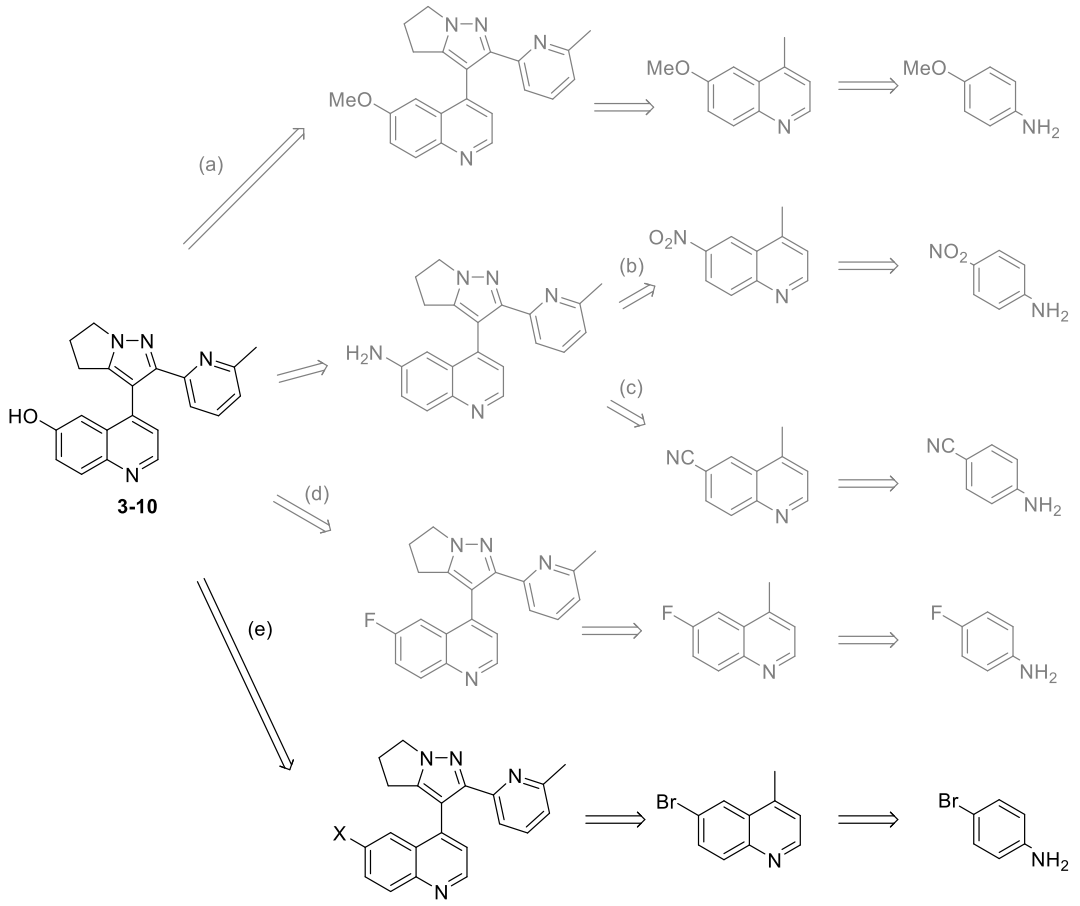


**Scheme 3-18**. Proposed synthesis of **3-10** from 4-bromoaniline.

A literature review revealed several methods to transform an aromatic bromine into a phenol. In 2010, the group of Ma[19] and, separately, also the group of Punniyamurthy[20] reported the synthesis of phenols from the corresponding aryl halides. After a substantial screen of solvents, ligands and substrates, Ma reported that the aryl bromide or iodide could be transformed into the corresponding phenol by treatment with CuI and 8-hydroxyquinoline in basic media (*tert*-butanol/DMSO/water). The reaction appeared to tolerate a variety of both EWG's and EDG's giving good yields (Scheme 3.19).

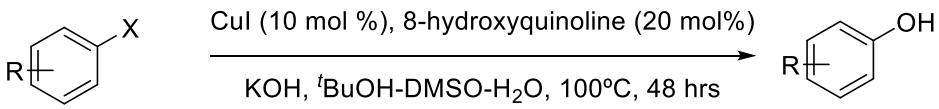


**Scheme 3.19**. Phenol formation as described by Ma and Punniyamurthy. (X = Br or I).

On the other hand, Bounaud *et al.*[21] reported the conversion of a bromo-quinoline to the corresponding phenol/hydroxy quinoline using Pd-X-Phos as the catalyst and KOH as the nucleophile.

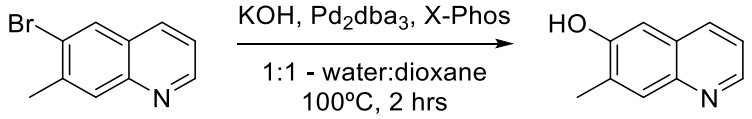


**Scheme 3.20.** Transformation of a bromo-quinoline into the corresponding alcohol by Bounaud *et al*.

With these precedents in mind we decided to synthesize the bromo-quinoline **3-28**. using a modified version of the Doebner-Miller reaction. However, when using the same method as in the synthesis of **3-3** the final product could not be easily purified since it co-precipitated with the oxidant (chloranil), or with its reduced form. Fortunately, we found that if the chloranil is simply replaced with air as the oxidant, the reaction proceeds smoothly, albeit slower than with the chloranil affording **3-28** as a hydrochloride salt (Scheme 3.21).

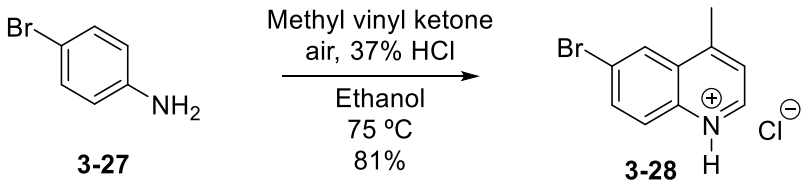


**Scheme 3.21**. Synthesis of **3-28**.

With the quinoline **3-28** prepared, we decided to use it as a model compound to search for the right conditions. We submitted **3-28** to the same reaction conditions as reported by Maurer *et al*, however no formation of the 6-hydroxy analogue **3-29** was visible after more than 2 days at 100 °C.[19] Conditions as described by Bounaud *et al* were then tried, and once again no trace of the alcohol was observed. One hypothesis regarding the reaction inactivity is that the substrate itself could be competing with the ligand in coordination with the copper and therefore deactivating the catalyst. We decided to consider palladium catalysed methods to perform the transformation of **3-28** to **3-29.** We tried repeating the reaction using Bounaud's conditions with **3-28**, however we did not observe any formation of the desired phenol **3-29** (Table 3.5).

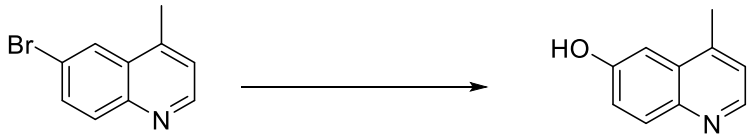


**3-28** **3-29**

| Reagents | Time | Temperature (°C) | Conversion |
|---|---|---|---|
| 4 eq. KOH, CuI, 2-methylquinolin-8-ol, $^{t}$BuOH, DMSO | 24 hrs | 100 | - |
| 4 eq. KOH, CuI, 2-methylquinolin-8-ol, $^{t}$BuOH, DMSO | 48 hrs | 100 | - |
| Pd(II)OAc (5%), +/- BINAP (15%), NaO$^{t}$Bu (1.5 eq.), $^{t}$BuOH (2 eq.), Toluene | 24 hrs | 90 | - |
| Pd(II)OAc (5%), +/- BINAP (15%), NaO$^{t}$Bu (1.5 eq.), $^{t}$BuOH (2 eq.), Toluene | 48 hrs | 90 | - |
| $Pd_2dba_3$ (2%), Xphos (8%), KOH (4 eq.), Dioxane, Water | o/n | 100 | - |
| $Pd_2dba_3$ (2%), Xphos (8%), KOH (4 eq.), Dioxane, Water | o/n | 50*-100 | - |

* Palladium and XPhos left to preform at 50 degrees for 30 minutes

**Table 3.5.** Attempts to convert **3-28** into **3-29**.

Having exhausted most of our options to do a direct transformation from a halogen, we sought to access the phenol indirectly via the boronic ester.

Synthetic methodologies to prepare aryl boronoic esters from aryl halides can be grouped into two categories. The first is the addition of an arylmagnesium,[22] aryllithium,[23] or less commonly, arylzinc [24] *(not drawn in the scheme)* to boronic ester as generalised in Scheme 3.22 below. Organometallic compounds are typically made by halogen metal exchange, or via transmetallation from another organometallic compound. This newly formed aryl-metal species is then able to attack boronic esters yielding aryl boronic esters.

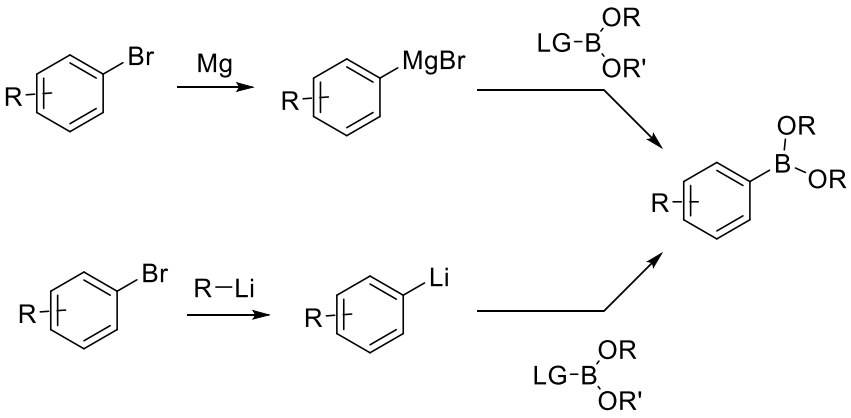


**Scheme 3.22**. Formation of boronic esters from the corresponding aryl bromides.

The main drawback with this method is that, in the case of organolithium, requires the use of highly reactive reagents (such as $^{t}$BuLi), and in the case of organomagnesium, is a very exothermic process. Substrate tolerance can be limited in these conditions and, in terms of safety, it would be advantageous to avoid this route if possible as we were searching for a safe and scalable process. With these concerns in hand, we first investigated the Miyaura borylation.

Miyaura and co-workers found that aryl bromides, iodides and triflates can be efficiently converted to the corresponding boronic esters via Pd catalysed cross coupling reactions with diboronyl esters such as $B_2Pin_2$.[25] The Miyaura borylation tolerates a wide range of functional groups, such as esters and nitriles, which would likely react with organomagnesium and organolithium reagents needed in the aforementioned transformation.[25] The coupling proceeds via Pd(0)/Pd(II) mechanism as shown in Scheme 3.23.[26]

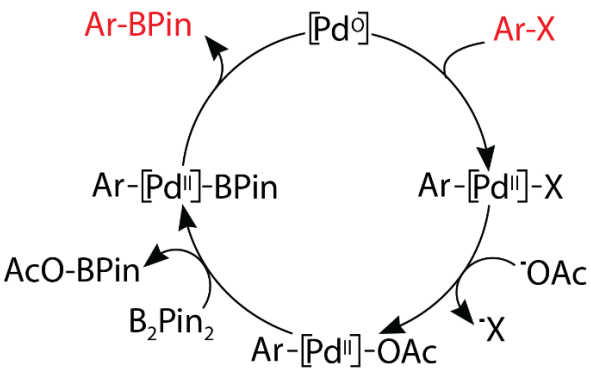


**Scheme 3.23**. Catalytic cycle of the Miyura borylation.

The mechanism involves the oxidative addition of an aryl halide or triflate to the $Pd^0$ species to form the Ar-$Pd^{II}$-X complex. This then exchanges the halide or triflate for an acetate before transmetallation with the $B_2Pin_2$ giving the Ar-$Pd^{II}$-BPin complex. Reductive elimination of the complex gives the desired aryl boric ester plus the starting $Pd^0$ catalyst, where the cycle can then repeat again.

Oxidation of boronic acids in basic media to the corresponding phenol has been known for over 85 years.[27] 27 years later, Kuivila studied and proposed a mechanism for the reaction between benzene-boronic acid and hydrogen peroxide (Figure 3.24).[28]

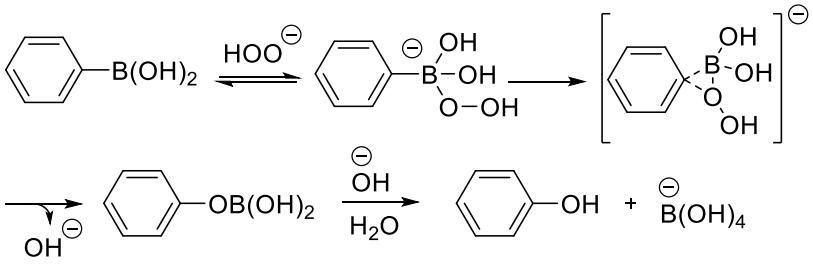


**Scheme 3.24**. Mechanism of the formation of a phenol from the corresponding boronic acid.

The mechanism starts with attack of the boronic acid by an equivalent of hydroperoxide, followed by a rearrangement to give the phenyl borate, and finally B-O cleavage by OH- to give the phenol.

We tested the Miyaura borylation using the model compound **3-28** with $B_2Pin_2$ as the cross-coupling partner. In 2 hours, no starting material was observed and after quench, the reaction mixture was purified by MPLC to give the desired arylbornoic ester in low yield. The low yield was attributed to the decomposition of the ester in the acidic silica to give the boronic acid that was then unable to be removed from the column due to its polar nature.

Instead of isolating the boronic ester **3-30**, we then attempted the oxidation of the boron without purification of the reaction mixture as shown in Scheme 3.25. Satisfactorily, the addition of 5 equivalents of NaOH followed by dropwise addition of $H_2O_2$ gave compound **3-29** in a low yield.

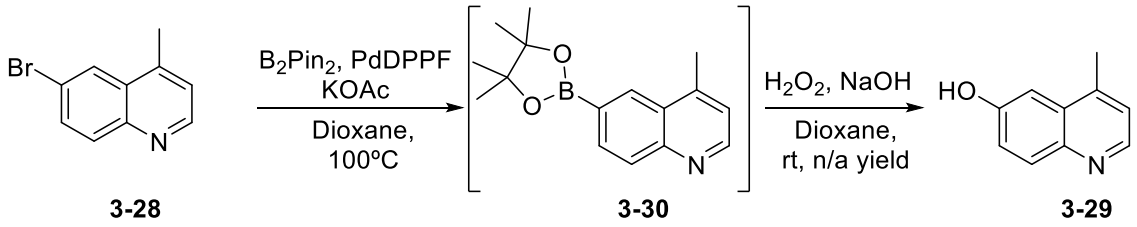


**3-28** **3-30** **3-29**

**Scheme 3.25.** Transformation of bromoquinoline **3-28** to the corresponding phenol **3-29** via boronic ester **3-30**.

After successfully testing our transformation of an aryl bromide to the corresponding phenol, albeit with a low yield, we then continued with route e toward the desired compound **3-10**.

As in the synthesis of **3-1**, $NaO^tBu$ was tested for the deprotonation of the methyl group of quinolone **3-28**. As with the synthesis of **3-13**, deprotonation of the bromo analogue was not possible with $NaO^tBu$. This was observed visually as there wasn't a colour change indicating the formation of the anion as there was in the cyano analogue. We performed a small screen of bases and conditions to optimise the reaction.

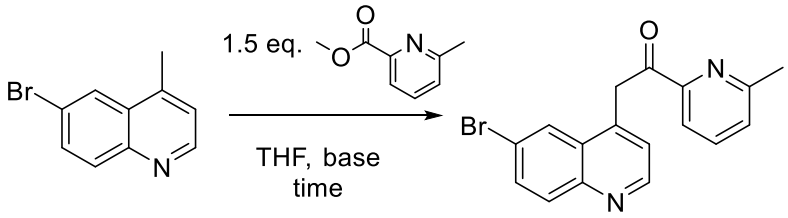


**3-28** **3-31**

| Entry | Base | Equivalents | Temp | Time | Conversion* | Yield |
|---|---|---|---|---|---|---|
| 1 | NaO$^t$Bu | 3,3 [a] | rt | 4 hours | 0 | 0 |
| 2 | NaO$^t$Bu | 3,3 [a] | 50 | 4 hours | 0 | 0 |
| 3 | LDA | 3,3 [a] | -78 - rt | on | 19% | - |
| 4 | NaHMDS | 2,4 | -78 - rt | on | 63% | - |
| 5 | NaHMDS | 2,4 | 0-rt | on | 52% | - |
| 6 | NaHMDS | 2,4 | -78 - rt | on | 82% | - |
| 7 | NaHMDS | 4 | -78 - rt | on | 100% | 88% |

*a the HCl salt was used. *conversion measured by $^1$H NMR*

**Table 3.6.** Optimisation of **3-28** to **3-31**.

Using LDA as the base resulted in conversion of the starting material to the product, however even at low temperatures, a highly coloured unidentified by-product was formed, suggesting that the reaction conditions were too harsh. When NaHMDS was used instead of LDA (pKa 26 vs 36), the reaction proceeded without any formation of the red by-product when conducted at -78$^o$C. Higher conversion was seen when the reaction mixture was left for 4 hours at -78$^o$C before the addition of the methyl ester (entry 4 vs entry 6). 4 equivalents of base were needed to achieve complete conversion. With a reliable method established to intermediate **3-31**, we then moved onto the next step in the synthesis.

Then, **3-31** was efficiently transformed into **3-33** using the same methodology used to make **3-1**. This was performed enabling us to have 2 grams of **3-33** to perform further tests with.

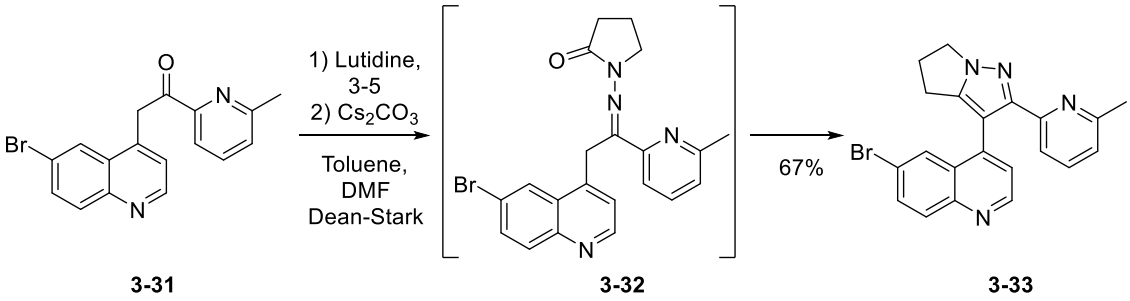


**Scheme 3.26**. Synthesis of compound **3-33**.

With compound **3-33** now in hand, we tested the Miyaura borylation under the same conditions used for model compound **3-28**. The reaction proceeded 'spot-to-spot' and once there was no sign of starting material, the reaction mixture was cooled down to rt, basified, and filtered through celite. Without any further purification, the boronic ester was oxidised, and after subsequent hydrolysis in the basic media, gave phenol **3-10** in a 77% yield after column chromatography. This is depicted below in Scheme 3.27.

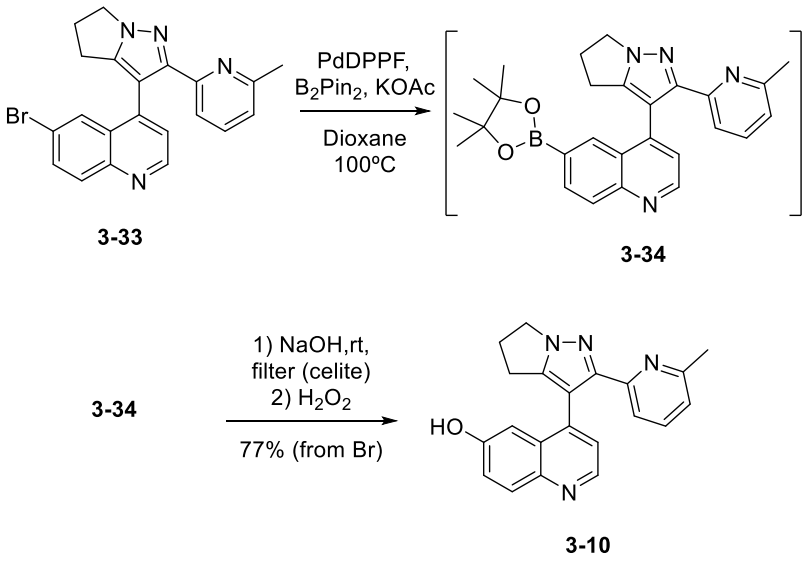


**Scheme 3.27**. Transformation of aryl bromide **3-33** to phenol **3-10**.

This process has since been scaled-up to in the group by Joan Matarín, obtaining **3-10** on a multi-gram scale which was of sufficient quantity to perform further *in vivo* biological tests in collaboration with the Batlle group.

## 3.4 Derivatives of 3-10

### 3.4.1 Design and synthesis of water-soluble derivatives of 3-10

With a procedure to access **3-10** on a gram scale, we designed and produced a new inhibitor which would overcome the drawbacks we had seen during the use of **3-1**. One of the drawbacks is the low solubility in aquous solutions, requiring repitative oral treatment by gavage. To generate a soluble formulation, we based our design and logic around Irinotecan.

Irinotecan is a prodrug of its active metabolite SN-38, as shown below in Figure 3.14.[29,30] The 4-piperidinopiperidine group in irinotecan is added to improve the solubility of SN-38 in aqueous media.

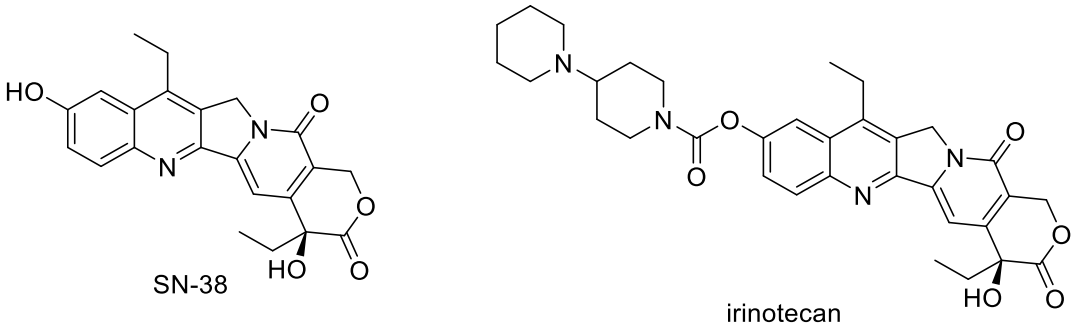


**Figure 3.14.** Structures of SN-38 and Irinotecan.

Importantly the 4-piperidinopiperidine group is cleaved via hydrolysis by various carboxylesterases *in vivo*.[30] We thought we could take advantage of this already established methodology in creating our own bioavailable and water soluble TGF-β inhibitor. We rationalised it could be made as shown in Scheme 3.28.

Fortunately, the [1,4'-bipiperidine]-1'-carbonyl chloride was commercially available therefore our first attempt to form compound **3-35** resulted in the obtention of the desired compound. Phenol **3-10** was reacted with 4-piperidinopiperidine-1-carbonyl chloride in DCM using pyridine as the base to capture the HCl produced as the reaction proceeds, and also using catalytic amounts of DMAP in an 87% yield.

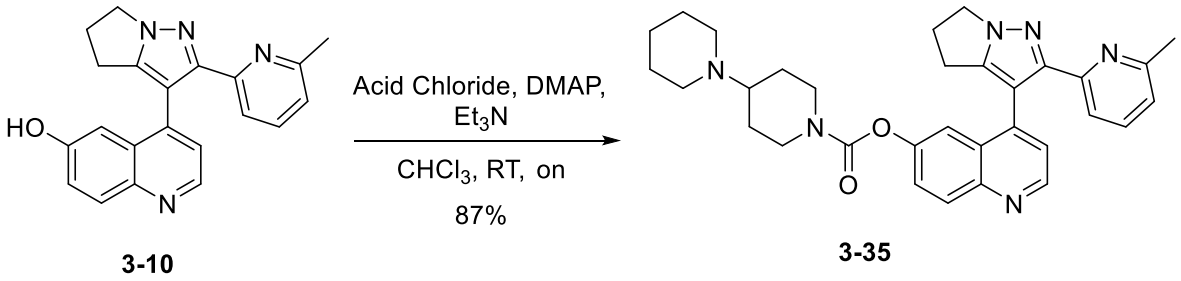


**3-10** **3-35**

**Scheme 3.28.** Synthesis of IrinOLY (**3-35**) from HOLY (**3-10**).

We then transformed **3-35** into the corresponding HCl salt with the foresight to aid *in vivo* formulation of the drug. The free base was dissolved in dioxane under $N_2$ where it was treated dropwise with 1.2 equivalents of 4M HCl in dioxane at room temperature with vigorous stirring. The reaction mixture was then taken to dryness *in vacuo* giving the desired compound that we named IrinOLY as the HCl salt (**3-36**).

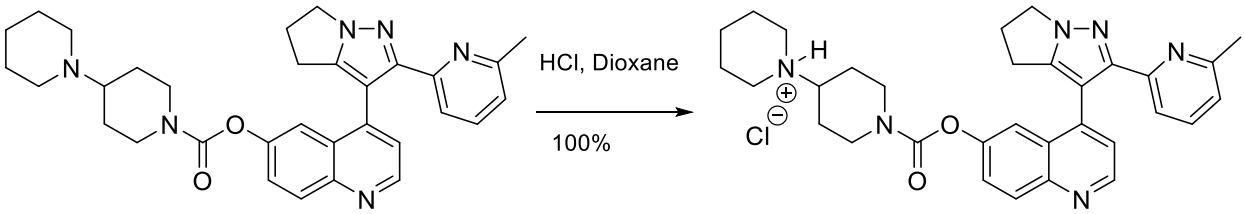


**3-35** **3-36**

**Scheme 3.29.** Synthesis of IrinOLY HCl salt **3-35**.

With the HOLY **3-10**, irinOLY **3-35**, and IrinOLY HCl salt **3-36** synthesised, we proceeded to explore their activity *in vivo*.

## 3.4.2 Synthesis of prodrug 3-38

As described in Chapter 5, we optimised a vanillone-based recognition fragment which can be specifically recognised by an exogenous enzyme known as LigF. This enzyme cleaves beta ether bonds (in red) as shown in the representation below, which in this case, the RO part of the molecule would be liberated as ROH.

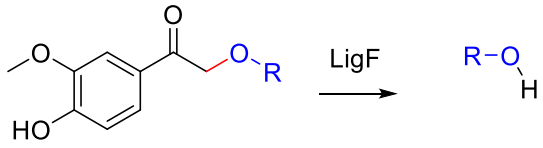


**Scheme 3.30**. Liberation of ROH from its corresponding beta-ether parent compound.

We wanted to extend the application of the technology developed in Chapter 5, and to see if it would also be expandable to other biologically interesting compounds such as **3-10**.

The intention was to have a prodrug of **3-10** with strongly reduced activity so that it could be administered in a model with little or no effect on the TGF-β pathway, unless the beta ether bond is cleaved. Depending on the distribution of the LigF enzyme, the active compound **3-10** would be locally released for instance in the tumour stroma, but not the wider circulation. The main advantage is that this would allow for high local doses and TGF-β inhibition, without systemic toxicity—an important issue going forward in combining immunotherapies.

Adapting the synthesis from that developed in chapter 5, we made compound **3-38** as shown in Schemes 31 and 32 below.

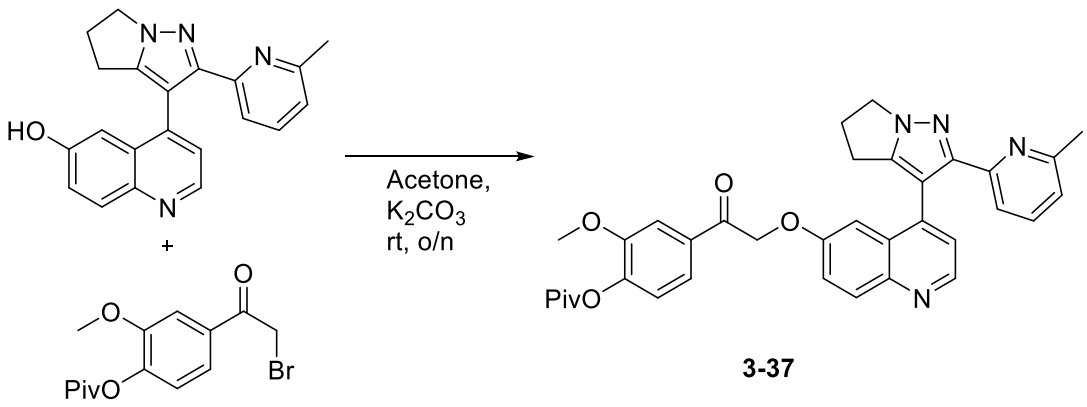


**Scheme 3.31.** Alkylation of **3-10** with pivoyl-protected alpha-bromo ketone.

The reaction proceeded with full conversion by TLC and **3-37** was used without any further purification. The pivaloyl group was deprotected by dissolving **3-37** in THF, followed by the addition of NaOH and being left to react overnight. Following column chromatography, the compound was then ready to be submitted to biological tests; we termed it VOLY, where 'V' stands for vanillone.

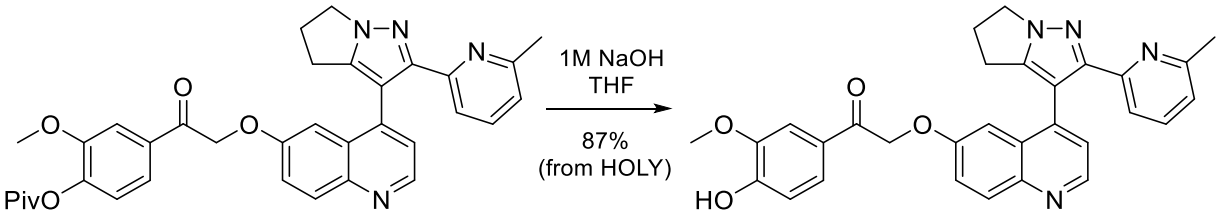


**3-37** **3-38**

**Scheme 3.32**. Deprotection of **3-37** to give **3-38**.

## 3.5 Biological assays of 3-10

As mentioned earlier, when TGF-β binds to the receptor, phosphorylation of the type 1 TGFBR occurs which in turn phosphorylates SMAD2/3, which then forms a complex with SMAD4 and enters the nucleus.

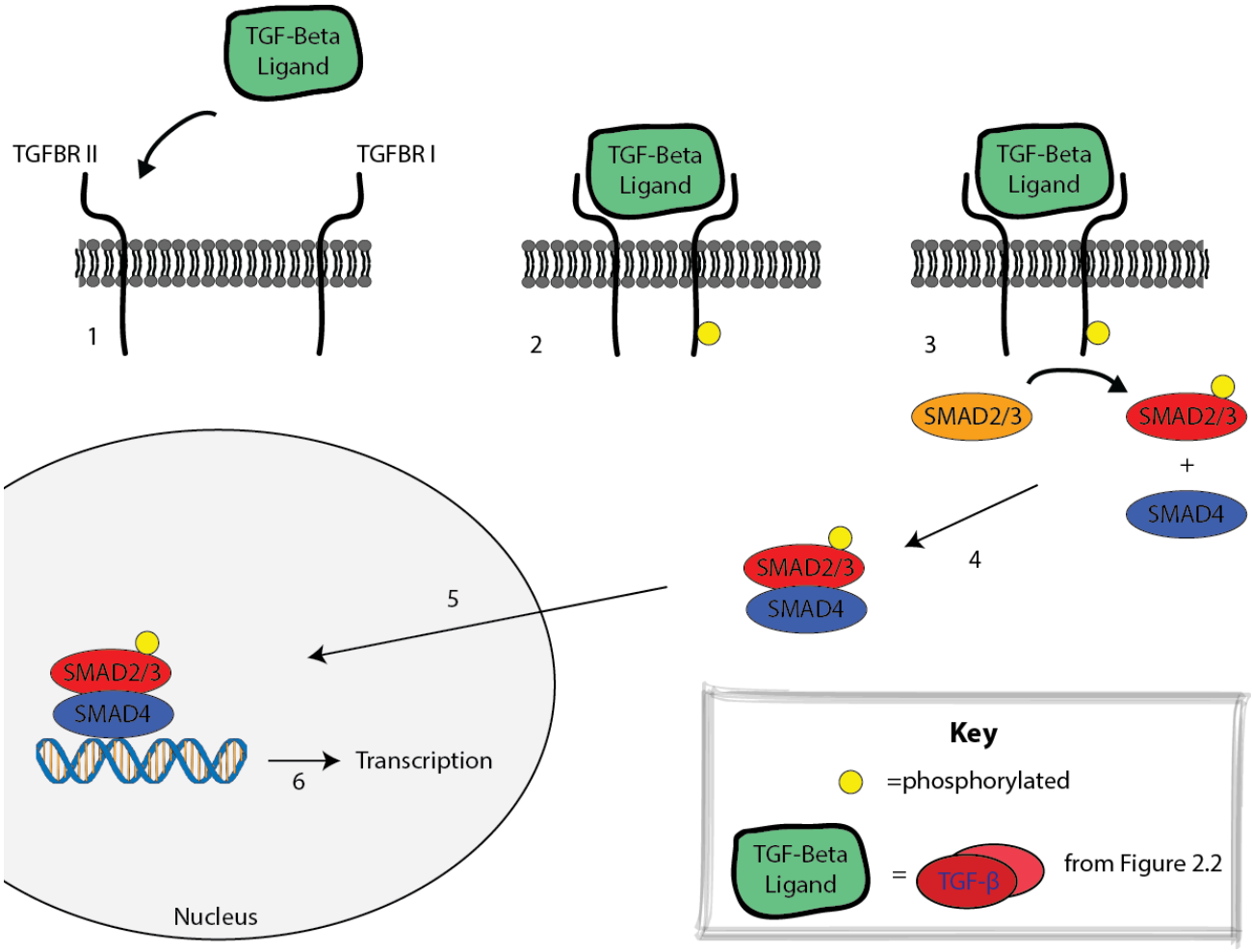


**Figure 3-15**. Overview of the TGF-β activation of SMADs.

The SMAD2/3-SMAD4 complex then binds to a promotor (or TGF-β response element) and with various co-factors, allows the transcription of various downstream genes. If we were to inhibit the TGFBR1 from being able to be phosphorylated, there wouldn't be any of the downstream effects observed, including gene transcription.

With this theory in mind, we mixed the firefly CAGA-luciferase (CAGA being a SMAD2/3-SMAD4 binding sequence) and the *Renilla* luciferase (*Rluc*) plasmids, and then co-transfected HEK293T cells with this stock solution. Firefly luciferase protein production thus reports the level of TGF-beta

signalling, while the renilla luciferase is expressed constitutively: this mainly marks transfection efficiency and cell viability. Upon treatment with various concentrations of the TGF-β inhibitor followed by treatment with TGF-β itself, the cells were lysed and the expression of the firefly luciferase measured in a luminometer following the addition of the luciferase substrate, luciferin.

Emission of light would imply an active TGF-β pathway as there had been the production of pSMAD2/3 – SMAD4, whereas no or little observed light would imply inhibition of the pathway by the inhibitor. Finally, the results could be normalised by the addition of Stop & Glo® which quenches the firefly luciferase enzyme/substrate and activates the *Renilla*, producing light which was again measured by the luminometer.

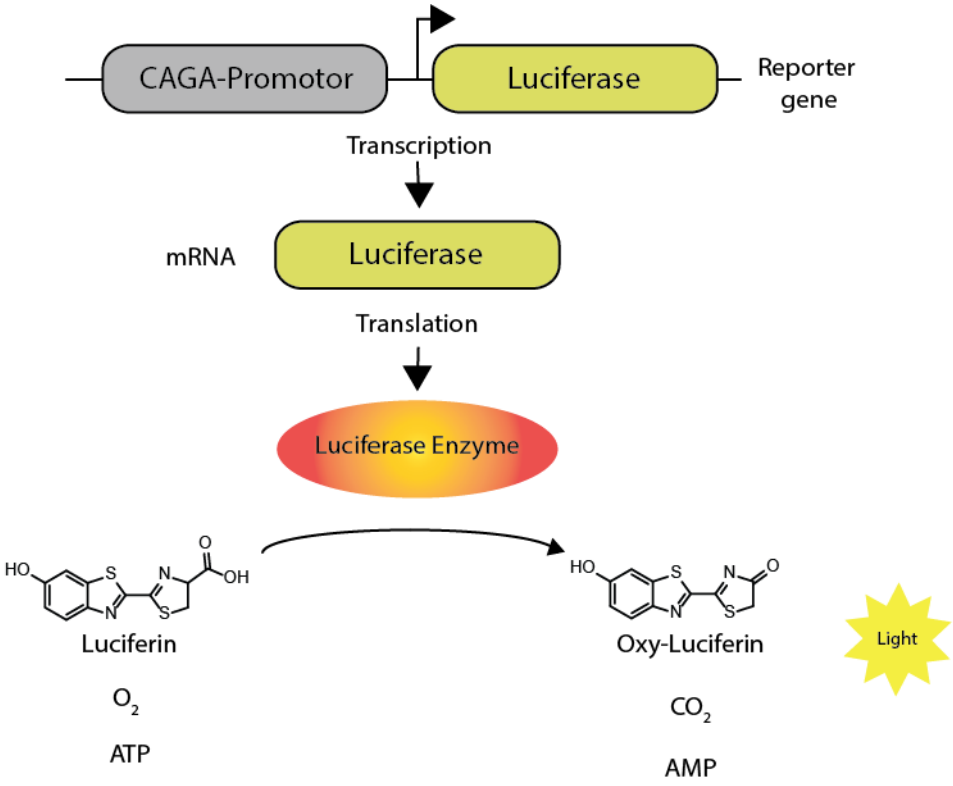


**Figure 3.16**. Overview of the luciferase assay.

After testing the inhibitors at various concentrations, we found that under the same conditions **3-1** had an IC value of 228 nM and that HOLY had an IC50 value of 133 nM - approximately twice as potent.

Interestingly, VOLY (**3-38**) was less active in the assay than **3-10**, meaning that there could be a window in which VOLY can be used as a pro-drug, which upon liberation by the exogenous enzyme Lig-F, could inhibit the TGF-β pathway in areas local to the tumour cells bearing Lig-F.

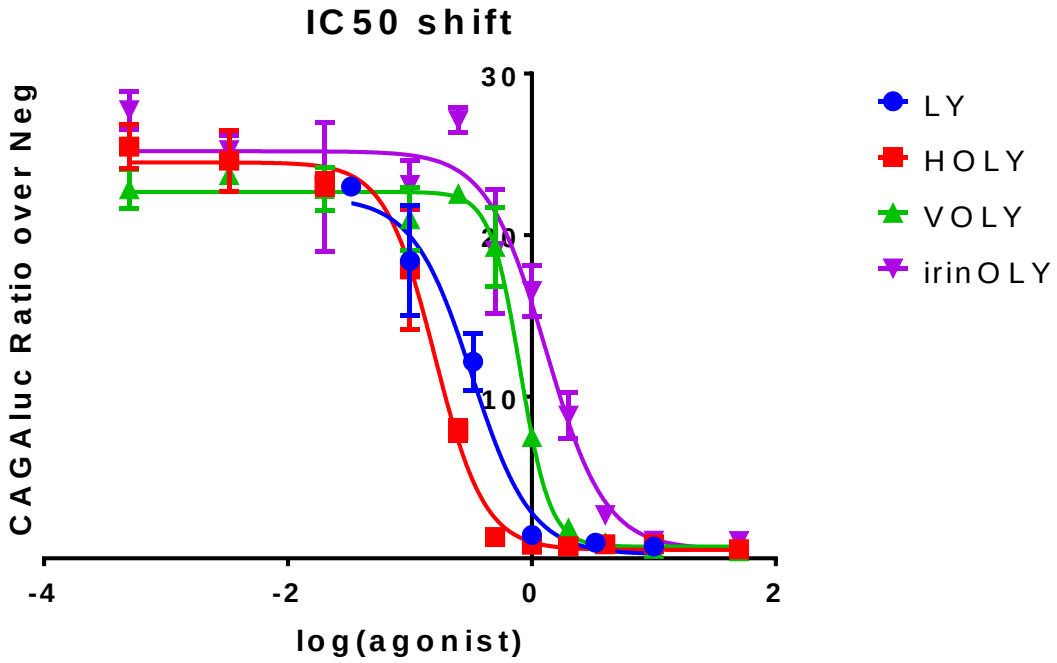


**Figure 3.17.** Comparison of the IC50 values of LY, HOLY, VOLY and IrinOLY.

As the cell culture did not contain the carboxyl esterases found in the liver, kidneys and intestine, we then moved to testing the three compounds *in vivo*.

Mice intrasplenically injected with mouse tumour organoids (see section 3.2.3) were treated on day 14 after tumour implantation with the compounds in wateous vehicle by gavage, twice daily. After 3 days, mice were sacrificed and tumours were taken; fixed slices were analysed by immunohistochemistry (Figure 3.18). Whereas SMAD2 phosporylation was clearly visible in the nuclei of stromal cells in tumour treated with vehicle control alone, Both HOLY and IrinOLY successfully abrogated TGF-β signalling to comparable extent as **3-1**. This suggests that IrinOLY was activated *in vivo* to generate HOLY, although specific evidence (such as serum detection of HOLY) was not collected.

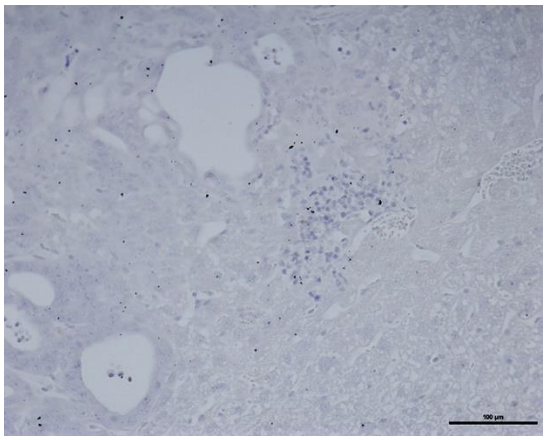

IrinOLY

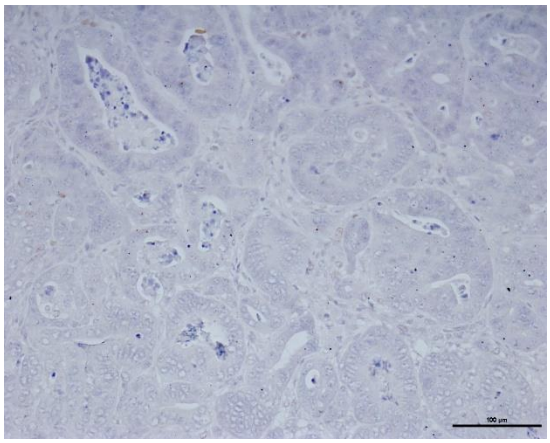

HOLY

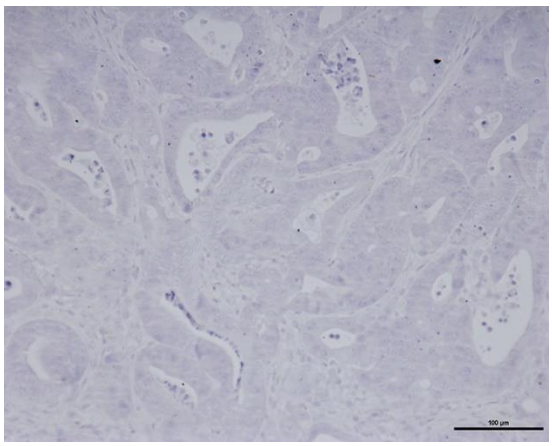

LY

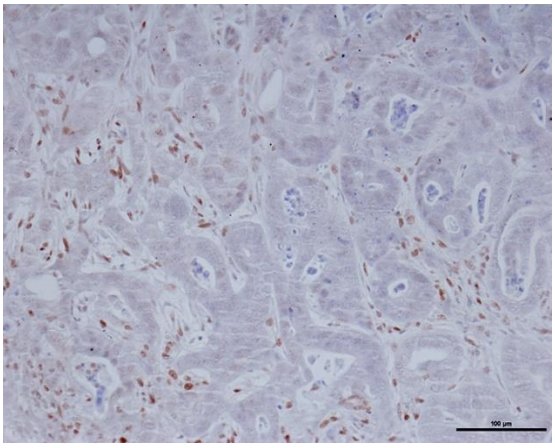

Control

**Figure 3.18.** pSMAD staining of tumours taken from *in vivo* experiments. (pSMAD can be seen in by the presence of the brown stained stromal cell nuclei in the control slide.).

We conclude that HOLY is an active TGF-β inhibitor with potential for derivitization, allowing both more soluble prodrugs, as well as locally and selectively cleavable prodrugs.

To compare *in vivo* efficacy of HOLY with **3-1**, we titrated twice-daily doses needed for inhibition of liver metastasis initiation in our mouse model (see section 3.2.3), comparing to an equivalent of the used human dose for **3-1** in clinical trials: 80 mg/kg. In mice, **3-1** only effectively works at doses at least 3-fold higher than the human dose, and frequently a 9x or 10x dose is used in the Batlle lab for reproducible inhibition of tumour formation. HOLY however, not only works effectively at human doses, but even at a 3-fold reduced dose (Figure 18).

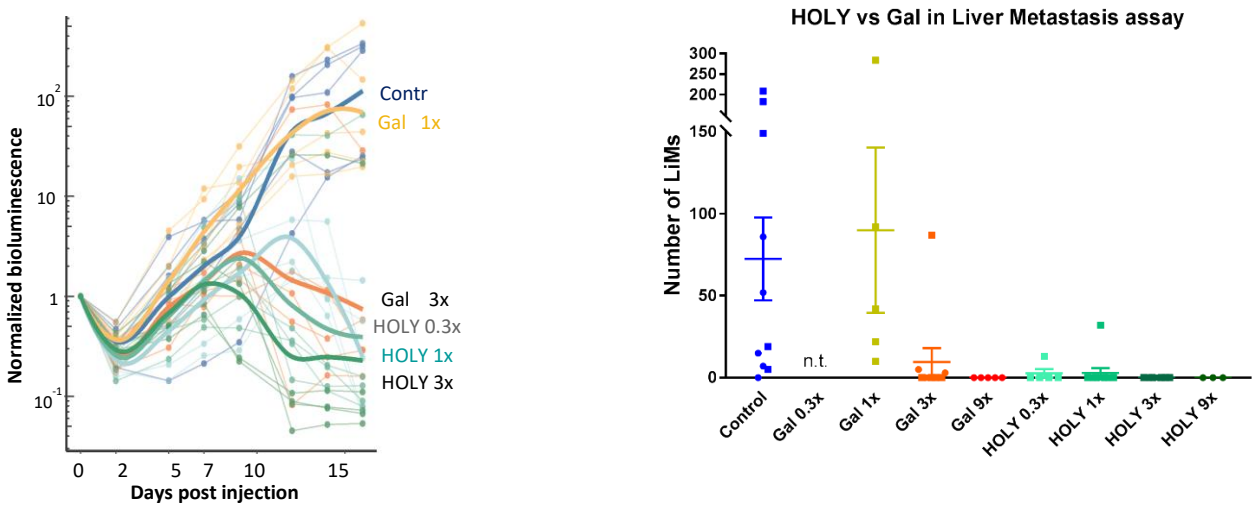


**Figure 3.19**. *In vivo* efficacy of **3-10** compared to **3-1**, at different doses. Left: quantification from bioluminescence imaging, individual mice and group LOESS averages are shown (thin and thick lines, respectively), normalized to the signal on the day of injection. Right: the number of counted liver metastases (LiMs) at the endpoint; day 24. Included are data from a separate experiment studying the dose range 1x-3x-9x. *n.t.: not tested.*

This indicates that the *in vivo* efficacy of HOLY is strongly improved when compared to **3-1**, to surprising levels when considering the moderate *in vitro* $IC_{50}$. This might have something to do with PD/PK characteristics.

In addition, the Batlle group together with Neus Prat of the IRB Barcelona histopathology department have analysed the murine toxicity profile of **3-1** and **3-10**. While the stronger efficacy of HOLY is associated to a hugh toxicity when using the 9x dose often required of galunisertib, toxicity of HOLY at effective doses 1x or lower the human equivalent were not associated with any toxicity studied. These studies include analyses of the heart valves, intestines, skin, liver, and thoracic and long bone cartilagous areas, with the latter two most affected at higher doses, sometimes leading to a caved in sternum (pectus excavatum) or an expansion in the epiphyseal bone formation zone (Table 3.6).

| Side effect | Gal (LY) | | | HOLY | | |
|---|---|---|---|---|---|---|
| | 1x | 3x | 9x | 0.3x | 1x | 3x |
| Pectus excavatum | 0 | ~10% | ~80% | 0 | 0 | ~25% |
| Epiphyseal expansion | 0 | 0 | n.d. | 0 | 0 | ~20% |
| **Cure rate** | **0%** | **~70%** | **~100%** | **~90%** | **~90%** | **100%** |

**Table 3.6**: Efficacy and toxicity comparison Gal vs HOLY. *0 is not observed; n.d: not determined*.

Together, this unexpectecly promising result suggests that HOLY, besides its advantages in derivatization, is by itself an interesting drug for further (commercial) development. A BioMedTec proposal has been submitted (together with the Batlle lab) to IRB Barcelona and Obra Social La Caixa to validate additional preclinical characteristics. Pending the outcomes, a patent will be drafted based on the strengths of HOLY, as well as the potential in further derivatives. In particular, if systemic doses of HOLY might still provoke some toxicity (be it likely reduced compared to galunisertib), targeted cleavage of a prodrug in e.g. the liver (site for most metastases for CRC patients) would be a major advantage in drug delivery and immunotherapeutic safety.

## 3.6 Conclusions

We synthesised hundreds of grams of the TGF-β inhibitor LY2157299 (**3-1**) developed by Eli Lilly and Company in order for the Batlle lab to carry out further *in vitro* and *in vivo* experiments to see the role that TGF-β plays in colorectal cancer. During synthesis of larger batches, we found that the particle size was larger due to slower crystallisation conditions and this resulted in difficulties in the formulation process. The particle size was reduced by a final fast precipitation process which we developed. These efforts resulted in three publications in high-impact jounals, namely Cancer Cell, Nature Genetics, and Nature.

We then designed a novel TGF-β inhibitor based on **3-1** with a phenol present, enabling the compounds properties to be modified as desired. First a small quantity of this new TGF-β inhibitor **3-10** (which we named HOLY) was made following a retrosynthetic analysis. It was then submitted to biological testing where it was shown to be 3 times more active than LY2157299. With these poisitive results, we then designed and carried out a scalable synthesis. With larger quantities of HOLY in hand, we transformed it into a compound which showed increased solubility in water, allowing for a far simpler formulation process for the subsequent *in vivo* experiments. This was then tested *in vivo* showing that it was able to inhibit TGF-β in a model system in the lab of Dr Eduard Batlle.

Surprisingly HOLY showed fewer side effects compared to treatment with LY2157299, including a reduction in the caved sternum (pectus excavatum) or an expansion in the epiphyseal bone formation zone.

## 3.7 References


[1] U. Mundla, Sreenivasa Reddy (Eli Lilly and company), *A Pyridin Quinolin Substituted Pyrrolo[1, 2-B] Pyrazole Monohydrate as a TGF- Beta Inhibitor*, **2007**.

[2] E. C. Taylor, N. F. Haley, R. J. Clemens, *J. Am. Chem. Soc.* **1981**, *103*, 7743–7752.

[3] F. Gellibert, J. Woolven, M.-H. Fouchet, N. Mathews, H. Goodland, V. Lovegrove, A. Laroze, V.-L. Nguyen, S. Sautet, R. Wang, *et al*., *J. Med. Chem.* **2004**, *47*, 4494–506.

[4] G. Dijkstra, W. H. Kruizinga, R. M. Kellogg, *J. Org. Chem.* **1987**, *52*, 4230–4234.

[5] J. Lu, S. Rohani, *Curr. Med. Chem.* **2009**, *16*, 884–905.

[6] A. Llinàs, J. M. Goodman, *Drug Discov. Today* **2008**, *13*, 198–210.

[7] D. V. F. Tauriello, A. Calon, E. Lonardo, E. Batlle, *Mol. Oncol.* **2017**, *11*, 97–119.

[8] A. Calon, E. Espinet, S. Palomo-Ponce, D. V. F. Tauriello, M. Iglesias, M. V. Céspedes, M. Sevillano, C. Nadal, P. Jung, X. H.-F. Zhang, *et al*., *Cancer Cell* **2012**, *22*, 571–584.

[9] J. Guinney, R. Dienstmann, X. Wang, A. de Reyniès, A. Schlicker, C. Soneson, L. Marisa, P. Roepman, G. Nyamundanda, P. Angelino, *et al*., *Nat. Med.* **2015**, *21*, 1350–1356.

[10] A. Calon, E. Lonardo, A. Berenguer-Llergo, E. Espinet, X. Hernando-Momblona, M. Iglesias, M. Sevillano, S. Palomo-Ponce, D. V. F. Tauriello, D. Byrom, *et al*., *Nat. Genet.* **2015**, *47*, 320–329.

[11] D. V. F. Tauriello, S. Palomo-Ponce, D. Stork, A. Berenguer-Llergo, J. Badia-Ramentol, M. Iglesias, M. Sevillano, S. Ibiza, A. Cañellas, X. Hernando-Momblona, *et al.*, *Nature* **2018**, *554*, 538–543.

[12] S. Herbertz, J. S. Sawyer, A. J. Stauber, I. Gueorguieva, K. E. Driscoll, S. T. Estrem, A. L. Cleverly, D. Desaiah, S. C. Guba, K. A. Benhadji, *et al.*, *Drug Des. Devel. Ther.* **2015**, *9*, 4479–4499.

[13] J. Rautio, N. A. Meanwell, L. Di, M. J. Hageman, *Nat. Rev. Drug Discov.* **2018**, *17*, 559–587.

[14] H.-Y. Li, W. T. McMillen, C. R. Heap, D. J. McCann, L. Yan, R. M. Campbell, S. R. Mundla, C.-H. R. King, E. a Dierks, B. D. Anderson, et al., *J. Med. Chem.* **2008**, *51*, 2302–2306.

[15] S. Herbertz, J. S. Sawyer, A. J. Stauber, I. Gueorguieva, K. E. Driscoll, S. T. Estrem, A. L. Cleverly, D. Desaiah, S. C. Guba, K. A. Benhadji, *et al*., *Drug Des. Devel. Ther.* **2015**, *9*, 4479–4499.

[16] N. A. Meanwell, *J. Med. Chem.* **2011**, *54*, 2529–2591.

[17] K. N. Campbell, I. J. Schaffner, *J. Am. Chem. Soc.* **1945**, *67*, 86–89.

[18] T. Cohen, A. G. Dietz, J. R. Miser, *J. Org. Chem.* **1977**, *42*, 2053–2058.

[19] S. Maurer, W. Liu, X. Zhang, Y. Jiang, D. Ma, *Synlett* **2010**, *2010*, 976–978.

[20] R. Paul, M. Ali, T. Punniyamurthy, *Synthesis (Stuttg).* **2010**, *2010*, 4268–4272.

[21] P.-Y. Bounaud, C. R. Smith, E. A. Jefferson, *Bicycle Triazoles as Protein Kinase Modulators*, **2008**.

[22] O. Baron, P. Knochel, *Angew. Chemie Int. Ed.* **2005**, *44*, 3133–3135.

[23] V. Bagutski, R. M. French, V. K. Aggarwal, *Angew. Chemie Int. Ed.* **2010**, *49*, 5142–5145.

[24] D. G. Hall, *Boronic Acids*, Wiley-VCH Verlag GmbH & Co. KGaA, Weinheim, Germany, **2011**.

[25] T. Ishiyama, M. Murata, N. Miyaura, *J. Org. Chem.* **1995**, *60*, 7508–7510.

[26] M. Peña-López, M. Ayán-Varela, L. A. Sarandeses, J. Pérez Sestelo, *Chemistry* **2010**, *16*, 9905–9909.

[27] A. D. Ainley, F. Challenger, *J. Chem. Soc.* **1930**, 2171–2180.

[28] H. G. Kuivila, A. G. Armour, *J. Am. Chem. Soc.* **1957**, *79*, 5659–5662.

[29] G. G. Chabot, *Clin. Pharmacokinet.* **1997**, *33*, 245–259.

[30] R. H. Mathijssen, R. J. van Alphen, J. Verweij, W. J. Loos, K. Nooter, G. Stoter, A. Sparreboom, *Clin. Cancer Res.* **2001**, *7*, 2182–2194.

# Chapter 4

# Guaymoxifen Background

# 4 Guaymoxifen Background

## 4.1 Introduction and history of Cre recombination

To silence a gene and study the resulting effects, a scientist has a few tools and methods at hand that he or she can use. 'Gene knockdown' is one of these and involves reducing the expression of the target gene. Common ways to achieve this alteration include small double-stranded interfering RNA (siRNA) as well as short-hairpin RNA (shRNA).[1][2] Both work in a similar fashion by binding specifically to the mRNA molecules produced from the transcription of the gene of interest. These newly formed sh/si-RNA-mRNA complexes are then degraded by natural biological processes, resulting in an overall decrease in the expression level of the target protein.

On the other hand, the complete and specific deletion of a gene from an entire genome is known as a 'knockout'. This is obtained by replacing the target gene with an artificial piece of DNA, which does not contain the genetic information necessary to express the corresponding protein. Usually, this artificial oligonucleotide contains a selection marker, such as neomycin resistance, so that cells whose transfection has been successful can be selected by survival after exposure to this antibiotic and be used in *in vitro* experiments. However, if mouse embryonic stem cells were genetically modified with such constructs, these cells could then be introduced into blastocysts (200-300 cells post fertilisation) and implanted into a surrogate mouse. Following a well-established breeding protocol, eventually a homozygous transgenic mouse is created and the effects of the knockout gene can be studied.[3] Difficulties arise though when this gene is essential for the growth and survival of the model being used. For example, TGF-β 1 null mice do not survive beyond 3-4 weeks due to organ failure.[4]

Since the 1990's, scientists have been trying to overcome the hurdles of conventional gene targeting. The efforts led to the development of what is known as a conditional gene knockout. The use of site-specific recombinase (SSR) systems, such as Flp/FRT and Cre-*Lox*, made possible to specifically knock-out a gene in a particular cell type and at a certain developmental stage.[5][6]

In the case of Cre-*Lox* recombination, the model needs to express a site-specific DNA recombinase known as Cre (**C**auses **re**combination) protein, preceded by a promoter of choice. The genome is also edited in such a way so that the gene of interest is flanked by two recognition sequences known as

*LoxP* (locus of X-over P1) sites. These serve as binding sites for the Cre enzyme, which upon their expression, acts as a pair of genomic scissors specifically cutting the DNA at the recognition sites (Figure 4.1). Depending on the directionality of the *LoxP* sites, the target gene can either be inverted or knocked out.

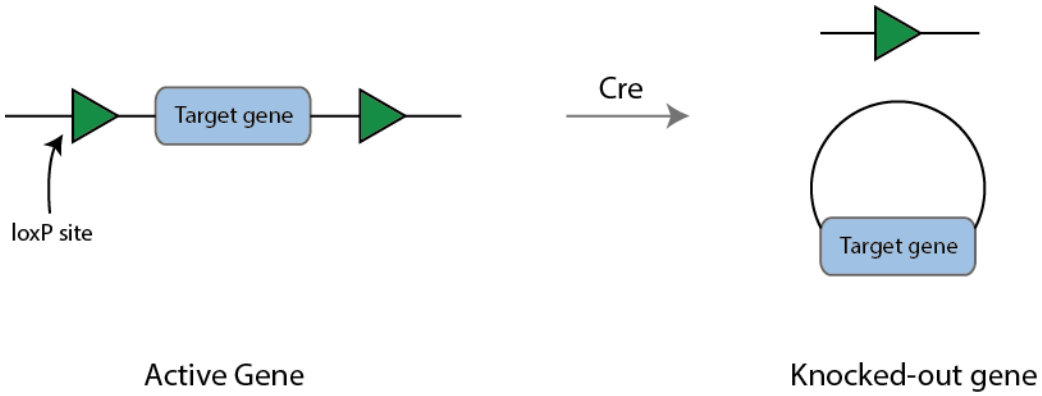


**Figure 4.1.** Illustration of a LoxP floxed gene before and after Cre recombination.

The success of this technology lies in the spatio-temporal control of the recombinase activity by means of the selected promoter. The use of a tissue-specific promoter is what allows for cell-type specificity. However, the Cre-promoter can be also combined with an inducible expression system, which is then responsible for the stage-specificity of the knockout. The transgenic animal develops as per the wild-type, until the moment when the activity of the promoter is purposely triggered by an exogenous source. Upon exposure to this external stimulus, the target gene is deleted from the genome and the function of its products can be studied.[7]

The most common inducible system for spatiotemporally controlled somatic mutagenesis was the tamoxifen (T)-inducible system. In this system, Cre is fused to a modified form of the oestrogen receptor (ER) called $ER^T$. This consists of the ligand binding domain of the natural receptor, however, mutated so not to have any affinity for the natural ligand 17β-oestradiol.[8] Instead, $ER^T$ binds the synthetic oestrogen antagonists ICI 182780 as well as tamoxifen - a common breast cancer drug - and its active metabolite 4-hydroxytamoxifen (4-OHT) (Figure 4.2).[9] This was later taken over by the $ER^{T2}$ variant due to its more specificity to 4-OHT.[10]

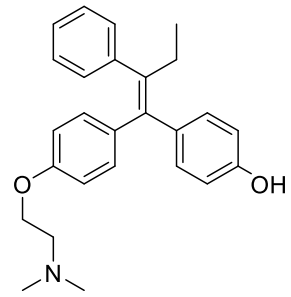


4-hydroxytamoxifen (4-OHT) **4-1**

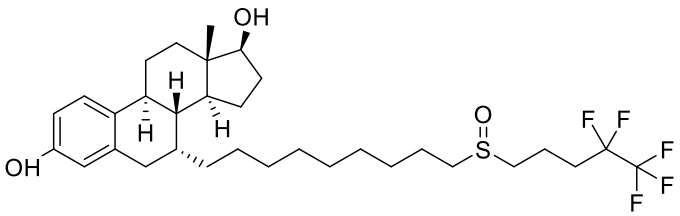


ICI 182780 (Fulvestrant)

**Figure 4.2.** $ER^{T2}$ ligands; 4-OHT (**4-1**) and Fulvestrant.

Like the natural oestrogen receptor, the Cre-$ER^{T2}$ fusion protein resides in the cytoplasm until the ligand binds to the receptor causing the nuclear translocation of the complex. Once in the nucleus, the Cre-$ER^{T2}$ complex recognises the *LoxP* sites and the Cre recombinase is finally able to exercise its function.

## 4.2 Tamoxifen

Tamoxifen was developed in the United Kingdom by Doris Richardson in 1966 at ICI (what is now AstraZeneca), and approved for use in postmenopausal patients with metastatic breast cancer in 1973.[11] Four years later, in 1977, it was also approved by the Food and Drug Administration (FDA) for use in the USA.[12]

Tamoxifen (**4-2**) is a **s**elective o**e**strogen **r**eceptor **m**odulator (SERM) whose mechanism of action is still poorly understood, however in breast tissues, it acts as an oestrogen antagonist thus inhibiting the growth of oestrogen-dependent tumours.[13] Although tamoxifen itself shows affinity to the oestrogen receptor, the active metabolites 4-hydroxy tamoxifen (**4-1**) and *N*-desmethyl-4-OHT (**4-3**) have ca. 100 fold higher affinity to the oestrogen receptor when compared to the parent compound (Figure 4.3). [14]

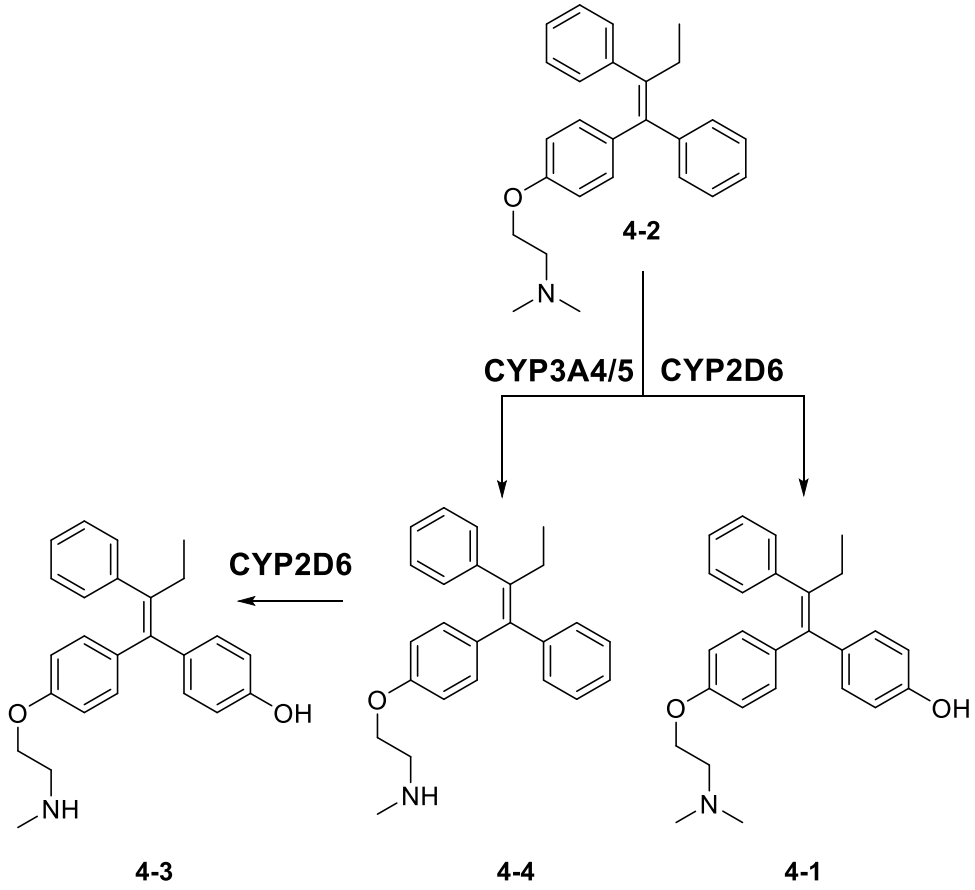


**Figure 4.3**. Tamoxifen and its main metabolites.

The difference in activity, however, is not limited only to its metabolite, but also to the *cis*/*trans* isomer of each tamoxifen derivative.

### 4.2.1 *Cis-trans* isomerism of tamoxifen and its metabolites

Due to the presence of a tetra-substituted double bond in its structure, tamoxifen as well its metabolites can exist as two isomers: either the (*E*) or the (*Z*) form (Figure 4.4). The two stereoisomers were found to have different affinities for the oestrogen receptor. In 1984, Katzenellenbogen *et al.* conducted an *in vitro* study using the MCF-7 breast cancer cell line, in which they evaluated the affinity to the oestrogen receptor of both (*E*)- and (*Z*)-tamoxifen as well as their respective 4-hydroxy metabolites. They compared the compounds affinity with respect to the endogenous ligand oestradiol, and concluded that if estradiol affinity to ER was defined as 100%, (*E*)-tamoxifen relative binding affinity was 0.3%, (*Z*)-tamoxifen was 2.5%, (*E*)-4-hydroxy tamoxifen was

1.8% and finally (*Z*)-4-hydroxy tamoxifen 310%. Cells treated with (*E*)-tamoxifen responded in a similar manner to cells treated with oestradiol. Specifically, (*E*)-tamoxifen was able to stimulate cell growth and to increase the activity of the plasminogen activator thus acting as an agonist, although as a very week one ($10^{-6}$ M needed vs $10^{-10}$ M for oestradiol). On the other hand, both 4-hydroxy analogues and the (*Z*)-tamoxifen displayed antagonistic properties by inhibiting cell growth.[15]

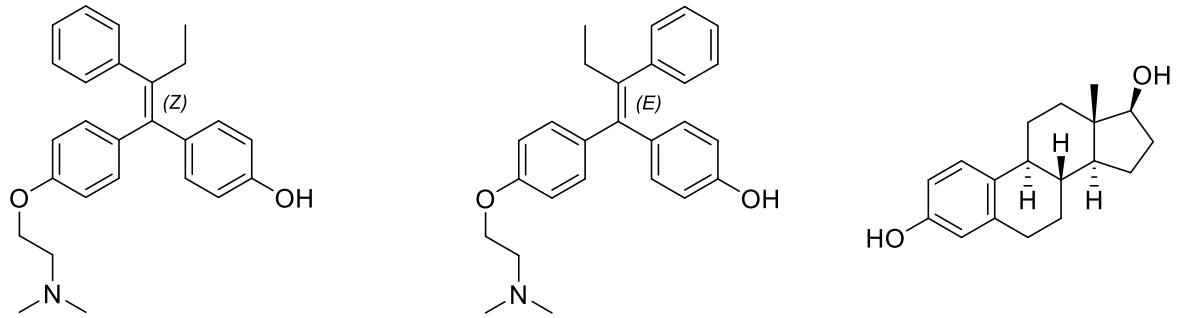


**4-1 (*Z*)** **4-1 (*E*)** Estradiol

**Figure 4.4**. Structures of (*E*) and (*Z*) - 4-hydroxytamoxifen, and estradiol.

## 4.2.2 Tamoxifen synthesis

In 1982, the group of Katzenellenbogen described one of the first syntheses of tamoxifen as shown below in Scheme 4.1.[16] The synthesis involves the Friedel-Crafts acylation of phenyl acetic acid with anisole forming compound **4-5**. The position in α to the ketone can then be deprotonated with a strong base and subsequently alkylated with iodoethane. Demethylation of the anisole residue is achieved in good yield using lithium ethane thiolate, and the newly formed phenol **4-7** is alkylated with 2-(dimethylamino) ethyl chloride to give product **4-8**. This can then be attacked at the carbonyl with phenyl magnesium bromide, and after acidic dehydration a 1.3:1 mixture of (*Z*):(*E*) tamoxifen.

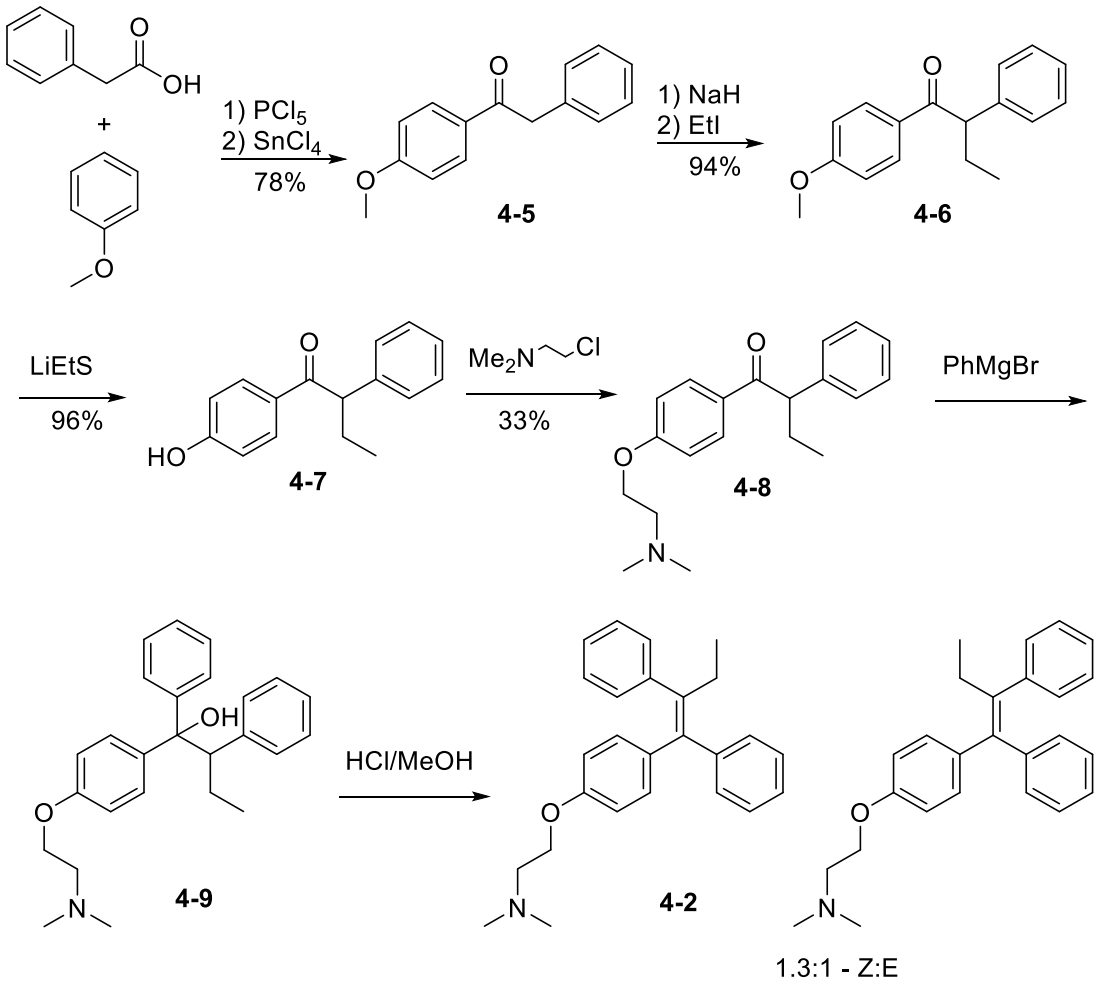


**Scheme 4.1**. Katzenellenbogen synthesis of tamoxifen.

Interestingly it possible to separate the mixture into each pure isomer using 9:1 benzene/trimethylamine, however, this would be impractical on an industrial scale.

Due to the fact that the (*Z*) isomer is the active form and that the (*E*) isomer acts as an agonist, it is necessary to make tamoxifen as only the (*Z*) isomer.

### 4.2.3 Stereospecific 4-hydroxytamoxifen synthesis

As mentioned above, 4-hydroxytamoxifen also can exist in either the (*E*) or the (*Z*) isomer. Although the molecule appears to be relatively simple, a synthesis arriving at just one of the isomers is a challenging one. Similar procedures have been employed to that of the synthesis of tamoxifen, although achieving a mix of isomers.[17][18]

The first stereospecific synthesis of 4-hydroxytamoxifen involved the carbometallation of alkynyl-silanes followed by subsequent coupling reactions as shown in Scheme 4.2.[19]

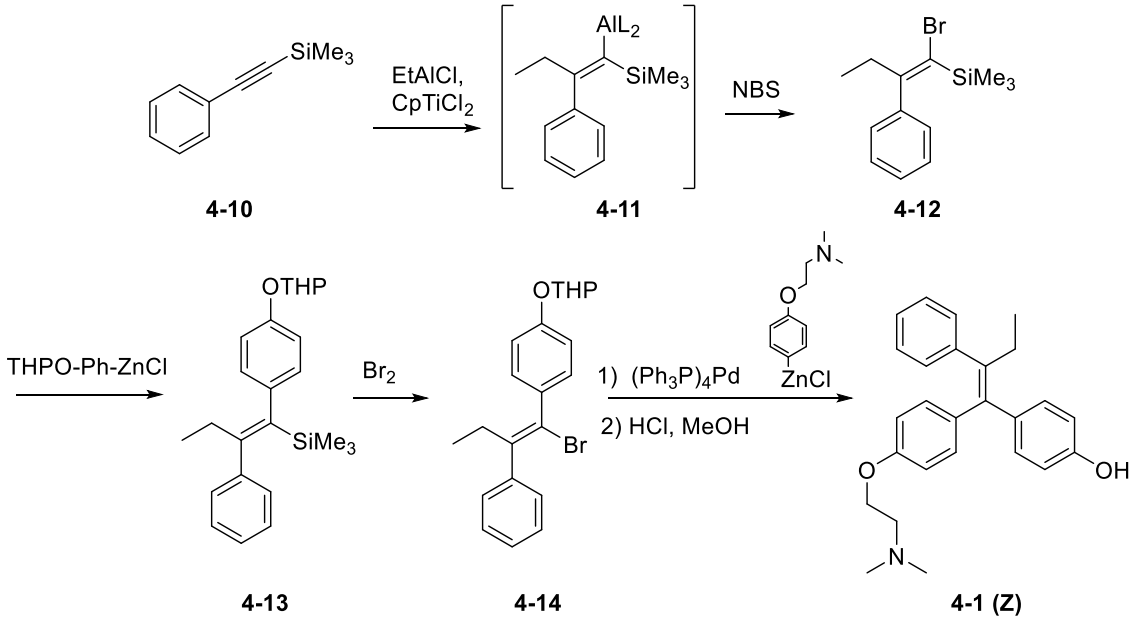


**Scheme 4.2.** The first stereospecific synthesis of 4-OHT.

This involves the addition of an ethyl chain and aluminium across the same face of the triple bond of **4-10** regioselectively. The subsequent exchange of the aluminium for a bromine followed by Negishi coupling gives the silylated intermediate **4-11**. This intermediate can then undergo silicon-bromine exchange giving **4-12**, and following a further Negishi coupling and acidic THP protection gives stereomerically pure 4-hydroxytamoxifen **4-1 Z**.

As this process is rather lengthy and time-consuming, Gauthier *et al*. published in 1996 a much shorter synthesis with the key step being the McMurry reaction as shown below in Scheme 4.3.[20]

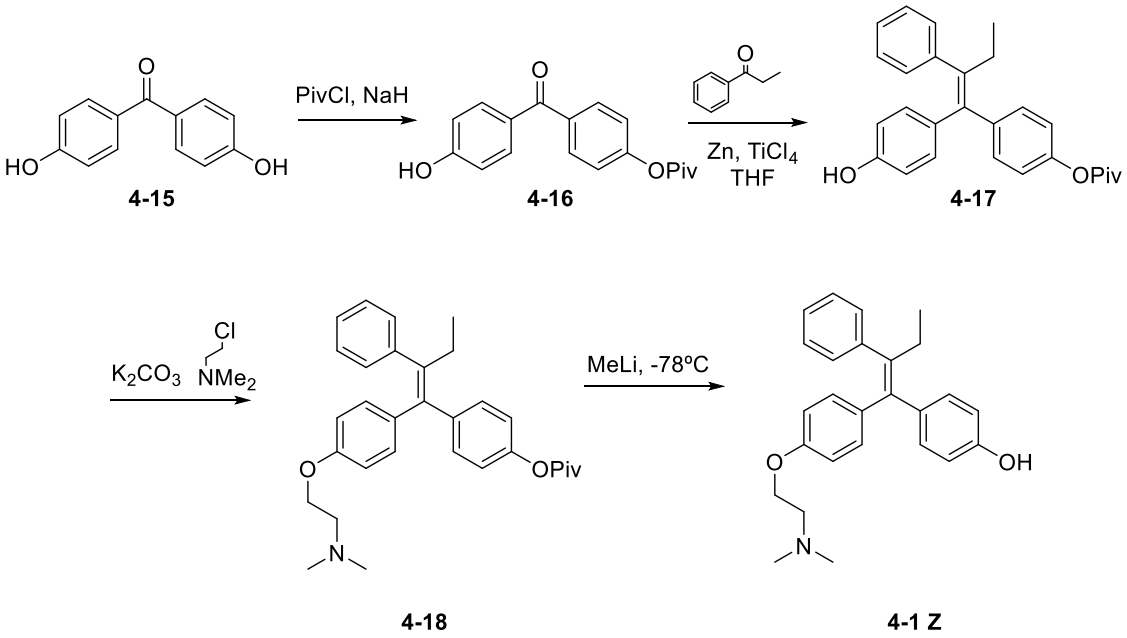


**Scheme 4.3.** Gauthier *et al.* synthesis of (*Z*)-4-OHT.

Desymmetrisation of the 4,4'-dihydroxybenzophenone with pivaloyl chloride afforded the corresponding ester **4-16**, which was then submitted to the McMurry reaction with propiophenone. This key step in this route is the McMurry reaction – the product of the reaction (**4-17**) has an E:Z ratio of 14:1 and following trituration from methanol, this increased to >100:1. The phenol of **4-17** was then alkylated with 2-(dimethylamino)ethyl chloride giving **4-18**, and following deprotection of the pivaloyl with MeLi at -78$^{o}$C and the following trituration from ethanol, gave 4-hydroxytamoxifen (**4-1**) in a >100:1 Z:E ratio.

Detsi *et al.* then further modified the synthesis with the use of the perfluorotolyl as the key component as shown below in Scheme 4.4[21]

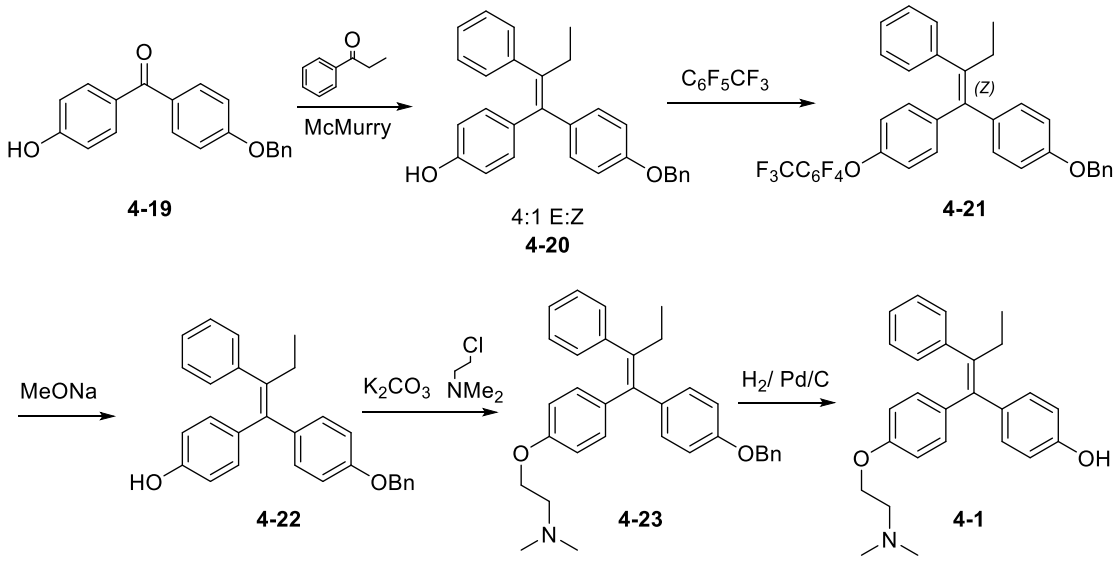


**Scheme 4.4.** Synthesis of 4-OHT by Detsi *et al.*

During the purification, intermediate **4-21** was left in the fridge where the mixture increased from 4:1 *Z*:*E* to completely the *Z* isomer. The now isomerically pure alkene could then be converted to 4-hydroxytamoxifen via selective deprotection of the perfluorotolyl group, alkylation of phenol **4-22**, and finally deprotection of the benzyl group via hydrogenolysis.

Later in 2010, Tsuji *et al.* developed methodology to synthesise 4-hydroxytamoxifen stereo- and regioselectively via the stannyllithiation of diarylacetylenes.[22] Within the paper, they described their route to *Z*-4-hydroxy tamoxifen as summarised in Scheme 4.5.

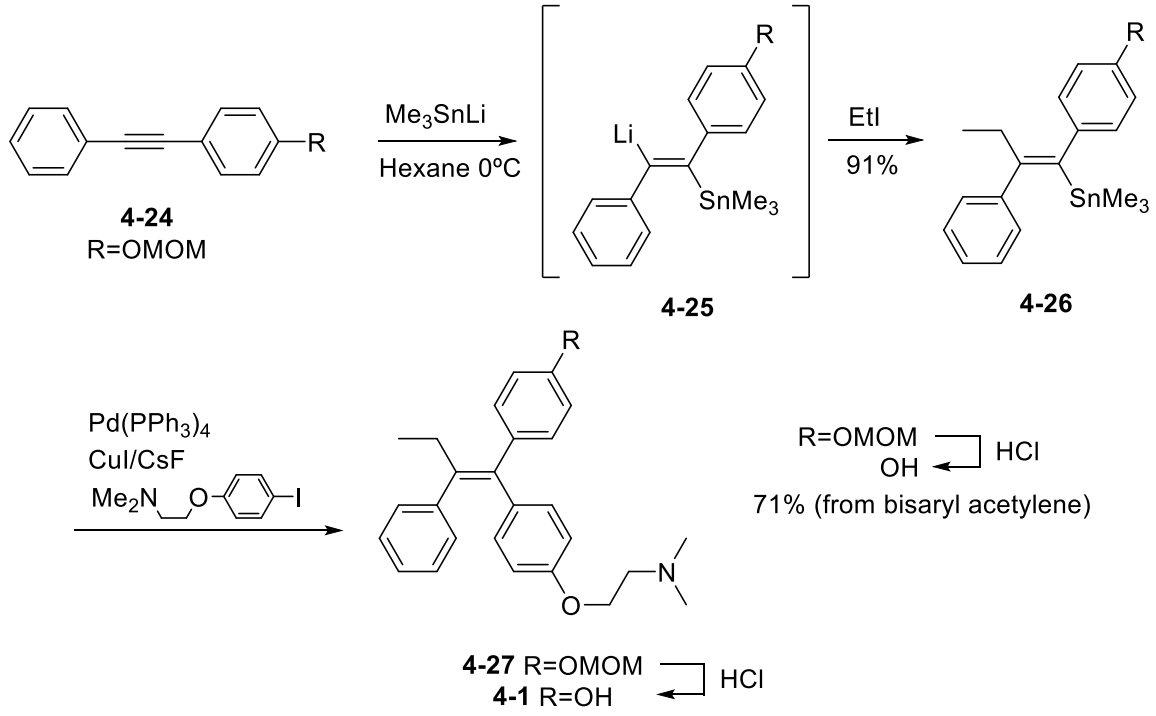


**Scheme 4.5.** Tsuji *et al.* synthesis of **4-1**.

The principle reason for the success of the selectivity of the subsequent alkylation, is that the trimethylstannyl lithium adds to the triple bond with 100% anti selectivity – the lithium ends up trans to the trimethyl tin moiety. The electronic effects of the aryl rings help control the regioselective outcome of the reaction. An electron-rich aryl places the stannyl group on the carbon to which it is itself attached.

Once the lithium intermediate **4-25** is formed, this readily attacks ethyl iodide forming stannylated intermediate **4-26**, and after a copper assisted Stille coupling, the MOM protected 4-hydroxytamoxifen is isolated. Facile removal of the MOM in acidic media liberates a mixture 95:5 of 4-hydroxytamoxifen and its regio-isomer as shown in Figure 4.6.

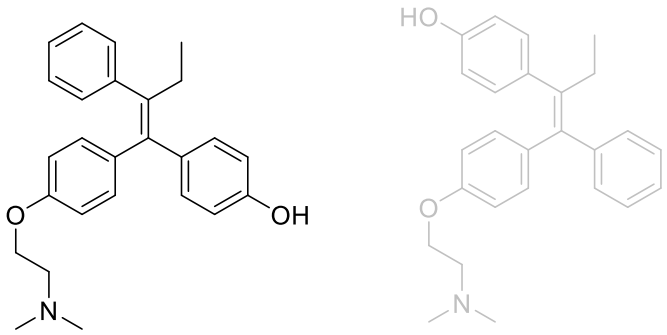


95:5

**Figure 4.6.** Ratio of final products by Tsuji *et al*.

To date, these are the main ways in which stereospecific 4-hydroxytamoxifen has been synthesised.

## 4.3 References


[1] K. a Whitehead, R. Langer, D. G. Anderson, *Nat. Rev. Drug Discov.* **2009**, *8*, 129–38.

[2] D. D. Rao, J. S. Vorhies, N. Senzer, J. Nemunaitis, *Adv. Drug Deliv. Rev.* **2009**, *61*, 746–59.

[3] C. Guan, C. Ye, X. Yang, J. Gao, *Genesis* **2010**, *48*, 73–85.

[4] A. B. Kulkarni, C. G. Huh, D. Becker, A. Geiser, M. Lyght, K. C. Flanders, A. B. Roberts, M. B. Sporn, J. M. Ward, S. Karlsson, *Proc. Natl. Acad. Sci. U. S. A.* **1993**, *90*, 770–4.

[5] S. M. Dymecki, *Proc. Natl. Acad. Sci. U. S. A.* **1996**, *93*, 6191–6.

[6] A. Nagy, *Genesis* **2000**, *26*, 99–109.

[7] M. Lewandoski, *Nat. Rev. Genet.* **2001**, *2*, 743–55.

[8] S. Hayashi, A. P. McMahon, *Dev. Biol.* **2002**, *244*, 305–18.

[9] R. Feil, J. Wagner, D. Metzger, P. Chambon, *Biochem. Biophys. Res. Commun.* **1997**, *237*, 752–7.

[10] A. K. Indra, X. Warot, J. Brocard, J. M. Bornert, J. H. Xiao, P. Chambon, D. Metzger, *Nucleic Acids Res.* **1999**, *27*, 4324–7.

[11] G. R. Bedford, D. N. Richardson, *Nature* **1966**, *212*, 733–734.

[12] V. C. Jordan, *Lancet. Oncol.* **2000**, *1*, 43–9.

[13] C. K. Osborne, *N. Engl. J. Med.* **1998**, *339*, 1609–18.

[14] D. P. Cronin-Fenton, P. Damkier, T. L. Lash, *Future Oncol.* **2014**, *10*, 107–22.

[15] B. S. Katzenellenbogen, M. J. Norman, R. L. Eckert, S. W. Peltz, W. F. Mangel, *Cancer Res.* **1984**, *44*, 112–9.

[16] D. W. Robertson, J. A. Katzenellenbogen, *J. Org. Chem.* **1982**, *47*, 2387–2393.

[17] C. Olier-Reuchet, D. J. Aitken, R. Bucourt, H.-P. Husson, *Tetrahedron Lett.* **1995**, *36*, 8221–8224.

[18] A. B. Foster, M. Jarman, O. T. Leung, R. McCague, G. Leclercq, N. Devleeschouwer, *J. Med. Chem.* **1985**, *28*, 1491–7.

[19] M. I. Al-hassan, *Synth. Commun.* **1989**, *19*, 1619–1623.

[20] S. Gauthier, J. Mailhot, F. Labrie, *J. Org. Chem.* **1996**, *61*, 3890–3893.

[21] A. Detsi, M. Koufaki, T. Calogeropoulou, *J. Org. Chem.* **2002**, *67*, 4608–4611.

[22] H. Tsuji, Y. Ueda, L. Ilies, E. Nakamura, *J. Am. Chem. Soc.* **2010**, *132*, 11854–5.

# Chapter 5

# Design and synthesis of compounds for spatiotemporal drug release

# 5 Design and synthesis of compounds for spatiotemporal drug release

## 5.1 Introduction

As explained in chapter one, our second goal was to design and develop a way to activate or delete a gene in cells at a specific location. In order to achieve this goal, and by using the Cre toolkit, we planned to locally activate the Cre enzyme by liberating 4-hydroxytamoxifen (4-OHT, **5-2**) only in cells that have encoded a specific xeno-enzyme. We selected LigF—an enzyme found in the lignin degradation pathway of the soil bacterium *Sphingobium sp.* (strain SYK6)—as the xeno-enzyme to be encoded in the DNA of tumour cells.[1] A tamoxifen prodrug was designed such that the enzymatic activity of LigF would liberate 4-hydroxytamoxifen (**5-2**). This part of the work was done by Daniele Tauriello from Batlle's group. This is conceptualised below in Figure 5.1 and Figure 5.2.

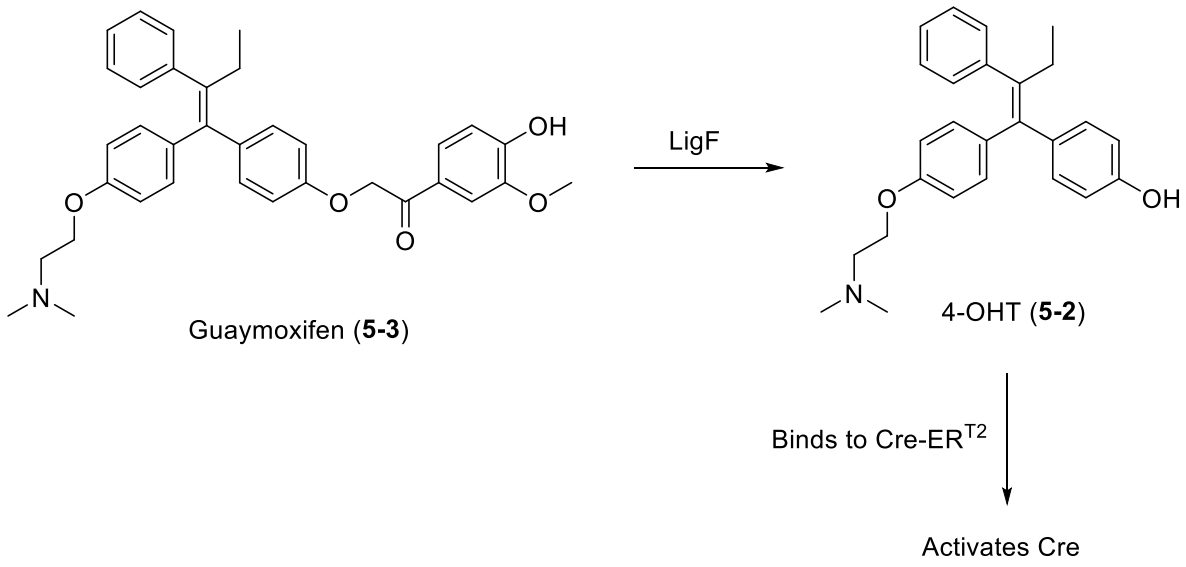


**Figure 5.1.** Schematic representation of the cleavage of the beta-ether bond, liberating 4-OHT.

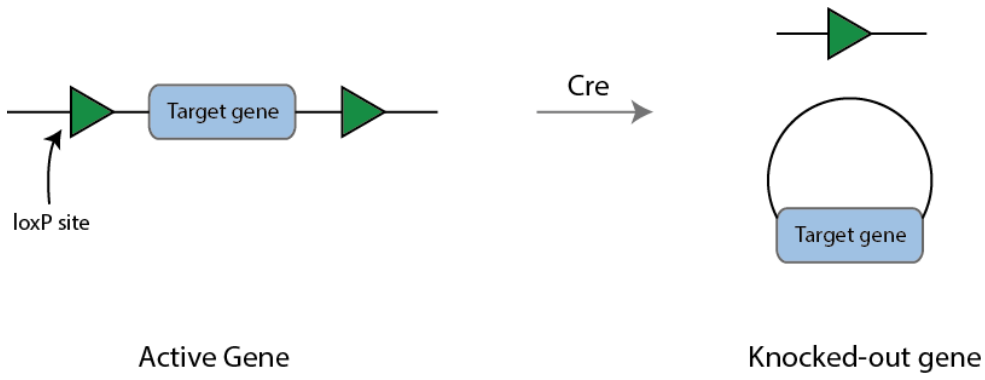


**Figure 5.2.** Effects on the target gene after recombination with Cre.

We designed the LigF recognition fragment to be attached to the phenol of **5-2**. The recognition fragment came from the skeleton of compound **5-1** which is the natural substrate of LigF. The bond highlighted in red is the one which is cleaved by the LigF enzyme, and would be also the point of cleavage in our prototype compound. Guaiacol (in grey) is liberated after the cleavage. According to our strategy, we designed compound **5-3** as our prototype compound. To simplify the synthesis, the hydroxymethyl group was removed from the recognition fragment as shown below in Figure 5.3.

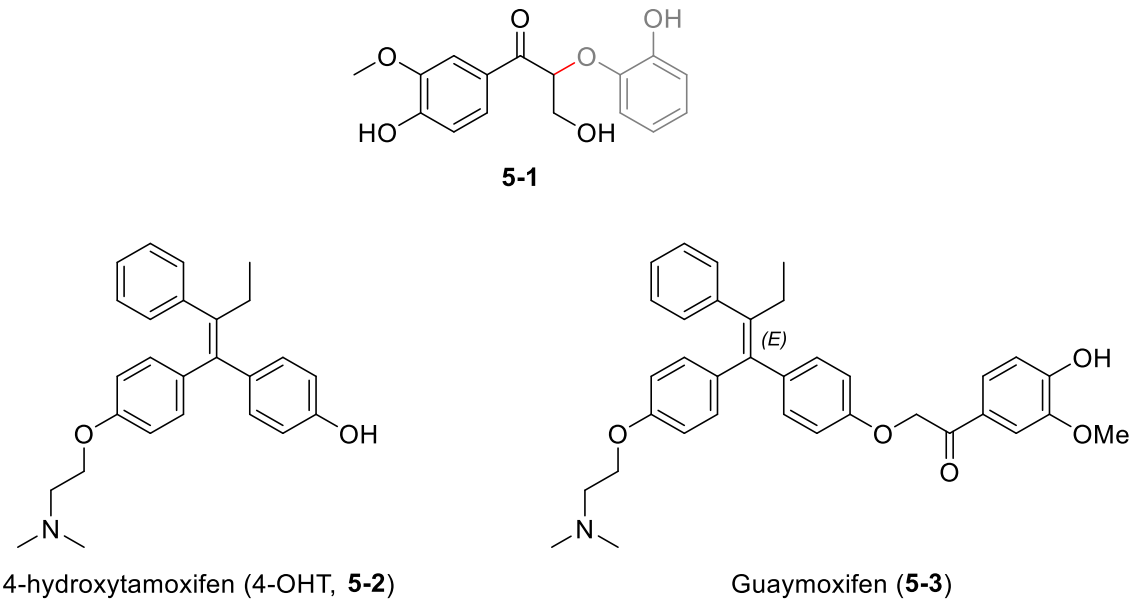


**Figure 5.3.** Structures of the natural LigF substrate (**5-1**), 4-OHT (**5-2**), and our target compound (**5-3**).

In order to study the kinetics of the cleavage of the ether bond in **5-3**, and also to know the selectivity of the enzyme for the recognition fragment, we thought that it would be easier to start liberating a fluorescent compound instead of liberating **5-2**. Consequently, we used model compound **5-4a** as a system to check if LigF worked in our hands (and inside our cancer cells), liberating the fluorescent 4-methylumbelliferone (**5-5,** 4-MU).

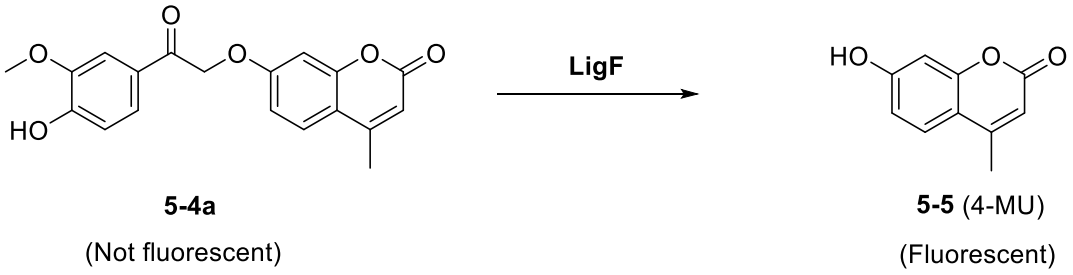


**Scheme 5.1**. Cleavage of the ester bond of **5-4a** by LigF, releasing **5-5**.

## 5.2 Testing the activity of the xeno-enzyme LigF

### 5.2.1 Synthesis of compound 5-4a

The synthesis of compound **5-4a** was planned by alkylation of the bromoketone **5-8a** with **5-5**, followed by deprotection of the benzyl group, giving the desired phenol. This was prepared following the procedure developed by Reiter *et al.*[1] The synthesis of **5-8a** was achieved by protecting the acetovanillone phenol **5-6** as a benzyl ether with a near-quantitative yield. Without any further purification, the crude of **5-7a** was then dissolved in ethanol at 60°C where bromine was added dropwise. The by-product of the reaction is HBr which conveniently self-catalyses the reaction, forming the enol which then attacks the molecular bromine. Simply cooling the reaction mixture to zero degrees afforded the crystallisation of the desired product **5-8a** from the reaction mixture, which could be then isolated as a white solid via filtration.

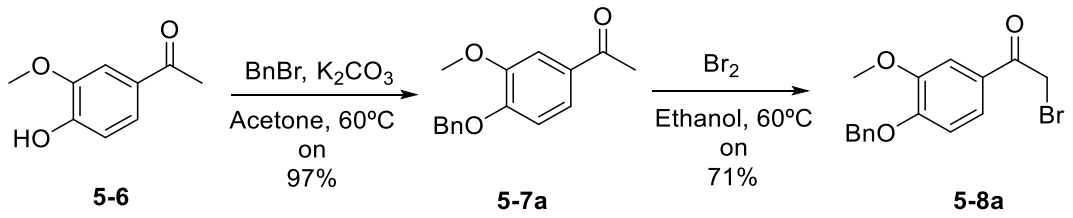


**Scheme 5.2.** Synthesis of **5.8a**.

We used pure alpha-bromo ketone **5-8a** to alkylate 4-methylumbeliferone (4-MU) giving intermediate **5-4b**. The benzyl group could then be removed by hydrogenolysis giving the compound **5-4a** (Scheme 5.3).

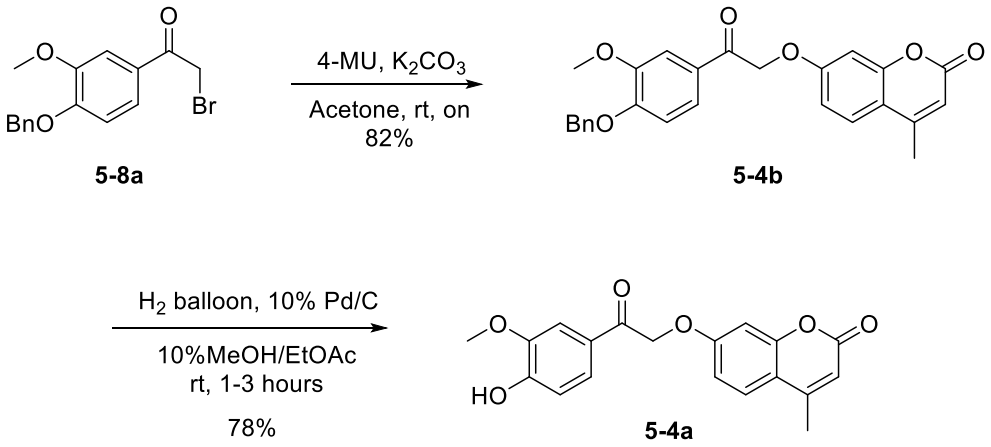


**Scheme 5.3.** Synthesis of **5-4a**.

## 5.2.2 Enzymatic *in vitro* cleavage of 5-4a by LigF

To test the enzymatic activity of LigF towards compound **5-4a**, pure LigF protein was needed. It was expressed by the Protein Expression Core Facility within the IRB Barcelona by inserting the His-tagged LigF DNA into a pOPINF vector and expressed in E. coli BL21 (DE3) Rosetta lysS cells. After expression and lysis, the protein was purified by using a nickel column followed by gel filtration. Noteworthy, the His tags were not removed from the protein after purification.

Due to a rapid rate of production of 4-MU (**5-5**) owing to the cleavage of the beta-ether bond of compound **5-4a**, we modified the protocol described by Masai by lowering the LigF enzyme loading.[2] With this optimised protocol now in hand, we incubated compound **5-4a** at room temperature in the presence of a buffer, glutathione (GSH) and LigF, and followed the cleavage by observing the production of 4-MU by fluorescence. Appropriate controls including wells containing no GSH, no LigF, and no **5-4a** were performed to ensure that the ether bond simply wasn't decomposing under the assay conditions and that it was, in fact, the enzyme doing the cleavage. This also confirmed that there wasn't an artefact present other than **5-5** which was contributing to the fluorescence. Gratifyingly, enzyme LigF cleaved product **5-4a** in approximately 30 min. As can be seen in Figure 5.4, after 40 minutes the reaction reached a plateau and did not progress further so we concluded that it reached completion.

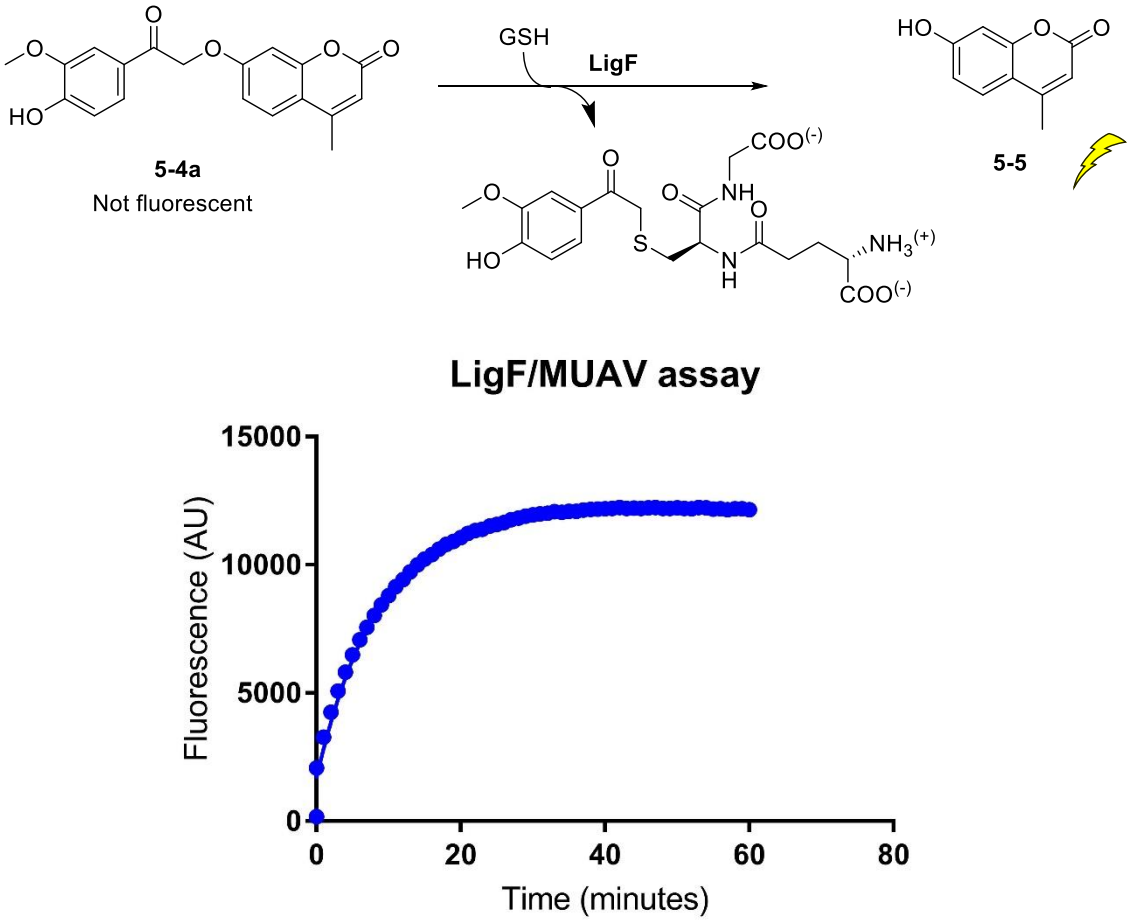


**Figure 5.4.** A graph to show the production of **5-5** vs. time.

Now knowing that **5-4a** was cleaved by LigF in the presence of GSH and in a buffer and was stable in the reaction media without LigF, we wanted to see if **5-4a** remained stable to the conditions found inside a cell. We also wanted to see if the xeno-enzyme would be able to cleave the beta ether bond in the cellular assay. A cellular assay is more complex due to the fact that there are many other proteins present when compared to the *in vitro* assay mentioned above. This experiment would provide more insight into the cellular permeability and stability of **5-4a**.

HEK293T cells were stably transduced with a lentiviral vector containing the bacterial LigF coding sequence under control of the phosphoglycerate kinase (PGK) promoter. Also encoded in the sequence was a resistance gene for puromycin. This was used as a selection tool so only the cells which had successfully incorporated the new DNA into their own genome survived exposure to

puromycin. With these cells now prepared, we proceeded to perform an *in vitro* cellular assay to measure the cleavage of the **5-4a** by LigF to produce 4-MU (**5-5**)

To the cell medium was added various concentrations of **5-4a**, namely 10, 30 and 100 µM. The cells were left under the appropriate conditions (see experimental section) where at various time points, aliquots of the cell medium were removed and the fluorescence was measured for each sample.

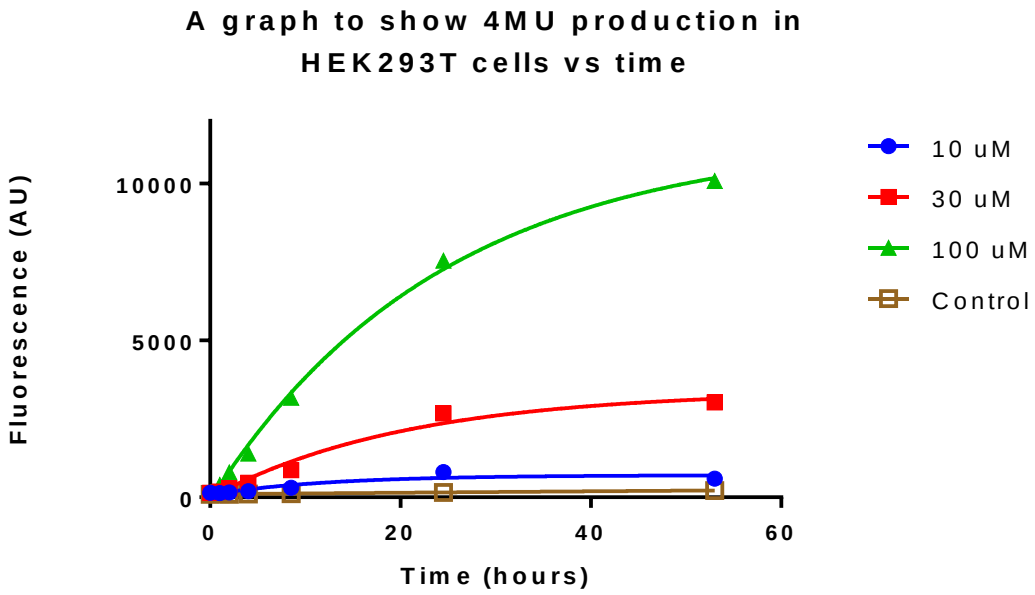


**Figure 5.5.** Production of 4-MU vs time.

As can be seen in Figure 5.5, the ether bond of **5-4a** was indeed cleaved by the LigF expressed by the cells. Importantly, no cleavage was observed in the control experiment: HEK293T cells expressing an empty vector (and not LigF). Increasing concentrations of **5-4a** resulted in increasing levels of fluorescence, meaning that more 4-MU was present which in turn means that more cleavage of the ether bond was being observed. These experiments indicated that LigF has activity inside mammalian cells and that there is no other enzyme capable of cleaving the beta ether bond, at least in the cells tested.

### 5.2.3 Optimisation of the recognition fragment.

Knowing now that our original system was working well with the isolated LigF both *in vitro* and in a cellular assay, we were interested in looking into the structural activity relationship (SAR) between the recognition fragment and the LigF enzyme. This would not only allow us to optimise the interaction between the LigF and the recognition fragment, but would also allow us to modulate the physical properties such as solubility, and also make it as close as possible to obeying Lipinski's rule of five. At this point, it was important to understand the specificity of LigF for the recognition fragment for us to decide whether we needed to aim for a single molecule, or to develop a small library of potential candidates to submit for biological testing.

Given the working *in vitro* assay, we kept 4-MU as the reporter for the cleavage of the ether bond by LigF, and systematically modified the recognition part of the molecule. Taking advantage of the synthetic route previously used to make compound **5-3** (MUAV), we planned to make the analogues as depicted in Scheme 5.4 below, focussing on *meta* and *para* aryl substituents.

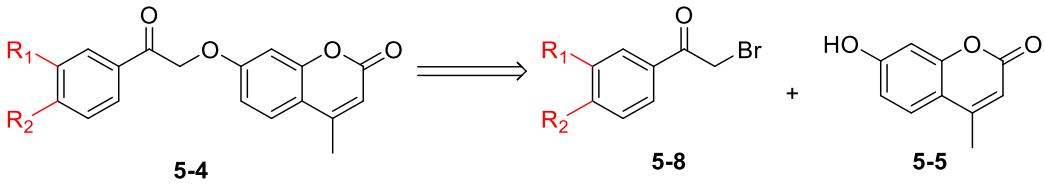


**Scheme 5.4**. Retrosynthetic analysis of the proposed SAR exploration.

These modifications would give us an indication as to which parts of the recognition fragment can be modified (perhaps improved), and which parts were essential for the activity of LigF.

The ketone precursors were either commercially available or were synthesised as follows. Compound **5-7e** was synthesised from 3,4-dihydroxybenzaldehyde (Scheme 5.5)

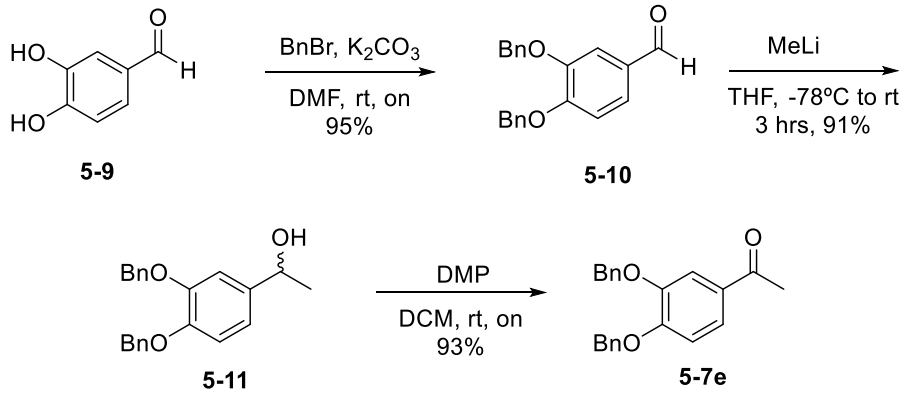


**Scheme 5.5**. Synthesis of **5-7e**.

To overcome problems with the deprotection of benzyl groups (*vida infra*), the bis-pivaloyl derivative **5-7f** was prepared.

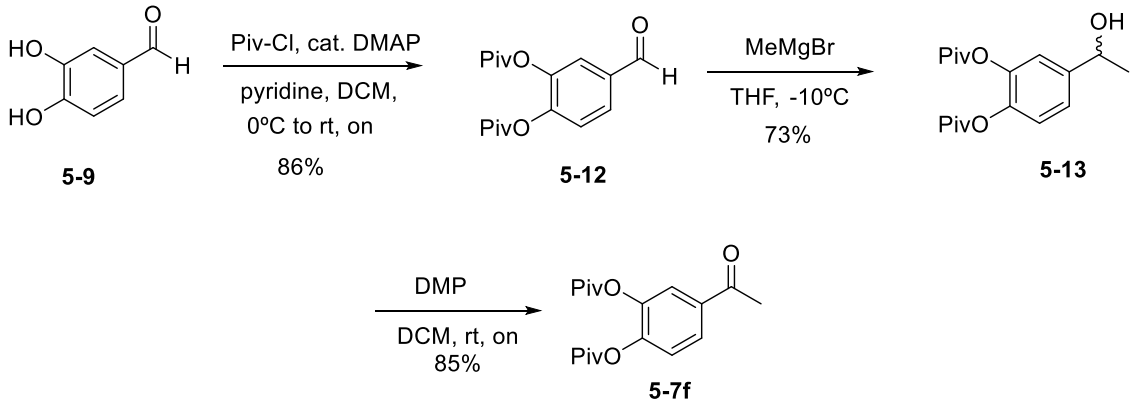


**Scheme 5.6.** Route to **5-7f**.

To finish our series of ketones needed in order to proceed to the bromination step, the phenols **5-14** and **5-15** below were protected giving the corresponding benzyl ethers.

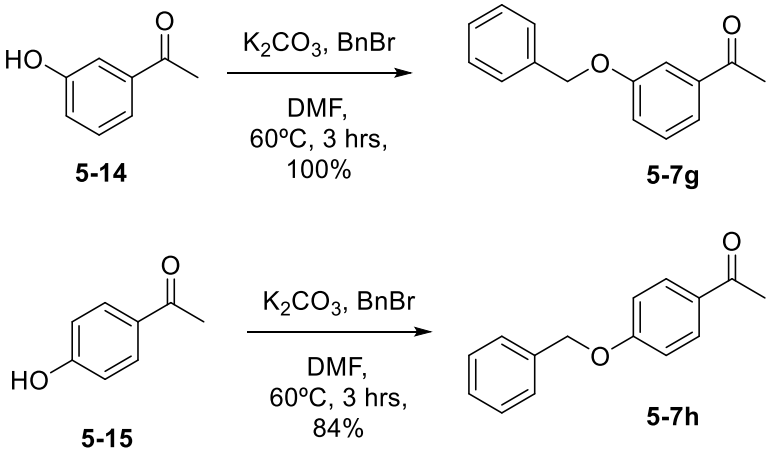


**Scheme 5.7.** Synthesis of **5-7g** and **5-7h**.

With the series of ketones in hand we then brominated them at the position alpha to the ketone. The reaction was performed under acidic conditions to prevent poly-bromination, as the haloform reaction can occur under basic conditions.

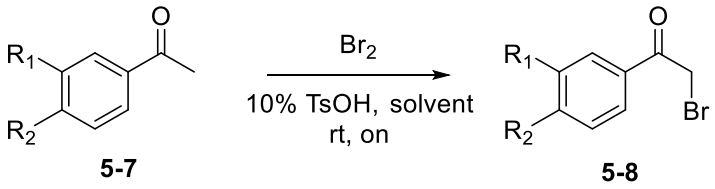


**5-7** **5-8**

| Entry | $R_1$ | $R_2$ | Solvent | Yield % | Product |
|---|---|---|---|---|---|
| **1** | OMe | OBn | EtOH | 64 | **5-8b** |
| **2** | OBn | OBn | MeCN | 54 | **5-8e**[b] |
| **3** | OPiv | OPiv | THF | 57 | **5-8f** |
| **4** | OBn | H | MeCN | 76 | **5-8g**[b] |
| **5** | H | OBn | DCM | 50 | **5.8h** |
| **6** | H | F | AcOH[a] | 81 | **5.8i** |
| **7** | H | Cl | AcOH[a] | n.d | **5.8j** |
| **8** | H | Br | AcOH[a] | n.d | **5.8k** |
| **9** | H | H | DCM | 57 | **5.8l** |

[a] no pTSA was added to the reaction mixture
[b] NBS was used instead of $Br_2$

**Table 5.1.** Bromination of methylketones **5-7**. Starting material is **5-7x**, where 'x' is the same designated letter as the product.

Apart from **5-7e** and **5-8g**, the ketones were brominated alpha to the carbonyl group using bromine at room temperature overnight in the solvent described in Table 5.1. Compounds without electron donating substituents on the aromatic ring were more problematic to brominate. Poly-bromination was observed in entries 6 to 8 when the reaction was ran in DCM. To suppress this unwanted side reaction, the solvent was changed to acetic acid which enabled us to access the desired alpha-bromo ketones.

**5-7f** was also brominated at the alpha ketone position using NBS. NBS was chosen instead of bromine as the by-product of the reaction with the **5-7** series of compounds and molecular bromine is HBr, whereas the by-product of the same reaction with NBS is succinimide. There was a concern that the HBr produced could lead to deprotection of the pivaloyl group, whereas the succinimide by-product should not do so. What was assumed to be over bromination was observed by TLC. We rationalised

the yield to be lower than with molecular bromine possibly due to the bromine reaction being auto-catalytic as it produces acid as the reaction progresses, possibly helping reduce poly-bromination. When using bromine and stopping the reaction the moment starting material was consumed, poly brominated appeared minimised to be and no significant amount of side products were observed by TLC

The isolated yields as shown in the table were moderate to good, yet note that during the purification using column chromatography, only tubes that contained one spot by TLC were combined. In all cases, the difference in rf between the starting material, product and what was presumed to be the di or tri brominated side product by TLC was minimal, so separation proved to be challenging. As only a small amount was needed for the assay, we did not invest time in optimising the reaction conditions.

The family of alpha-bromo ketones were then transformed into the corresponding beta keto ethers by the reaction with 4-methylumbeliferone in acetone and in basic media as shown below in Table 5.2. After the reaction was complete, the solvent was removed and the remaining solid split between water and chloroform. The reaction products tended to be very insoluble in most organic solvents and appeared to be most soluble in chloroform which is why it was used as the extraction solvent. However in some cases such as compound **5-4e** (entry 2), the aqueous phase had to be extracted with 5% methanol in chloroform as the compound proved to be very insoluble in organic solvent, including chloroform alone.

**Table 5.2.** Reaction of bromoketones **5-8** with 4-MU.

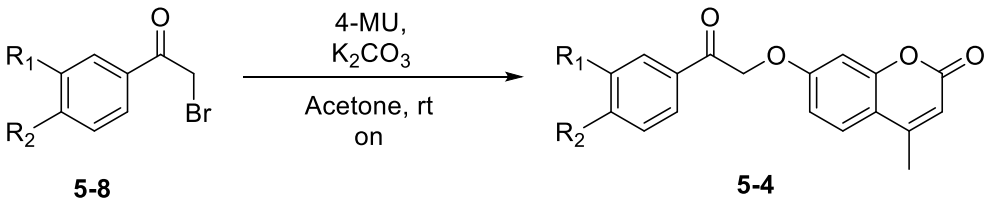


**5-8** **5-4**

| Entry | $R_1$ | $R_2$ | Starting material | Product |
|---|---|---|---|---|
| **1** | OMe | OBn | **5-8b** | **5-4b** |
| **2** | OBn | OBn | **5-8e** | **5-4e** |
| **3** | OPiv | OPiv | **5-8f** | **5-4f** |
| **4** | OBn | H | **5-8g** | **5-4g** |
| **5** | H | OBn | **5.8h** | **5-4h** |
| **6** | H | F | **5.8i** | **5-4i** |
| **7** | H | Cl | **5.8j** | **5-4j** |
| **8** | H | Br | **5.8k** | **5-4k** |
| **9** | H | H | **5.8l** | **5-4l** |

This insoluble character of the compounds meant that during the purification, they came off the silica column over many fractions. It was important for us to have the least possible amount of 4-methylumbeliferone in the sample as to keep the background fluorescence in the subsequent assay to a minimum. For this reason, and for the fact that we needed few milligrams for the test, we again only took the fractions that were a single spot by TLC. This selectivity contributed to the lower than desired yield. As with the previous bromination step, we did not invest time in optimising the reaction conditions.

Benzylic compounds **5-4b, 5-4e, 5-4g** and **5-4h** were also subjected to hydrogenolysis catalysed by Pd/C to give the corresponding phenols. Compounds **5-4b, 5-4g and 5-4h** were deprotected uneventfully in 10% ethanol in ethyl acetate (Scheme 5.8). However, compound **5-4e** under the same conditions did not afford the corresponding diol product **5-4o**. We tried to obtain **5-4o** by deprotection of the pivaloyl groups. However, no product was able to be isolated. Starting material had been consumed after 2 hours, however upon acidification of the reaction mixture to pH 5 with ammonium chloride and extraction with EtOAc followed by 5% methanol in chloroform, no product was seen in either of the organic fractions. We postulated that the product of the reaction either decomposed, or it was too insoluble in the solvents that were tried to extract it from the reaction

crude. Due to these challenges, attempts at trying to synthesize this target compound was abandoned.

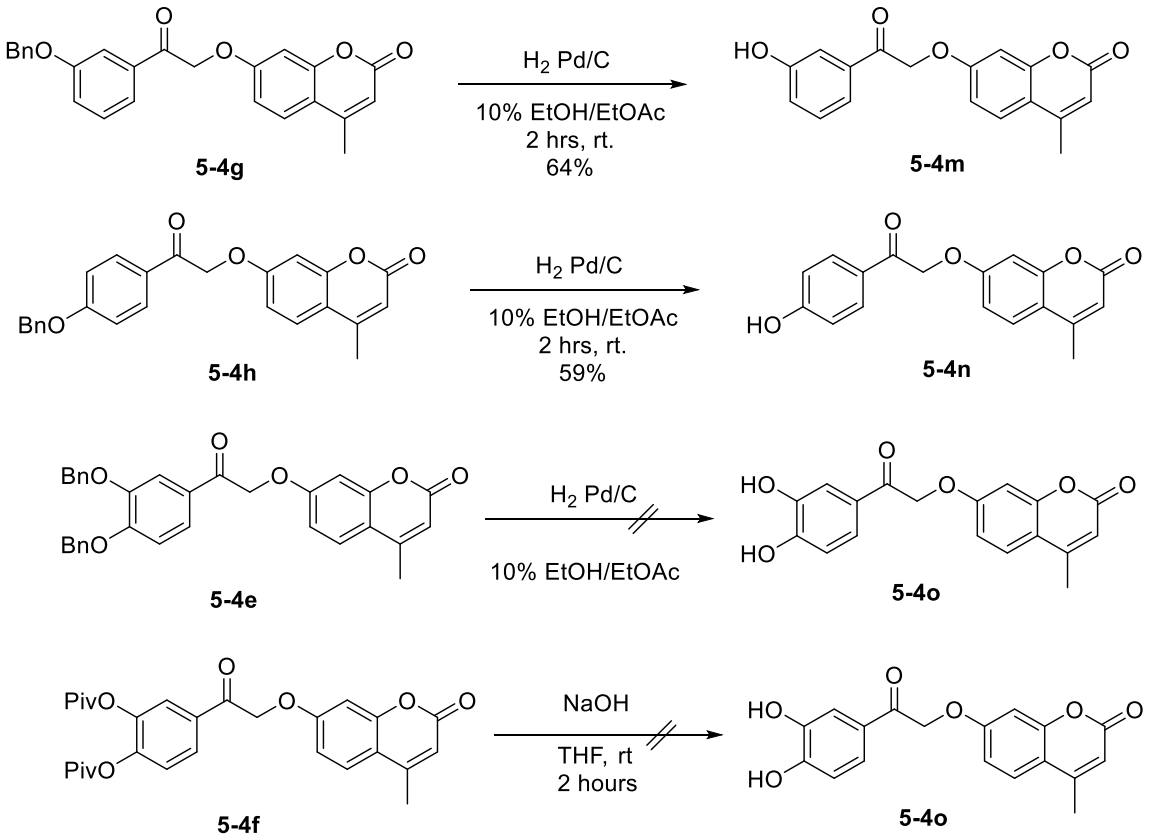


**Scheme 5.8.** Synthesis of various final compounds.

Compound **5-4p** was made by the reaction of compound **5-4a** with methyl iodide in acetone with $K_2CO_3$ as shown below in Scheme 5.9.

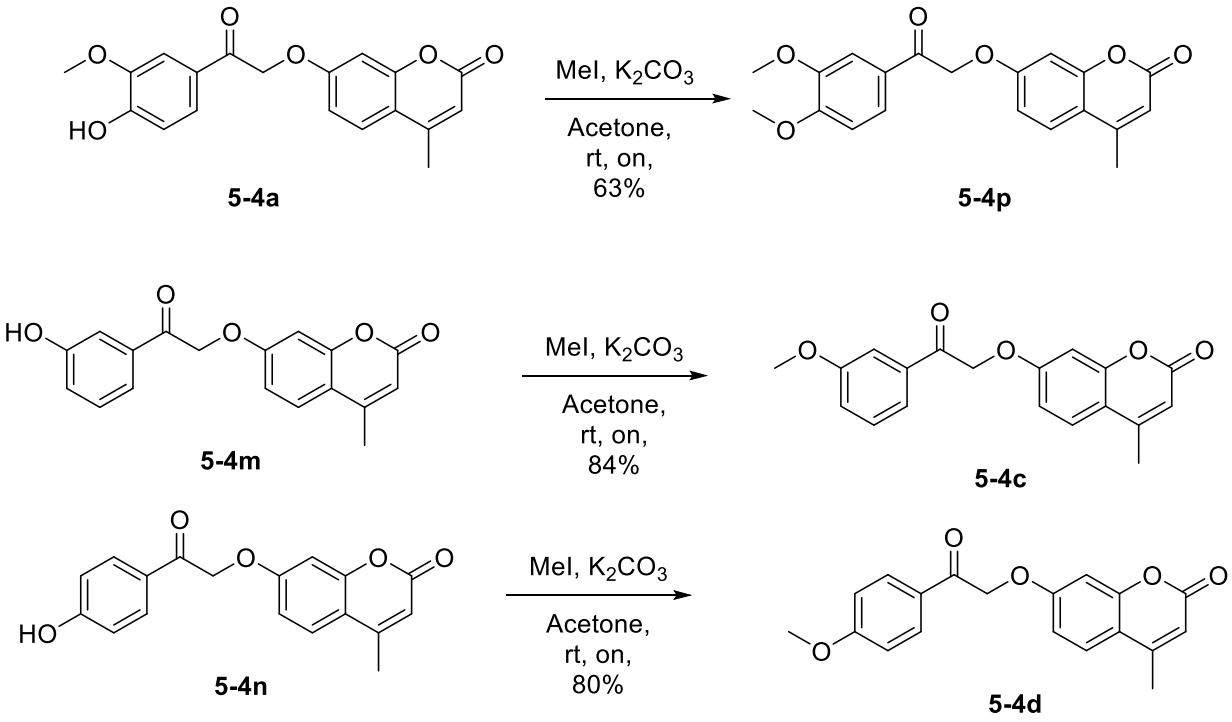


**Scheme 5.9.** Methylation of **5-4a**, **5-4m** and **5-4n**.

Now with the small library of compounds **5-4** in hand, we sought to determine whether LigF was able to cleave the beta keto ether bond, liberating 4-MU. Table 5.3 summarises the compounds used in the assay, using the same conditions established previously.

**Table 5.3.** Compounds used in the LigF assay.

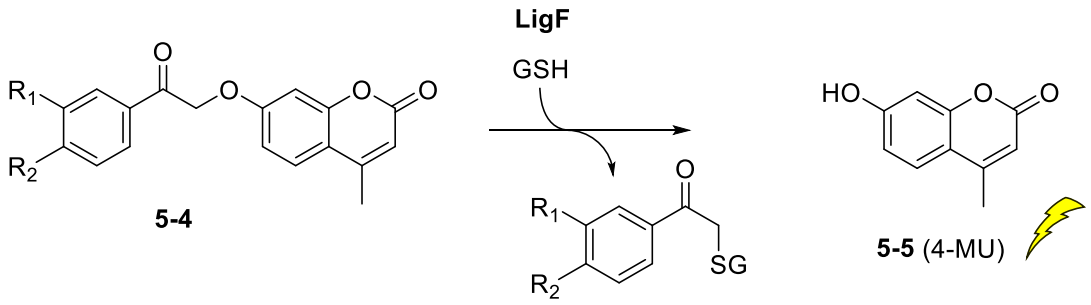


| Entry | $R_1$ | $R_2$ | Starting material |
|---|---|---|---|
| **1** | OMe | OH | **5-4a** |
| **2** | OMe | OBn | **5-4b** |
| **3** | OMe | H | **5-4c** |
| **4** | H | OMe | **5-4d** |
| **5** | OBn | OBn | **5-4e** |
| **6** | OBn | H | **5-4g** |
| **7** | H | OBn | **5-4h** |
| **8** | H | F | **5-5i** |
| **9** | H | Cl | **5-4j** |
| **10** | H | Br | **5-4k** |
| **11** | H | H | **5-4l** |
| **12** | OH | H | **5-4m** |
| **13** | H | OH | **5-4n** |

As can be seen in Figure 5.6, only entry 1 (**5-4a**) was cleaved significantly in the presence of LigF, liberating 4-MU. This showed us that LigF appeared to be specific to the 3-methoxy-4-hydroxyphenyl fragment. Compound **5-4b** was of particular interest as it had been previously reported that LigF could cleave the beta ether bond. However, our results went against what was claimed by Reiter *et. al.* where they had drawn the Bn protected variant.[1] We suggest that this is a mistake in the drawing of the structure. **5-4c** and **5-4m** also seemed to show cleavage of the beta ether bond, however this was significantly less than that of **5-4a**.

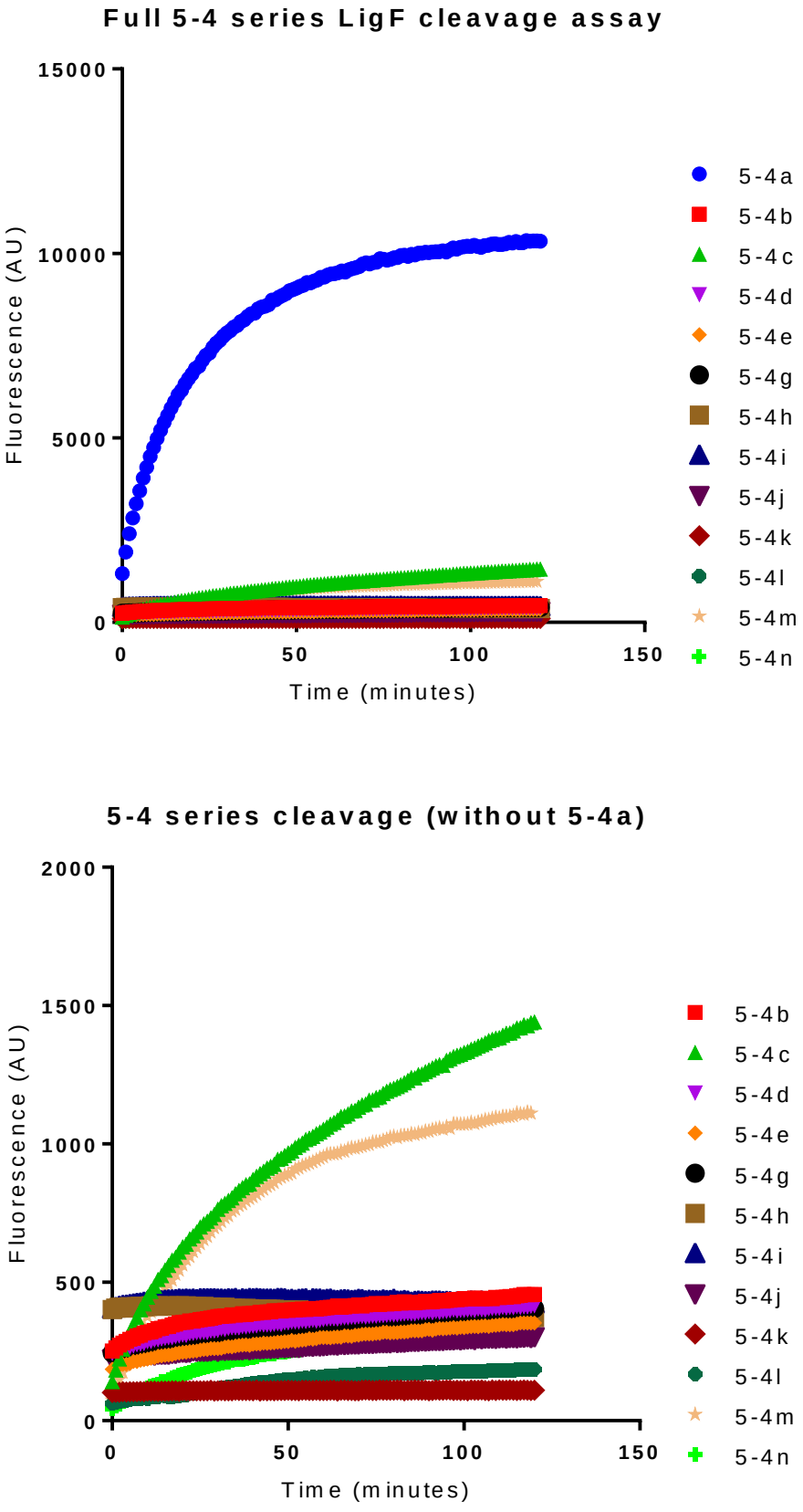


**Figure 5.6**. Graphs to show the cleavage of the **5-4** series over time. Top: Combined **5-4** series. Bottom: Combined series with **5-4a** omitted for clarity.

Knowing now that there is little to no room for improvement in the substituents attached to the aryl ring on the recognition fragment, we continued our original plan and kept the target molecule as shown in Figure 5.1.

## 5.3 Synthesis of Guaymoxifen (5-3)

### 5.3.1 Retrosynthetic analysis of Guaymoxifen (5-3)

Having completed the SAR analysis of the recognition fragment, we embarked upon the synthesis of our target compound for biological testing – Guaymoxifen (**5-3**). Our first approach was to use the same methodology that was used in the preparation of the 4-methylumberliferone derivative **5-4a**, which was alkylation of 4-hydroxytamoxifen (4-OHT) **5-2** with bromoketone **5-5b** followed by hydrogenolysis of the benzyl group (Scheme 5.8).

(*Z*)-4-hydroxytamoxifen (**5-2Z**) is not a common reagent, and its high cost means that it is prohibitive in practical terms as a starting material for anything other than a few milligrams. Its high cost is not only because it is difficult to prepare, but also as the activation of Cre *in vivo*, as well as in the treatment of breast cancer, uses Tamoxifen.

4-OHT, on the other hand, is used for *in vitro* experiments. Compared to *in vivo* experiments, *in vitro* experiments only require a very small amount of 4-OHT. Also, in an *in vivo* setting, the liver oxidises tamoxifen (a prodrug) giving the active metabolite 4-OHT, and obviously this is not possible *in vitro*.[3][4]

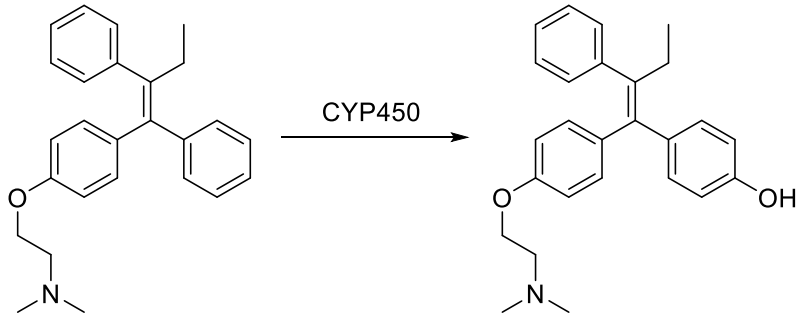


**Figure 5.7.** Oxidation of tamoxifen to 4-hydroxytamoxifen by CYP450 enzymes.

As just mentioned, tamoxifen is a pro-drug that is oxidised in the liver affording the active metabolite **5-1**. However, since we wanted to activate Cre in a specific cell we cannot use just tamoxifen, as the liver would release 4-OHT systemically.

## 5.3.2 Attempts of synthesis of 4-hydroxytamoxifen (5-2) via borylstannylation of acetylenes

We thought that the Takaki synthesis of tamoxifen (see background in chapter 4) could be adapted to our needs either as a source of 4-hydroxytamoxifen (**5-2**) or as a route to other precursors of **5-3**.[5] Our retrosynthetic analysis is shown in Scheme 5.8.

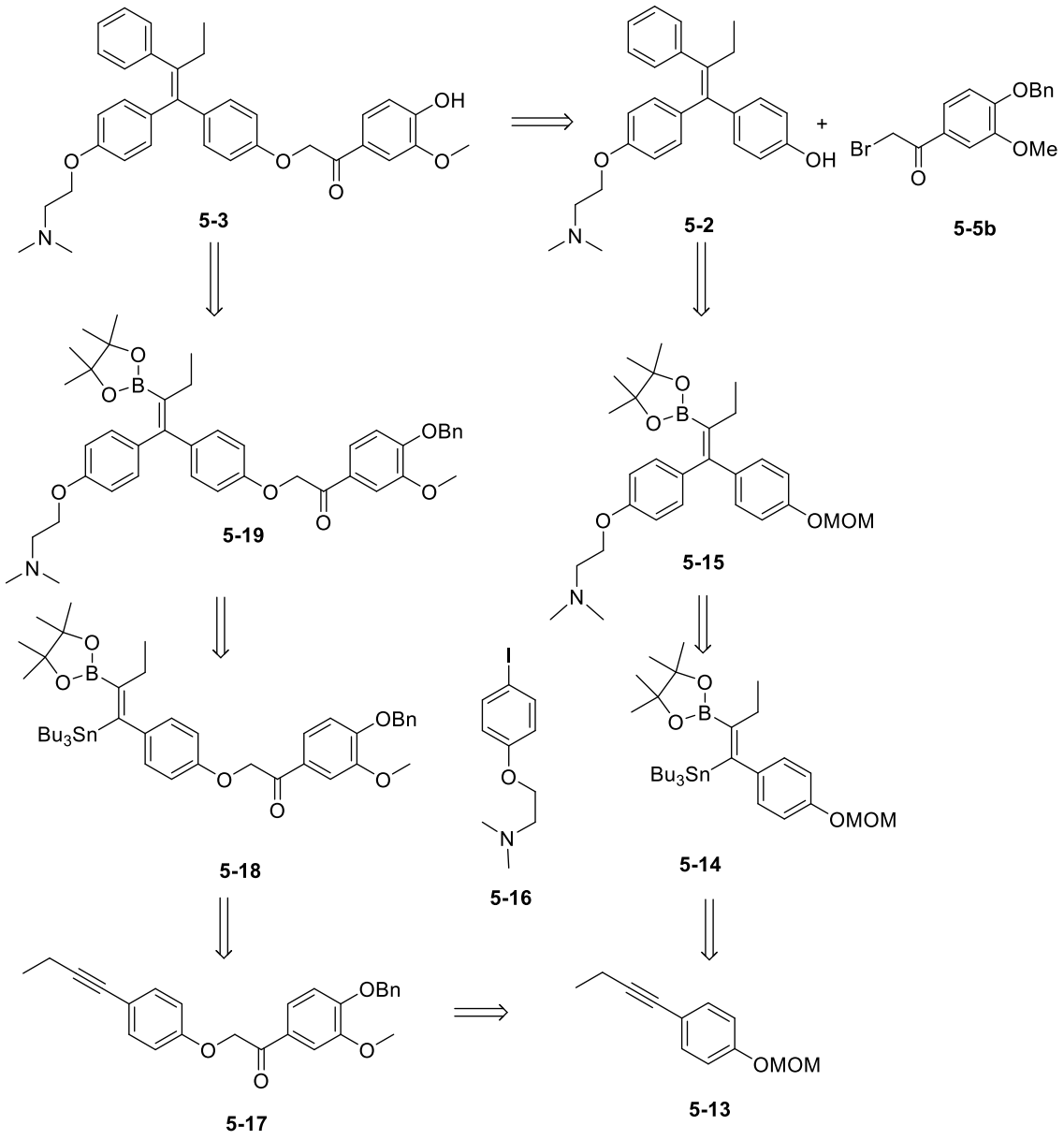


**Scheme 5.8**. Retrosynthetic analysis of Guaymoxifen **5-3**.

Based on the retrosynthetic analysis of Scheme 5.8, we planned to synthesise **5-1** using the chemistry developed by Takaki. The synthesis of the starting alkyne **5-13** was relatively straightforward (Schemes 5.9 and 5.10). First, 4-iodophenol was protected as a methoxymethyl acetal (MOM) using MOM-Cl in THF with sodium hydride as the base, giving **5-20**. The resulting crude reaction mixture was pure by $^1$H NMR, so it was used without purification for the next step.

Compound **5-20** was then subjected to Sonogashira coupling with TMS acetylene using $Pd(PPh_3)_2Cl_2$ and CuI as the catalysts, and $Et_3N$ both as the base and the solvent yielding the corresponding alkyne **5-21**. Cooling the reaction mixture to room temperature in air and filtration through a Celite pad was sufficient to purify the reaction mixture for the next step.

The TMS protecting group was removed from the alkyne under basic conditions using $K_2CO_3$ in a mixture of 2:1 DCM:MeOH. Following quench with water and subsequent extraction with $Et_2O$, the product was purified by column chromatography affording compound **5-22** as a pale-yellow oil in an 86% yield over the three steps.

It is worth noting that we chose not to go from **5-20** to **5-22** directly, as this would involve the use of acetylene gas. We thought that this would have been an added and unnecessary safety risk, as well as the additional complexity of working with a gas.

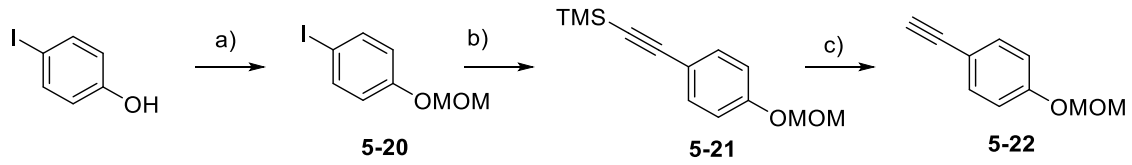


**Scheme 5.9**. a) NaH, MOM-Cl, THF. 100% b) $Et_3N$ (neat), CuI, $Pd(PPh_3)_2Cl_2$, TMS-acetylene, 100%. c) $K_2CO_3$, MeOH, DCM. 86%

Initial attempts of alkylation of **5-22** with ethyl iodide using n-butyl lithium as the base resulted in incomplete reaction crudes despite varying the amounts of base, electrophile, time and temperature. In the end the optimal condition was using LDA at 0 $^oC$ to deprotonate the terminal alkyne, and leaving the reaction mixture for 20 minutes when it turned from yellow to orange. Ethyl iodide was then added dropwise to the reaction mixture and left to warm to room temperature overnight. The reaction was cooled to 0 °C where it was quenched with water and after extraction, the mixture was purified by flash column chromatography giving product **5-13** in a 96% yield.

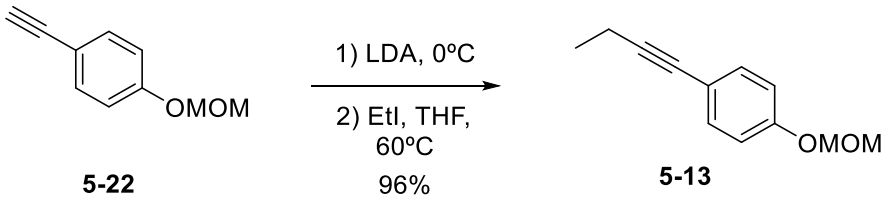


**Scheme 5.10**. Ethylation of **5-22.**

We next moved on to investigate the borylstannylation reaction of **5-13**, the key step of our retrosynthesis for **5-2**. According to Takaki's paper, the BPin and the tributyl tin not only added *cis* across the double bond but also regioselectively (>99:1) with the stannyl moiety in the geminal position to the Ph and the BPin in the geminal position to the ethyl chain.

We first made the active copper catalyst by dissolving copper (II) acetate and tricyclohexylphosphine in degassed methanol and stirring at 80$^{o}$C for 30 minutes. A colourless solution formed, and the solvent was then removed *in vacuo* in a Schlenk tube, taking care to keep the reaction mixture out of contact with oxygen and water.

Bis(pinacolato)diborane, tributyltin methoxide, alkyne **5-13** and toluene were then added to the reaction mixture and left at room temperature for 20 hours to react. The mixture was then diluted with ethyl acetate and brine, and then purified by column chromatography following the work-up. The product was isolated in a 50% yield, with the major impurity being the destannylated product **5-23** as shown in Scheme 5.11.

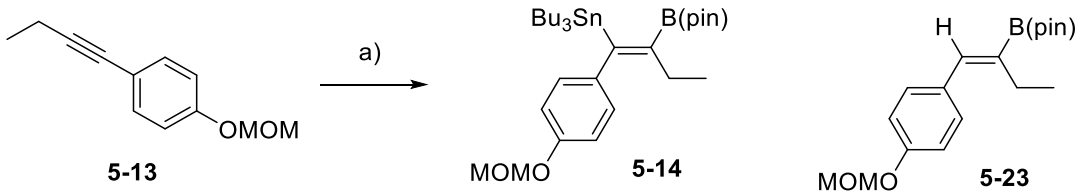


**Scheme 5.11**. a) $Cu(OAc)_2$, $PCy_3$, MeOH, $Bu_3SnOMe$, $B_2Pin_2$, rt, 20 hours, 49%.

We were now ready to attempt the Stille coupling, using 4-(2-(dimethylamino)ethoxy)-1-iodobenzene (**5-16**) as the aromatic coupling partner, which was easily prepared from 4-iodophenol (Scheme 5.12).

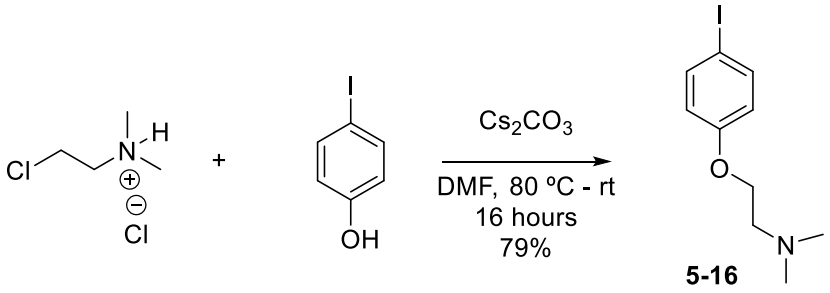


**Scheme 5.12.** Alkylation of iodophenol to give **5-16.**

Unfortunately, in our hands and following Takaki's procedure (Scheme 5.13), no trace of the Stille coupling product **5-15** was observed. Column chromatography of the reaction mixture gave us some insight to why no product was formed. No starting material was recovered and the two major by-products were both the destannylated alkene **5-23** as well as the destannylated-deborylated alkene **5-25**.

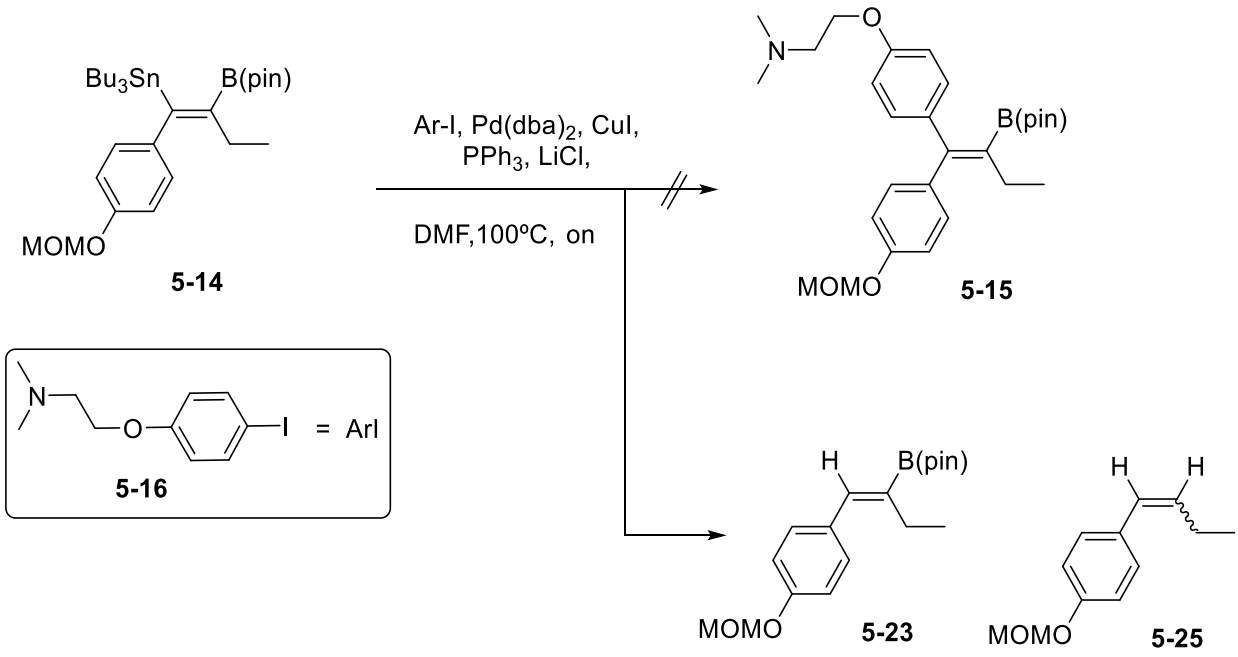


**Scheme 5.13.** Attempted Stille coupling of **5-14**.

The failure of this reaction led us to test many Stille coupling reactions with other conditions and reagents. We synthesised iodo compound **5-26** from *p*-iodophenol, which has a masked version of the side chain of tamoxifen. Treatment of 4-iodophenol with glycidol, using trimethylamine as the base in ethanol afforded diol **5-27** in a quantitative yield. Compound **5-27** was then protected as the dimethyl acetal by reaction with with 2,2-dimethyoxypropane in acetone, using TsOH as the catalyst in a 10% loading.

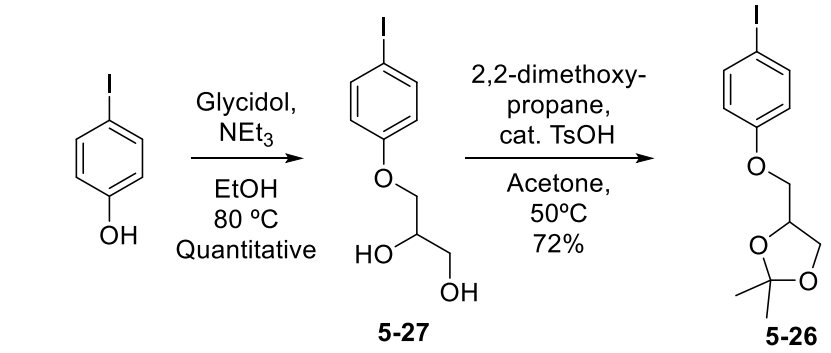


**Scheme 5.14.** Synthesis of **5-26**.

With iodo compounds **5-16** and **5-26** in hand we assayed the Stille coupling with **5-23**. Attempts are summarised in Table 5.4.

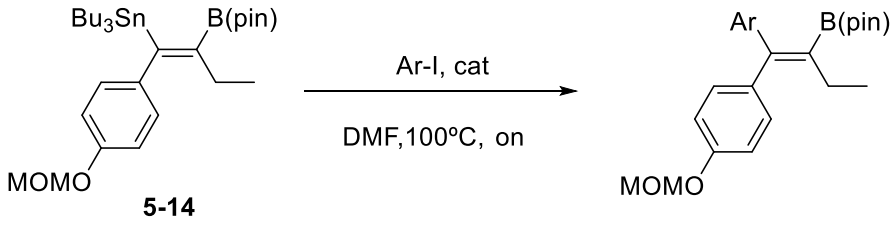


| Catalyst | Ligand | Co-Catalyst | Temp | Ar-I |
|---|---|---|---|---|
| $Pd(dba)_2$ | $PPh_3$ | CuI | 100ºC | a |
| $Pd(dba)_2$ | $PPh_3$ | CuI | 60 - 100ºC | a |
| $PdCl_2(MeCN)_2$ | $PPh_3$ | - | 100ºC | a |
| $Pd(dba)_2$ | $PPh_3$ | CuI | 100ºC | b |
| $Pd(dba)_2$ | $PPh_3$ | CuI | 60 - 100ºC | b |
| $Pd(dba)_2$ | $AsPh_3$ | CuI | 100ºC | c |
| $Pd(dba)_2$ | $PPh_3$ | CuI | 100ºC | c |

a) Compound **5-16**. b) 1-iodo-4-methoxybenzene. c) compound **5-26**.

**Table 5.4.** Attempts of Stille coupling on compounds **5-14**.

Unfortunately, no coupling product was observed in any of the reactions. In view of the negative results, we tried to change the MOM protecting group of the starting alkyne to both the THP and pivaloyl protecting groups. The THP group was introduced by the reacting the 4-iodophenol with 3,4-

dihydropyran using PPTS as the catalyst. Once protected, compound **5-28** was then reacted with TMS acetylene via Sonogashira coupling giving compound **5-29** in a 98% yield after chromatography. Unfortunately, deprotection of the TMS group proved to be more complicated. Attempts to deprotect under basic conditions using $K_2CO_3$ in a mixture of 2:1 DCM:MeOH - which worked for the deprotection of compound **5-21** - were not successful. Heating the reaction mixture resulted in decomposition of the molecule and gave a complex mixture of products.

Parallel to the previous THP analogue reactions, pivaloyl was also explored as a protecting group for the phenol in the model reaction. As in the case of the THP analogue **5-28**, the protection proceeded in a quantitative yield, before being submitted to Sonogashira coupling with TMS-acetylene under the same conditions mentioned above. As before, attempts to deprotect the TMS compound **5-31** resulted in decomposition of the molecule.

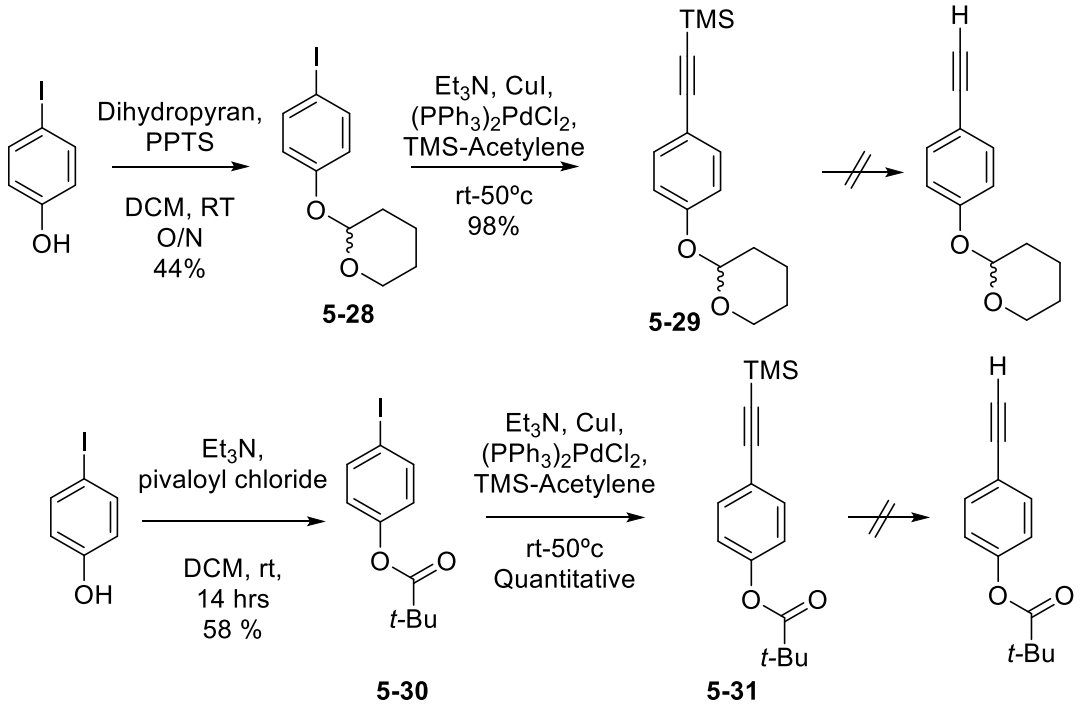


**Scheme 5.15.** Synthesis of TMS-protected acetylenes.

The difficulties in the synthesis of 4-OHT led us to consider buying a sample to speed up the project. Although it is prohibitively expensive to use as starting material on a gram scale, we purchased a small amount of isomerically pure (Z)-4-OHT from LKT Laboratories.

### 5.3.3 Attempts of synthesis Guaymoxifen (5-3) from commercial 4-hydroxytamoxifen (4-OHT, 5-2)

We planned to make a small amount of Guaymoxifen from commercial (*Z*)-4-OHT (**5-2**) to confirm the cleavage of the recognition fragment by LigF, and perhaps perform some initial cell-based assays depending on the quantity available. Although it is extremely expensive, we purchased a small amount of isomerically pure (*Z*)-4-OHT from LKT Laboratories. Following our retrosynthetic analysis in Scheme 5.2, we planned to alkylate (*Z*)-4-OHT with the alpha-bromo ketone **5-5b**. Should this route be successful, we planned to make 4-OHT by one of the several syntheses described in the literature that are reviewed in the previous chapter. Our first efforts were devoted to the synthesis of **5-2** using **5-1** as a starting material. We performed a range of conditions as summarised in Table 5.5.

**Table 5.5**. Attempts to alkylate 4-hydroxytamoxifen with bromoketone **5-5b**.

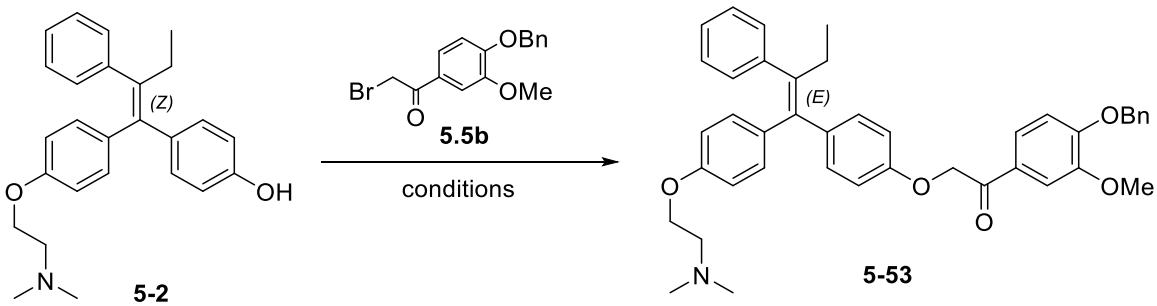


| Solvent | Temp | Base | Time | Result |
|---|---|---|---|---|
| Acetone | rt | $K_2CO_3$ | 2 hrs | no reaction |
| Acetone | rt | $Cs_2CO_3$ | on | no reaction |
| DMF | rt | $Cs_2CO_3$ | on | no reaction |
| MIK | rt | $Cs_2CO_3$ | 3hrs | no reaction |
| THF | rt | $Et_3N$ | 6 hrs | no reaction |
| Acetone | 60°C | $K_2CO_3$ | 2 hrs | decomposition |

To our surprise, none of the conditions tried resulted in the desired product **5-3**. In the crude reaction mixture, the alpha bromo ketone **5-5b** could be seen along with the (*Z*)-4-OHT as well as the varying amounts of the (*E*)-4-OHT from the isomerisation depending on reaction conditions. We propose the isomerisation could be going through the following mechanism.

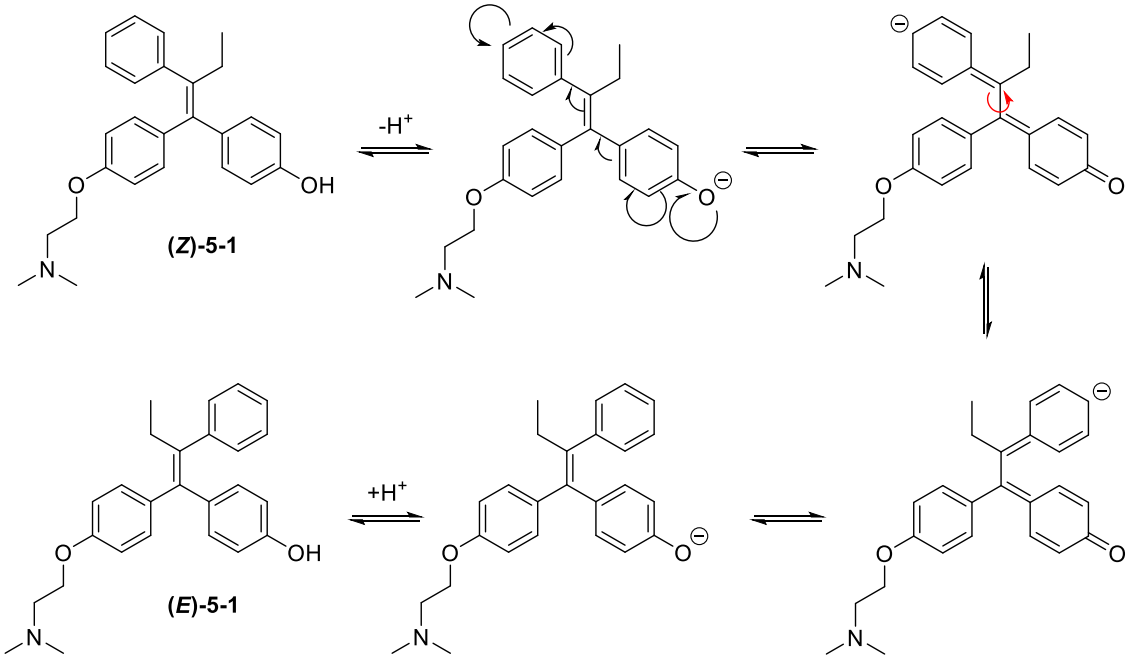


**Figure 5.8**. Proposed mechanism of isomerisation of 4-OHT.

Having learnt the difficulty of alkylating 4-OHT with the alpha bromo ketone **5-5b**, we sought other routes to our target compound.

### 5.3.4 Attempts of synthesis Guaymoxifen (5-3) by borylstannation of acetylene 5-17

We tried to borylstannaylate alkyne **5-17**, with the recognition fragment incorporated into the structure according with the retrosynthetic analysis of Scheme 5.9. The rationale was that the borylstannylation can be performed on ethers as we saw in the synthesis of **5-14**, therefore we envisaged that this reaction could be feasible.

We first tried to prepare **5-17** from 4-iodophenol via Sonogashira with trimethylsilyl acetylene as as before. 4-iodophenol was treated with bromo ketone **5-5b** and $K_2CO_3$ in DMF and left at 50 °C overnight, giving compound **5-32** in an 88% yield after recrystallisation. The compound seemed to be particularly insoluble in most organic solvents, and was therefore recrystallized from EtOH instead of purification through silica.

**5-32** was then subjected to Sonogashira coupling with TMS-acetylene under the same conditions as before to give target intermediate **5-33**. Unfortunately, we were not able to deprotect the TMS group of **5-33** under the same conditions as for **5-21**. As in the cases of the Piv (**5-31**) and the THP (**5-29**) analogues, attempts at deprotection of the TMS group resulted in decomposition.

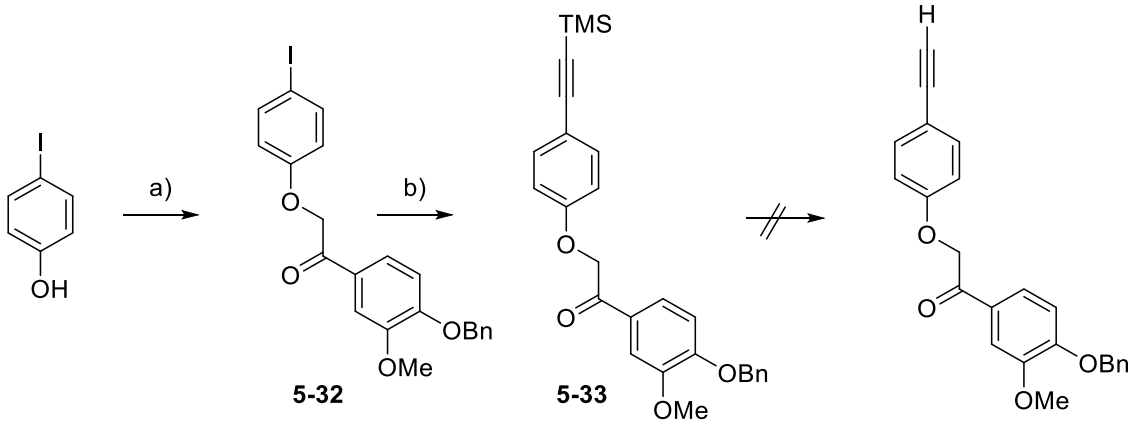


**Scheme 5.16**. Synthesis of **5-33**. a) **5-8a**, $K_2CO_3$, DMF, 50 °C, on, 88%. b) THF, $Et_3N$, CuI, $Pd(PPh_3)_2Cl_2$, TMS-acetylene, 100%.

To solve this problem, we thought of performing the Sonogashira coupling of **5-32** with 1-butyne instead of trimethylsilyl acetylene to avoid the deprotection and alkylation. However, 1-butyne is a gas at room temperature (boiling point is 8 °C) and this creates handling and safety issues.

Methodology developed by Maaliki *et. al*. led us to explore the decarboxylative variant using 2-pentynoic acid as a 1-butyne surrogate.[6]

The decarboxylative Sonogashira was then performed with compound **5-32** without deviation from the described protocol. The reaction appeared to commence at room temperature as upon addition of the 2-pentynoic acid to the reaction mixture, bubbling was observed. Regardless it was heated to 50°C for two hours. Following purification through silica, the compound was isolated in a 94 % yield. The final route to our target intermediate is shown below in Scheme 5.17.

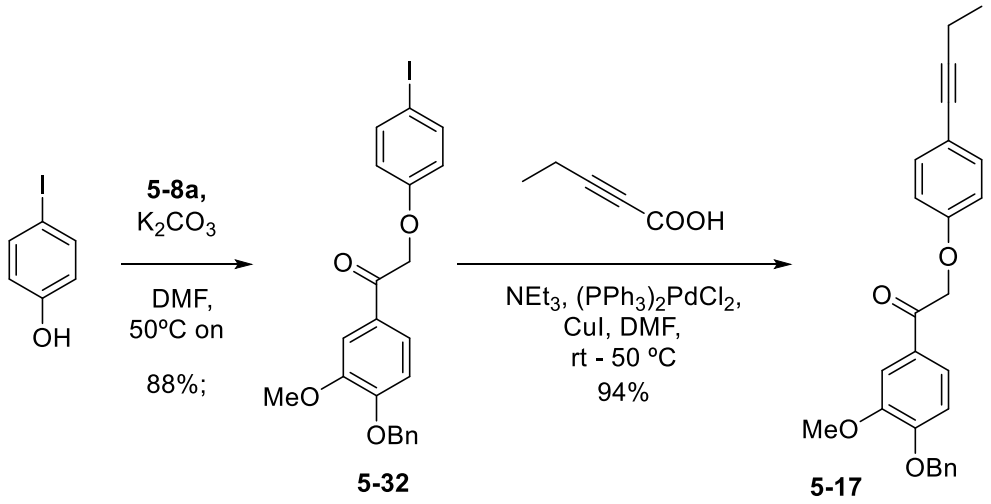


**Scheme 5.17**. Synthesis of **5-17**.

With our alkyne in hand, we then attempted the borylstannylation as shown below in Scheme 5.18.

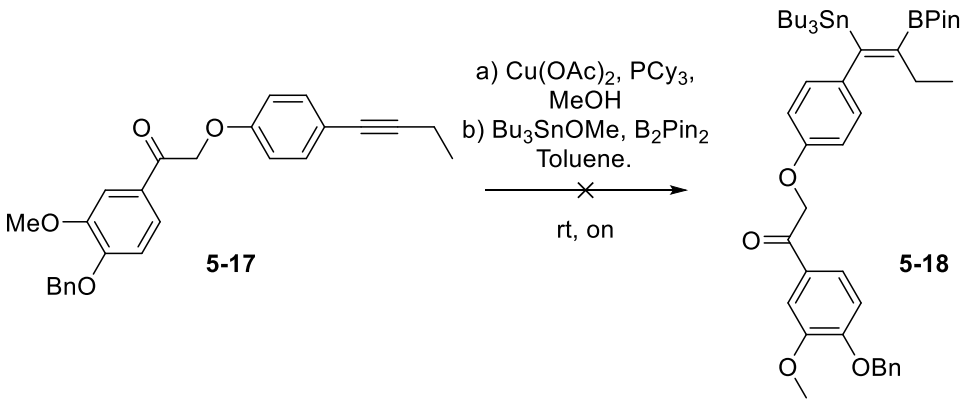


**Scheme 5.18**. Attempts at synthesis of **5-18**.

We attempted the borylstannylation of compound **5-17** five times in total. After the first two attempts did not lead to the product, we suspected that there might be an issue with some of the starting materials. We then distilled the tin coupling partner, replaced the bis(pinacolato)borane with a new one, a new batch of $Cy_3P$ was also used (and analysed by $^{31}P$ NMR before use), however the reaction would not seem to go ahead. The reaction temperature was also reduced, and the reaction followed carefully by TLC, however no reaction was observed.

To assure that there was not a problem in preparation of the reaction, diphenylacetylene as described in the original publication was used as a test. The reaction went to complete conversion, therefore we concluded the problem was with the substrate and not with how we were setting up the reaction.

As the MOM-protected compound **5-13** was able to be borylstannylated, we postulated that the problem could be with the carbonyl group as both compound **5-17** and compound **5-13** otherwise contain the same functional groups. We proposed that we could reduce the carbonyl, protect it, perform the borylstannylation and then at some point later in the synthesis, could deprotect and re-oxidise back to the ketone.

Compound **5-17** was dissolved in methanol and then left to react with $NaBH_4$ overnight. After work-up with $NH_4Cl$, a crude NMR was ran and it showed a ca. 20% amount of an impurity, which appeared to be the corresponding alkene **5-35** coming from reduction of the alkyne.

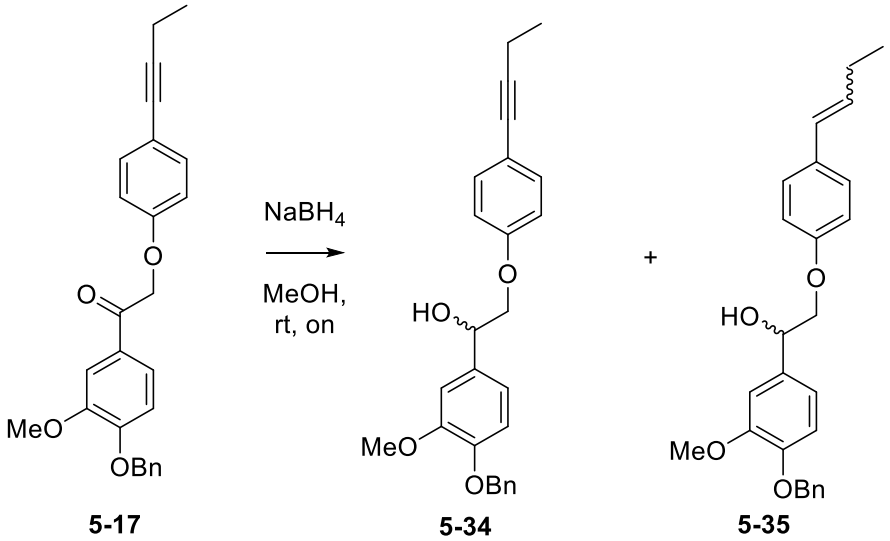


**5-17** **5-34** **5-35**

**Scheme 5.19**.

Changing the reducing agent to $NaCNBH_3$ or to $NaBH(OAc)_3$ did not result in reduction of the triple bond, however neither did it result in the reduction of the carbonyl. The reaction was found to perform best with addition of $NaBH_4$ at 0°C and stopping the reaction when it could be seen by TLC that the over-reduced product was forming. The advantage of this was that the alcohol could be separated easily from the starting material. Alcohol **5-34** was then protected as a TIPS ether. It was important to use TIPS-OTf and not TIPS-Cl as the latter proved to be very sluggish.

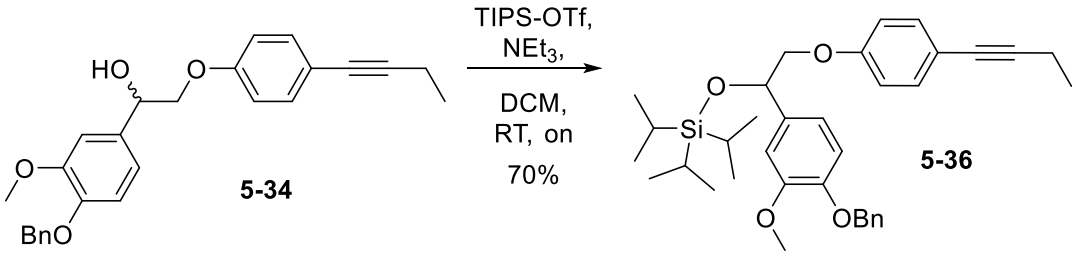


**Scheme 5.20**. TIPS protection of **5-34**.

Upon quenching with water, the excess TIPS-OTf yielded a by-product which could not be separated from the product by chromatography due to them having a similar rf. We proposed that this product was either the TIPS-OH, or the dimer formed from TIPS-OH reacting with a TIPS-OTf giving TIPS-O-TIPS. We postulated that quenching the reaction with another compound to modulate the polarity of the by-product could be a way to allow purification of the product. We chose ethanolamine as it was cheap, contained a primary alcohol that should react quickly with the excess TIPS-OTf, and also had a basic amine meaning that it could be removed with a lightly acidic wash. This was indeed the case and after quenching with excess ethanolamine, leaving for 2 hours, followed by 3 washes with $NH_4Cl$, protected alcohol **5-36** was obtained pure in a 70% yield.

The product was then submitted to the borylstannylation reaction where no product was seen in three repeat runs. Facing recurrent difficulties during the borylstannylation route, we explored a further coupling route using a different methodology.

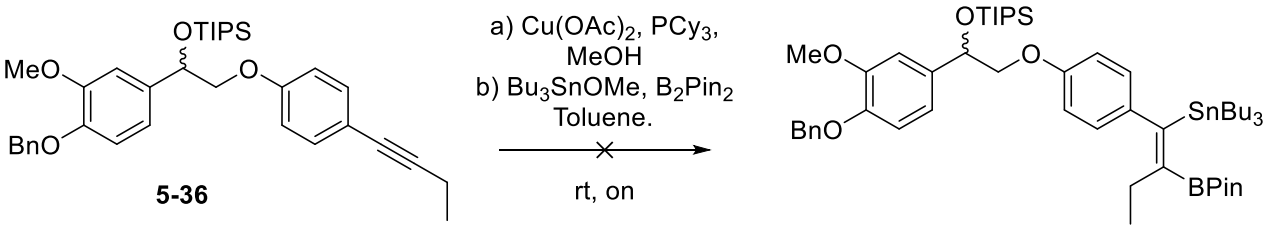


**Scheme 21**. Attempted borylstannylation of **5-35**.

### 5.3.5 Attempted Guaymoxifen (5-2) synthesis via sequential Suzuki reaction of a bis-borylated compound

Shimizu *et al.* described that the geminal boronic ester **5-37** can be transformed selectively into the corresponding mono-coupled compound **5-38**.[7] This occurs with complete control of stereochemistry, where the mono-coupled partner reacts *trans* to the aromatic moiety. Then a second Suzuki coupling can be carried out at the remaining borylated position.

The first Suzuki reaction goes under very mild conditions, and it a one-pot manner Shimizu *et al* were able to achieve selective coupling of the boron esters one at a time. This was done by modulating the reaction temperature – upon consumption of starting material **5-37**, they added an equivalent of a different aryl iodide and increased the reaction temperature to 100 degrees where the second coupling reaction could take place. The second coupling reaction occurred with no significant isomerisation of the double bond.

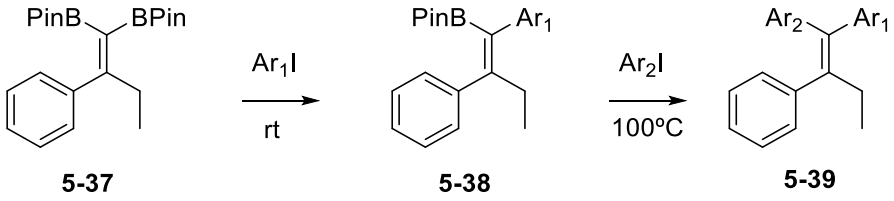


**Scheme 5.22.** Shimizu *et al.* synthesis of tetrasubstituted alkenes.

This methodology was of particular interest to us: not only was it an elegant and relatively inexpensive way to our target compound, but it is also flexible. Should after *in vitro* or *in vivo* testing, further modifications to the structure be required, this approach could give us speedy access to a library of compounds due to the late point of divergence. Thus we designed a new retrosynthetic analysis (Scheme 5.23).

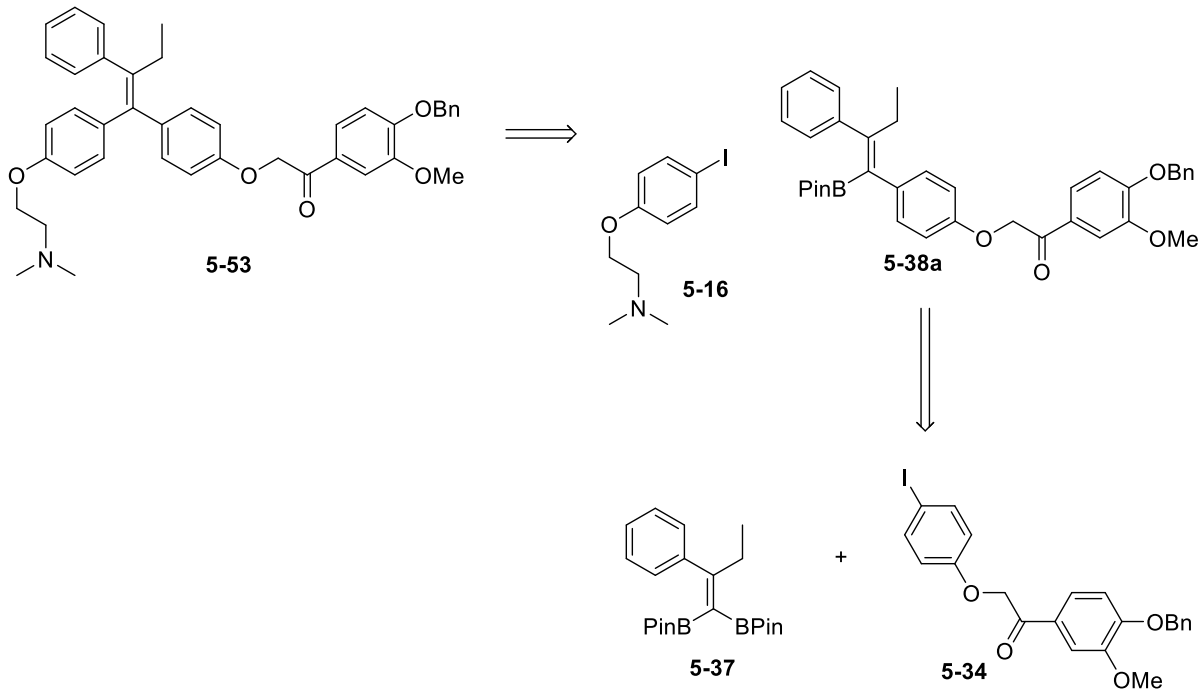


**Scheme 5.23**. Retrosynthetic analysis base on a sequential double Suzuki coupling.

Efficient access to compound **5-37** was achieved using modifications to the literature procedure. Propiophenone was converted into the corresponding hydrazone **5-40** via its addition into an excess of hydrazine in ethanol at 0 °C. The order of addition was crucial as it avoided the formation of what was presumed to be a dimer side-product. The hydrazone **5-40** was alsnot stable in the presence of silica as decomposition was seen upon rotation and re-running a TLC plate. Due to this instability, the crude was carried onto the next step without purification.

Following the procedure described by Zhao *et al.* and Korotchenko *et al.*, hydrazone **5-40** was converted into the corresponding geminal dibromo compound **5-41**.[8][9] The loading of $CBr_4$ was lowered with respect to the reported procedure as it proved to be easier to separate the product from the unreacted starting material as opposed to separating the product from unreacted $CBr_4$. To transform it into the corresponding germinal bis(pinacolato) borane **5-37**, **5-41** was lithiated at -110°C in an ethanol/$N_2$ bath before being treated with bis(pinacolato)diboron, affording the product after flash column chromatography. From here we were able to test the sequential Suzuki reactions.

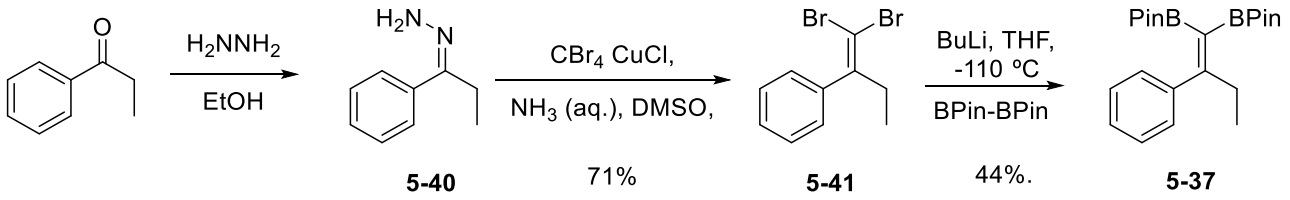


**Scheme 5.24**. Route to intermediate **5-37**.

First, coupling substrate **5-34** was made easily from 4-iodophenol as described earlier (Scheme 5.17). This was then reacted using the conditions described Shimizu *et al*, who claimed to achieve excellent trans selectivity with respect to the aryl group ion only 5 hours at rt. However, in our hands the reaction appeared to go a lot faster by TLC - in less than 30 minutes the starting material was consumed. Following work-up an *E*:*Z* ratio of 85:15 was observed by proton NMR. This ratio was improved to 93:7 by keeping the reaction in the dark and cooling the reaction mixture to 0 °C before addition of the catalyst and then allowing the mixture to warm to rt overnight. The reaction was successfully scaled up to 0.5 gram for optimisation of the following reaction. It is possible that cooling the reaction down below 0 °C could result in even higher selectivity.

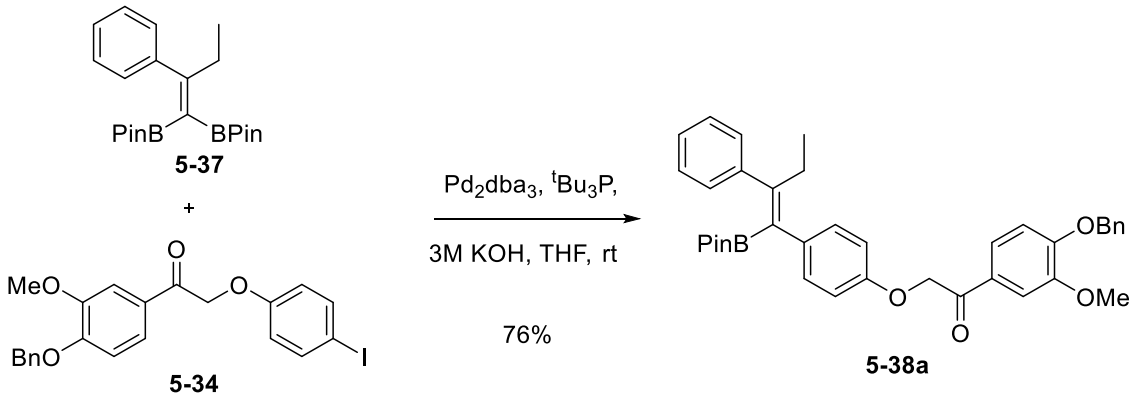


**Scheme 5.25**. First Suzuki coupling of compound **5-37**.

At this point, all was left was to perform the second Suzuki coupling to introduce the final aryl fragment to make compound **5-53** or a masked version. Coupling of aryl iodide **5-16** was attempted using the conditions described by the authors. These gave a complex mixture of products, none of which seemed to be the desired product. Various other conditions were tried as shown below in Table 5.6.

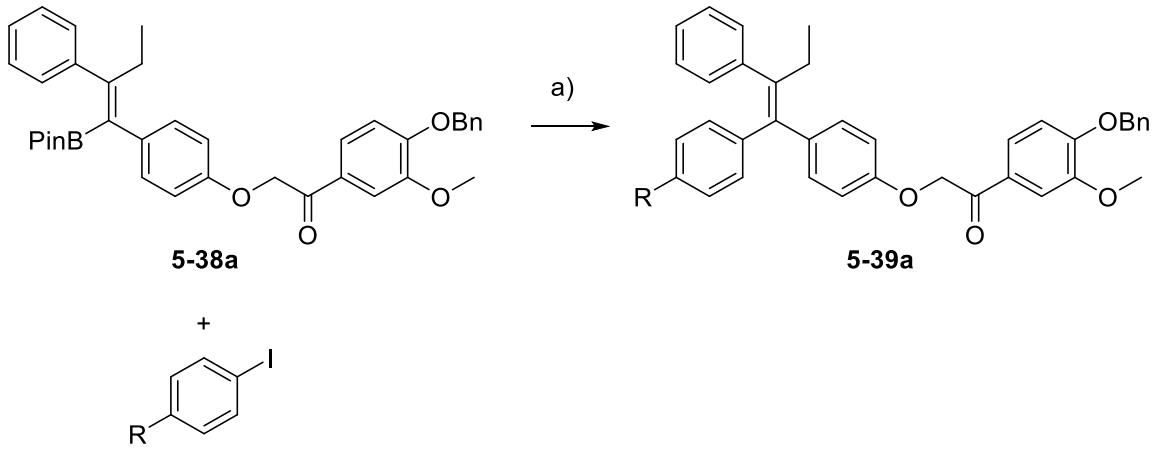


**Scheme 5.26**. a) $Pd_2dba_3$, base, solvent, temperature described in table below.

| Entry | Ar-I | Solvent | Base | Yield |
|---|---|---|---|---|
| 1 | **5-16** | Dioxane | KOH | - |
| 2 | i) **5-34**, ii) **5-16** | THF | KOH | - |
| 3 | 4-iodoanisole | THF | $K_3PO_4$ | - |
| 4 | **5-26** | THF | $K_3PO_4$ | - |

**Table 5.6.** Conditions used in Scheme 5.26. In entry 2, **5-37** was used as SM, forming **5-38a** *in situ*.

Although it was reported that similar couplings are possible using **5-16**, we were concerned that the dimethyl amino chain was interfering with the reaction so we attempted the coupling with partner **5-26** (protected diol) instead. As was the case with the previous reaction, the coupling gave a complex mixture of compounds, and no sign of the product was observed.

The failure of these coupling approaches drove us to focus on the more traditional McMurry approach.

## 5.3.6 Guaymoxifen (5-3) synthesis via McMurry coupling

Based on the synthesis of 4-OHT described by Gauthier *et al*, we envisaged a retrosynthetic analysis based on the McMurry reaction which allows the formation of a double bond from two carbonyls.[10] The retrosynthetic analysis (Scheme 5.27) involves the introduction of the dimethylaminoethyl chain at the end of the synthesis since we found that alkylaton of 4-OHT with bromoketone **5-5b** is not possible.

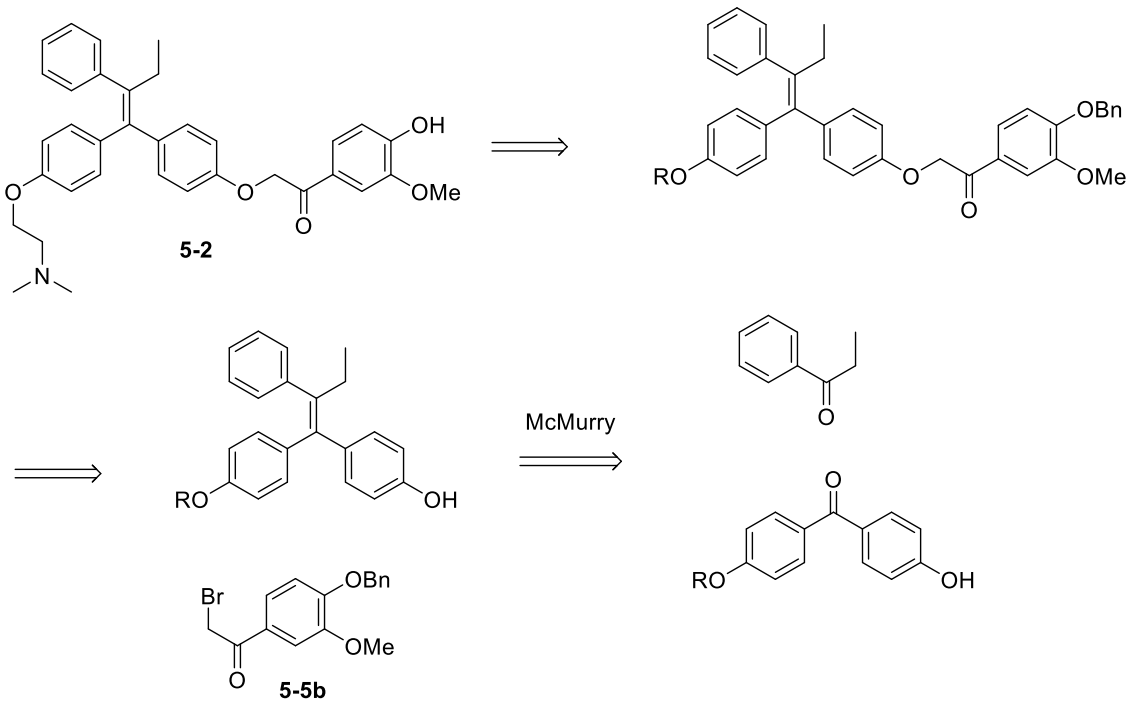


**Scheme 5.27**. Retrosynthetic analysis based on the McMurry reaction.

The reaction involves the reduction of one carbonyl compounds yielding a radical anion. This radical forms a carbon-carbon bond with the other ketone which, after reduction gives rise a 1,2-diolate. The 1,2-diolate can then be deoxygenated by treatment of low-valent titanium with heating forming the alkene as shown below in Scheme 5.28.[11]

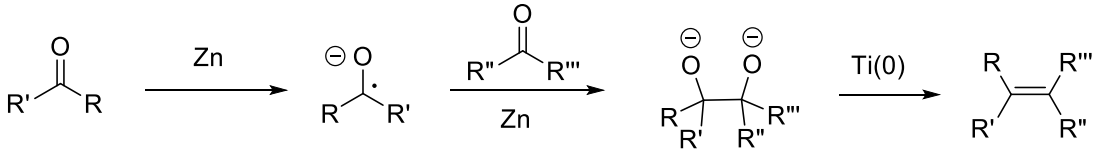


**Scheme 5.28**. Mechanism of the McMurry reaction.

The McMurry reaction between propiophenone and diol **5-41** took place in a notable 70 % yield. The reaction was scaled up to the 20 g scale so we could obtain relatively large quantities of diol **5-43**.

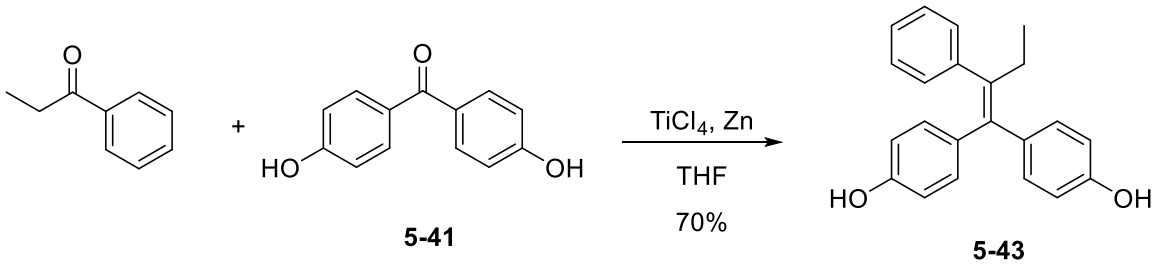


**Scheme 5.29**. Formation of **5-43** via the McMurry reaction.

In 1996, Gauthier *et al* described the use of the pivaloyl protecting group as a means to direct the outcome of a McMurry reaction.[10] In this particular example, they described a novel route to (Z)-4-OHT in only four steps, with a high stereoselectivity >100:1, and a global yield of 10%. This approach involves first the desymmetrisation of diol **5-41**. This is achieved by deprotonation with an excess of NaH, followed by the addition of pivaloyl chloride. We repeated their methodology on a 5 g scale, and after two hours the reaction was quenched giving a theoretical 1:2:1 – SM:Prod:Bis-Piv. These were then easily separated by column chromatography.

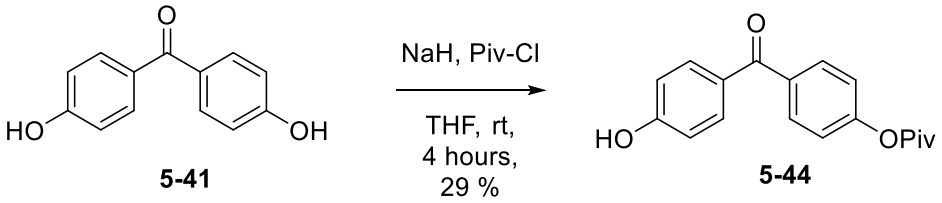


**Scheme 5.30**. Mono-pivaloyl protection of **5-41**.

The monoprotected diol **5-44** was then subjected to McMurry conditions: First titanium (IV) chloride was reduced by addition to zinc dust at 0°C under $N_2$, followed by refluxing for two hours giving the reactive titanium (II) chloride species. At which point the reaction mixture was cooled to 0°C, and to it was added a solution of 3:1 molar ratio of propiophenone and the monoprotected diol **5-44**. The reaction was quenched with ammonium chloride after being heated up to reflux for a further 2 hours.

This procedure afforded a 53% yield of the McMurry product with a 5:1 ratio in favour of the desired stereoisomer **5-45**. Following titration this increased to 15:1, however this led to a reduction in yield to 37%. As this could be optimised at a later date, this was sufficient as a proof of principle and we used this product for further reactions.

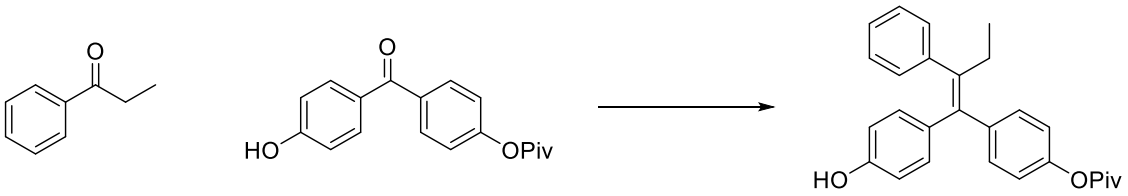


**5-44** **5-45**

**Scheme 5.31**. McMurry reaction or **5-44** to give **5-45**.

The now stereomerically enriched alcohol **5-45** was then attempted to be used to attack glycidol, which we had previously been found to be the best electrophile. Table 5.7 summarising the reaction conditions tried is shown below. Frustratingly, not only did the reaction not work as planned, various sub-products were formed. Sub-product a was reasoned to originate from the transesterification of the starting material, which in turn would explain the presence of diol **5-43**.

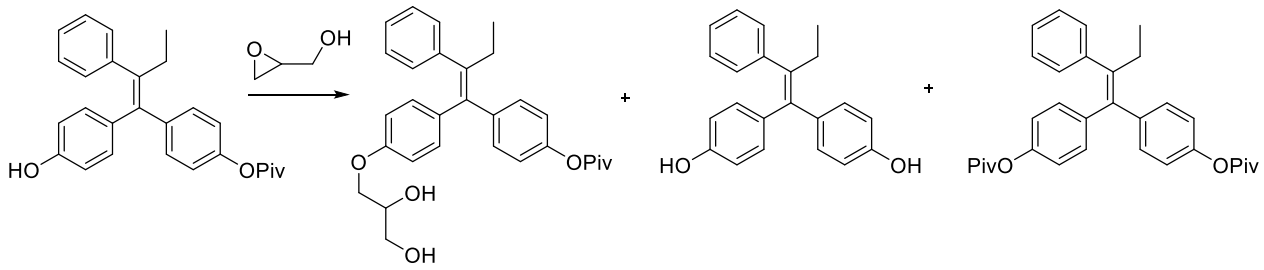


**5-45** **5-46** **5-43** **5-47**

| Entry | Solvent | Base | Temperature | Time | Product |
|---|---|---|---|---|---|
| 1 | MeCN | $NEt_3$ | reflux | on | Mixture |
| 2 | EtOH | $NEt_3$ | reflux | on | Diol |
| 3 | Acetone | $NEt_3$ | reflux | on | Mixture |
| 4 | THF | $NEt_3$ | reflux | on | Mixture |
| 5 | Dioxane | $NEt_3$ | reflux | on | Mixture |
| 6 | Acetone | $K_2CO_3$ | reflux | on | Mixture |
| 7 | Acetone | $K_2CO_3$ | RT - reflux | on | Mixture |

**Table 5.7**. Summary of the attempted synthesis of **5-46** from **5-45**.

Entries 6 and 7 depict our attempts to reproduce the experiment described in the publication. As before, efforts including distillation of the amine prior to use did not affect the outcome of the reaction, and no trace of product was seen in the crude NMR. Mass recovery in most cases was accounted for and greater than 70%, so it was not suspected to have been lost during the work up.

We rationalised that the low reactivity towards the electrophiles of compound **5-45** could be due to the negative charge being stabilised by the conjugated pi system as in compound **5-43**, but also further deactivated to nucleophilic attack by the electron withdrawing effects of the ester group.

Another possible explanation could be the ester moiety acts as a way to increase the ability for the conjugated system to act as a leaving group, as the corresponding anion is stabilised by the ester.

With a better understanding of the limitations of the tamoxifen core reactivity, we postulated that starting from diol **5-43** could provide us with a route to our target compound **5-3**, albeit as a mixture of isomers. Happily, we were able to open glycidol with bis-phenol **5-43** giving a 1:2:1 mixture of the **5-43:5-46:5-48** in the crude reaction mixture, and **5-46** was able to be isolated in a 36% yield.

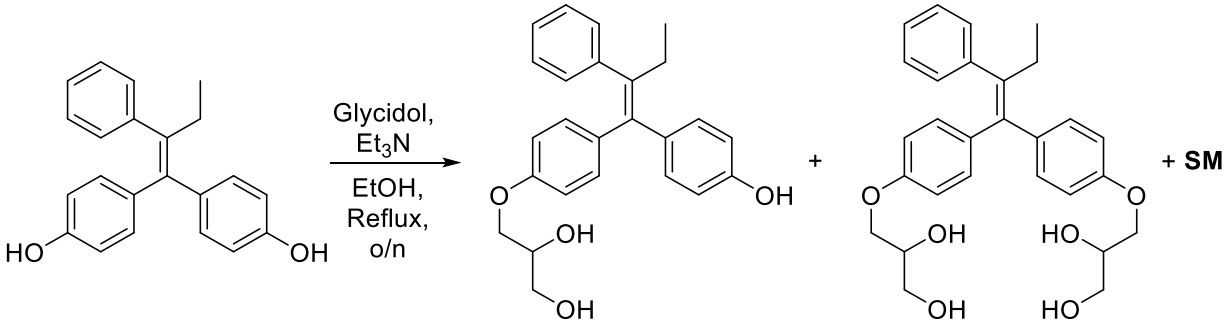


**5-43** **5-46** **5-48**

**Scheme 5.33**

As the next goal would be to alkylate the remaining phenol, we first had to protect the 1,2-diol moiety to ensure there wasn't any reaction between it and the alpha bromo ketone **5-5b**. This was achieved by acetal protection of **5-46** with 2,2-dimethoxypropane gave us **5-49** in an 87% yield. Alkylation with the alpha bromo ketone also proceeded in good yield, giving us access for the first time of the dissymmetrical alkylated bis phenol core **5-50**. From here we could then move on to the alkylation with alpha bromo ketone **5-5b**. This proceeded in good yield, giving us access for the first time to the dissymmetrical alkylated bis-phenol core **5-50** (Scheme 5.34).

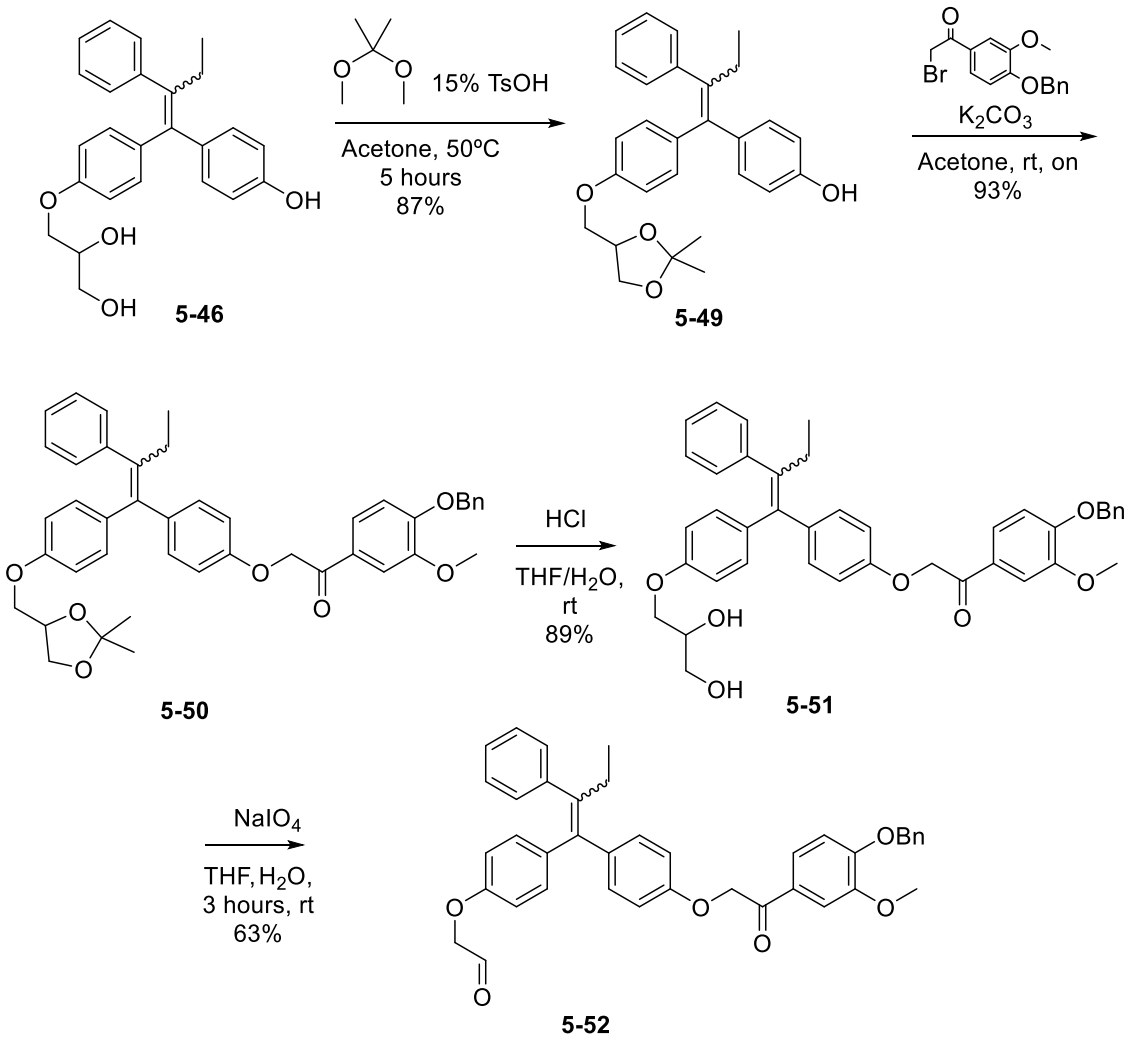


**Scheme 5.34**. Synthesis of aldehyde **5-52** from **5-46**.

From compound **5-50**, we then deprotected the acetal under acidic conditions giving diol **5-51** with an excellent yield. The diol was then subjected to oxidative cleavage using $NaIO_4$, yielding the corresponding aldehyde **5-52**. A subsequent reductive amination with dimethylamine lead us to the benzyl protected target compound **5-53**. The benzyl group was then deprotected via hydrogenolysis leading to a 1:1 E:Z mix of, finally, our target compound.

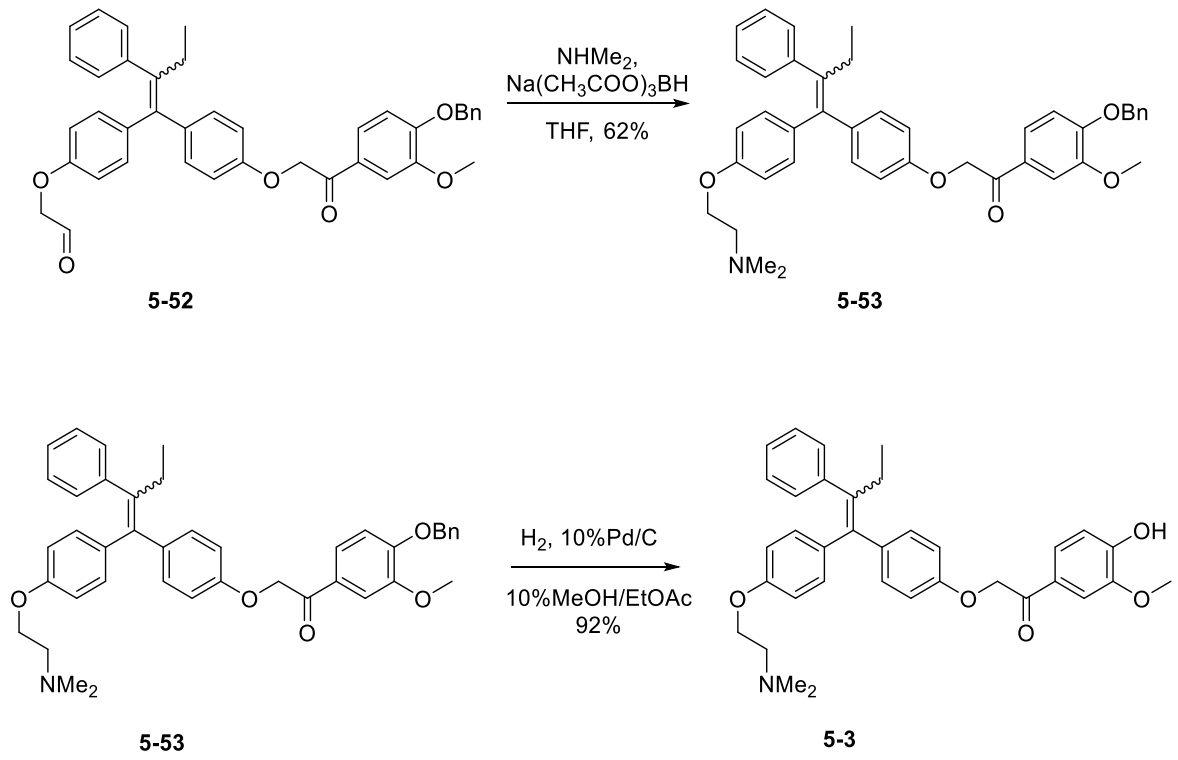


**Scheme 5.35**. First synthesis of Guaymoxifen from aldehyde **5-52**.

With the desired compound in hand, but as a mixture of diastereomers, we attempted to enrich **5-3** by crystallisation with the hope that we would be able to preferentially crystallise one isomer over the other. We tried an extensive range of solvents, including mixtures of solvents, however we were not able to achieve a crystalline solid form – only oils or gums. We then tried to form a solid as an HCl salt. This also was not the case, so we moved onto the next goal of the project: to obtain the stereomerically pure forms of Guaymoxifen (**5-3**).

### 5.3.7 Obtaining both (*Z*) and (*E*)-Guaymoxifen by HPLC chromatography

With a solid route to Guaymoxifen in hand, we wanted to see if each of the stereoisomers were stable, and if both isomers were cleaved by LigF at the same rate. Given the complexity of a sterospecific synthesis, the fastest way to access this was to separate the compounds via preparative HPLC.

Although the final product can be analytically separated by HPLC, its preparative separation by HPLC was envisaged to be too difficult (Figure 5.9).

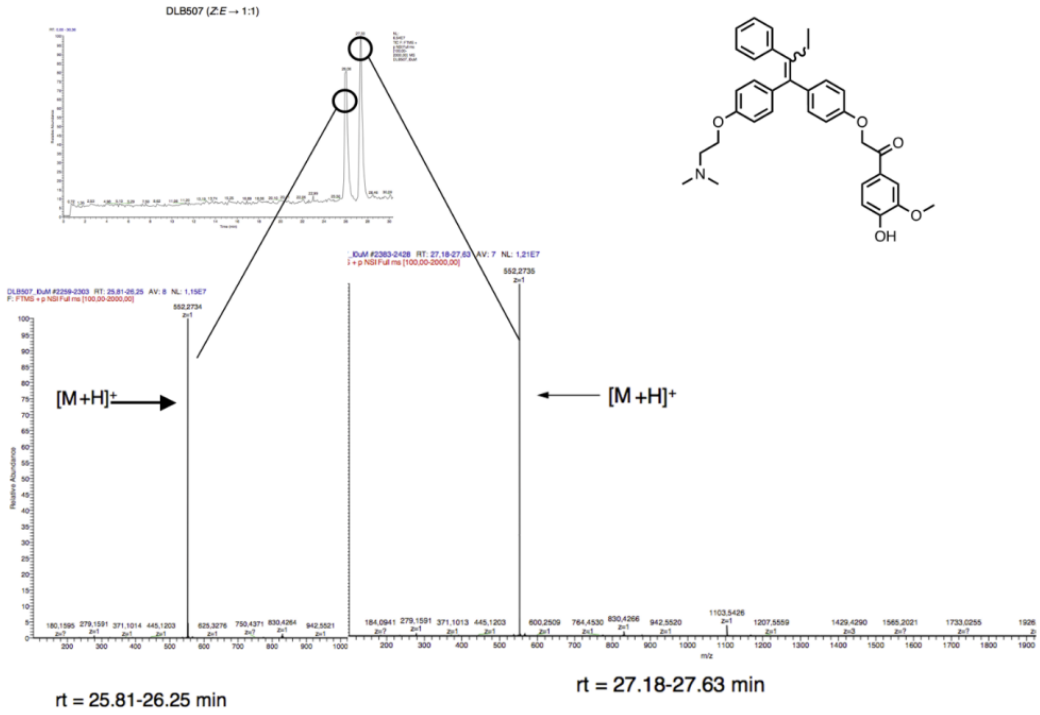


**Figure 5.9.** HPLC-MS of Guaymoxifen (**5-3**) as a mixture of diastereomers.

Having quantities of the intermediates in hand, we chose to analyse them via analytical HPLC to see which had the best separation between the two stereoisomers.

We chose intermediate **5-51** as it appeared to have the best separation, and rather than separating the final compound, we could perform chemistry on the purified isomers to check their stability towards isomerisation under a variety reaction conditions. Moreover, this could show us some possible limitations of the planned future stereospecific synthesis. The synthesis was performed as outlined in the Scheme 5.36.

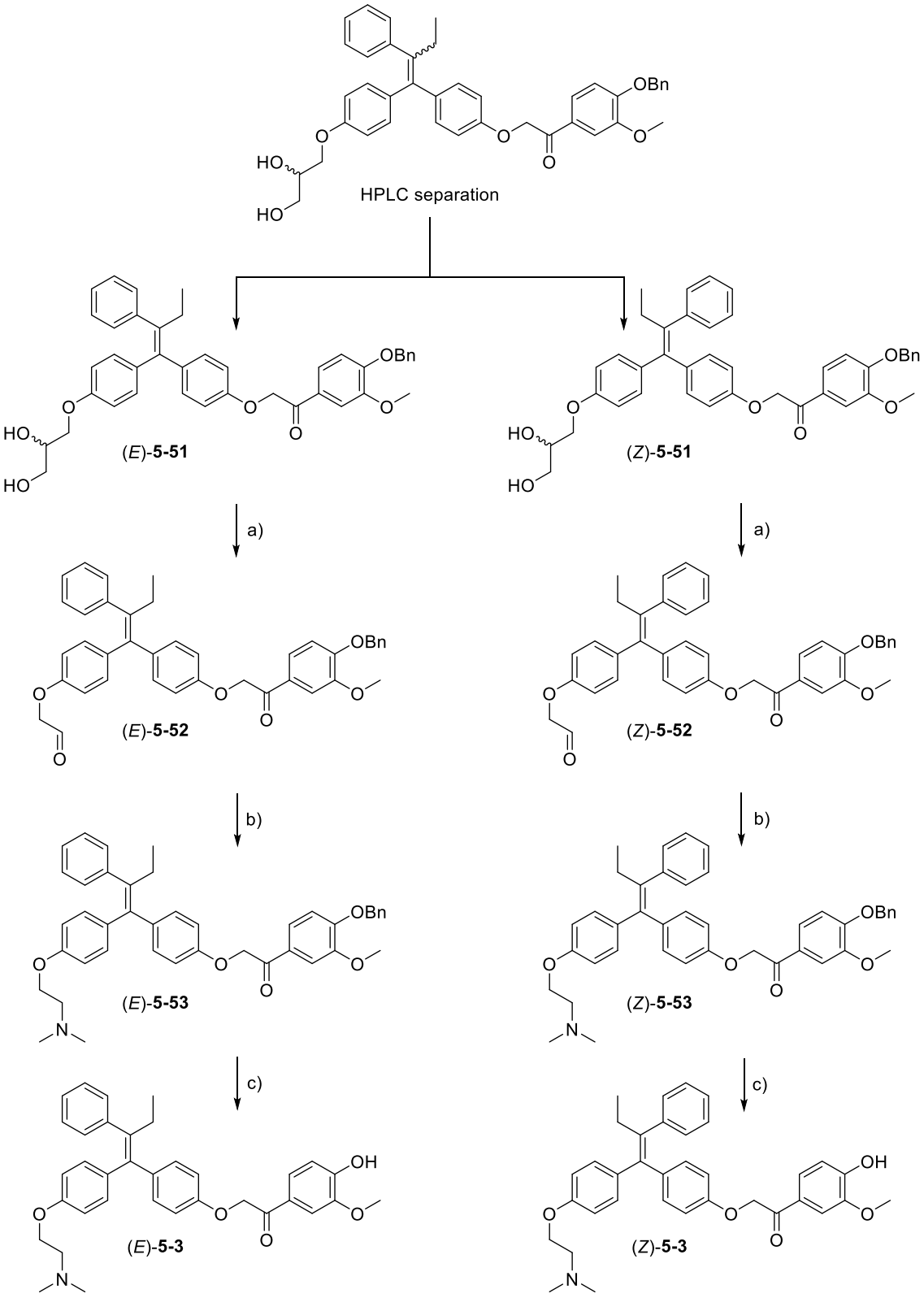


**Scheme 5.36.** $NaIO_4$, Silica, THF; b) $NMe_2H$, $NaBH(OAc)_3$, c) 10% Pd/C, $H_2$, 10% EtOH/EtOAc.

Various injections in the HPLC yielded ca. 100 mg of each isomer of **5-51**. Following the methodology developed previously, each stereo-pure diol was treated with $NaIO_4$ affording aldehydes (*E*)-**5-53** and (*Z*)-**5-53**. The aldehyde was then subjected to a reductive amination with dimethyl amine and sodium triacetoxyborohydride, leading to the protected target compounds. Subsequent removal of the benzyl group via hydrogenolysis afforded each of the stereo isomers of **5-3**. Importantly the stereoisomers remained stable to isomerisation during the three reactions.

Furthermore, a sample of each stereoisomer was dissolved in *d*-chloroform. $^{1}H$ NMR experiments were ran after one hour, four hours, overnight, three days and finally after a week. During this time no isomerisation of the double bond was observed in solution. In contrast, 4-OHT isomerised to a 1.2:1 ratio of the *Z:E* during 16 hours under the same conditions. We rationalised that the alkylation of the phenol impeded the isomerisation mechanism proposed in Scheme 5.37.

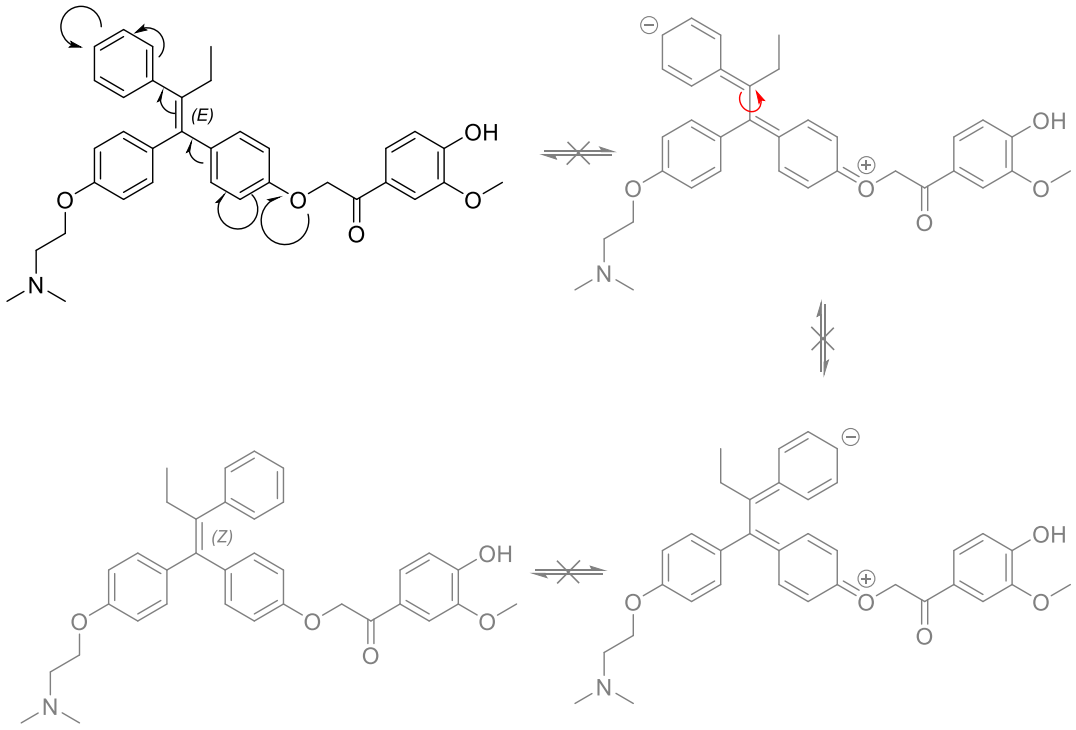


**Scheme 5.37**.

## 5.4 Biological tests results of Guaymoxifen

### 5.4.1 *In vitro* test of Guaymoxifen

Now with our target compound in hand for the first time, we wanted to test whether the beta ether bond could be cleaved by the LigF enzyme. This was crucial to the project, as the 4-OHT being released would be the active molecule invoking the desired biological change. Unlike the 4-methyl umberliferone, 4-OHT is not fluorescent so we were not able to follow the cleavage using the fluorimeter.

In our first attempt to follow the cleavage, we incubated Guaymoxifen in 20 mM Tris HCl buffered at pH 7.6, along with 1 mM of glutathione and the LigF enzyme overnight. In the morning, we extracted the aqueous phase with ethyl acetate and tried to follow the reaction progression by TLC. Unfortunately we weren't able to see either the starting material or the 4-OHT by TLC, perhaps due to the low concentration.

Together with the mass spectrometry core facility, we designed an experiment to see if the Guaymoxifen is cleaved to liberate 4-OHT. Firstly, conditions to separate the two isomers of 4-OHT were found.

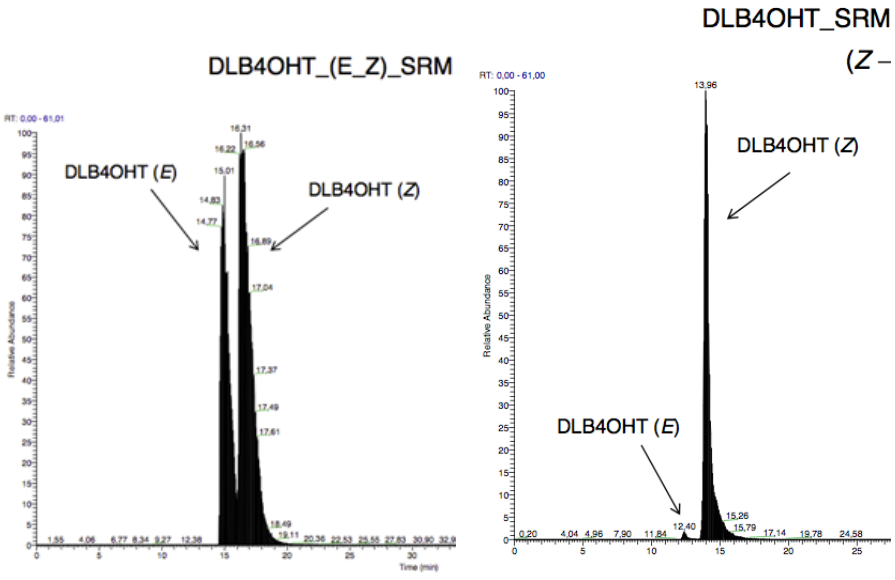


**Figure 5.10**. HPLC-MS of a diastereomeric mixture of 4-OHT (**5-3**) and commercial sample of (Z)-4OHT.

Using the same gradient, there was a clear separation between Guaymoxifen and 4-OHT giving us the conditions to follow the cleavage of Guaymoxifen by LigF. Also both the *E* and *Z* isomers of 4-OHT, and the *E* and *Z* isomers of Guaymoxifen separated under the same conditions. This meant that we were able to follow the cleavage of each isomer of Guaymoxifen.

Thankfully, LigF was able to cleave the beta ether bond linking the recognition fragment and the 4-OHT core, producing 4-OHT. Note that the molecule remained intact when all the other components were present bar the LigF in the control experiments. Unexpectedly the *E*-Guaymoxifen cleaved at a faster rate than the *Z* isomer. This was very fortunate as this allows us to liberate the isomer (Z)-4-OHT) we want. The fact that *E*-Guaymoxifen cleaves to give (Z)-4-OHT is due to the Cahn-Ingold-Prelog priority rules.

The cleavage of Guaymoxifen reached a plateau of 50% after approximately 30 hours and arrived half way to the plateau after 3 hours, which we envisaged to be a sufficient rate to be a useful tool *in vivo*.

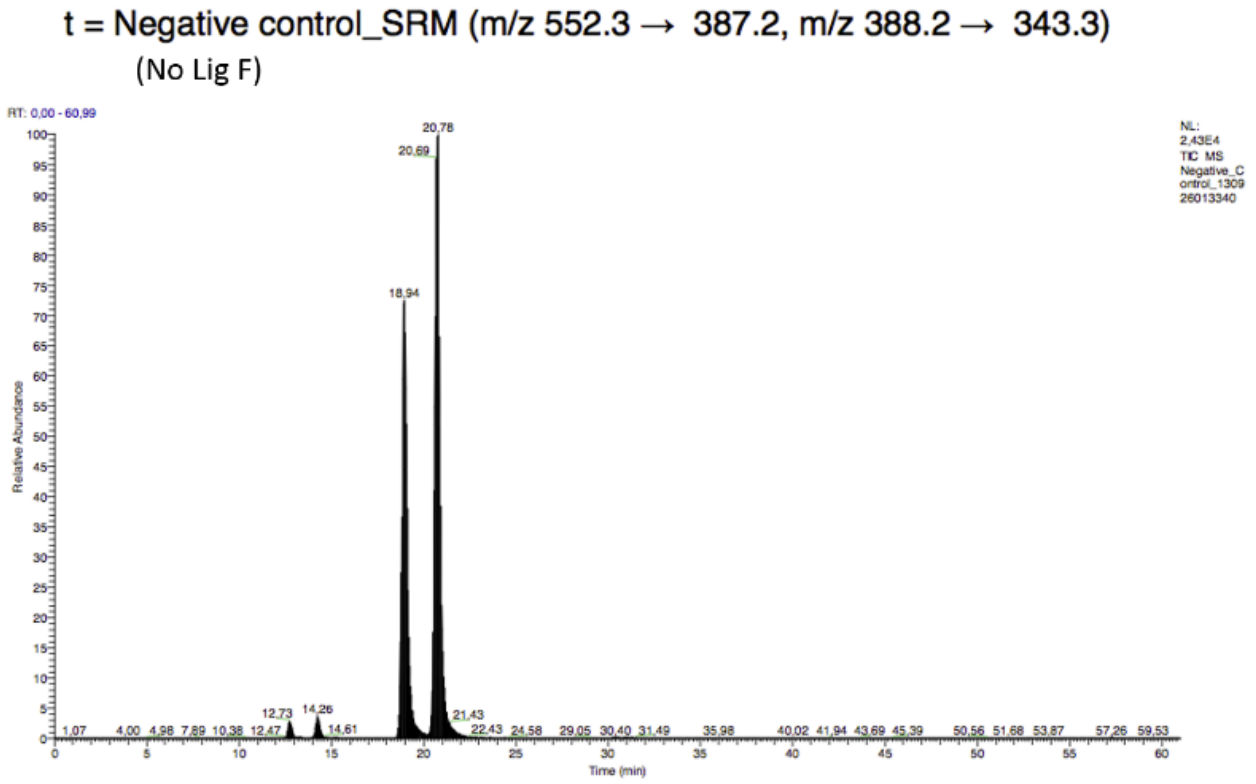


a)

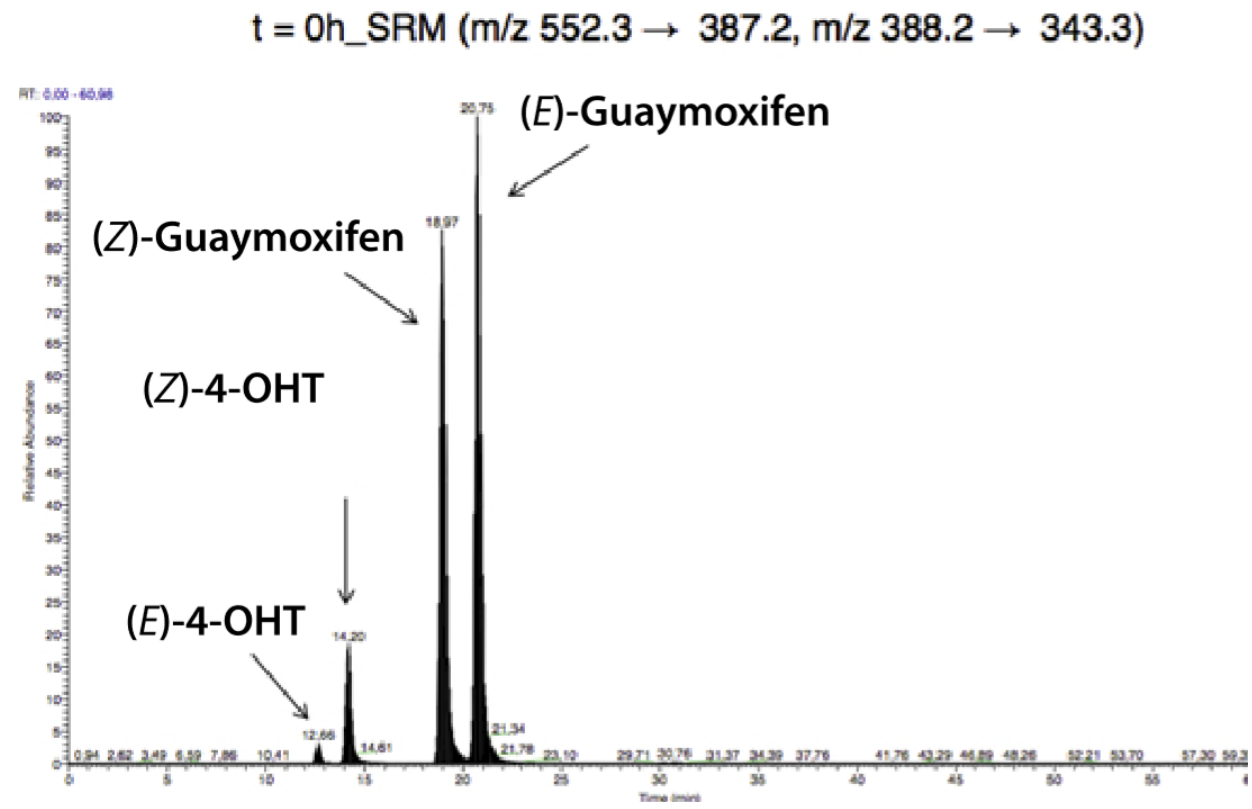
t = 0h_SRM (m/z 552.3 → 387.2, m/z 388.2 → 343.3)
(E)-Guaymoxifen
(Z)-Guaymoxifen
(Z)-4-OHT
(E)-4-OHT
Relative Abundance
Time (min)

b)

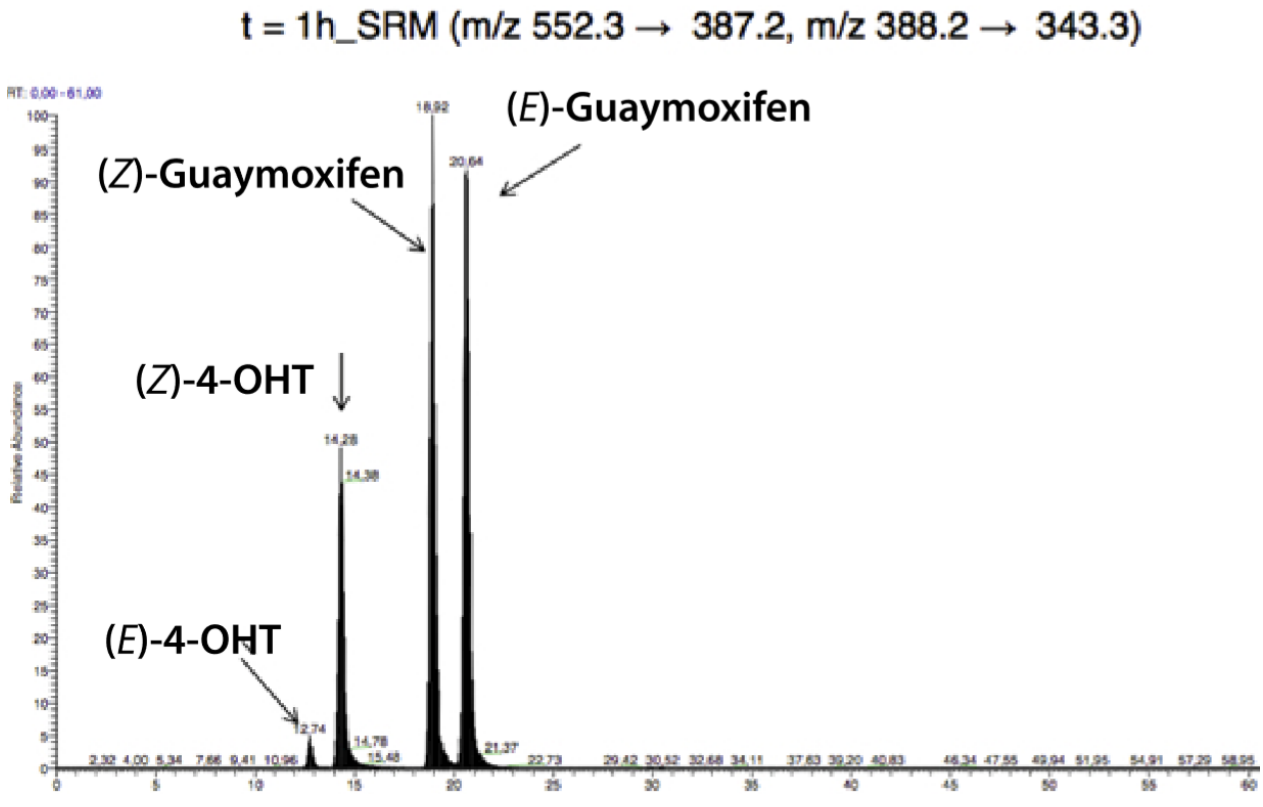
t = 1h_SRM (m/z 552.3 → 387.2, m/z 388.2 → 343.3)
(E)-Guaymoxifen
(Z)-Guaymoxifen
(Z)-4-OHT
(E)-4-OHT
Relative Abundance

c)

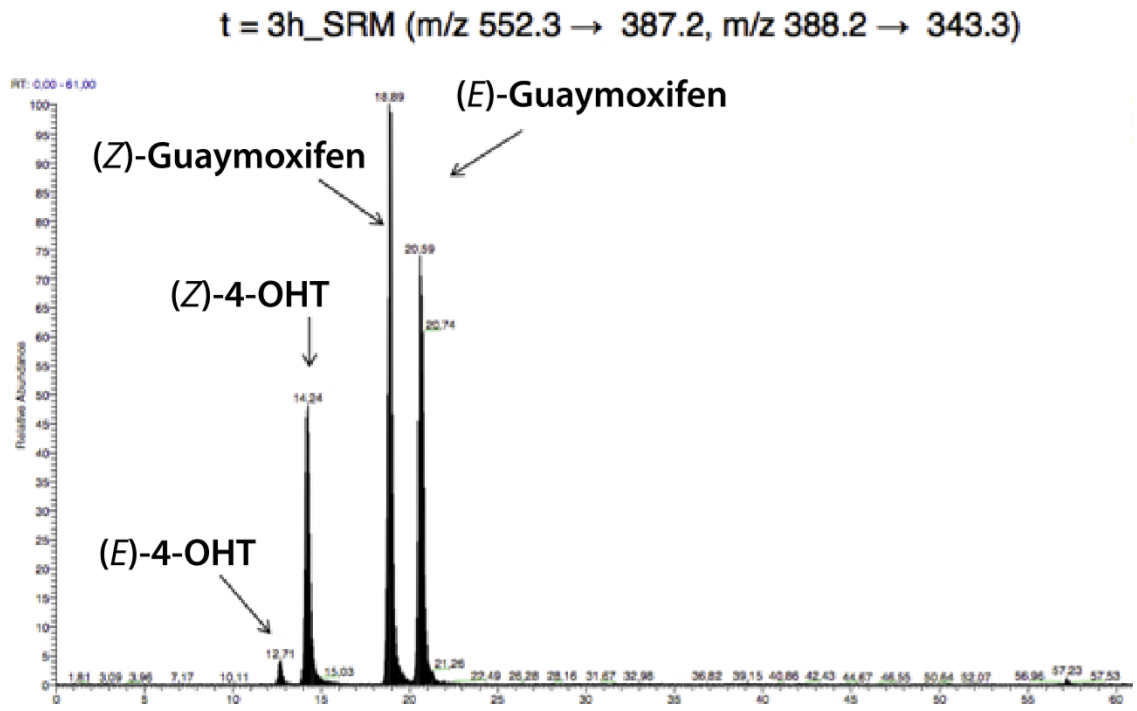


d)

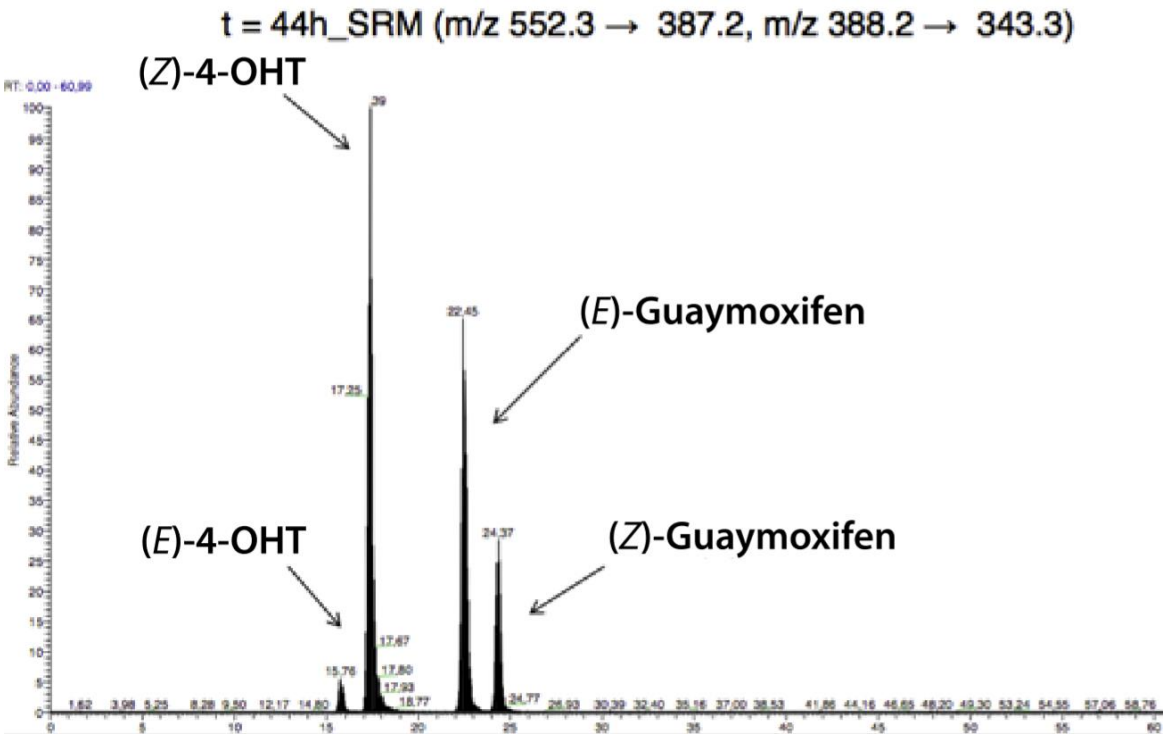


e)

**Figure 5.11.** HPLC-MS experiment of the cleavage of the beta ether bond of Guaymoxifen by LigF, giving 4-OHT. a) negative control. b) Time = 0. c) Time = 1 hour. d) Time = 3 hours. e) Time = 44 hours.

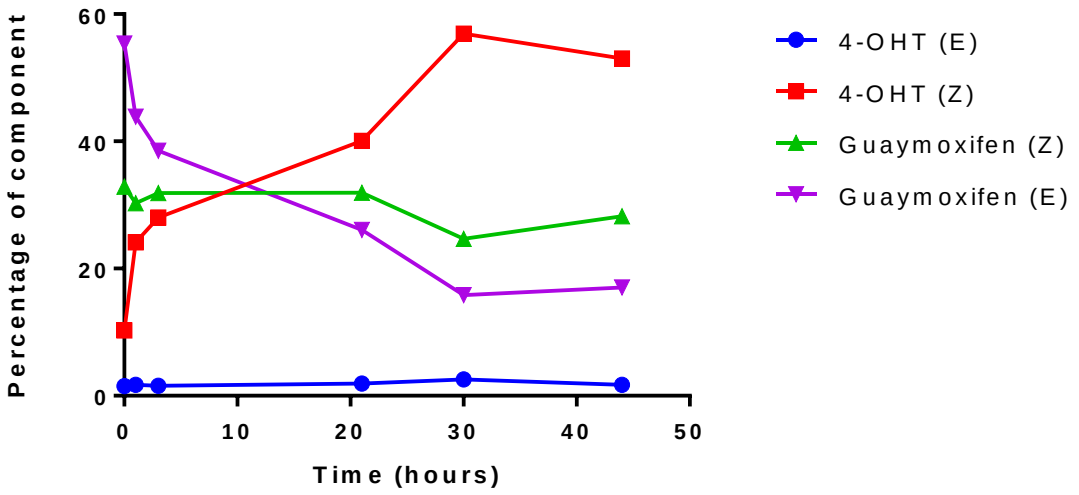


**Figure 5.12**. Quantification of the conversion of Guaymoxifen to 4-OHT vs time.

This mass spectroscopy gave us some useful insight into where we should go from here. To avoid any potential toxicity or other unwanted secondary effects, we need to make selectively the *E*-Guaymoxifen. However, with the *E/Z* Guaymoxifen in hand and before reembarking on a challenging synthesis of a tetra-substituted olefin, we needed to test to see if the Guaymoxifen worked in a cellular assay.

## 5.4.2 Cellular tests of Guaymoxifen

One of the potential hurdles and unanswered questions at this point was that if the Guaymoxifen would be able to pass through the cell membrane and, upon coming into contact with the LigF, be transformed into the 4-OHT inside the cell. The second hurdle was if the newly liberated 4-OHT would be able to leave the cell bearing the LigF and diffuse into a cell nearby bearing the CRe-ER$^{T2}$ toolkit.

To answer this question, we designed an experiment using a cell culture with two types of cells. Mouse embryonic fibroblasts (MEFs) were used from a genetic model bearing *Ub-creERT2;R26-mTmG* as shown below in Figure 5.13.

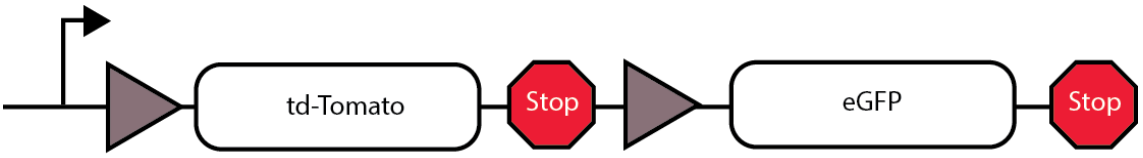


**Figure 5.13.** Gray triangles depict LoxP sites.

Before interacting with 4-OHT, the system expresses the membrane bound tdTomato (tandem dimer tomato), which is a red fluorescent protein. Upon treatment with 4-OHT the CRe-ER$^{T2}$ toolkit becomes activated and excises the area between loxP sites, including the tdTomato gene and a stop site, leaving the enhanced green fluorescent protein (eGFP) in proximity of the promotor. Effectively this means that when the system comes into contact with 4-OHT, the cells stop their production of tdTomato and proceed to express the eGFP. This genetic switch can be efficiently quantified by flow cytometry analysis.

These reporter MEFs were co-cultured with mouse tumour organoids using methodology developed in the Batlle lab.[12] These organoids were then infected in solution with a lentiviral vector so they were able to express the LigF protein. The appropriate control experiments were also performed ensuring that recombination could only occur by the Guaymoxifen entering a MEF cell, being cleaved by LigF and after leaving the MEF, entering the mouse tumour cell and activating the recombinase system.

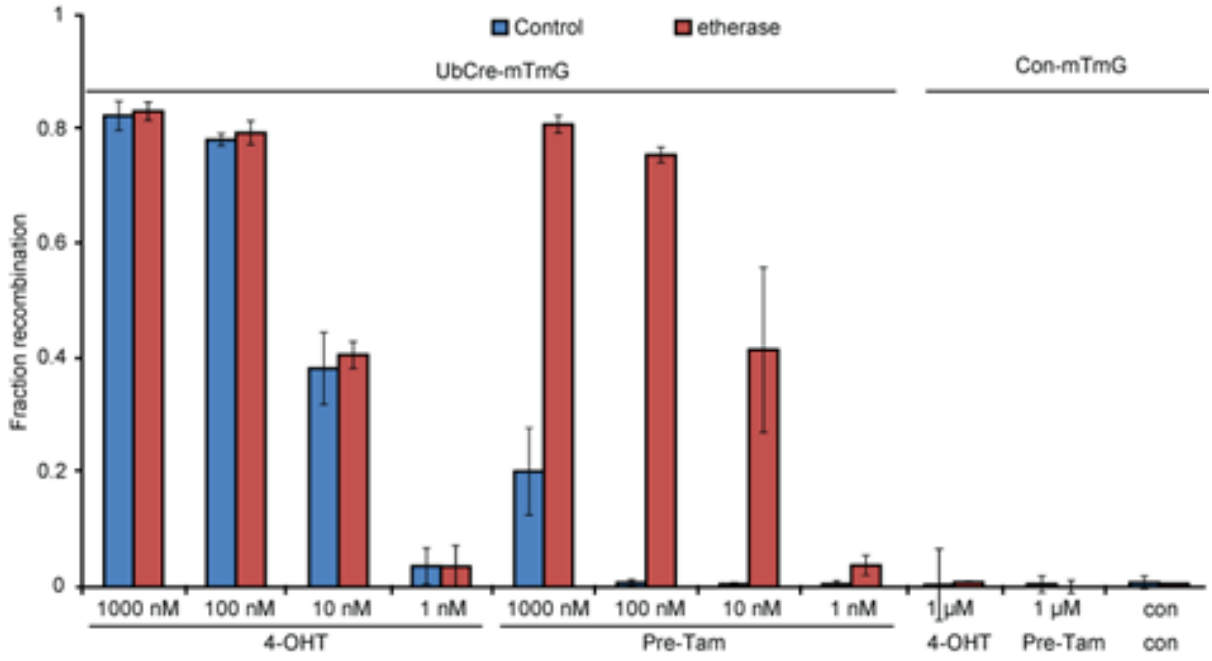


**Figure 5.14**. **5-3** is shown as 'Pre-Tam'. 'Con' is the control experiment.

There was a very strong correlation between the fraction of recombination driven by direct addition of (*Z*)-4-OHT and that induced by Guaymoxifen. This implies that under these conditions, the cleavage of the Guaymoxifen was close to quantitative. At 1000 nM of Guaymoxifen, there was a slight amount of recombination. This could be due to the fact that Guaymoxifen itself has a slight affinity ($10^{-2}$ – $10^{-3}$) for the $ER^{T2}$ or that the Guaymoxifen sample itself had a between 0.1-1% impurity of 4-OHT.

We designed a different experiment to confirm that the system worked in other cell types and using a different reporter method. This time we infected HEK293T cells with PGK-LigF using again a lentiviral. These HEK cells were then co-cultured with the human CRC cell line LS173T which were engineered to express a dominant negative TCF4-$ER^{T2}$ fusion protein. Upon activation with 4-OHT, the fusion protein enters the nucleus of the cell and inhibits some WNT target gene transcription. The levels of gene expression can then be measured by quantitative PCR (qPCR) expression assays. In this particular case, we measured the expression of ASCL2 and KRT20, which are a stem cell gene repressed by 4-OHT and a differentiation gene activated by 4-OHT, respectively.

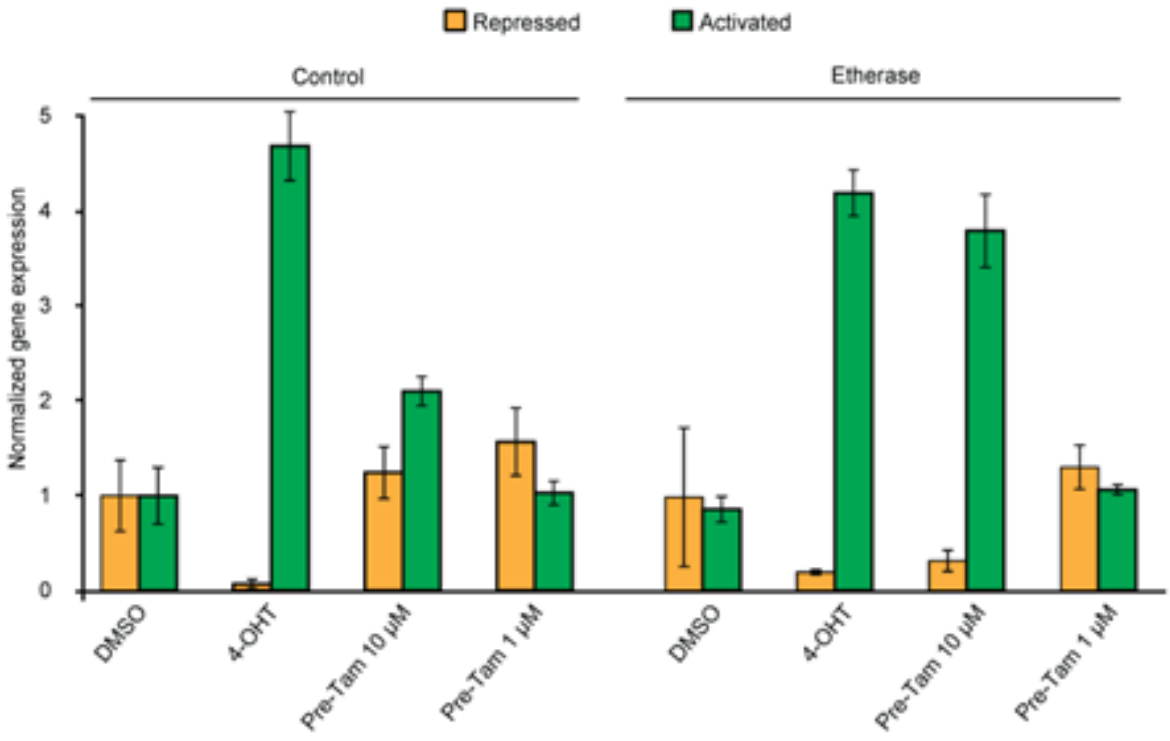


**Figure 5.15**. Normalised gene expression. **5-3** is shown as 'Pre-Tam'. 'Con' is the control experiment.

Using a different reporter cell line and method, and also a different cell line expressing the LigF enzyme, we still observed the co-culture system working as we desired it to.

## 5.5 Conclusions

In chapter 5, we described the design of Guaymoxifen (**5-3**) based on a combination of the drug 4-hydroxytamoxifen (**5-2**) and part of the natural polymer lignin – specifically the part which is recognised by the enzyme LigF. Before embarking on the synthesis of Guaymoxifen, we first sought to optimise the recognition fragment – the part of the **5-3** which would be cleaved by the exogenous enzyme LigF, thus liberating 4-hydroxy tamoxifen (**5-2**).

A series of alpha-bromo ketones were synthesized with strategic variations on the aryl ring. These were then reacted with 4-methylumberliferone (**5-5**), and in some cases further modifications were performed post-reaction with **5-5**, forming a family of compounds whose ability to be cleaved by the exogenous enzyme LigF was tested *in vitro*. If the beta-ether bond was cleaved by LigF, **5-5** is released which itself is a fluorescent compound. As the alkylated derivatives of **5-5** were not fluorescent, the cleavage of the beta-ether bond could be measured in real-time using a fluorimeter by the amount of **5-5** produced. Only significant cleavage was seen of one member of the family (**5-4a**), and therefore this structure was chosen as the one used in compound Guaymoxifen.

Following numerous routes attempted, Guaymoxifen was successfully synthesised as a mixture of *E* and *Z* isomers. It was then submitted to two main biological tests. The first was with the reaction between LigF (expressed by the Protein expression core facility at IRB Barcelona) and Guaymoxifen *in vitro*. The reaction was followed by mass spectrometry, and liberation of **5-2** from the reaction between **5-3** and glutathione catalysed by LigF was seen as time progressed, indicating that our original hypothesis of LigF being able to transform **5-3** into **5-2** was correct.

LigF was then encoded into the HEK293T cells. These cells were then co-cultured with cells which respond to treatment with **5-2** (reporter cells). Upon treatment with **5-3**, the reporter cells responded by activation of Cre recombination. This implied various important points - **5-3** was able to pass through the cell wall and enter into the cell; LigF inside the cell was able to convert **5-3** into **5-2**; **5-2** was then able to leave the cell and enter into another cell in the surrounding area and activate the Cre toolkit.

Knowing that our compound was working in a biological setting, both *E* and *Z* isomers of Guaymoxifen were synthesized as single isomers.

## 5.6 References


[1] J. Reiter, H. Strittmatter, L. O. Wiemann, D. Schieder, V. Sieber, *Green Chem.* 2013, *15*, 1373.

[2] E. Masai, A. Ichimura, Y. Sato, K. Miyauchi, Y. Katayama, M. Fukuda, *J. Bacteriol.* **2003**, *185*, 1768–75.

[3] M. S. Singh, P. A. Francis, M. Michael, *The Breast* **2011**, *20*, 111–118.

[4] D. P. Cronin-Fenton, P. Damkier, T. L. Lash, *Future Oncol.* **2014**, *10*, 107–22.

[5] Y. Takemoto, H. Yoshida, K. Takaki, *Chemistry* **2012**, *18*, 14841–4.

[6] C. Maaliki, Y. Chevalier, E. Thiery, J. Thibonnet, *Tetrahedron Lett.* **2016**, *57*, 3358–3362.

[7] M. Shimizu, C. Nakamaki, K. Shimono, M. Schelper, T. Kurahashi, T. Hiyama, *J. Am. Chem. Soc.* **2005**, *127*, 12506–7.

[8] L.-M. Zhao, H.-S. Jin, J. Liu, T. C. Skaar, J. Ipe, W. Lv, D. A. Flockhart, M. Cushman, *Bioorg. Med. Chem.* **2016**, *24*, 5400–5409.

[9] V. N. Korotchenko, A. V. Shastin, V. G. Nenajdenko, E. S. Balenkova, *J. Chem. Soc. Perkin Trans. 1* **2002**, *2*, 883–887.

[10] S. Gauthier, J. Mailhot, F. Labrie, *J. Org. Chem.* **1996**, *61*, 3890–3893.

[11] J. E. McMurry, L. R. Krepski, *J. Org. Chem.* **1976**, *41*, 3929–3930.

[12] D. V. F. Tauriello, S. Palomo-Ponce, D. Stork, A. Berenguer-Llergo, J. Badia-Ramentol, M. Iglesias, M. Sevillano, S. Ibiza, A. Cañellas, X. Hernando-Momblona, et al., *Nature* **2018**, *554*, 538–543.

# Chapter 6

# Conclusions

In chapter 3 of this doctoral thesis, we have synthesised hundreds of grams of the TGF-β inhibitor LY2157299 (Galunisertib). This product was used by the group of Eduard Batlle in their investigations into the roles that TGF-β plays in colorectal cancer. During the initial synthesis and subsequent scale up, we overcame hurdles including optimisation of the penultimate step of the reaction - giving reproducible results - as well as optimising conditions of the final solid form to provide a product which is suitable for formulation for the *in vivo* experiments.

After discovering some of the drawback of LY2157299, we designed and synthesised a novel TGF-β inhibitor which we named HOLY (**3-10**). HOLY proved to be nearly 10x more potent than the original compound and shows a very significant reduction in the negative physical effects that were observed when administering LY2157299 at a therapeutic dose *in vivo*.

HOLY was designed to be a compound which could be transformed into a prodrug, and therefore modulation of various properties could be achieved with careful modification of the structure. This was demonstrated by modification of the phenol of HOLY to give a substituted carbamate inspired by the structure of Irinotecan and was subsequently named IrinOLY. It was hypothesised that this carbamate would be enzymatically cleaved *in vivo,* releasing the active TGF-β inhibitor. When tested *in vivo*, this IrinOLY was shown to be a potent TGF-β inhibitor as well as a compound much more comfortable to formulate when compared to LY2157299. Other potential advantages of this novel compound, such as infusion via an osmotic pump, are yet to be explored and will be done so in the near future.

In chapter 5 of this doctoral thesis, we designed a molecule which was capable of being cleaved at a specific point by an exogenous enzyme (LigF), releasing the active compound 4-hydroxy tamoxifen. After the cleavage, 4-OHT would then be able to activate the Cre toolkit and therefore performing specific genetic modifications to cells in the vicinity from where the 4-OHT was released.

In order for the 4-hydroxytamoxifen to be released, a beta ether bond needed to be cleaved by the enzyme LigF. The fragment containing the beta ether bond had various points in which modifications could be possible to modulate properties such as solubility and bioavailability, however specificity for the LigF enzyme needed to be maintained. In order to synthesise the optimum compound(s), first a structure activity relationship study was performed on the recognition fragment of the part of the desired compound that LigF would cleave.

A small library of compounds bearing on one side various strategic modification of the original ligand to LigF, and on the other side the reporter 4-methylumberliferone. This enabled us to perform modifications on the recognition fragment, test the new modifications in front of the LigF enzyme, and then perform further modifications based upon these results.

A synthesis the optimised recognition fragment covalently bound to 4-hydroxy tamoxifen was then designed, synthesised, and tested both *in vitro*. The tests showed that 4-OHT was indeed cleaved in all three of the aforementioned settings, and so we sought to synthesise the target compound in its pure isomeric form.

Following many attempts at complex coupling reactions, we eventually reached our target compound isomerically-pure following preparative HPLC of a key intermediate of the initial synthesis. The corresponding isomers were then transformed successfully into both the *E* and the *Z* isomers of Guaymoxifen.

# Chapter 7

# Experimental

# 7 Experimental

## 7.1 General methods and instrumentation

All reactions were carried out under an inert atmosphere ($N_2$) unless otherwise stated, with the nitrogen gas being passed through a column of Drierite® before use, and the reaction flasks were flame dried before use. Anhydrous THF, DCM and diethyl ether were taken from the Innovative Technology Inc. Puresolv Solvent Purification System (SPS). Other anhydrous solvents were purchase from Sigma-Aldrich and used without any further purification or drying.

Starting materials were purchased from the following suppliers and were used without any further purification: Sigma-Aldrich, Manchester Organics, TCI, or Fluorochem.

All experiments were monitored by analytical thin-layer chromatography (TLC) using silica gel TLC-aluminium sheets (Merck 60 $F_{254}$). The results were visualised under a UV lamp (either 254 or 365 nm) and revealed using a $KMnO_4$ stain when necessary.

Flash column chromatography was performed on either a CombiFlash ® (Teledyne Isco), or on the Puriflash 430 (Interchim) unless otherwise stated. The mobile phase was either a gradient of hexane/ethyl acetate, or a gradient of dichlormethane/methanol. In some cases where a basic nitrogen was present on the molecule being purified, the column was preconditioned with a 2.5 % triethylamine solution in hexanes.

Samples for NMR were dissolved in either $CDCl_3$, $CD_3OD$, DMSO or $D_2O$. The spectra was then recorded on one of the following instruments:

- Varian-Unity 300: $^1H$ NMR (300 MHz) and $^{13}C$ NMR (75 MHz)
- Mercury 400: $^1H$ NMR (400 MHz) and $^{13}C$ NMR (100 MHz)
- Varian-Unity 500: $^1H$ NMR (500 MHz) and $^{13}C$ NMR (125 MHz)

$^1H$ and $^{13}C$ spectra were referenced to residual solvent peaks and/or tetramethylsilane.[1] The coupling constants were measured in hertz (Hz).

High resolution mass spectrometry experiments were performed either in the IRB core facility, or in the CCiT (Centres Científics i Tecnològics) at the Facultat de Química (Universitat de Barcelona).

All IR spectra were performed using the film method on a NaCl disc and recorded on a Thermo Nicolet Nexus Ft-IR Fourier transform spectrometer.

Ultra-high-pressure liquid chromatography mass spectroscopy (UPLC-MS) analysis was performed using an Acquity high class (PDA eλ detector, Quaternary solvent manager, and a FNT sample manager) coupled to a SQ detector 2. An Acquity BEH C18 (50 x 2 mm x 1.7 µM) column was used, with the mobile phases being MeCN (0.07% formic acid) and water (0.1% formic acid), with a flow rate of 0.6 mL $min^{-1}$. Samples were prepared for analysis by dissolving in either HPLC-grade MeCN, iPrOH, MeOH, MilliQ water, or a mixture thereof. All samples were filtered through a 22 µm filter before being injected into the UPLC-MS.

## 7.2 Experimental methods for Chapter 3

**6-cyano-4-methylquinolin-1-ium chloride, (3-3)**

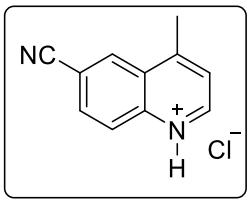


To a stirred solution of 4-aminobenzonitrile (300 g, 2.54 mol) and chloranil (668 g, 2.72 mol, 1.07 equiv.) in ethanol (2.7 L, 9 volumes) at rt was added 37% HCl (654 mL, 7.62 mol, 3 equiv.) over fifteen minutes in a 10 L reactor equipped with mechanical stirring. After stirring for five minutes at rt the reaction mixture was heated to 75˚C where methyl vinyl ketone (310 mL, 3.81 mol, 1.5 equiv.) diluted in ethanol (300 mL, 1 volume) was added to the reaction mixture over thirty minutes. After four hours, no starting material was observed by TLC. The reaction was cooled to 60˚C where it was diluted with THF (3.3 L, 11 volumes), stirred for an hour at 60˚C and then left to cool to rt overnight. The suspension was filtered through a sintered Büchner funnel. The residue was rinsed with THF (2 x 900 mL, 6 volumes in total) and then dried at 50˚C overnight in a vacuum oven to give the title compound (422 g, 81%) as a brown solid. Spectra conformed to compound previously described in the literature.[2]

**$^1$H NMR (400 MHz, DMSO-$d_6$) δ** 9.14 (d, *J* = 5.0 Hz, 1H), 8.92 (d, 1H), 8.38 (d, *J* = 8.8 Hz, 1H), 8.26 (dd, *J* = 8.8, 1.7 Hz, 1H), 7.81 (d, *J* = 5.0 Hz 1H), 2.88 (s, 3H).

**4-(2-(6-methylpyridin-2-yl)-2-oxoethyl)quinoline-6-carbonitrile, (3-4)**

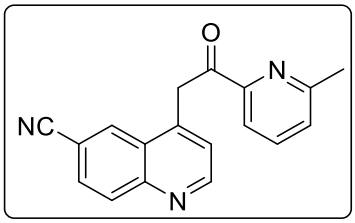


To a stirred suspension of 6-cyano-4-methylquinolin-1-ium chloride (196 g, 713 mmol) in THF (1.9 L, 10 volumes) at 5 ˚C under a nitrogen atmosphere was added NaO$^t$Bu (303 g, 3.16 mol, 3.3 equiv.) portionwise keeping the temperature below 25 ˚C. The reaction mixture was stirred for 0.5 h followed by addition of methyl 6- methylpicolinate (217 g, 1.44 mmol, 1.5 equiv.) diluted in THF (190 mL, 1 volume) at such a rate the internal temperature stayed below 20˚C. After 3 hours the reaction had completed and was cooled to 5 ˚C and then quenched with HCl (2M) until pH 8-9. The mixture was extracted with EtOAc (2 × 1 L, 20 volumes), the combined organic extracts were dried ($MgSO_4$) and the solvent removed *in vacuo*. The residue was redissolved in MeOH (2 L, 10 volumes) at reflux and slowly cool to rt, then to 0˚C in an ice bath. The suspension was filtered through a sintered Büchner funnel and the residue was washed with chilled MeOH (600 mL, 3 equiv.)

and dried in a vacuum oven overnight at 40˚C to afford the title compound (209.8 g, 76.2%) as a brown solid. Spectra conformed to compound previously described in the literature.[2]

**$^1$H NMR (400 MHz, cdcl3) δ** 8.98 (d, J = 4.4 Hz, 1H), 8.63 (d, J = 1.5 Hz, 1H), 8.20 (d, J = 8.4 Hz, 1H), 7.89 – 7.81 (m, 2H), 7.76 (t, J = 7.7 Hz, 1H), 7.54 (d, J = 4.4 Hz, 1H), 7.41 (d, J = 7.7 Hz, 1H), 5.03 (s, 2H), 2.72 (s, 3H).

**4-chloro-N'-(diphenylmethylene)butanehydrazide, (3-7)**

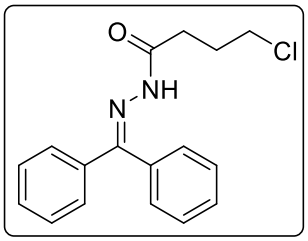


To a stirred solution of benzophenone hydrazone (200 g, 1.019 mol) and pyridine (82 mL, 1.019 mol, 1 equiv.) in DCM (1 L) at rt and under $N_2$, was added 4-chlorobutyryl chloride (114 mL, 1.019 mol, 1 equiv.) at such a rate that the reaction mixture was at a gentle reflux. The reaction mixture was stirred for 30 minutes, cooled to rt in a water bath, then quenched and the salts extracted with water (2 x 500 mL). The organic layer was dried ($MgSO_4$) and the solvent removed *in vacuo* to afford the titled compound as a (295 g, 96%) as a pale yellow solid. Spectra conformed to compound previously described in the literature.[3]

$^1$H NMR (400 MHz, Chloroform-*d*) δ 8.41 (br s, 1H), 7.59 - 7.20 (m, 10H), 3.69 (t, *J* = 6.4 Hz, 2H), 3.04 (t, *J* = 7.2 Hz, 2H), 2.22 (p, *J* = 6.8 Hz, 2H).

**1-((diphenylmethylene)amino)pyrrolidin-2-one, (3-8)**

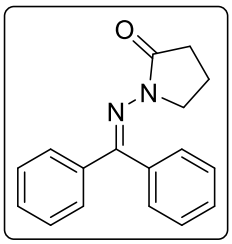


To a stirred solution of **3-7** (100 g, 0.332 mol) in THF (700 mL) at 0˚C and under $N_2$ was added 95% sodium hydride (8.36 g, 0.349 mol, 1.05 equiv.) portionwise. The reaction mixture was stirred for 30 minutes at 0˚C before being warmed to rt and left for 2 hours, where it was quenched with saturated $NH_4Cl_{(aq)}$ and extracted with EtOAc (2 x 300 mL). The combined organic extracts were dried ($MgSO_4$), evaporated to give the titled compound (83.3 g, 94.8%) as a pale yellow solid. Spectra conformed to compound previously described in the literature.[3]

**$^1$H NMR (400 MHz, Chloroform-*d*)** δ 7.64 – 7.28 (m, 10H), 3.32 (t, *J* = 7.0 Hz, 2H), 2.32 (t, *J* = 8.0 Hz, 2H), 1.92 (p, *J* = 7.5 Hz, 2H).

**2-oxopyrrolidin-1-aminium tosylate, (3-5)**

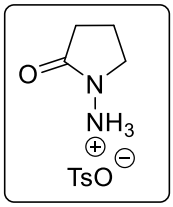

To a stirred solution of **3-8** (50 g, 0.189 mol) in toluene (750 mL, 15 volumes) at 50 ˚C was added water (3.4 mL, 0.189 mol, 1 equiv.) and p-TSA (32.95g, 0.189 m, 1 equiv.). The reaction mixture was stirred for 2 hrs and then cooled to rt and concentrated to 33% of the initial volume. The precipitate was filtered through a sintered Büchner funnel, washed with toluene (2 x 100 mL, 4 volumes in total) and dried in a vacuum oven at 35˚C overnight to give title compound (43.3 g, 84.4%) as a white solid. Spectra conformed to compound previously described in the literature.[2]

**$^1$H NMR (400 MHz, DMSO-$d_6$)** δ 7.46 (d, *J* = 8.2 Hz, 2H), 7.10 (d, *J* = 8.3 Hz, 2H), 3.46 (t, *J* = 7.0 Hz, 2H), 2.33 – 2.28 (m, 2H), 2.27 (s, 3H), 2.01 (p, *J* = 7.3 Hz, 2H).

**4-(2-(6-methylpyridin-2-yl)-5,6-dihydro-4H-pyrrolo[1,2-b]pyrazol-3-yl)quinoline-6-carbonitrile, (3-9)**

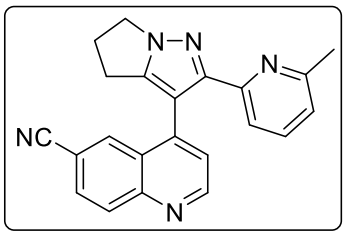

To a stirred solution of **3-4** (78.8 g, 0.274 mol) in DMF (472 mL, 6 volumes), toluene (780 mL, 10 volumes), 2,6-lutidine (78.8 mL, 1 volume) at rt was added **3-5** (74.62 g, 0.274 mol, 1 equiv.). The reaction mixture was stirred at rt for 5 minutes and then heated to reflux under Dean-Stark conditions until most of the starting material had been consumed by TLC. The reaction mixture was cooled to rt where it was charged with $Cs_2CO_3$ (148 g, 0.455 mol, 1.66 equiv.) and heated back to reflux. The reaction was monitored for disappearance of the intermediate and once all was consumed, toluene was distilled from the reaction mixture until the internal temperature of the reaction reached 145˚C indicating that most of the toluene had being distilled. The reaction mixture was then cooled to rt and diluted with water (1100 mL, 17 volumes). The resulting suspension stirred for 2 hours at rt, filtered through a sintered Büchner funnel, and the precipitate washed with water (320 mL, 4 volumes). The solid was dried in a vacuum oven at 45˚C overnight to give the title compound (137.5 g, 78.9%) as a light brown solid. Spectra conformed to compound previously described in the literature.[2]

**$^1$H NMR (400 MHz, DMSO-$d_6$) δ** 9.00 (d, *J* = 4.5 Hz, 1H), 8.16 (d, *J* = 8.7 Hz, 1H), 8.09 (d, *J* = 1.8 Hz, 1H), 7.94 (dd, *J* = 8.7, 1.9 Hz, 1H), 7.68 – 7.59 (m, 2H), 7.56 (d, *J* = 4.5 Hz, 1H), 6.95 (d, *J* = 7.2 Hz, 1H), 4.29 (t, *J* = 7.3 Hz, 2H), 2.88 (s, 2H), 2.63 (p, *J* = 7.1 Hz, 2H), 2.05 (s, 3H).

**4-(2-(6-methylpyridin-2-yl)-5,6-dihydro-4H-pyrrolo[1,2-b]pyrazol-3-yl)quinoline-6-carboxamide monohydrate, (3-1)**

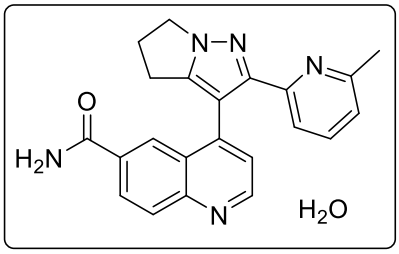


To a stirred solution of **3-9** (137.5 g, 0.39 mol) in DMSO (820 mL, 6 volumes) was added $K_2CO_3$ (10.8 g, 78.2 mmol, 0.2 eq) at rt and stirred for 30 minutes. 30% $H_2O_2$ (49.79 mL, 0.488 mol, 1.25 equiv.) was then diluted with water (70 mL, 0.5 volumes). This solution was then added dropwise over 2 hrs to the reaction mixture ensuring the reaction mixture stays below 40˚C. After a further hour, no starting material was visible by TLC and the reaction was slowly quenched with sodium sulphite (29.5 g, 0.234 mol, 0.6 equiv.) in water (1.23 L, 9 volumes) keeping the temperature below 40˚C, and after all the quench was added, was left for a further hour at rt. The reaction mixture was checked for the presence of peroxide (Quantofix®), followed by addition of 32% HCl (148 mL, 1.08 volumes), stirred for 30 minutes, activated charcoal (14 g, 10% wt) was added and the reaction mixture was stirred for a further hour. The suspension was then filtered through celite, diluted with MeOH (143 mL, 1.05 volumes) and taken to pH8-9 with NaOH (2M), ensuring the reaction mixture stayed below 30˚C. The suspension was then filtered, and the resulting solid suspended in 3:1 acetone:water (3.8 L, 28 volumes) at reflux and held at there for 1.5 hrs before being filtered. The filtrate was then distilled until half of the original volume remained (1.9 L, 14 volumes), at which point the reactor was allowed to cool to rt overnight, followed by cooling to 0˚C for one hour the following morning. The product was filtered and dried in a vacuum oven for 24 hrs at 45˚C giving the title compound (113g, 78.4%). Due to the large particle size of a slow crystallisation, a portion of the product (25.4g) was then dissolved in the minimum amount (approximately 6 volumes) of 60:40 EtOH:MeCN at reflux and this solution was then quickly added to ice cooled water (500 mL, 20 volumes) and stirred for a further hour at 0˚C. The suspension was filtered, and the product was dried in a vacuum oven for 24 hrs at 45˚C affording the titled compound (24.8g, 97.6% recovery) as a fine white powder. Spectra conformed to compound previously described in the literature.[2]

**$^1$H NMR (400 MHz, Chloroform-*d*)** δ 8.92 (d, *J* = 4.5 Hz, 1H), 8.19 (d, *J* = 1.9 Hz, 1H), 8.13 (d, *J* = 8.8 Hz, 1H), 8.08 (dd, *J* = 8.8, 1.9 Hz, 1H), 7.37 (d, *J* = 4.5 Hz, 1H), 7.30 (t, *J* = 7.7 Hz, 1H), 7.04 (d, *J* = 7.8 Hz, 1H), 6.90 (d, *J* = 7.7 Hz, 1H), 6.23 (br s, 1H), 5.78 (br s, 1H), 4.35 (t, *J* = 7.3 Hz, 2H), 2.91 (t, *J* = 7.1 Hz, 2H), 2.68 (p, *J* = 7.3 Hz, 2H), 2.23 (s, 3H), 2.04 (s, 2H).

**6-methoxy-4-methylquinoline, (3-12)**

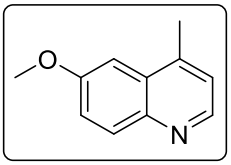

To a stirred solution of *p*-anisidine (5 g, 40.6 mmol) and $ZnCl_2$ (719 mg, 5.3 mmol, 0.13 equiv.) in ethanol (20 mL) at rt was added $FeCl_3$ (17.45 g, 107.6 mmol, 2.65 equiv.) portionwise over 30 minutes. The reaction mixture was stirred for 30 minutes, when methyl vinyl ketone (3.38 mL, 40.6 mmol, 1 equiv.) was added and heated to 75˚C for two hours. It was then cooled to rt and poured into NaOH (1M, 220 mL) at 0˚C. The mixture was extracted with EtOAc (3 × 40 mL) and the combined organic extracts were dried ($MgSO_4$), evaporated and the residue was chromatographed (0-100% EtOAc in hexanes) to give the title compound (2.88 g, 41%) as a brown oil. Spectra conformed to compound previously described in the literature.[4]

**$^1$H NMR (400 MHz; $CDCl_3$) δ** 8.65 (d, *J* = 4.4 Hz, 1H), 8.02 (d, *J* = 9.2 Hz, 1H), 7.37 (dd, *J* = 9.2, 2.8 Hz, 1H), 7.21 (d, *J* = 4.4 Hz, 1H), 7.19 (d, *J* = 2.8 Hz, 1H), 3.96 (s, 3H), 2.67 (s, 3H).

**2-(6-methoxyquinolin-4-yl)-1-(6-methylpyridin-2-yl)ethan-1-one, (3-13)**

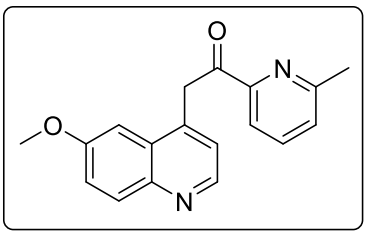

To a stirred solution of **3-12** (2.5 g, 14.4 mmol) in THF (80 mL) at -78 ˚C was added LDA (33.19 mmol, 2.3 equiv.). The reaction mixture was stirred for 30 minutes when methyl 6- methylpicolinate (3.27 g, 21.6 mmol, 1.5 eq) was added dropwise to the reaction mixture over 30 minutes. The reaction was left at -78˚C and allowed to warm to rt overnight. It was then quenched with sat. $NH_4Cl$ (20 mL), diluted with EtOAc (40 mL) and the phases separated. The aqueous phase was extracted with chloroform (2 x 50 mL), the combined organic extracts were dried ($MgSO_4$), evaporated and the residue was chromatographed (0-100% EtOAc in hexanes) to give the title compound (1.91 g, 51%) as a brown oil;

**$^{1}$H NMR (400 MHz; $CDCl_3$) δ** 8.70 (m, 1H), 8.04 – 7.95 (m, 1H), 7.84 (d, *J* = 7.6Hz, 1H), 7.71 (t, *J* = 7.7 Hz, 1H), 7.43 – 7.31 (m, 4H), 4.95 (s, 2H), 3.83 (s, 3H), 2.67 (s, 3H).

**$^{13}$C NMR (101 MHz, $CDCl_3$) δ** 198.23, 158.05, 157.80, 152.16, 147.52, 144.50, 140.42, 137.23, 131.46, 128.92, 127.22, 123.77, 121.54, 119.56, 102.46, 55.39, 40.75, 24.41.

I**R (Film):** 3377, 3065, 2969, 2932, 2827, 1693, 1624, 1577, 1520, 1242, 1230 $cm^{-1.}$

**HRMS (ESI):** m/z [M + H]+ calculated for $C_{18}H_{16}N_2O_2$: 292.1212; found: 292.1208.

**6-methoxy-4-(2-(6-methylpyridin-2-yl)-5,6-dihydro-4H-pyrrolo[1,2-b]pyrazol-3-yl)quinoline, (3-14)**

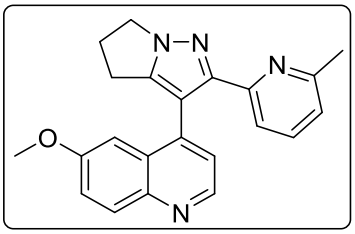

To a stirred solution of **3-13** (1.60 g, 5.47 mmol) in DMF (9.6 mL, 6 volumes), toluene (16 mL, 10 volumes) and 2,6-lutidine (1.6 mL, 1 volume) at rt was added 1-aminopyrrolidin-2-one tosylate salt (1.49 g, 5.47 mmol, 1 eq) and stirred at rt for 5 minutes. The reaction was heated to reflux under Dean-Stark conditions until most of the starting material had been consumed by TLC. The reaction mixture was cooled to rt where it was charged with $Cs_2CO_3$ (3.029g, 9.299 mmol, 1.7 equiv.), left for 5 minutes before being heated back to reflux. The reaction was monitored for disappearance of the intermediate and once all was consumed, the reaction was cooled to rt and split between water (50 mL) and EtOAc (50 mL). The aqueous phase was extracted (2 x 25 mL), the combined organic extracts were washed with 5% LiCl aqueous solution (2 x 50 mL) and the organic layer was dried ($MgSO_4$), evaporated and the residue was chromatographed (0-10% MeOH in DCM). The fractions containing the product were dissolved in a small amount of $CHCl_3$ and diluted slowly with hexane until the mixture appeared to be slightly cloudy. The flask was left in the fridge for 48 hours were crystals were formed. (1.28 g, 67%) as a white solid;

**$^{1}$H NMR (400 MHz, $cdcl_3$) δ** 8.74 (d, *J* = 4.4 Hz, 1H), 7.98 (d, *J* = 9.2 Hz, 1H), 7.35 – 7.20 (m, 4H), 6.96 – 6.85 (m, 3H), 4.37 (t, *J* = 7.2 Hz, 2H), 3.54 (s, 3H), 2.91 (br s, 2H), 2.75 – 2.65 (m, 2H), 2.38 (s, 3H).

**$^{13}$C NMR (101 MHz, cdcl$_3$) δ** 158.62, 157.67, 153.65, 151.83, 147.66, 146.69, 144.89, 139.90, 136.43, 131.17, 128.25, 122.41, 122.22, 121.93, 119.50, 110.50, 104.00, 55.52, 48.46, 26.19, 24.58, 23.32.

**HRMS (ESI):** m/z [M + H]+ calculated for $C_{22}H_{20}N_4O$: 356.1637; found: 356.1639.

**4-(2-(6-methylpyridin-2-yl)-5,6-dihydro-4H-pyrrolo[1,2-b]pyrazol-3-yl)quinolin-6-ol, (3-10)**

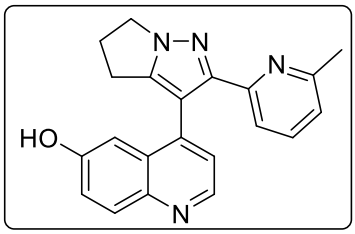


Method 1:

To a stirred solution of **3-14** (432 mg, 1.21 mmol) in acetic acid (5 mL) at rt was added HBr (5 mL, 44.45 mmol, 36.7 equiv.). The reaction mixture was stirred for 48hrs at 120 ˚C before being cooled to rt and the solvent removed *in vacuo*. The residue was split between water (5 mL) and EtOAc (10 mL) and taken to pH 8 with 40% NaOH, phases separated, and the aqueous phase extracted with EtOAc (3 x 10 mL). The combined organic extracts were dried ($MgSO_4$), evaporated and the residue was suspended in refluxing toluene for one hour before been cooled to rt over an hour. The solid was filtered and dried *in vacuo* to give the title compound (328 mg, 79%) as an off white solid:

**$^{1}$H NMR (400 MHz, dmso) δ** 9.66 (s, 1H), 8.58 (d, J = 4.4 Hz, 1H), 7.86 (d, J = 9.0 Hz, 1H), 7.56 (t, J = 7.7 Hz, 1H), 7.48 (d, J = 7.8 Hz, 1H), 7.29 – 7.16 (m, 2H), 6.96 (d, J = 7.5 Hz, 1H), 6.91 (d, J = 2.7 Hz, 1H), 4.27 (t, J = 7.2 Hz, 2H), 2.79 (t, J = 6.5 Hz, 2H), 2.69 – 2.55 (m, 2H), 1.89 (s, 3H).

**$^{13}$C NMR (101 MHz, dmso) δ** 156.49, 155.08, 152.01, 151.70, 146.55, 146.24, 143.18, 139.37, 136.48, 130.60, 128.71, 122.47, 121.16, 117.73, 109.89, 106.98, 47.86, 25.53, 23.41, 22.50.

**IR (film):** 3412, 2949, 2833, 1650, 1618, 1508, 1236, 1010 cm$^{-1}$

**HRMS (ESI):** m/z [M + H]+ calculated for $C_{21}H_{18}N_4O$: 342.1481; found: 342.1480.

**4-(2-(6-methylpyridin-2-yl)-5,6-dihydro-4H-pyrrolo[1,2-b]pyrazol-3-yl)quinoline-6-carboxylic acid, (3-19)**

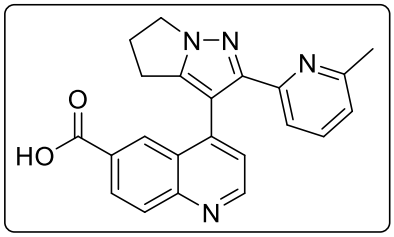

**3-1** (1 g, 2.71 mmol) was dissolved in 37% HCl (2.5 mL) and then heated to 110˚C in a sealed tube and left overnight. The reaction was cooled to rt, diluted with water (10 mL) then taken to pH 5 with $NaHCO_3$. The white precipitate was filtered and dried under vacuum to give the title compound as a white solid (828 mg, 83 %). Spectra conformed to compound previously described in the literature.[5]

**$^1$H NMR** (400 MHz, DMSO-$d_6$) δ 12.92 (s, 1H), 8.94 (d, *J* = 4.3 Hz, 1H), 8.30 (s, 1H), 8.14 – 8.02 (m, 2H), 7.67 – 7.53 (m, 2H), 7.48 (d, *J* = 4.4 Hz, 1H), 6.91 (d, *J* = 6.9 Hz, 1H), 4.34 – 4.28 (m, 2H), 2.88 (s, 2H), 2.65 (q, *J* = 7.1 Hz, 2H), 1.66 (s, 3H).

**$^{13}$C NMR** (101 MHz, DMSO-$d_6$) δ 166.95, 156.25, 151.85, 151.36, 149.52, 147.20, 143.21, 136.68, 129.69, 129.35, 127.93, 127.47, 126.64, 122.59, 121.19, 117.53, 109.06, 48.01, 25.52, 23.05, 22.32.

**M.P.:** 277-279 ˚C

**UPLC-MS:** 372 m/z [M+H]

**1,3-bis(4-(2-(6-methylpyridin-2-yl)-5,6-dihydro-4H-pyrrolo[1,2-b]pyrazol-3-yl)quinolin-6-yl)urea, (3-20)**

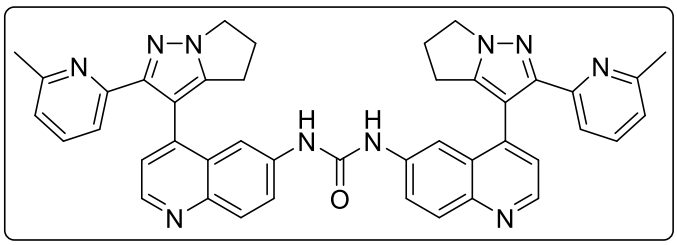

To a stirred suspension of **3-19** (295 mg, 0.796 mmol) in toluene (8 mL) at rt under a $N_2$ atmosphere was added $Et_3N$ (111 µL, 0.796 mmol, 1 equiv.) followed by DPPA (172 µL, 0.796 mmol, 1 equiv.) 10 minutes later. The reaction mixture was heated to 70˚C at which point the suspension became a solution. It was left for an hour when it was then further heated slowly to 95˚C where bubbling (presumed to be $N_2$) was observed. Once the bubbling became less frequent, the reaction was heated to 100˚C and held there for 2 further hours before being cooled to rt and diluted carefully with water (8 mL) while stirring

vigorously. After stirring at rt overnight, the reaction was diluted with $CHCl_3$, the organic phase washed with water (2 x 5 mL), saturated $NaHCO_3$ (2 x 5 mL), dried ($MgSO_4$) and concentrated to half the volume *in vacuo*. The precipitate was filtered through a sintered Büchner funnel and the solid dried under high vacuum to give the title compound (174 mgs, 61.7%) as a white solid

**$^1$H NMR (400 MHz, $CDCl_3$) δ** 8.67 (d, *J* = 4.5 Hz, 2H), 8.08 (s, 2H), 7.89 (s, 1H), 7.33 (t, *J* = 7.8 Hz, 1H), 7.30 – 7.13 (m, 2H), 6.99 (d, *J* = 7.6 Hz, 1H), 6.90 (d, *J* = 7.8 Hz, 1H), 4.15 (br s, 2H), 2.76 (ddd, *J* = 46.2, 32.1, 18.7 Hz, 2H).

**$^{13}$C NMR (101 MHz, cdcl$_3$) δ** 158.78, 153.06, 152.99, 152.93, 151.05, 147.40, 144.91, 139.58, 138.62, 138.52, 137.82, 136.61, 130.26, 128.98, 128.17, 127.85, 125.24, 123.11, 122.90, 122.34, 119.56, 111.37, 49.76, 48.24, 25.91, 24.07, 23.48.

**HRMS (ESI):** m/z [M + H]+ calculated for $C_{43}H_{36}N_{10}O$: 708.3074; found: 708.3073

**tert-butyl (4-(2-(6-methylpyridin-2-yl)-5,6-dihydro-4H-pyrrolo[1,2-b]pyrazol-3-yl)quinolin-6-yl)carbamate, (3-21)**

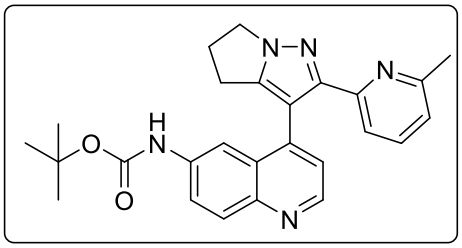

To a stirred suspension of **3-19** (100 mg, 0.270 mmol) in toluene (2 mL) at rt under a $N_2$ atmosphere was added $Et_3N$ (46 µL, 0.270 mmol, 1 equiv.) followed by DPPA (64 µL, 0.270 mmol, 1 equiv.) 10 minutes later. The reaction mixture was heated to 70˚C at which point the suspension became a solution. It was then further heated slowly to 95˚C where bubbling (presumed to be $N_2$) was observed. Once the bubbling became less frequent, the reaction was cooled to 70˚C and was added $^t$BuOH (39 µL, 0.405 mmol, 1.5 equiv.), held there for 2 further hours before being cooled to rt and diluted carefully with water (8 mL) while stirring vigorously. After stirring at rt overnight, the reaction was diluted with $CHCl_3$, the organic phase washed with water (2 x 5 mL), saturated $NaHCO_3$ (2 x 5 mL), dried ($MgSO_4$) and concentrated *in vacuo*. The residue was chromatographed (0-10% MeOH in DCM) to give title compound (74 mgs, 64%) as a thick colourless oil.

**$^{1}$H NMR (400 MHz, cdcl$_3$) δ** 8.69 (d, J = 4.5 Hz, 1H), 8.04 (d, J = 9.7 Hz, 1H), 7.78 – 7.72 (m, 2H), 7.32 – 7.22 (m, 1H), 7.20 (d, J = 4.5 Hz, 1H), 6.93 (t, J = 7.2 Hz, 2H), 6.78 (s, 1H), 4.32 (t, J = 7.2 Hz, 2H), 2.88 (s, 2H), 2.71 – 2.58 (m, 2H), 2.38 (s, 3H), 1.47 (s, 9H).

**$^{13}$C NMR (101 MHz, cdcl3) δ** 158.34, 153.54, 152.55, 151.47, 148.31, 146.79, 145.38, 140.27, 136.51, 136.16, 130.45, 127.83, 123.01, 122.34, 121.72, 119.47, 112.65, 110.07, 80.67, 48.30, 28.26, 26.01, 24.41, 23.39.

**IR (neat) 3427, 3230, 2975, 2975, 2923, 2217, 1729, 1569 cm$^{-1}$;**

**HRMS (ESI):** m/z [M + H]+ calculated for $C_{26}H_{27}N_5O_2$: 441.2165: 708.3074; found: 441.2460

**6-fluoro-4-methylquinoline, (3-26)**

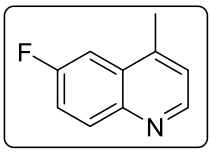


To a stirred solution of 4-fluoroaniline (1 g, 9.00 mmol) and chloranil (2.65 g, 10.8 mmol, 1.2 equiv.) in ethanol (15 mL, 15 volumes) at rt was added 37% HCl (2.25 mL, 27 mmol, 3 equiv.) over five minutes. After stirring for five minutes at rt the reaction mixture was heated to 75˚C where methyl vinyl ketone (1.13 mL, 13.5 mmol, 1.5 equiv.) was added to the reaction mixture over thirty minutes. After four hours, no starting material was observed by TLC. The reaction was cooled to 60˚C where it was diluted with THF (18 mL, 18 volumes), stirred for an hour at 60˚C and then left to cool to rt overnight. The suspension was filtered through a sintered Büchner funnel. The residue was rinsed with THF (2 x 5 mL, 10 volumes in total) and then dried at under vacuum oven to give the title compound (1.28 g, 72%) as a light yellow solid. The salt was suspended in $CHCl_3$ and taken to pH 8 with $NaHCO_3$ to afford a pale yellow sold which darkened upon standing (980 mgs 94% with respect to the salt). Spectra conformed to compound previously described in the literature.[6]

**$^{1}$H NMR (400 MHz, dmso) δ** 9.10 (d, *J* = 5.3 Hz, 1H), 8.48 (dt, *J* = 9.3, 4.8 Hz, 1H), 8.18 (dd, *J* = 9.9, 2.7 Hz, 1H), 8.08 – 7.97 (m, 1H), 7.91 (d, *J* = 5.2 Hz, 1H), 2.88 (s, 3H).

**6-bromo-4-methylquinoline, (3-28)**

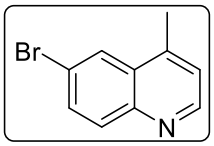


To a stirred solution of 4-bromoaniline (20 g, 117 mmol) and chloranil (34.7 g, 141 mmol, 1.2 equiv.) in ethanol (200 mL, 10 volumes) at rt was added 37% HCl (29.3 mL, 351 mmol, 3 equiv.) over five minutes. After stirring for five minutes at rt the reaction mixture was heated to 75˚C where methyl vinyl ketone (15.45 mL, 190.5 mmol, 1.5 equiv.) diluted in ethanol (15 mL, 1 volume) was added to the reaction mixture over thirty minutes. After four hours, no starting material was observed by TLC. The reaction was cooled to 60˚C where it was diluted with THF (165 mL, 11 volumes), stirred for an hour at 60˚C and then left to cool to rt overnight. The suspension was filtered through a sintered Büchner funnel. The residue was rinsed with THF (2 x 45 mL, 6 volumes in total) and then dried at 50˚C overnight in a vacuum oven to give the title compound (21.1 g, 81%) as a brown solid. Spectra conformed to compound previously described in the literature.[7]

**$^1$H NMR (400 MHz, $CDCl_3$) δ** 8.78 (d, *J* = 4.4 Hz, 1H), 8.16 – 8.14 (m, 1H), 7.97 (d, *J* = 9.0 Hz, 1H), 7.77 (dd, *J* = 9.0, 2.2 Hz, 1H), 7.25 (dd, *J* = 4.4, 0.9 Hz, 1H), 2.68 (d, *J* = 0.9 Hz, 3H).

**$^{13}$C NMR (101 MHz, dmso) δ** 145.76, 138.20, 135.96, 133.04, 129.21, 127.79, 125.12, 123.25, 122.18, 19.24.

**4-methyl-6-(4,4,5,5-tetramethyl-1,3,2-dioxaborolan-2-yl)quinoline, (3-30)**

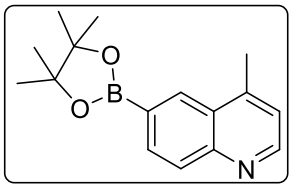


To a flame dried flask under $N_2$ was added **3-28** (250 mgs, 1.13 mmol), $Pd(dppf)Cl_2$ (82 mgs, 0.113 mmol, 0.1 eq.), KOAc (331 mgs, 3.38 mmol, 3 equiv.) and bis(pinacolato)diboron (314 mgs, 1.24 mmol, 1.1 eq). To the reaction flask was then added degassed dioxane (15 mL) and heated to 100˚C for 2 hours, at which point the reaction was cooled to rt and split into two portions. One half was used as described below to make **3-29**, and other half filtered through a pad of celite, and split between water (15 mL) and EtOAc (15 mL). The phases were separated, the aqueous layer was extracted with EtOAc (1 x 10 mL), the organic phases combined, dried ($MgSO_4$) and chromatographed to give title compound as a colourless oil (2 mg). The purified product was injected into the UPLC, and the mass corresponded to the desired titled compound.

**UPLC-MS:** 270.3 (M+H)

**4-methylquinolin-6-ol, (3-29)**

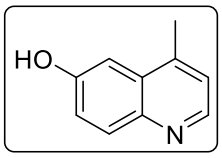

The half of the reaction mixture from above was then basified with 1M NaOH (1 mL, 1 mmol, 2 eq) and dioxane (2 mL). To the reaction mixture was added $H_2O_2$ (0.676 mmol, 1.2 eq) and stirred at rt for 2 hours. After 2 hrs, it then quenched with 1.6 M sodium sulphite (1 mM, 625 µL). After stirring for 30 minutes, the reaction mixture was checked for the presence of peroxide, before being taken to pH 8 with 37% HCl. The mixture was diluted with water (5 mL) and extracted with EtOAc (3 × 5 mL). The combined organic extracts were dried ($MgSO_4$), evaporated and the residue was chromatographed (0-100% EtOAc in hexanes). A small quantity of solid remained after chromatography, and was submitted to UPLC-MS. The mass matched that of the desired phenol **3-29**.

**UPLC-MS:** 160.2 (M+H)

**2-(6-bromoquinolin-4-yl)-1-(6-methylpyridin-2-yl)ethan-1-one, (3-31)**

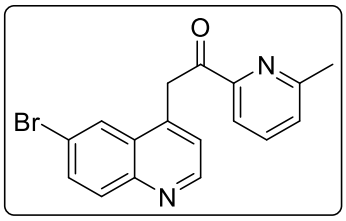

To a stirred solution of **3-28** (3.70 g, 14.31 mmol) in THF (60 mL) at -78˚C was added 1M NaHMDS (57 mL, 57 mmol, 4 equiv.). The reaction mixture was stirred for 3 hrs followed by the addition of methyl 6-methylpicolinate (2.60 g, 17.17 mmol, 1.2 equiv.) diluted in THF (7.4 mL, 2 volumes) dropwise over 30 minutes. The reaction was left to warm to rt overnight and then cooled to 0˚C and taken to pH 1 with 3M HCl. It was allowed to warm to rt over one hour and then taken to pH 8 with solid $NaHCO_3$. The mixture was diluted with water (50 mL) and extracted with EtOAc (1 x 100 mL) followed by $CHCl_3$ (1 × 100 mL). The combined organic extracts were dried ($MgSO_4$), evaporated and the residue was recrystallised from MeOH (30 mL, 8 volumes) to give title compound (2.57 g, 53%) as an off-white solid. Spectra conformed to compound previously described in the literature.[7]

**$^1$H NMR (400 MHz, cdcl3) δ** 8.84 (d, *J* = 4.4 Hz, 1H), 8.36 (d, *J* = 2.1 Hz, 1H), 7.97 (d, *J* = 9.0 Hz, 1H), 7.86 (d, *J* = 7.7 Hz, 0H), 7.75 (dd, *J* = 9.0, 2.2 Hz, 1H), 7.73 (t, *J* = 7.7 Hz, 1H), 7.43 (d, *J* = 4.4 Hz, 1H), 7.38 (d, *J* = 8.6 Hz, 1H), 4.96 (s, 1H), 2.70 (s, 2H).

**$^{13}$C NMR (101 MHz, cdcl3) δ** 197.87, 158.43, 152.01, 150.47, 147.24, 141.30, 137.39, 132.77, 131.95, 129.36, 127.58, 127.09, 124.09, 120.89, 119.76, 40.53, 24.60.

**6-bromo-4-(2-(6-methylpyridin-2-yl)-5,6-dihydro-4H-pyrrolo[1,2-b]pyrazol-3-yl)quinoline, (3-33)**

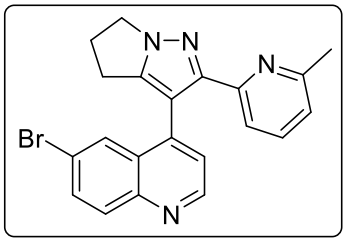


To a stirred solution of **3-31** (2.57 g, 7.53 mmol) in DMF (15.5 mL, 6 volumes), toluene (26 mL, 10 volumes) and 2,6-lutidine (2.6 mL, 1 volume) at rt was added 1-aminopyrrolidin-2-one tosylate salt (2.05 g, 7.53 mmol, 1 equiv.) and stirred at rt for 5 minutes. The reaction was heated to reflux under Dean-Stark conditions until most of the starting material had been consumed by TLC. The reaction mixture was cooled to rt where it was charged with $Cs_2CO_3$ (4.17 g, 12.8 mmol, 1.7 equiv.) and heated back to reflux. The reaction was monitored for disappearance of the intermediate and once all was consumed, toluene was distilled until the reaction mixture reacted 145˚C and then cooled to rt, split between water (30 mL) and EtOAc (30 mL) and the phases separated. The aqueous phase was extracted with EtOAc (2 x 20 mL), the combined organic extracts were washed with 5% LiCl aqueous solution (2 x 20 mL) and the organic layer was dried ($MgSO_4$), evaporated and the residue was chromatographed (0-10% MeOH in DCM) to give the title compound (2.05 g, 67%) as a brown solid.

**1H NMR (400 MHz, cdcl3) δ** 8.85 (d, J = 4.4 Hz, 1H), 7.98 (d, J = 8.9 Hz, 1H), 7.92 (d, J = 2.2 Hz, 1H), 7.71 (dd, J = 8.9, 2.2 Hz, 1H), 7.35 (t, J = 7.7 Hz, 1H), 7.31 (d, J = 4.4 Hz, 1H), 7.11 (d, J = 7.8 Hz, 1H), 6.92 (d, J = 7.6 Hz, 1H), 4.37 (t, J = 7.2 Hz, 2H), 2.90 – 2.84 (m, 2H), 2.75 – 2.66 (m, 2H), 2.24 (s, 3H).

**13C NMR (101 MHz, cdcl3**) **δ** 158.22, 153.60, 153.24, 151.25, 150.22, 147.11, 146.66, 140.88, 136.29, 132.50, 131.34, 128.72, 128.66, 123.03, 121.77, 120.20, 118.86, 48.33, 25.98, 24.19, 23.15.

**UPLC-MS:** 407 m/z [M+H]

**4-(2-(6-methylpyridin-2-yl)-5,6-dihydro-4H-pyrrolo[1,2-b]pyrazol-3-yl)quinolin-6-ol, (3-10)**

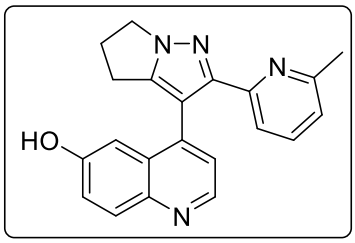


Method 2:

To a flame dried flask under $N_2$ was added **3-33** (200 mg, 0.493 mmol), $Pd(dppf)Cl_2$ (36 mgs, 0.050 mmol, 0.1 eq.), KOAc (145 mgs, 1.48 mmol, 3 equiv.) and bis(pinacolato)diboron (137 mgs, 0.542 mmol, 1.1 eq). To the reaction flask was then added degassed dioxane (5 mL) and heated to 100˚C for 2 hours, at which point the reaction was cooled to rt, and diluted with 1M NaOH (4.93 mL, 4.93 mmol, 10 equiv.) and 30% $H_2O_2$ (46.6 µL, 0.542 mmol, 1.1 equiv.) added dropwise. After 2 further hours at rt, the reaction was quenched with 1.6 M sodium sulphite (1 mM, 625 µL). After stirring for 30 minutes, the reaction mixture was checked for the presence of peroxides, filtered through a pad of celite and taken to pH 8 with 37% HCl. The mixture was diluted with water (5 mL) and extracted with EtOAc (3 × 5 mL) and chloroform (1 x 5 mL). The combined organic extracts were dried ($MgSO_4$), evaporated and the residue was chromatographed (0-100% EtOAc in hexanes) to give title compound (130 mgs, 77%)**.**

**$^1$H NMR (400 MHz, dmso) δ** 9.66 (s, 1H), 8.58 (d, J = 4.4 Hz, 1H), 7.86 (d, J = 9.0 Hz, 1H), 7.56 (t, J = 7.7 Hz, 1H), 7.48 (d, J = 7.8 Hz, 1H), 7.29 – 7.16 (m, 2H), 6.96 (d, J = 7.5 Hz, 1H), 6.91 (d, J = 2.7 Hz, 1H), 4.27 (t, J = 7.2 Hz, 2H), 2.79 (t, J = 6.5 Hz, 2H), 2.69 – 2.55 (m, 2H), 1.89 (s, 3H).

**$^{13}$C NMR (101 MHz, dmso) δ** 156.49, 155.08, 152.01, 151.70, 146.55, 146.24, 143.18, 139.37, 136.48, 130.60, 128.71, 122.47, 121.16, 117.73, 109.89, 106.98, 47.86, 25.53, 23.41, 22.50.

**IR (film):** 3412, 2949, 2833, 1650, 1618, 1508, 1236, 1010 $cm^{-1}$

**4-(2-(6-methylpyridin-2-yl)-5,6-dihydro-4H-pyrrolo[1,2-b]pyrazol-3-yl)quinolin-6-yl [1,4'-bipiperidine]-1'-carboxylate, (3-35)**

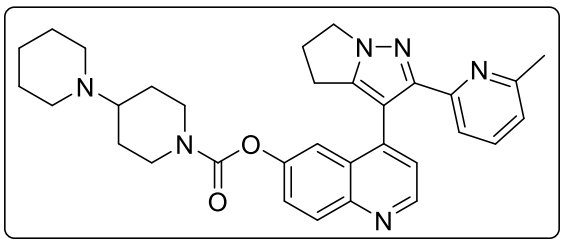

A solution of **3-10** (47 mg, 0.14 mmol) in 3 mL of $CHCl_3$ was prepared and transferred, under $N_2$ to a Schlenk flask containing 3 Å activated molecular sieves. The solution was stirred at room temperature for 1 hour. A solution of [1,4'-bipiperidine]-1'-carbonyl chloride (32 mg, 0.14 mmol, 1 eq.), $Et_3N$ (23 µL, 0.17 mmol, 1.2 eq.) and a crystal of 4-dimethylaminopyridine in 1 mL of $CHCl_3$ was then added dropwise. The resulting mixture was stirred overnight. Some starting material was detected by TLC the following day, so another solution of [1,4'-bipiperidine]-1'-carbonyl chloride (16 mg, 0.07 mmol, 0.5 eq.), $Et_3N$ (12 µL, 0.08 mmol, 0.6 eq.) and a crystal of 4-dimethylaminopyridine in 0.5 mL of $CHCl_3$ was added to the reaction mixture and it was stirred overnight. The reaction was quenched by adding 20 mL of $H_2O$. The resulting aqueous layer was extracted with EtOAc (3 x 20 mL), dried over $MgSO_4$ and concentrated to afford the crude product which was purified by column chromatography (eluted with a gradient of 10-20% MeOH in DCM) to obtain 64 mg (87%) of the desired product as an orange oil.

**$^1$H NMR (400 MHz, dmso) δ** 8.80 (d, *J* = 4.4 Hz, 1H), 8.01 (d, *J* = 9.1 Hz, 1H), 7.56 (dd, *J* = 24.0, 7.5 Hz, 2H), 7.47 (dd, *J* = 9.1, 2.6 Hz, 1H), 7.38 (d, *J* = 4.4 Hz, 1H), 7.28 (d, *J* = 2.6 Hz, 1H), 6.95 (d, *J* = 7.8 Hz, 1H), 4.27 (t, *J* = 7.2 Hz, 2H), 4.01 (dd, *J* = 37.1, 14.3 Hz, 2H), 3.65 – 3.14 (m, 1H), 2.81 (d, *J* = 16.6 Hz, 4H), 2.61 (m, 3H), 1.82 (s, 3H), 1.74 (d, *J* = 10.6 Hz, 3H), 1.44 (m, 10H).

**$^{13}$C NMR (101 MHz, dmso) δ** 156.59, 152.55, 151.92, 151.57, 149.18, 148.60, 147.08, 145.62, 141.10, 136.57, 130.20, 127.54, 124.70, 122.63, 121.25, 117.67, 116.92, 109.27, 61.31, 49.59, 47.95, 25.53, 23.29, 22.41.

**UPLC-MS:** 537.8 (M+H)

**1-(1-(((4-(2-(6-methylpyridin-2-yl)-5,6-dihydro-4H-pyrrolo[1,2-b]pyrazol-3-yl)quinolin-6-yl)oxy)carbonyl)piperidin-4-yl)piperidin-1-ium chloride, (3-36)**

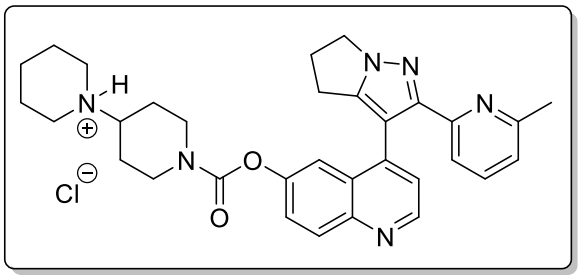

Compound **3-35** (65 mg, 0.12 mmol) was dissolved in DCM (1.5 mL) and treated with 0.3 mL (1.21 mmol) of a 2M solution of HCl in dioxane during 2h. Then the solvent was removed to afford a pale orange solid (70 mg, 100%).

**$^{1}$H NMR (400 MHz, Methanol-d4) δ** 9.18 (d, J = 5.6 Hz, 1H), 8.35 (d, J = 9.2 Hz, 1H), 8.12 (d, J = 5.6 Hz, 1H), 8.06 (t, J = 7.9 Hz, 1H), 8.02 – 7.93 (m, 2H), 7.74 (d, J = 7.9 Hz, 1H), 7.28 (d, J = 7.9 Hz, 1H), 4.56 – 4.39 (m, 3H), 4.31 – 4.28 (m, 1H), 3.59 – 3.56 (m, 2H), 3.52 – 3.45 (m, 2H), 3.19 – 2.95 (m, 6H), 2.88 (s, 3H), 2.85 – 2.81 (m, 1H), 2.25 – 2.20 (m, 2H), 2.01 – 1.85 (m, 7H), 1.60 – 1.50 (m, 1H) ppm.

**$^{13}$C NMR (101 MHz, Methanol-d4) δ** 157.0, 153.3, 153.2, 152.2, 151.0, 147.2, 146.1, 145.5, 144.9, 137.62, 131.4, 129.3, 128.0, 124.6, 124.5, 124.1, 119.5, 111.0, 66.9, 64.6, 51.4, 50.4, 44.3, 44.0, 27.5, 27.2, 27.1, 24.5, 24.2, 22.9, 20.1, 15.5 ppm.

**IR (Film):** 3411, 3048, 2933, 2857, 1716, 1589, 1420, 1195, 1020, 804 $cm^{-1}$.

**HRMS (ESI):** m/z [M + H]+ calculated for C32H37N6O2: 537.2973; found: 537.2968.

**Mp:** 214-215 °C.

**1-(4-hydroxy-3-methoxyphenyl)-2-((4-(2-(6-methylpyridin-2-yl)-5,6-dihydro-4H-pyrrolo[1,2-b]pyrazol-3-yl)quinolin-6-yl)oxy)ethan-1-one, (3-38)**

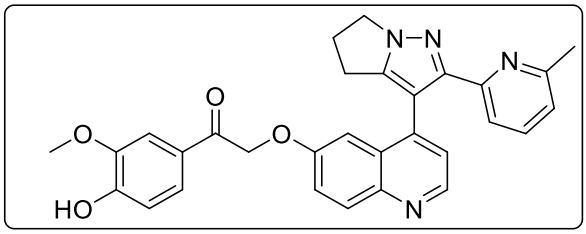

4-(2-(6-methylpyridin-2-yl)-5,6-dihydro-4H-pyrrolo[1,2-b]pyrazol-3-yl)quinolin-6-ol (42 mg, 0.12 mmol) and $Cs_2CO_3$ (134 mg, 0.41 mmol) were dissolved in 1.5 mL of anhydrous DMF and heated, under $N_2$ atm. at 60 ºC for 1.5 h. A solution of 4-(2-bromoacetyl)-2-methoxyphenyl pivalate in 0.5 mL of anhydrous DMF was then added via cannula to the bright green suspension. The resulting mixture was stirred at at 60 °C for 2 hours. Then the reaction was cooled to room temperature, diluted with water (15 mL), and then quenched with 0.5 mL of a 1M solution of HCl. The resulting aqueous layer was extracted with EtOAc (3 x 20 mL), the organic layer was dried over anhydrous $MgSO_4$ and the solvent removed *in vacuo*. The crude was purified via column chromatography (0 to 20 % of MeOH in DCM) to yield 51.9 mg (82 %) of the title compound as a brown oil.

**1H NMR (400 MHz, $CDCl_3$) δ** 8.73 (d, J = 4.6 Hz, 1H), 8.11 (d, J = 9.2 Hz, 1H), 7.50 (d, J = 1.9 Hz, 1H), 7.47 – 7.43 (m, 2H), 7.32 – 7.26 (m, 2H), 7.06 – 6.95 (m, 3H), 6.89 (d, J = 7.6 Hz, 1H), 4.94 (bs, 2H), 4.27 (t, J = 7.3 Hz, 2H), 3.93 (s, 3H), 2.82 (bs, 2H), 2.61 (bs, 2H), 2.24 (s, 3H) ppm.

**13C NMR (101 MHz, $CDCl_3$) δ** 192.3, 158.5, 156.3, 153.4, 152.0, 151.6, 147.5, 147.2, 146.9, 144.2, 141.1, 136.5, 130.7, 128.3, 127.1, 123.5, 122.7, 122.6, 122.0, 119.2, 114.5, 110.2, 110.1, 105.7, 70.4, 56.2, 48.4, 26.0, 24.3, 23.2 ppm.

**IR (Film):** 3074, 2958, 2925, 1686, 1620, 1589, 1509, 1428, 1274, 1225, 1198, 1088 $cm^{-1}$.

**HRMS (ESI):** m/z [M + H]+ calculated for $C_{30}H_{27}N_4O_4$: 507.2027; found: 507.2016.

**Mp:** 162-163 °C.

# Chapter 5

**1-(4-(benzyloxy)-3-methoxyphenyl)ethan-1-one, (5-7a)**

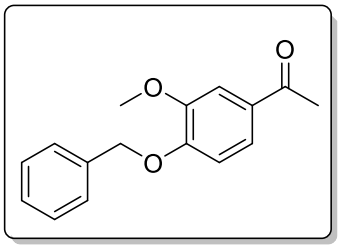

To a stirred solution of acetovanillone (6 g, 36.1 mmol) in DMF (120 mL) at rt was added $K_2CO_3$ (7.48 g, 54.15 mmol, 1.5 equiv.) followed by benzyl bromide dropwise (4.66 mL, 38.99 mmol, 1.08 equiv.). The reaction mixture was stirred for 14 hrs at 40 ˚C before being cooled down to rt where it was poured into 1L of water/ice mixture and stirred for 10 minutes. The suspension was then filtered using a Büchner funnel under vacuum, the solid rinsed with water (3 x 70 mL) at 0˚C, before being left under vacuum in the Büchner funnel for one hour. The solid was then transferred into a round bottom flask and dried to a constant weight on the high vacuum line giving 8.99g (97% yield) of the titled compound. [8]

**$^1$H NMR (400 MHz, Chloroform-d) δ** 7.55 (d, J = 2.0 Hz, 1H), 7.50 (dd, J = 8.4, 2.0 Hz, 1H), 7.43 (dd, J = 8.2, 1.4 Hz, 2H), 7.38 (m, 2H), 7.34 – 7.29 (m, 1H), 6.91 – 6.87 (m, 1H), 5.23 (s, 2H), 3.94 (s, 3H), 2.55 (s, 3H).

**1-(4-(benzyloxy)-3-methoxyphenyl)-2-bromoethan-1-one, (5-8a)**

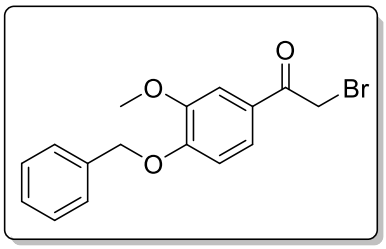

To a stirred solution of ketone **5-7a** (7.86g, 30.69 mmol) in EtOH (150 mL) at 60 ˚C was added bromine (4.90g, 30.69 mmol, 1 equiv.). The reaction mixture was stirred for 6 h, before being left to cool slowly to room temperature overnight. In the morning the reaction mixture was cool to 0 ˚C where it was left stirring for an hour. It was then filtered through a glass Buchner funnel, washed with cold EtOH (2 x 30 mL), and then left to dry on the high vacuum line. This afforded the title compound (7.25g, 71%) as a white solid pure by $^1$H NMR, and conforming to the structure as previously described in the literature.[9]

**$^1$H NMR (400 MHz, cdcl$_3$) δ** 7.58 – 7.49 (m, 2H), 7.46 – 7.29 (m, 5H), 6.92 (d, *J* = 8.4 Hz, 1H), 5.25 (s, 2H), 4.39 (s, 2H), 3.95 (s, 3H).

**7-(2-(4-(benzyloxy)-3-methoxyphenyl)-2-oxoethoxy)-4-methyl-2H-chromen-2-one, (5-4b)**

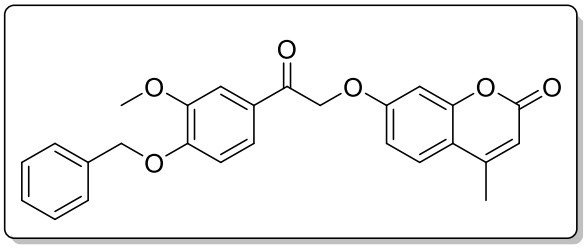

To a stirred solution of 4- methylumberliferone (400 mg, 2.27 mmol) in acetone (30 mL) at 25 °C was added alpha-bromo ketone **5-8a** (967 mg, 2.72 mmol, 1.2 equiv.). The reaction mixture was stirred for 16 h, before being filtered and the solid residue washed with acetone (2 x 30 mL). The solvent was then removed under reduced pressure, before being suspended in toluene and heated until a solution was formed. The flask was then left to cool to RT over 90 minutes, where it was filtered, washed with cold toluene (10 mL), and left to dry on the high vacuum line. This afforded the titled compound as a white solid (801 mg, 82%) and the structure conformed to that previously reported.[10]

**$^1$H NMR (400 MHz, cdcl$_3$) δ** 7.57 – 7.30 (m, 8H), 6.94 (d, *J* = 4.5 Hz, 2H), 6.78 (d, *J* = 2.5 Hz, 1H), 6.14 (d, *J* = 1.2 Hz, 1H), 5.31 (s, 2H), 5.26 (s, 2H), 3.95 (s, 3H).

**7-(2-(4-hydroxy-3-methoxyphenyl)-2-oxoethoxy)-4-methyl-2H-chromen-2-one, (5-4a)**

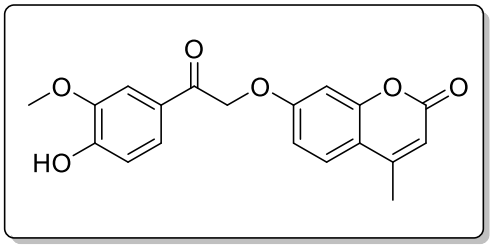

To a pressure reactor was added **5-4b** (500mg, 1.16 mmol) and 10% Pd/C (25mg, 5% wrt to mass of sm) in degassed 10% MeOH/EtOAc (10 mL) at rt. The reactor was charged with 1 bar(g) of hydrogen and the reaction followed by TLC by taking samples using an appropriate needle which is able to withstand pressure. After 4 hours, the starting material had been consumed. The hydrogen was released from the reactor and replaced with nitrogen via 3 vacuum-nitrogen cycles. The reaction mixture was diluted with $CHCl_3$ (20 mL) and filtered through Celite. The filtrate was concentrated under reduced pressure. The crude was chromatographed (0-10% MeOH:DCM) to give title compound **5-4a** (307 mg, 78%) as a white solid. The spectral data was consistent with that reported in the literature.[11]

**$^1$H NMR (400 MHz, Chloroform-*d*) δ** 7.59 – 7.55 (m, 2H), 7.51 (d, J = 8.8 Hz, 1H), 7.00 (d, J = 8.1 Hz, 1H), 6.94 (dd, J = 8.8, 2.6 Hz, 1H), 6.79 (d, J = 2.6 Hz, 1H), 6.18 (br s, 1H), 6.14 (d, J = 1.2 Hz, 1H), 5.33 (s, 2H), 3.97 (s, 3H), 2.39 (d, J = 1.2 Hz, 3H).

**3,4-bis(benzyloxy)benzaldehyde, (5-10)**

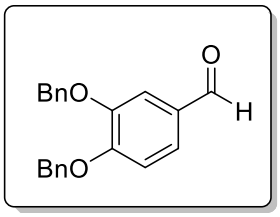


To a solution of 3,4-dihydroxybenzaldehyde (1 g, 7.24 mmol) in DMF (20 mL) under $N_2$ was added $K_2CO_3$ (2.1g, 15.20 mmol, 2.1 eq) and left to stir for 20 minutes. Benzyl bromide (1.84 mL, 15.20 mmol, 2.1 eq) was then added dropwise at room temperature over 5 minutes and left for one hour. It was then heated up to 60 degrees where it was left overnight. The following morning all the starting material had disappeared by TLC, the reaction was cooled down to room temperature, diluted with water (200 mL) and EtOAc (30 mL) and left to stir for 15 minutes. The phases were separated, the aquous phase was extracted with EtOAc (3x 20 mL), the combined organic phases were then washed with a 10% CuSO4(aq.) solution (2 x 15 mL) and dried over MgSO4. The solvent was removed to give the title compound as an off-white solid (2.2g, 95% yield). The structure conformed to that previously described in the literature.[12]

**1H NMR (400 MHz, cdcl3) δ** 9.81 (s, 1H), 7.51 – 7.25 (m, 12H), 7.02 (d, J = 8.2 Hz, 1H), 5.25 (s, 2H), 5.21 (s, 2H).

**1-(3,4-bis(benzyloxy)phenyl)ethan-1-ol, (5-11)**

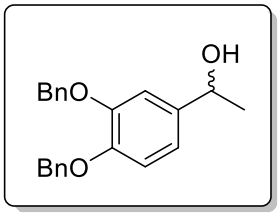


A solution of aldehyde **5-10** (100mgs, 0.314 mmol) was cooled down to -78 ˚C in THF (3 mL) under N2 was added MeLi (196 µL, 0.377 mmol, 1.2 eq) dropwise. The reaction mixture was allowed to warm to room temperature over 3 hours, where it was quenched with excess $NH_4Cl$ (3 mL) and diluted with TBME (3 mL). The phases were separated, the organic phase was extracted wth TBME (2 x 3 mL), the oganic phases were combined and dried over MgSO4 and then concentrated in vacuo to give the title compound (95 mg, 91% yield). The spectra matched the one reported previously in the literature.[13]

**1H NMR (400 MHz, cdcl3) δ** 7.49 – 7.26 (m, 10H), 7.01 (d, J = 1.9 Hz, 1H), 6.87 (m, 2H), 5.17 (s, 2H), 5.15 (s, 2H), 4.80 (qd, J = 6.6, 2.7 Hz, 1H), 1.70 (d, J = 3.2 Hz, 1H), 1.43 (d, J = 6.4 Hz, 3H).

**1-(3,4-bis(benzyloxy)phenyl)ethan-1-one, (5-7e)**

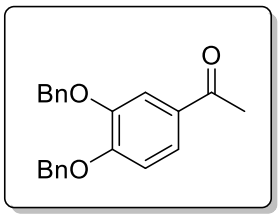


To a solution of alcohol **5-11** (312 mg, 0.93 mmol) in $CH_2Cl_2$ was added Dess-Martin periodinane (435 mg, 1.02 mmol, 1.1 eq) at room temperature. The reaction mixture was stirred overnight at room temperature, where it was quenched the following morning with excess 10% $Na_2S_2O_{3\ (aq)}$, followed by washing with 10% $NaHCO_{3(aq)}$. The organic phase was dried ($MgSO_4$), the solvent was removed in vacuo where the residue was purified through silica giving the titled compound (287 mg, 93% yield) as a white solid. The spectra matched the one reported previously in the literature.[14]

**$^1$H NMR (400 MHz, cdcl3) δ** 7.58 (d, J = 1.6 Hz, 1H),7.51 (dd, J = 8.2, 1.5 Hz, 1H), 7.30 - 7.48 (m, 10H), 6.91 (d, J = 7.2 Hz, 1H), 5.18 (s, 2H), 5.21 (s, 2H), 2.51 (s, 3H).

**4-formyl-1,2-phenylene bis(2,2-dimethylpropanoate), (5-12)**

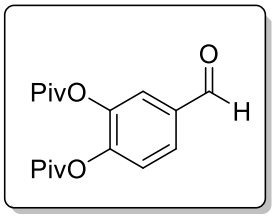


To a solution of 3,4-dihydroxybenzophenone(2.5 g, 18.1 mmol) in THF (50 mL) at 0 °C was added $Et_3N$ (6.31 mL, 45.25 mmol, 2.5 eq.), DMAP (a few crystals) followed by pivoyl chloride (5.35 mL, 43.44 mmol, 2.4 eq.). The reaction was left to warm to room temperature overnight where it was then quenched with saturate ammonium chloride (20 mL) and diluted with EtOAc (20 mL). The phases were separated, the aquous was extracted with EtOAc (2 x 20 mL), the combined organic phases were then washed with 10% $NaHCO_3$ (30 mL), dried over then ($MgSO_4$), the solvent was removed in vacuo where the residue was purified through silica giving the titled compound (4.76 g, 86 % yield). The spectra matched the one reported previously in the literature.[15]

**$^1$H NMR (400 MHz, cdcl3) δ** 9.96 (s, 1H), 7.77 (dd, J = 8.3, 1.9 Hz, 1H), 7.68 (d, J = 1.9 Hz, 1H), 7.34 (d, J = 8.3 Hz, 1H), 1.37 (s, 9H), 1.36 (s, 9H).

**4-(1-hydroxyethyl)-1,2-phenylene bis(2,2-dimethylpropanoate), (5-13)**

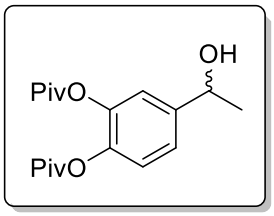


To a stirred solution of aldehyde **5-12** (5.545 g, 18.11 mmol) in THF (40 mL) at -10 ˚C and under $N_2$ was added 3M methyl magnesium bromide solution (6.04 mL, 18.12 mmol, 1. eq.) dropwise over 30 minutes. The reaction was left at -10 ˚C and followed by TLC, where upon disappearance of the starting material, the reaction was carefully quenched with excess saturated ammonium chloride (20 mL) and diluted with EtOAc (40 mL). The phases were then separated, the organic phase was dried ($MgSO_4$) and the solvent removed *in vacuo*. The crude was then purified to give the titled compound as a thick colourless oil. (4.267 g, 73.1%).

**$^1$H NMR (400 MHz, cdcl$_3$) δ** 7.20 (dd, *J* = 8.3, 2.0 Hz, 1H), 7.14 (d, *J* = 2.0 Hz, 1H), 7.08 (d, *J* = 8.3 Hz, 1H), 4.87 (q, *J* = 6.5 Hz, 1H), 1.47 (d, *J* = 6.5 Hz, 4H), 1.34 (s, 10H), 1.33 (s, 9H).

**$^{13}$C NMR (101 MHz, cdcl$_3$) δ** 175.95, 175.92, 144.42, 142.46, 141.61, 123.28, 123.20, 120.38, 69.55, 39.11, 39.11 27.22, 27.21, 25.11.

**4-acetyl-1,2-phenylene bis(2,2-dimethylpropanoate), (5.7f)**

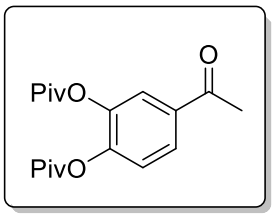


To a stirred solution of alcohol **5-13** (4.27 g, 13.23 mmol) in DCM (100 mL) was added Dess-Martin periodinane (6.17 g, 14.55 mmol, 1.1 eq.) portion-wise at room temperature. The reaction mixture was left at rt overnight, before being diluted with 10% sodium thiosulfite (30 mL). The aqueous was extracted with DCM (40 mL), the combined organic extracts were washed with 10% $NaHCO_3$ (20 mL), and then dried over $MgSO_4$. The organic phase was then evaporated to dryness, before being purified by flash column chromatography giving the titled compound as a white solid (3.62 g, 85.4 %) yield. The spectra matched with those reported in the literature.[16]

**$^1$H NMR (400 MHz, cdcl$_3$) δ** 7.83 (dd, *J* = 8.5, 2.1 Hz, 1H), 7.72 (d, *J* = 2.1 Hz, 1H), 7.25 (d, *J* = 8.5 Hz, 1H), 2.59 (s, 3H), 1.36 (s, 9H), 1.35 (s, 9H).

**$^{13}$C NMR (101 MHz, cdcl$_3$) δ** 196.10, 175.67, 175.38, 146.69, 142.73, 135.30, 126.54, 123.63, 123.55, 27.21, 27.14, 26.55.

**1-(3-(benzyloxy)phenyl)ethan-1-one, (5-7g)**

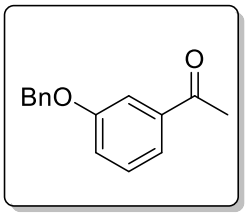


To a stirred solution of 3'-hydroxyacetophenone (0.95g, 7.35 mmol) in DMF (20 mL) at rt was added $K_2CO_3$ and stirred for 10 minutes. To the reaction mixture was then added dropwise benyl bromide (0.95 mL, 8.09mmol, 1,1 eq.) before being heated to 60 ˚C for 3 hours. After all SM was consumed by TLC, the reaction was cooled to room temperature, before being diluted with water (140 mL) and EtOAc (20 mL). The phases were separated, and the aqueous layer was extracted with EtOAc (2 x 20 mL). The combined organic extracts were washed with 10% $CuSO_{4\ (aq.)}$ (40 mL) before being dried over $MgSO_4$. The organic phase was then evaporated to dryness giving the titled compound as a white solid (quantitative yield). The spectra matched the one reported previously in the literature.[17]

**$^1$H NMR (400 MHz, cdcl3) δ** 7.59 – 7.53 (m, 2H), 7.46 – 7.29 (m, 6H), 7.18 (m ,1H), 5.12 (s, 2H), 2.59 (s, 3H).

**1-(4-(benzyloxy)phenyl)ethan-1-one, (5-7h)**

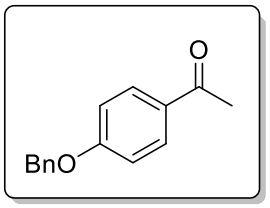


To a stirred solution of 4'-hydroxyacetophenone (0.5g, 3.67 mmol) in DMF (10 mL) at rt was added $K_2CO_3$ and stirred for 10 minutes. To the reaction mixture was then added dropwise benyl bromide (0.47 mL, 4.04 mmol, 1.1 eq.) before being heated to 60 ˚C for 3 hours. After all SM was consumed by TLC, the reaction was cooled to room temperature, before being diluted with water (70 mL) and EtOAc (10 mL). The phases were separated, and the aqueous layer was extracted with EtOAc (2 x 10 mL). The combined organic extracts were washed with 10% $CuSO_{4\ (aq.)}$ (2 x 20 mL) before being dried over $MgSO_4$. The organic phase was then evaporated to dryness giving the titled compound as a white solid (697 mg, 84 % yield). The spectra matched the one reported previously in the literature.[18]

**$^1$H NMR (400 MHz, cdcl3) δ** 7.94 (d, J = 9.0 Hz, 2H), 7.45 – 7.33 (m, 5H), 7.01 (d, J = 9.0 Hz, 2H), 5.14 (s, 2H), 2.55 (s, 3H)

**1-(3,4-bis(benzyloxy)phenyl)-2-bromoethan-1-one, (5-8e)**

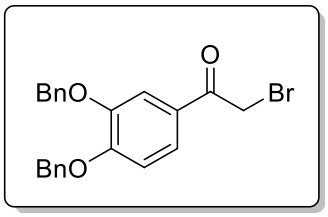


To a stirred solution of **5-7e** (332 mgs, 1 mmol) was added in MeCN (10 mL) was added TsOH (190 mgs, 1 mmol, 1 eq.) and stirred for 10 minutes at room temperature. NBS (182 mgs, 1.02 mmol, 1.02 eq.) was then added to the reaction mixture portionwise. After 60 hours, the solvent was removed in vacuo and the residue was purified by flash column chromatography using a gradient of hexane – EtOAc giving the titled compound as a thick oil (223 mgs, 54% yield) which conformed with spectra previously described in the literature.[19]

**$^1$H NMR (400 MHz, cdcl$_3$) δ** 7.61 (d, *J* = 2.1 Hz, 1H), 7.56 (dd, *J* = 8.4, 2.1 Hz, 1H), 7.46 – 7.26 (m, 4H), 6.95 (d, *J* = 8.5 Hz, 1H), 5.25 (s, 1H), 5.21 (s, 1H), 4.34 (s, 1H).

**4-(2-bromoacetyl)-1,2-phenylene bis(2,2-dimethylpropanoate), (5-8f)**

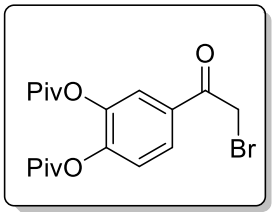


To a stirred solution of ketone **5-7f** (1 g, 3.12 mmol) in THF (20 mL) at rt was added dropwise $Br_2$ (160 µL, 3.12 mmol, 1 eq.) and left to react for 8 hours. The reaction mixture was quenched with excess 10% sodium thiosulfate $_{(aq.)}$, diluted with EtOAc (20 mL) and the phases separated. The aqueous was extracted with $CHCl_3$ (20 mL), the combined organic extracts were dried over $MgSO_4$. The organic phase was then evaporated to dryness, before being purified by flash column chromatography giving the titled compound as a white solid (706 mg, 57 % yield).

**$^1$H NMR (400 MHz, cdcl3) δ** 7.86 (dd, J = 8.5, 2.1 Hz, 1H), 7.77 (d, J = 2.1 Hz, 1H), 7.29 (d, J = 8.5 Hz, 1H), 4.42 (s, 1H), 1.37 (s, 1H), 1.36 (s, 1H).

**$^{13}$C NMR (101 MHz, cdcl3) δ** 189.63, 175.74, 175.44, 147.54, 143.16, 132.20, 127.31, 124.55, 124.02, 39.49, 39.36, 30.60, 27.37, 27.31.

**1-(3-(benzyloxy)phenyl)-2-bromoethan-1-one, (5-8g)**

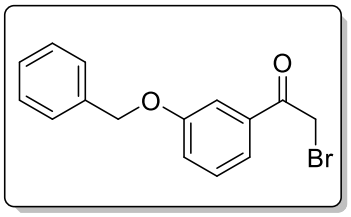


To a stirred solution of 1-(3-(benzyloxy)phenyl)ethan-1-one (1.66g, 7.346 mmol) in MeCN (25 mL) was added TsOH (1.40g, 7.37 mmol, 1 eq.) and stirred for 10 minutes at room temperature. NBS (1.33g, 7.49 mmol, 1.02 eq) was then added to the reaction mixture portionwise. After 24 hours, the solvent was removed in vacuo and the residue was purified by flash column chromatography using a gradient of hexane – EtOAc giving the titled compound as a white solid (1.70g, 76% yield) which conformed with spectra previously described in the literature.[20]

**$^1$H NMR (400 MHz, cdcl$_3$) δ** 7.64 – 7.53 (m, 1H), 7.49 – 7.28 (m, 3H), 7.24 – 7.18 (m, 1H), 5.12 (s, 1H), 4.43 (s, 1H).

**1-(4-(benzyloxy)phenyl)-2-bromoethan-1-one, (5-8h)**

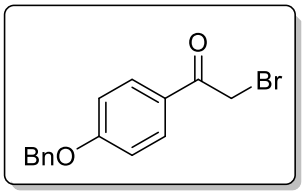


To a stirred solution of **5-7h** (852 mg, 3.76 mmol) in DCM (40 mL) at rt was added $Br_2$ and left to react for 4 hours. The reaction mixture was quenched with excess 10% sodium thiosulfate $_{(aq.)}$, and the phases separated. The aqueous was extracted with DCM (20 mL), the combined organic extracts were dried over $MgSO_4$. The organic phase was then evaporated to dryness, before being purified by flash column chromatography giving the titled compound as a white solid. (572 mg, 50% yield). The spectra matched the one reported previously in the literature.[21]

**$^1$H NMR (400 MHz, cdcl3) δ** 8.00 – 7.94 (m, 2H), 7.45 – 7.32 (m, 5H), 7.07 – 7.01 (m, 2H), 5.15 (s, 2H), 4.39 (s, 2H).

**2-bromo-1-(4-fluorophenyl)ethan-1-one, (5-8i)**

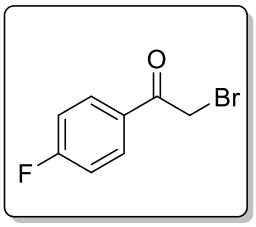


To a stirred solution of 4'-fluoroacetophenone (0.875 mL, 7.24 mmol) in acetic acid (15 mL) and protected from light, was added molecular bromine (0,373 mL, 7.24 mmol, 1 eq.) dropwise at room temperature over 30 minutes. The reaction mixture was left to stir overnight, before being quenched with 10% sodium thiosulfate (15 mL). The reaction was diluted with water (10 mL) and TBME (20 mL), the aqueous phase was extracted with TBME (2 x 20 mL). The organic phases were combine and with vigorous stirring, 10% $_{(aq.)}$ $NaHCO_3$ was added slowly until the aqueous layer remained > pH 7. The phases were separated, and the organic was washed with brine (2 x 15 mL) before being dried over $MgSO_4$. The compound was purified by flash column chromatography to give the titled compound as a light yellow solid (1.27g, 81% yield).[22]

**$^1$H NMR (400 MHz, cdcl3) δ** 8.00 – 7.93 (m, 2H), 7.14 – 7.07 (m, 2H), 4.41 (s, 2H).

**2-bromo-1-(4-chlorophenyl)ethan-1-one. (5-8j)**

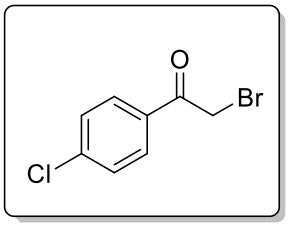


To a stirred solution of **5-7j** (938 µL, 7.24 mmol) in acetic acid (15 mL) and protected from light, was added molecular bromine (0.373 mL, 7.24 mmol, 1 eq.) dropwise at room temperature over 45 minutes. The reaction mixture was left to stir for 6 hours, before being diluted with acetone (1.5 mL) and water (0.5 mL) and left to stir overnight. The solvents were removed under reduced pressure, and the crude was diluted with DCM (15 mL) and 10% $_{(aq.)}$ $NaHCO_3$ and stirred vigorously for 5 minutes. The phases were then separated, the organic phase was dried over $MgSO_4$, before being concentrated to dryness *in vacuo* giving the titled compound. No further purification was performed.

**UPLC-MS**: 234.7 (M+H)

**2-bromo-1-(4-bromophenyl)ethan-1-one. (5-8k)**

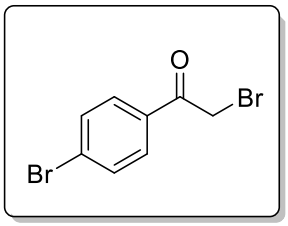


To a stirred solution of 5-7k (1 g, 3.62 mmol) in acetic acid (5 mL) and protected from light, was added molecular bromine (0.147 mL, 3.62 mmol, 1 eq.) dropwise at room temperature over 45 minutes. The reaction mixture was left to stir for 6 hours, before being diluted with acetone (1.5 mL) and water (0.5 mL) and left to stir overnight. The solvents were removed under reduced pressure, and the crude was diluted with DCM (15 mL) and 10% $_{(aq.)}$ $NaHCO_3$ and stirred vigorously for 5 minutes. The phases were then separated, the organic phase was dried over $MgSO_4$, before being concentrated to dryness *in vacuo* giving the titled compound. No further purification was performed.[23]

**UPLC-MS**: 279.1 (M+H)

**2-bromo-1-phenylethan-1-one. (5-7l)**

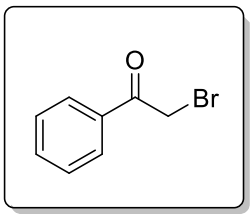


To a stirred solution of acetophenone (1 g, 8.32 mmol) in DCM was added bromine (428 µL, 8.32 mmol, 1 eq.) dropwise at room temperature over 10 mins. The solution was stirred for 3 hours, before being quenched with excess 10% sodium thiosulfate$_{(aq.)}$, and the phases separated. The organic layer was dried ($MgSO_4$) and reduced to dryness *in vacuo*, before being purified by flash column chromatography, giving the titled compound (951 mgs, 57% yield). The spectra matched those previously reported in the literature.[24]

**$^1$H NMR (400 MHz, cdcl$_3$) δ** 8.03 – 7.93 (m, 2H), 7.64 – 7.58 (m, 1H), 7.53 – 7.44 (m, 2H), 4.46 (s, 2H).

**7-(2-(3,4-bis(benzyloxy)phenyl)-2-oxoethoxy)-4-methyl-2H-chromen-2-one, (5-4e)**

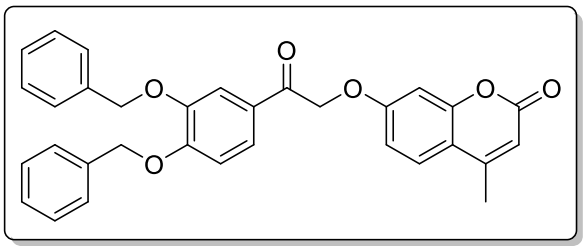

To a stirred solution of 4- methylumberliferone (56.7 mg, 0.322 mmol) in acetone (3 mL) at 25 ˚C was added alpha-bromo ketone **5-8e** (159 mg, 0.387 mmol, 1.2 equiv.). The reaction mixture was stirred for 16 h, before being filtered and the solid residue washed with acetone (2 x 30 mL). The reaction mixture was then diluted with water (2 mL) and DCM (10 mL), the phases were separated, the aqueous layer was then extracted with chloroform (2 x 5 mL), the organic phases were then combined, dried ($MgSO_4$), and the solvent was then removed under reduced pressure. The residue was purified by flash column chromatography (0-50 % EtOAc in hexanes), affording the titled compound as a white solid (48 mg, 29 %).

**$^1$H NMR (400 MHz, cdcl$_3$) δ** 7.63 – 7.27 (m, 13H), 6.97 (d, *J* = 8.4 Hz, 1H), 6.91 (dd, *J* = 8.8, 2.5 Hz, 1H), 6.75 (d, *J* = 2.5 Hz, 1H), 6.13 (d, *J* = 1.1 Hz, 1H), 5.26 (s, 2H), 5.25 (s, 2H), 5.21 (s, 2H), 2.38 (s, 3H).

**$^{13}$C NMR (101 MHz, cdcl3) δ** 191.49, 161.03, 160.93, 155.06, 154.04, 152.33, 148.91, 136.52, 136.15, 128.66, 128.58, 128.12, 128.05, 127.47, 127.37, 127.05, 125.69, 122.84, 114.23, 113.65, 113.03, 112.61, 112.36, 101.85, 71.23, 70.85, 70.30, 18.65.

**UPLC-MS**: 507.5 (M+H).

**4-(2-((4-methyl-2-oxo-2H-chromen-7-yl)oxy)acetyl)-1,2-phenylene bis(2,2-dimethylpropanoate), (5-4f)**

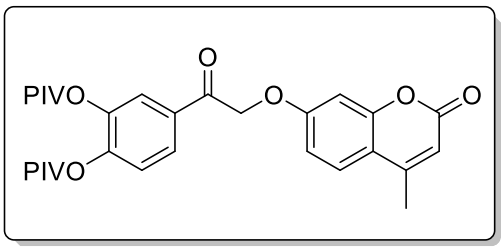


To a stirred solution of alpha bromo ketone **5-8f** (700 mg, 1.69 mmol) in acetone (17 mL) was added $K_2CO_3$ (233 mg, 1.69 mmol, 1 eq.) followed by 4-methylumberliferone (238.6 mg, 1.35 mmol, 0.8 eq.). The reaction mixture was stirred at room temperature for 4 hours where no 4-MU was visible by TLC. The reaction mixture was then evaporated to dryness, before being purified by flash column chromatography (DCM/MeOH) giving the titled compound (424 mg 64 % yield).

**$^{1}$H NMR (400 MHz, cdcl$_3$) δ** 7.88 (dd, *J* = 8.5, 2.1 Hz, 1H), 7.77 (d, *J* = 2.1 Hz, 1H), 7.52 (d, *J* = 8.8 Hz, 1H), 7.31 (d, *J* = 8.4 Hz, 1H), 6.92 (dd, *J* = 8.8, 2.6 Hz, 1H), 6.84 (d, *J* = 2.5 Hz, 1H), 6.16 (d, *J* = 1.0 Hz, 1H), 5.32 (s, 1H), 2.57 – 2.23 (m, 1H), 1.37 (s, 1H), 1.36 (s, 1H).

**$^{13}$C NMR (101 MHz, cdcl$_3$) δ** 191.54, 175.58, 175.26, 160.97, 160.65, 155.06, 152.28, 147.57, 143.10, 132.17, 126.23, 125.80, 124.06, 123.64, 114.46, 112.53, 112.35, 102.16, 77.19, 70.65, 39.32, 39.21, 27.20, 27.13, 18.65.

**7-(2-(3-(benzyloxy)phenyl)-2-oxoethoxy)-4-methyl-2H-chromen-2-one, (5-4g)**

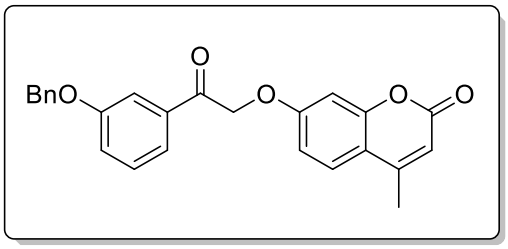


To a stirred solution of the alpha-bromoketone **5-8g** (1.7 g, 5.57 mmol, 1,2 eq.) in acetone (18 mL) was added 4-methylumberliferone (0.817 g, 4.64 mmol, 1 eq.) and $K_2CO_3$ (1.283 g, 9.28mmol, 2 eq.) at room temperature. After stirring overnight, the reaction mixture was heated to 60 degrees for an hour, before being cooled back to room temperature, where the solvent was removed *in vacuo*. The residue was split between water (10 mL) and EtOAc (30 mL), the phases were separated and the aqueous phase was extracted with EtOAc (1 x 20 mL). The residue was then purified by flash column chromatography over a gradient of $CHCl_3$/MeOH, to give the titled compound (1.19 g, 64 % yield)

**$^{1}$H NMR (400 MHz, dmso) δ** 7.67 (d, *J* = 8.8 Hz, 1H), 7.65 – 7.59 (m, 2H), 7.54 – 7.44 (m, 1H), 7.44 – 7.28 (m, 7H), 7.06 (d, *J* = 2.5 Hz, 1H), 7.01 (dd, *J* = 8.8, 2.6 Hz, 1H), 6.20 (s, 1H), 5.71 (s, 2H), 5.19 (s, 2H), 2.39 (d, *J* = 1.0 Hz, 3H).

**$^{13}$C NMR (101 MHz, dmso) δ** 193.98, 161.49, 160.53, 159.00, 155.09, 153.82, 137.12, 136.00, 130.52, 128.92, 128.41, 128.25, 126.87, 120.91, 120.88, 114.20, 113.86, 113.01, 111.73, 102.07, 71.07, 69.99, 18.59.

**IR (film):** 3383, 2949, 2830, 1655, 1447, 1386, 1013 cm$^{-1}$

**UPLC-MS**: 401.8 (M+H)

**7-(2-(4-(benzyloxy)phenyl)-2-oxoethoxy)-4-methyl-2H-chromen-2-one, (5-4h)**

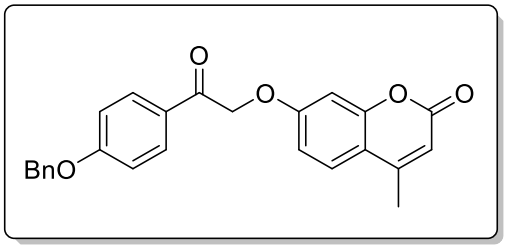


To a stirred solution of the **5-8h** (50 mg, 0.164 mmol, 1,2 eq.) in acetone (10 mL) was added 4-methylumberliferone (24 mg, 0.137 mmol, 1 eq.) and $K_2CO_3$ (38 mg, 27.4 mmol, 2 eq.) at room temperature. After stirring overnight, the solvent was removed *in vacuo* and the residue was stirred vigorously for one hour in 15 volumes of $CHCl_3$, 0.75 volumes of MeOH and 5 volumes of water. The residue was then purified by flash column chromatography over a gradient of $CHCl_3$/MeOH, to give the titled compound in a 56% yield (31 mg).

**UPLC-MS**: 401.6 (M+H)

**7-(2-(4-fluorophenyl)-2-oxoethoxy)-4-methyl-2H-chromen-2-one, (5-4i)**

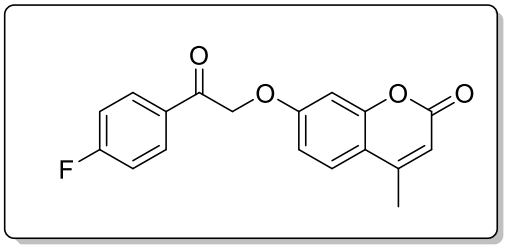


To a stirred solution of **5-8i** (50 mg, 0.230 mmol, 1,2 eq.) in acetone (10 mL) was added 4-methylumberliferone (34 mg, 0.192 mmol, 1 eq.) and $K_2CO_3$ (54 g, 0.384 mmol, 2 eq.) at room temperature. After stirring overnight, the solvent was removed *in vacuo* and the residue was stirred vigorously for one hour in 15 volumes of $CHCl_3$, 0.75 volumes of MeOH and 5 volumes of water. The residue was then purified by flash column chromatography over a gradient of $CHCl_3$/MeOH, to give the titled compound in an 66% yield (39 mg). The spectra matched those previously reported in the literature.[25]

**$^1$H NMR (400 MHz, cdcl$_3$) δ** 8.01 – 7.97 (m, 2H,), 7.45 (d, *J* = 8 Hz, 1H), 7.18 – 7.10 (m, 2H), 6.88 (dd, *J* = 2.5, 9 Hz, 1H), 6.74 (d, *J* = (2.4 Hz, 1H), 6.10 (q, *J* = 1.6 Hz, 1H), 5.27 (s, 2H), 2.37 (d, (1 Hz, 3H)

**UPLC-MS**: 313.4 (M+H)

**7-(2-(4-chlorophenyl)-2-oxoethoxy)-4-methyl-2H-chromen-2-one, (5-4j)**

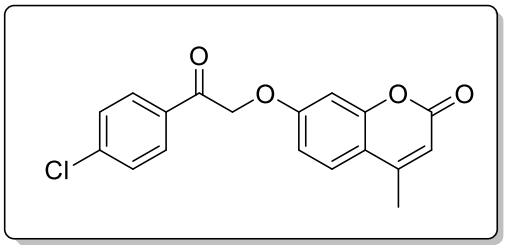


To a stirred solution of the crude **5-8j** (125 mg, 0.535 mmol, 1,2 eq.) in acetone (5 mL) was added 4-methylumberliferone (78 mg, 0.446 mmol, 1 eq.) and $K_2CO_3$ (124 mg, 892 mmol, 2 eq.) at room temperature. After stirring overnight, the solvent was removed *in vacuo* and the residue was stirred vigorously for one hour in 15 volumes of $CHCl_3$, 0.75 volumes of MeOH and 5 volumes of water. The residue was then purified by flash column chromatography over a gradient of $CHCl_3$/MeOH, to give the titled compound in an 35% yield (37 mg). The spectra matched those previously reported in the literature. [26]

**$^1$H NMR (400 MHz, cdcl$_3$) δ** 7.99 – 7.89 (m, 2H), 7.51 (m, 4H), 6.93 (dd, *J* = 8.8, 2.6 Hz, 1H), 6.79 (d, *J* = 2.6 Hz, 1H), 6.16 (d, *J* = 1.2 Hz, 1H), 5.32 (s, 2H), 2.40 (d, *J* = 1.2 Hz, 3H).

**7-(2-(4-bromophenyl)-2-oxoethoxy)-4-methyl-2H-chromen-2-one, (5-4k)**

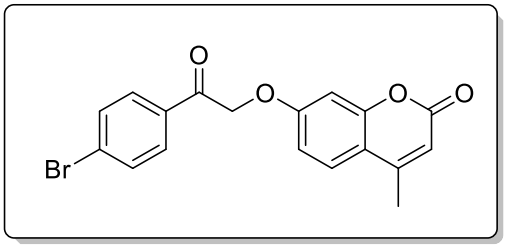


To a stirred solution of **5-8k** (63 mg, 0.227 mmol, 1,2 eq.) in acetone (10 mL) was added 4-methylumberliferone (33 mg, 0.189 mmol, 1 eq.) and $K_2CO_3$ (52 mg, 378 mmol, 2 eq.) at room temperature. After stirring overnight, the solvent was removed *in vacuo* and the residue was stirred vigorously for one hour in 15 volumes of $CHCl_3$, 0.75 volumes of MeOH and 5 volumes of water. The residue was then purified by flash column chromatography over a gradient of $CHCl_3$/MeOH, to give the titled compound in an 37 % yield (31 mg).

**UPLC-MS:** 374.2 (M+H)

**4-methyl-7-(2-oxo-2-phenylethoxy)-2H-chromen-2-one, (5-4l)**

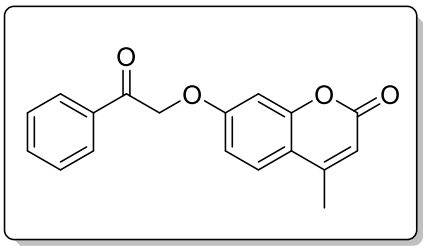

To a stirred solution of **5-8l** 248 mg, 1.248 mmol, 1,2 eq.) in acetone (10 mL) was added 4-methylumberliferone (200 mg, mmol, 1 eq.) and $K_2CO_3$ (188 mg, 1.362 mmol, 1.2 eq.) at room temperature. After stirring for 3 days, the reaction mixture was diluted with water (10 mL) and EtOAc (30 mL), the phases separated, and the aqueous phase was extracted with EtOAc (3 x 10 mL). The combined organic extracts were combined, dried over $MgSO_4$, concentrated to dryness *in vacuo*. The residue was then purified by flash column chromatography to give the titled compound (182 mg, 61 % yield).[25]

**$^1$H NMR (400 MHz, cdcl$_3$) δ** 8.01 – 7.97 (m, 2H), 7.65 (ddd, *J* = 6.9, 4.1, 1.3 Hz, 1H), 7.56 – 7.50 (m, 3H), 6.95 (dd, *J* = 8.8, 2.6 Hz, 1H), 6.80 (d, *J* = 2.6 Hz, 1H), 6.15 (d, *J* = 1.3 Hz, 1H), 5.38 (s, 2H), 2.39 (t, *J* = 1.5 Hz, 3H).

**7-(2-(3-hydroxyphenyl)-2-oxoethoxy)-4-methyl-2H-chromen-2-one, (5-4m)**

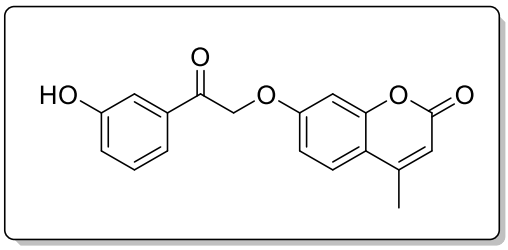

To a solution of **5-4g** (40 mg, 0.1 mmol) in 10% ethanol in ethyl acetate was added 10% Pd/C (10% by weight, 4 mg) under $N_2$. The solution was bubbled with stirring for 20 minutes with $N_2$ gas. The flask was placed under vacuum before the atmosphere being replaced with hydrogen (balloon). The reaction was followed by TLC, and immediately upon consumption of starting material was stopped by replacing the atmosphere with nitrogen following cycles of vacuum and nitrogen. The residue was filtered through Celite before being purified by column chromatography giving the title compound (20 mg, 64 % yield).

**UPLC-MS:** 311.6 (M+H)

**7-(2-(4-hydroxyphenyl)-2-oxoethoxy)-4-methyl-2H-chromen-2-one, (5-4n)**

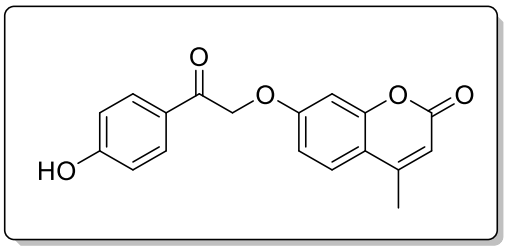

To a solution of **5-4g** (40 mg, 0.1mmol) in 10% ethanol in ethyl acetate was added 10% Pd/C (10% by weight, 4 mg) under $N_2$. The solution was bubbled with stirring for 20 minutes with $N_2$ gas. The flask was placed under vacuum before the atmosphere being replaced with hydrogen (balloon). The reaction was followed by TLC, and upon consumption of starting material was stopped by replacing the atmosphere with nitrogen following cycles of vacuum and nitrogen. The residue was filtered through Celite before being purified by column chromatography giving the title compound (18 mg, 59 % yield)

**UPLC-MS:** 311.6 (M+H)

**7-(2-(3,4-dimethoxyphenyl)-2-oxoethoxy)-4-methyl-2H-chromen-2-one, (5-4p)**

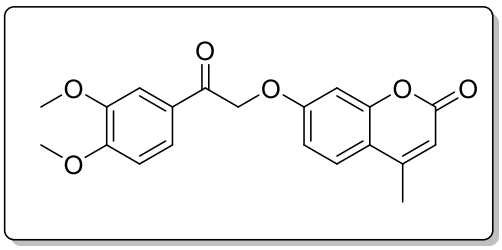

To a solution of **5-4a** (100 mg, 0.294 mmol) in acetone (10 mL) at room temperature was added $K_2CO_3$ (81 mg, 0.588 mmol, 2 eq.) and MeI (417 mg, 2.94 mmol, 10 eq.) and left to stir overnight. The following morning, the solvent was removed *in vacuo* and the residue was stirred vigorously for one hour in 15 volumes of $CHCl_3$, 0.75 volumes of MeOH and 5 volumes of water. The residue was then purified by flash column chromatography over a gradient of $CHCl_3$/MeOH, to give the titled compound in an 63 % yield (65 mg). The spectra matched those previously reported in the literature.[27]

**$^1$H NMR (400 MHz, $CDCl_3$) δ** 7.62 (dd, J = 8.22, 2.06 Hz, 1H), 7.51–7.42 (m, 2H), 7.08–6.89 (m, 2H), 6.79 (d, J = 2.77 Hz, 1H), 6.14 (d, J = 1.38 Hz, 1H), 5.33 (s, 2H), 3.99 (s, 3H), 3.91 (s, 3H), 2.40 (d, 1.37 Hz)

**7-(2-(3-methoxyphenyl)-2-oxoethoxy)-4-methyl-2H-chromen-2-one, (5-4c)**

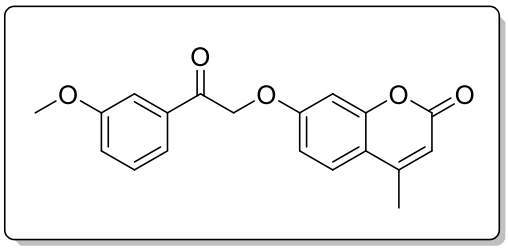

To a stirred solution of **5-4m** (23 mg, 0.071 mmol) in acetone (5 mL) at room temperature was added $K_2CO_3$ (20 mg, 0.142 mmol, 2 eq.) and MeI (101 mg, 0.71 mmol, 10 eq.) and left to stir overnight. The following morning, the solvent was removed *in vacuo* and the residue was stirred vigorously for one hour in 15 volumes of $CHCl_3$, 0.75 volumes of MeOH and 5 volumes of water. The residue was then purified by flash column chromatography over a gradient of $CHCl_3$/MeOH, to give the titled compound in an 84 % yield (20.1 mg). The structure conformed to that previously reported in the literature.[25]

**UPLC-MS**: 325.6 (M+H)

**7-(2-(4-methoxyphenyl)-2-oxoethoxy)-4-methyl-2H-chromen-2-one, (5-4d)**

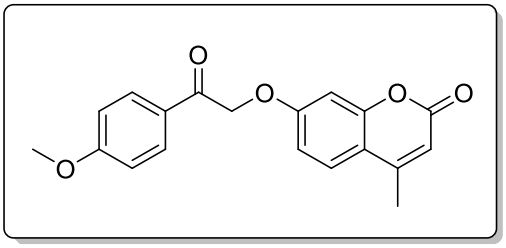

To a stirred solution of **5-4n** (23 mg, 0.071 mmol) in acetone (5 mL) at room temperature was added $K_2CO_3$ (20 mg, 0.142 mmol, 2 eq.) and MeI (101 mg, 0.71 mmol, 10 eq.) and left to stir overnight. The following morning, the solvent was removed *in vacuo* and the residue was stirred vigorously for one hour in 15 volumes of $CHCl_3$, 0.75 volumes of MeOH and 5 volumes of water. The residue was then purified by flash column chromatography over a gradient of $CHCl_3$/MeOH, to give the titled compound in an 80 % yield (19mg). The structure conformed to that previously reported in the literature.[25]

**UPLC-MS**: 325.5 (M+H)

**1-iodo-4-(methoxymethoxy)benzene, (5-20)**

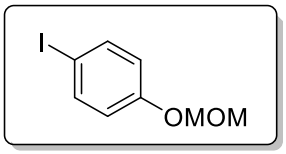


To a stirred solution of 4-iodophenol (6 g, 27.27 mmol) in THF (120 mL) and under $N_2$ was added 60% NaH (2.18 g, 54.54 mmol, 2 eq.) and left to stir for 20 minutes at room temperature. MOM-Cl (2.07 mL, 27.27 mmol, 1 eq.) was added to the reaction mixture dropwise and left to stir overnight at room temperature. The following morning the reaction was carefully quenched with brine (50 mL) and diluted with $Et_2O$ (70 mL). The organic phase was dried ($MgSO_4$), and the solvent removed *in vacuo*. The residue was used without any further purification, giving the titled compound as a colourless oil (7.2 g, 100 % yield). The spectra matched those previously reported in the literature.[28]

**$^1$H NMR (400 MHz, cdcl3) δ** 7.58 – 7.54 (m, 2H), 6.84 – 6.79 (m, 2H), 5.14 (s, 2H), 3.46 (s, 3H).

**((4-(methoxymethoxy)phenyl)ethynyl)trimethylsilane, (5-21)**

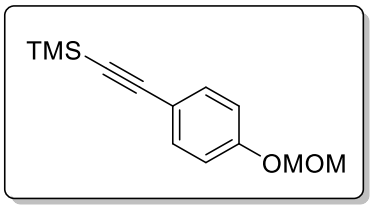


To a stirred solution of **5-20** (7.2 g, 27.27 mmol) in excess degassed $Et_3N$ (90 mL) was added CuI (209.5 mgs, 1.1 mmol, 4 mol %) and bis (triphenylphosphine) palladium (II) dichloride (382 mg, 0.55 mmol, 2 mol %) at room temperature. TMS-acetylene (4.62 mL, 32.72 mmol, 1.2 eq.) was added dropwise and stirred for 20 minutes before being heated to 50 degrees and left stirring for 90 minutes. The reaction mixture was then allowed to cool down to room temperature, the reaction mixture was filtered through celite, and the solvent was removed *in vacuo*. The residue was partitioned between EtOAc (30 mL) and water (20 mL), and the phases were separated. The organic phase was dried ($MgSO_4$) and the solvent was then removed *in vacuo*, giving the titled compound (6.39 g, 100 % yield). The spectra matched those previously reported in the literature.[29]

**$^1$H NMR (400 MHz, cdcl3) δ** 7.42 – 7.36 (m, 2H), 6.98 – 6.91 (m, 2H), 5.17 (s, 2H), 3.47 (s, 3H), 0.24 (s, 9H).

**1-ethynyl-4-(methoxymethoxy)benzene, (5-22)**

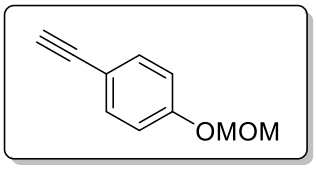


To a stirred solution of **5-21** (6.39 g, 27.27 mmol) in DCM (200 mL) and MeOH (100 mL) was added $K_2CO_3$ (12.99g, 54.54 mmol, 2 eq.), and left to stir for 3 hours at room temperature. The reaction mixture was then evaporated to dryness, and the resulting residue diluted with water (70 mL) and $Et_2O$ (70 mL). After stirring for 10 minutes, the phases were separated, and the aqueous phase extracted with $Et_2O$ (2 x 35 mL). the organic extracts were combined, dried over $MgSO_4$, and the solvent removed *in vacuo*. The resulting crude was then purified by flash column chromatography (0- 10% EtOAc in pentane) giving the titled compound as a yellow oil (3.78 g, 23.31 mmol, 85.5% yield). The spectra matched those previously reported in the literature. [30]

**$^1$H NMR (400 MHz, cdcl$_3$) δ** 7.45 – 7.39 (m, 2H), 7.01 – 6.96 (m, 2H), 5.18 (s, 2H), 3.47 (s, 3H), 3.00 (s, 1H).

**1-(but-1-yn-1-yl)-4-(methoxymethoxy)benzene, (5-13)**

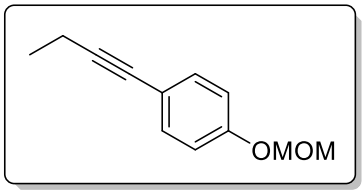


To stirred solution of DIPA (2.16 mL, 15.41 mmol, 1.25 eq.) in THF (35 mL) was added 2.5 M n-BuLi (5.91 mL, 14.79 mmol, 1.2 eq.) dropwise at 0 °C. After stirring for 30 minutes, a solution of **5-22** (2.0 g, 12.33 mmol, 1 eq.) in THF (20 mL) at 0 degrees was added dropwise to the reaction mixture. After 30 minutes, EtI (1.45 mL, 18.50 mmol, 1.5 eq.) was added dropwise to the reaction mixture and was allowed to warm to room temperature over an hour, before being heated to 60 degrees for a further hour. The reaction mixture was then cooled to room temperature before being diluted with $Et_2O$ (30 mL), followed by being quenched dropwise with brine (30 mL). the residue was then purified by flash column chromatography giving the titled compound in a 96% yield (2.52 g, 11.89 mmol).

**$^1$H NMR (400 MHz, cdcl$_3$) δ** 7.34 – 7.29 (m, 2H), 6.97 – 6.90 (m, 2H), 5.16 (s, 2H), 3.47 (s, 3H), 2.40 (q, *J* = 7.5 Hz, 2H), 1.22 (t, *J* = 7.5 Hz, 3H).

**(E)-tributyl(1-(4-(methoxymethoxy)phenyl)-2-(4,4,5,5-tetramethyl-1,3,2-dioxaborolan-2-yl)but-1-en-1-yl)stannane, (5-14)**

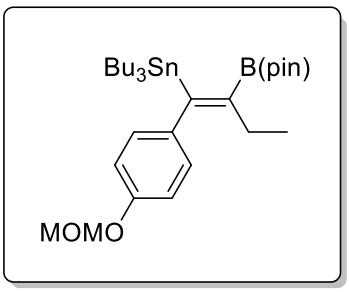


To a flame dried Schlenk under $N_2$ was added copper (II) acetate (2.85 mg, 2 mol%) and tricyclohexylphosphine (15.46 mg, 7 mol %). The mixture was suspended in anhydrous MeOH (2 mL) and heated to 80 degrees for 30 minutes where a colourless solution was formed. The solvent was then removed *in vacuo*, and the atmosphere replaced again with nitrogen. **5-13** (150 mg, 0.788 mmol, 1 eq.), bis(pinacolato)diboron (260 mg, 1.024 mmol, 1.3 eq.) and tributyltin methoxide (0.285 mL, 1.024 mmol, 1.3 eq.) were added to the Schlenk flask followed by toluene (2 mL). the reaction mixture was left to react for 20 hours before being diluted with EtOAc (2 mL) and brine (2 mL). After stirring for 1 hour, the phases were separated, the aqueous layer extracted with EtOAc (2 x 1mL), and the organic extracts combined and dried over $MgSO_4$. The residue was then passed through a $K_2CO_3$ plug, before being purified by flash column chromatography, yielding the 234 mg of the titled compound (49% yield) as a colourless oil.

**$^1$H NMR (400 MHz, cdcl$_3$) δ** 6.96 – 6.89 (m, 2H), 6.73 – 6.66 (m, 3H), 5.15 (s, 2H), 3.48 (s, 3H), 2.05 (q, *J* = 7.4 Hz, 2H), 1.43 – 1.30 (m, 7H), 1.29 (s, 12H), 1.20 (dq, *J* = 14.1, 7.1 Hz, 6H), 0.88 – 0.68 (m, 17H).

**2-(4-iodophenoxy)-N,N-dimethylethan-1-amine, (5-16)**

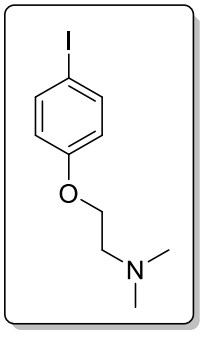


To a solution of iodophenol (5 g, 22.73 mmol) in DMF (30 mL) was added to $Cs_2CO_3$ (25.9 g, 79.55 mmol, 3.5 eq.) and heated to 80 degrees for 30 minutes. 2-Chloro-N,N-dimethylethylamine hydrochloride (6.54 g, 45.45 mmol, 2 eq.) was then added to the reaction mixture portionwise after being cooled to room temperature. The reaction was stirred at rt and left overnight to react. The reaction mixture was then poured into water (200 mL) and diluted with EtOAc (100 mL). The phases were separated, and the aqueous layer was extracted with EtOAc (2 x 50 mL), and the combined orgic extracts were dried ($MgSO_4$) and the solvent was then removed *in vacuo.* The residue

was then purified by flash column chromatography giving the titled compound (5.22 g, 79 % yield). The spectra matched those previously reported in the literature.[31]

**$^1$H NMR (400 MHz, cdcl$_3$) δ** 7.56 – 7.51 (m, 2H), 6.72 – 6.66 (m, 2H), 4.03 (t, *J* = 5.7 Hz, 2H), 2.73 (t, *J* = 5.7 Hz, 2H), 2.34 (s, 3H).

**3-(4-iodophenoxy)propane-1,2-diol, (5-27)**

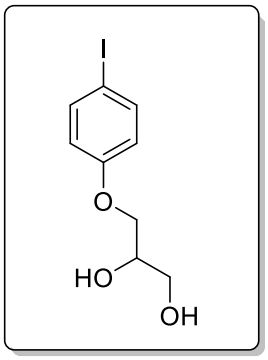


To a solution of iodophenol (1.22g, 5.54mmol) in EtOH (20 mL) was added to $Et_3N$ (0.927 mL, 6.65 mmol, 1.2 eq.) followed by glycidol (0.75 mL, 11.09 mmol, 2 eq.), before being heated up to 80 degrees in a sealed flask overnight. The solvent was removed *in vacuo* and the residue was split between water (20 mL) and EtOAc (20 mL), the phases were separated, the aqueous phase was extracted with EtOAc (2 x 10 mL), the combined organic extracts were washed with saturated ammonium chloride (10 mL), dried ($MgSO_4$) and the solvent was then removed *in vacuo*, where the residue was then purified through silica giving the titled compound (1.62 g, 100 % yield). The spectra matched those previously reported in the literature.[32]

**$^1$H NMR (400 MHz, cdcl$_3$) δ** 7.58 – 7.56 (d, 2H, *J* = 8.2 Hz), 6.71 – 6.67 (d, 2H, *J* = 8.2 Hz), 4.11 (m, 1H), 4.02 – 4.00 (m, 2H), 3.90 – 3.83 (m, 1H), 3.76 – 3.73 (m, 1H).

**4-((4-iodophenoxy)methyl)-2,2-dimethyl-1,3-dioxolane, (5-26)**

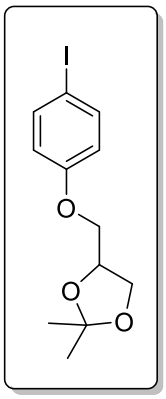


**5-27** (1.612 mgs, 5.54mmol) was added to a flask under $N_2$ and dissolved in acetone (30 mL) at room temperature where *p*-TSA (100 mg, cat.) and 2,2-dimethoxypropane (1.35 mL, 11.08 mmol, 2 eq.) was added at 50 degrees and left to react for 16 hours. The following morning the reaction mixture was cooled to rt where it was diluted with 10% $NaHCO_3$ (30 mL) and EtOAc (30 mL), the phases were separated and the aqueous layer was extracted with EtOAc (2 x 20 mL), the organic layers were combined and dried over $MgSO_4$, before being concentrated *in vacuo*. The residue was then purified through silica giving the titled compound (1.31 mgs, 71.6 % yield) as a colourless oil. The spectra matched those previously reported in the literature.[33]

**$^{1}$H NMR (400 MHz, cdcl$_3$) δ** 7.67 – 7.41 (m, 2H), 6.72 – 6.67 (m, 2H), 4.51 – 4.40 (m, 1H), 4.16 - 3.89 (m, 4H), 1.45 (s, 3H), 1.40 (s, 3H).

**$^{13}$C NMR (101 MHz, cdcl3) δ** 158.43, 138.22, 116.92, 109.82, 83.24, 73.85, 68.86, 66.71, 26.76, 25.32.

**2-(4-iodophenoxy)tetrahydro-2H-pyran, (5-28)**

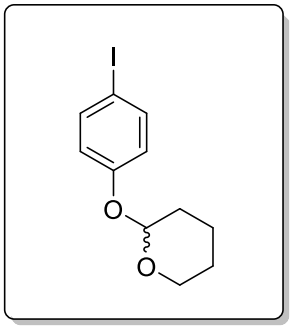


To a stirred solution of iodophenol (1 g, 4.55 mmol) in DCM (25 mL) was added dihydropyran (1.25 mL, 13.65 mmol, 3 eq.) and pyridinium *p*-toluenesulfonate (114 mg, 0.455 mmol, 10 mol %). The reaction was stirred at rt overnight, where the following morning the reaction mixture was diluted with 10% $NaHCO_3$ (10 mL), the phases were separated and the aqueous layer was extracted with DCM (1 x 10 mL), the organic layers were combined and dried ($MgSO_4$), before being concentrated *in vacuo*. The residue was then purified through silica giving the titled compound (608 mgs, 44 % yield) as a colourless oil.

**$^{1}$H NMR (400 MHz, cdcl$_3$) δ** 7.73 – 7.41 (m, 2H), 6.93 – 6.62 (m, 2H), 5.37 (t, *J* = 3.2 Hz, 1H), 4.00 – 3.49 (m, 2H), 1.95 – 1.42 (m, 5H).

**2-(4-iodophenoxy)tetrahydro-2H-pyran, (5-29)**

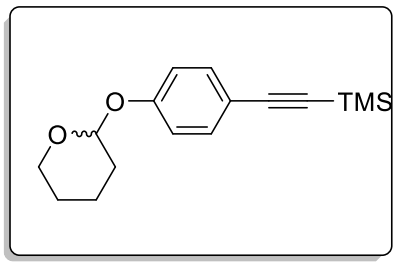


To a stirred solution of THP-iodophenol (608 mgs, 2 mmol) in excess degassed $Et_3N$ (20 mL) was added CuI (15 mg, 0.08 mmol, 4 mol %) and Bis (triphenylphosphine) palladium (II) dichloride (28 mg, 0.04 mmol, 2 mol %) at room temperature. TMS-acetylene (0.340 mL, 2.4 mmol, 1.2 eq.) was added dropwise and stirred for 20 minutes before being heated to 50 degrees and left stirring for 90 minutes. The reaction mixture was then allowed to cool down to room temperature, filtered through celite and the solvent was removed *in vacuo*. The residue was partitioned between EtOAc (20 mL) and water (10 mL), and the phases were separated. The organic phase was washed with 1M HCl (10 mL), brine (10 mL), the phases were separated, the organic phase was dried ($MgSO_4$) and the solvent was then removed *in vacuo*, giving the titled compound (535 mg, 97.5% yield).

**$^1$H NMR (400 MHz, cdcl$_3$) δ** 7.20 (q, *J* = 4.8 Hz, 2H), 6.79 (d, *J* = 1.2 Hz, 2H), 5.23 (t, *J* = 3.2 Hz, 1H), 3.90 – 3.20 (m, 2H), 1.86 – 1.07 (m, 6H), 0.04 (s, 9H).

**4-iodophenyl pivalate, (5-30)**

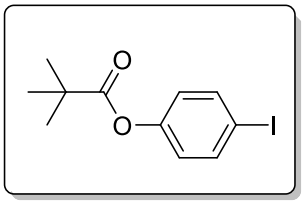

To a stirred solution iodophenol (1 g, 4.55mmol) in DCM (20 mL) under $N_2$ was added $NEt_3$ (0.762 mL, 5.46 mmol, 1.1 eq.), followed by pivaloyl chloride (0.560 mL, 4.55 mmol, 1 eq.) dropwise. The reaction was left for 14 hours at room temperature where it was quenched with excess saturated ammonium chloride and stirred for 20 minutes. The organic phase was then washed with 10% $NaHCO_3$ (10 mL), the organic extracts were combined, dried ($MgSO_4$) and the solvent removed *in vacuo*. The residue was purified by flash column chromatography giving the titled compound as a thick oil (804 mg, 58.1 % yield). The spectra matched those previously reported in the literature.[34]

**$^1$H NMR (400 MHz, cdcl$_3$) δ** 7.61 (d, J = 8.2 Hz, 2H), 6.81 (d, J = 8.3 Hz, 2H), 1.33 (s, 9H).

**4-((trimethylsilyl)ethynyl)phenyl pivalate, (5-31)**

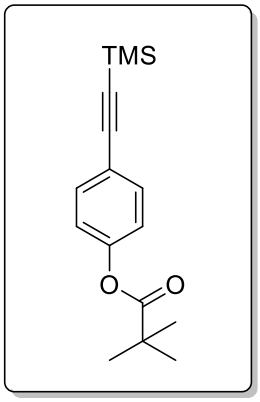


To a stirred solution of **5-30** (304 mg, 1 mmol) in excess degassed $Et_3N$ (10 mL) was added CuI (7.6 mg, 0.04 mmol, 4 mol %) and bis (triphenylphosphine) palladium (II) dichloride (14.03 mg, 0.02 mmol, 2 mol %) at room temperature. TMS-acetylene (169 µL, 1.2 mmol, 1.2 eq.) was added dropwise and stirred for 20 minutes before being heated to 50 degrees and left stirring for 90 minutes. The reaction mixture was then allowed to cool down to room temperature, where the solvent was removed *in vacuo*. The residue was partitioned between EtOAc (10 mL) and water (10 mL), and the phases were separated. The organic phase was filtered through celite, the celite was washed with EtOAc (10 mL) and the solvent was then removed *in vacuo*, where the residue was used without further purification for the next step**.** The spectra matched those previously reported in the literature.[35]

**$^1$H NMR (400 MHz, cdcl$_3$) δ** 7.49 – 7.43 (m, 2H), 7.03 – 6.97 (m, 2H), 1.34 (s, 9H), 0.24 (s, 9H).

**1-(4-(benzyloxy)-3-methoxyphenyl)-2-(4-iodophenoxy)ethan-1-one,** (**5-32**)

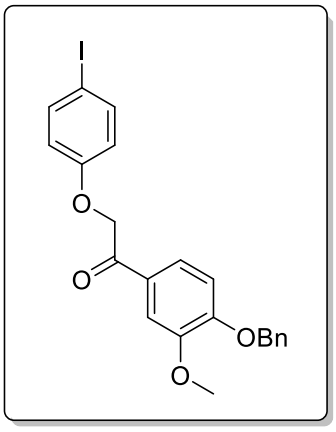


To a stirred solution of iodophenol (3.75 g, 17.05 mmol) in DMF (80 mL) was added $K_2CO_3$ (2.82 g, 20.4 mmol, 1.2 eq.) and alpha bromo ketone **5-8a** (6 g, 17.9 mmol, 1.05 eq.). The reaction was left to stir overnight at 50 degrees, before the reaction mixture was cooled down to room temperature and diluted with water (300 mL), $CHCl_3$ (100 mL) and MeOH (5mL). The aqueous layer was extracted with 5% MeOH in $CHCl_3$ (4 x 50 mL). All of the combined organic extracts were dried over $MgSO_4$ and the solvent was then removed *in vacuo*. The resulting crude was then diluted with EtOH (125 mL) and heated to reflux. Once a clear solution was formed, the heating was turned off and the mixture allowed to slowly cool to room temperature, before being cooled in an ice bath for 30 minutes. The mixture was then filtered through a sintered Buchner funnel, giving the titled compound as an off white solid (7.12 g, 88 % yield).

**$^1$H NMR (400 MHz, dmso) δ** 7.67 (dd, *J* = 8.4, 2.0 Hz, 1H), 7.61 – 7.52 (m, 2H), 7.50 – 7.28 (m, 6H), 7.19 (d, *J* = 8.5 Hz, 1H), 6.88 – 6.70 (m, 2H), 5.53 (s, 2H), 5.22 (s, 2H), 3.84 (s, 3H).

**$^{13}$C NMR (101 MHz, dmso) δ** 193.03, 158.45, 152.96, 149.42, 138.28, 136.88, 128.94, 128.48, 128.30, 127.75, 122.87, 117.90, 112.90, 110.83, 83.83, 70.34, 70.31, 56.10.

**HRMS (ESI):** m/z [M + H]+ calculated for $C_{22}H_{19}IO_4$: 474.0328; found: 474.0320.

**IR (Film):** 2917, 2851, 2362, 1731, 1679, 1586, 1551, 1415 $cm^{-1}$

**1-(4-(benzyloxy)-3-methoxyphenyl)-2-(4-((trimethylsilyl)ethynyl)phenoxy)ethan-1-one, (5-33)**

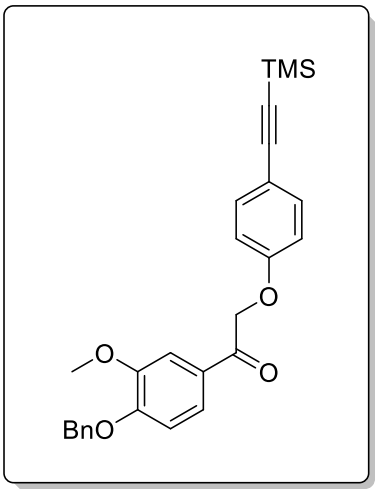


To a solution of **5-32** (400 mg, 0.843 mmol) in THF (5 mL) was added $Et_3N$ (10 mL). The mixture was degassed by with bubbling $N_2$ for 10 minutes. CuI (6.44 mg, 2 mol %) and $Pd(PPh_3)_2Cl_2$ (11.8 mg, 4 mol %) were then added to the reaction mixture, followed by dropwise addition of TMS acetylene (143 µL, 1.01 mmol, 1.2 eq.). The reaction mixture was then heated to 60 degrees for 90 minutes where it was then cooled down to room temperature, before being filtered through a pad of Celite. The resulting solution was concentrated to dryness *in vacuo*, diluted with EtOAc (20 mL) and $NH_4Cl$ (10 mL). The phases were separated, and the organic layer was washed with $NH_4Cl$ (10 mL), the phases separated, and the organic layer was then dried over $MgSO_4$, and concentrated to dryness *in vacuo*. The residue was used without further purification for the next step.

**$^1$H NMR (400 MHz, cdcl$_3$) δ** 7.59 – 7.51 (m, 1H), 7.46 – 7.29 (m, 3H), 6.91 (d, *J* = 8.2 Hz, 1H), 6.84 (dd, *J* = 9.2, 2.5 Hz, 1H), 5.24 (s, 1H), 5.20 (s, 1H), 3.94 (s, 1H).

**1-(4-(benzyloxy)-3-methoxyphenyl)-2-(4-(but-1-yn-1-yl)phenoxy)ethan-1-one, (5-17)**

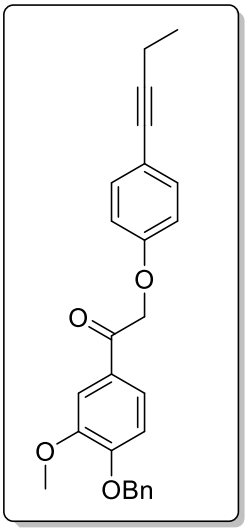


To a solution of **5-32** (1 g, 2.11 mmol) in degassed DMF (20 mL) was added CuI (40 mg, 0.211 mmol, 10 mol %), $Pd(PPh_3)_2Cl_2$ (73 mg, 0.105 mmol, 5 mol %) and $Et_3N$ (0.88 mL, 6.33 mmol, 3 eq.) at room temperature under $N_2$. 2-Pentynoic acid (410 mg, 4.22 mmol, 2 eq.) was then added to the reaction mixture and was left to react for 2 hours at room temperature, before being heated to 50 degrees for a further hour. The reaction was then cooled to room temperature before being filtered through a pad of Celite. The resulting solution was concentrated to dryness *in vacuo*, diluted with $CHCl_3$ (20 mL) and $NH_4Cl$ (10 mL). The phases were separated and the organic layer was washed with $NH_4Cl$ (10 mL), 10% copper sulphate solution (2x 10 mL), the phases separated, and the organic layer was then dried over $MgSO_4$ and concentrated to dryness *in vacuo*. The crude was then purified by flash column chromatography giving the titled compound in a 94% yield (795 mg).

**$^1$H NMR (400 MHz, cdcl$_3$) δ** 7.60 – 7.52 (m, 1H), 7.48 – 7.28 (m, 2H), 5.24 (s, 1H), 5.19 (s, 1H), 3.94 (s, 1H), 2.39 (q, *J* = 7.5 Hz, 1H), 1.22 (t, *J* = 7.5 Hz, 1H).

**1-(4-(benzyloxy)-3-methoxyphenyl)-2-(4-(but-1-yn-1-yl)phenoxy)ethan-1-ol, (5-34)**

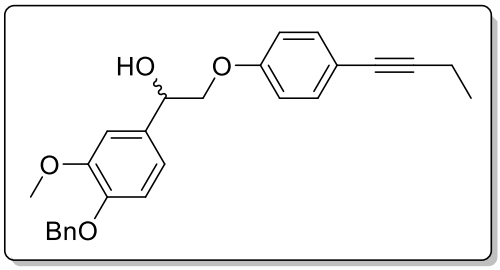


To a solution of **5-17** (480 mg, 1.2 mmol) in THF (20 mL) was added $NaBH_4$ (50 mg, 1.32 mmol, 1.1 eq.) at -12 degrees. The reaction mixture was kept at -12 degrees until nearly all the SM had disappeared by TLC, at which point it was quenched with excess saturated ammonium chloride and diluted with EtOAc (20 mL), the phases separated, the aqueous layer extracted with chloroform (20 mL), and the combined organic layers dried over $MgSO_4$, before being concentrated to dryness *in vacuo*. The resulting crude was then columned by flash column chromatography giving the titled compound (351 mg, 73 %)

**$^1$H NMR (400 MHz, cdcl$_3$) δ** 7.49 – 7.26 (m, 1H), 7.02 (s, 1H), 6.88 (s, 1H), 6.85 – 6.78 (m, 1H), 5.15 (s, 1H), 5.03 (dd, *J* = 8.6, 2.5 Hz, 1H), 4.08 – 3.94 (m, 1H), 3.90 (s, 1H), 2.77 (d, *J* = 1.3 Hz, 1H), 2.40 (q, *J* = 7.5 Hz, 1H), 1.22 (t, *J* = 7.5 Hz, 1H).

**$^{13}$C NMR (101 MHz, cdcl3) δ** 157.76, 149.84, 148.04, 137.05, 132.90, 132.66, 128.53, 127.83, 127.22, 118.54, 116.84, 114.48, 113.95, 109.90, 90.34, 79.38, 73.34, 72.31, 71.05, 56.03, 13.99, 13.06.

**IR (film):** 3490, 3033, 2966, 2932, 2865, 1603, 1499, 1245 cm$^{-1}$

**HRMS (ESI):** m/z [M + H]+ calculated for $C_{26}H_{26}O_4$: 402.1831; found: 402.1836.

**(1-(4-(benzyloxy)-3-methoxyphenyl)-2-(4-(but-1-yn-1-yl)phenoxy)ethoxy) triisopropylsilane, (5-36)**

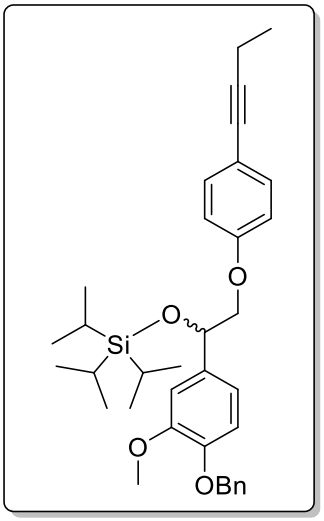


To a stirred solution of **5-34** (2.0 g, 4.97 mmol) in DCM (50 mL) under $N_2$ was added triethylamine (1.04 mL, 7.46 mmol, 1.5 eq.) and DMAP (61 mg, .497 mmol, 10 mol %) After stirring for 10 minutes, TIPS-OTf (1.27 mL, 4.72 mmol, 0.95 eq.) was added dropwise over 20 minutes, and the mixture left to react overnight. The following morning, 2-amino ethanol (680 mg, 10 mmol, 2 eq.) was added dropwise to the reaction mixture and left for an hour. The reaction mixture was then diluted with water (30 mL), and the organic phase washed with saturated ammonium chloride (2 x 30 mL), dried ($MgSO_4$) before being concentrated to dryness *in vacuo*. The resulting crude was purified by flash column chromatography giving the titled compound (1.43 g, 52 % yield).

**$^1$H NMR (400 MHz, cdcl$_3$) δ** 7.44 (d, *J* = 6.9 Hz, 2H), 7.40 – 7.27 (m, 5H), 7.04 (s, 1H), 6.84 (s, 2H), 6.77 – 6.72 (m, 2H), 5.14 (s, 2H), 5.08 (dd, *J* = 7.6, 4.0 Hz, 1H), 4.03 – 3.83 (m, 5H), 2.39 (q, *J* = 7.5 Hz, 2H), 1.22 (t, *J* = 7.5 Hz, 3H), 1.16 – 1.07 (m, 3H), 1.05 (d, *J* = 6.3 Hz, 9H), 0.99 (d, *J* = 6.8 Hz, 9H).

**(Z)-(1-phenylpropylidene)hydrazine,** (**5-40**)

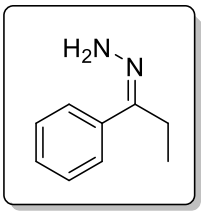


To a stirred solution of hydrazine monohydrate (1.81 mL, 37.26 mmol, 5 eq.) at 0 degrees was added a 0 degrees-solution of propiophenone (1g, 7.45 mmol, 1 eq.) in EtOH (15 mL). The mixture was left to warm to room temperature over an hour, before being heated to 50 degrees for 4 hours. The reaction mixture was then cooled to 0 degrees in an ice bath, before being diluted with DCM (50 mL) and water (20 mL). The phases were separated, and the organic phase dried over $MgSO_4$. The crude was used in the following reaction without any purification as decomposition was observed in previous experiments following purification by thin layer chromatography.

The spectra matched those previously reported in the literature.[36]

**$^1$H NMR (400 MHz, cdcl$_3$) δ** 7.67 – 7.23 (m, 1H), 2.65 (q, *J* = 7.7 Hz, 1H), 1.18 (t, *J* = 7.7 Hz, 1H).

**(1,1-dibromobut-1-en-2-yl)benzene, (5-41)**

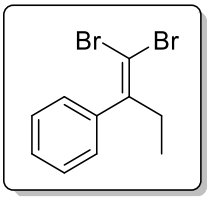


To a stirred solution of **5-40** (1.1 g, 7.45 mmol, 1 eq.) in DMSO (7 mL) was added CuCl (72.7 mg, 0.745 mmol, 10 mol %), 25% $NH_3$ solution in water (2.5 mL) and $CBr_4$ (2.48 g, 7.45 mmol, 1 eq.) at room temperature. After stirring for 24 hours, the reaction mixture was diluted with water (80 mL) and DCM (40 mL). The phases were separated and the aqueous phase was extracted with DCM (2 x 40 mL), the combined organic phases were then washed with a 10% solution of copper sulphate (2 x 40 mL), dried over MgSO4, before being concentrated to dryness *in vacuo*. The crude was then purified by flash column chromatography (100% hexanes) to give the titled compound (1.53 g, 71 % yield). Care was taken to ensure no $CBr_4$ remained by looking for the absence of a peak at -30 ppm in the $^{13}C$ NMR which corresponds to the carbon of $CBr_4$. The spectra matched those previously reported in the literature.[36][37]

**$^1$H NMR (400 MHz, cdcl$_3$) δ** 7.42 – 7.27 (m, 1H), 7.20 – 7.13 (m, 1H), 2.61 (q, *J* = 7.5 Hz, 1H), 0.98 (t, *J* = 7.5 Hz, 1H).

**2,2'-(2-phenylbut-1-ene-1,1-diyl)bis(4,4,5,5-tetramethyl-1,3,2-dioxaborolane), (5-37)**

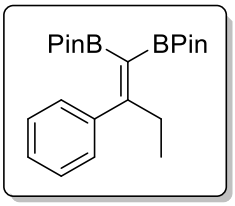


A solution of **5-41** (250 mg, 0.862 mmol) in THF (3 mL) and $Et_2O$ (2 mL) under $N_2$ was cooled to -110 degrees in an ethanol/$N_2$ (liquid) bath. To the solution was added a 1.4M solution of n-BuLi (0.616 mL, 0.862 mmol, 1 eq.) dropwise. The solution turned yellow and was left at -110 degrees for 10 minutes where bis(pinacolato)diboron (219 mg, 0.862 mmol, 1 eq.) was added at once. The solution turned deep red followed by purple, at which point it was covered with tin foil and left in the bath to warm slowly to room temperature overnight. The following morning the colourless solution was diluted with TBME (5 mL) and saturated $NH_4Cl_{(aq.)}$ (5 mL). The phases were separated, and the aqueous phase was extracted with TBME (2 x 5 mL), the combined organic phases were dried over MgSO4, before being concentrated to dryness *in vacuo*. The crude was then purified by flash column chromatography to give the titled compound (146 mg, 44 % yield).

The spectra matched those previously reported in the literature.[38]

**$^1$H NMR (400 MHz, cdcl$_3$) δ** 7.27 – 7.19 (m, 1H), 2.71 (q, *J* = 7.5 Hz, 1H), 1.28 (s, 1H), 1.03 (s, 1H), 0.92 (t, *J* = 7.5 Hz, 1H).

**(E)-1-(4-(benzyloxy)-3-methoxyphenyl)-2-(4-(2-phenyl-1-(4,4,5,5-tetramethyl-1,3,2-dioxaborolan-2-yl)but-1-en-1-yl)phenoxy)ethan-1-one, (5-38a)**

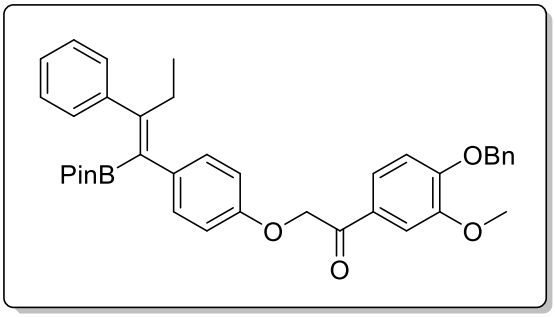


To a flame dried Schlenk tube under $N_2$ was added $^tBu_3P$ (10.5 mg, 0.052 mmol, 20 mol %) and $Pd_2dba_3$ (12 mg, 0.013 mmol, 5 mol 5%) and degassed THF (1 mL). The mixture was left to stir at room temperature for ten minutes before cooling down to -12 degrees in an ice bath. To the mixture was then added aryl iodide **5-32** (123.5 mg, 0.260 mmol, 1 eq.), **5-37** (100 mg, 0.260 mmol, 1 eq.) and more degassed THF (1.5 mL) previously cooled to -12 degrees. The reaction was kept isolated from light as a precaution and left to stir to room temperature overnight. The following morning the reaction mixture was diluted with TBME (4 mL) and $NH_4Cl_{(aq.)}$ (4 mL). The phases were separated, and the aqueous phase was extracted with TBME (2 x 5 mL), the combined organic phases were dried over MgSO4, before being concentrated to dryness *in vacuo*. The crude was then purified by flash column chromatography to give the titled compound (119 mg, 76 % yield).

**$^1$H NMR (400 MHz, cdcl$_3$) δ** 7.63 – 7.56 (m, 2H), 7.45 – 7.24 (m, 10H), 7.18 – 7.10 (m, 2H), 6.95 – 6.88 (m, 3H), 5.25 (s, 2H), 5.21 (s, 2H), 3.95 (s, 3H), 2.42 (q, J = 7.5 Hz, 2H), 0.99 (s, 12H), 0.84 (t, J = 7.5 Hz, 3H).

**$^{13}$C NMR (101 MHz, cdcl$_3$) δ** 193.27, 156.46, 153.59, 152.99, 149.74, 143.66, 136.11, 134.79, 129.57, 128.70, 128.43, 128.15, 128.05, 127.83, 127.17, 126.94, 122.63, 114.55, 112.24, 110.83, 83.23, 70.95, 70.83, 56.11, 27.06, 24.37, 13.25.

**IR (film):** 3380, 2975, 2926, 2868, 2246, 1687, 1598, 1499, 1265 cm$^{-1}$

**UPLC-MS:** 605.5 (M+H)

**4,4'-(2-phenylbut-1-ene-1,1-diyl)diphenol, (5-43)**

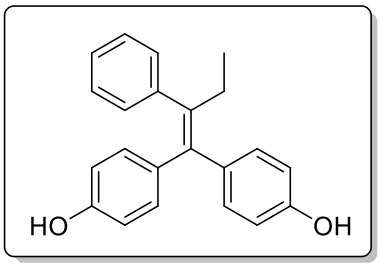


To a suspension of Zn dust (24.41 g, 373.44 mmol, 8 eq.) in THF (200 mL) under $N_2$ was added $TiCl_4$ (20.48 mL, 186.4 mmol, 4 eq.) dropwise at 0 degrees. After all the $TiCl_4$ was added to the suspension, the reaction mixture was heated up to reflux for 2 hours, before it was then cooled down to room temperature. A solution of 4,4'-dihydroxybenzophenone (10 g, 46.6 mmol, 1 eq.) and propiophenone (18.98 g, 139.8 mmol, 3 eq.) in THF (200 mL) was added dropwise to the reaction mixture, stirred for 5 minutes, before being heated again to reflux for three hours. After being cooled to room temperature, the reaction mixture was carefully quenched with saturated 10% $K_2CO_3$ (300 mL) and diluted with TBME (200 mL). The phases were separated, and the aqueous layer was extracted with TBME (2 x 100 mL), the organic layers were combined, washed with brine (100 mL) and dried over $MgSO_4$, before being concentrated *in vacuo*. The residue was then purified through silica giving the titled compound (10.4 g, 70.4 % yield) as a white solid. The spectra matched those previously reported in the literature.[39]

**$^1$H NMR (400 MHz, cdcl$_3$) δ** 7.22 – 6.99 (m, 4H), 6.86 – 6.77 (m, 1H), 6.77 – 6.67 (m, 1H), 6.52 – 6.39 (m, 1H), 2.48 (q, *J* = 7.4 Hz, 1H), 0.92 (t, *J* = 7.4 Hz, 2H).

**4-(4-hydroxybenzoyl)phenyl pivalate, (5-44)**

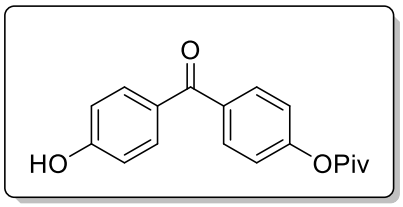


To a stirred solution of 4,4'- dihydroxybenzophenone (5.0 g, 23.34 mmol) in THF (55 mL) under $N_2$ was added 60% NaH (1.70 g, 42.17 mmol, 2 eq.), followed by pivaloyl chloride (3.16 mL, 25.67 mmol, 1.1 eq.) dropwise 20 minutes later. The reaction was left for 4 hours at room temperature where it was quenched carefully with excess saturated ammonium chloride, and diluted with EtOAc. The phases were separated, the aqueous phase was extracted with EtOAc (2 x 50 mL), the organic extracts were combined, dried ($MgSO_4$) and the solvent removed *in vacuo*. The residue was purified by flash column chromatography giving the titled compound (2.0 g, 28.7% yield) The spectra matched those previously reported in the literature.[40]

**$^1$H NMR (400 MHz, cdcl$_3$) δ** 7.83 – 7.74 (m, 1H), 7.20 – 7.16 (m, 1H), 6.94 – 6.86 (m, 1H), 1.39 (s, 2H).

**(E)-4-(1-(4-hydroxyphenyl)-2-phenylbut-1-en-1-yl)phenyl pivalate, (5-45)**

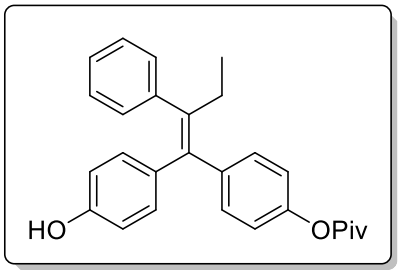


To a suspension of Zn (3.5 g. 53.6 mmol, 8 eq.) in THF (60 mL) under $N_2$ was added $TiCl_4$ (2.94 mL, 26.8 mmol, 4 eq.) dropwise at 0 degrees. After all the $TiCl_4$ was added to the suspension, the reaction mixture was heated up to reflux for 2 hours, before it was then cooled down to room temperature. A solution of mono-piv **5-44** (2.0 g, 6.70 mmol, 1 eq.) and propiophenone (2.69 mgs, 20.1 mmol, 3 eq.) in THF (60 mL) was added dropwise to the reaction mixture, stirred for 5 minutes, before being heated again to reflux for three hours. After being cooled to room temperature, the reaction mixture was carefully quenched with saturated 10% $K_2CO_3$ (100 mL) and diluted with TBME (50 mL). The phases were separated and the aqueous layer was extracted with TBME (3 x 50 mL), the organic layers were combined, washed with brine (50 mL) and dried over $MgSO_4$, before being concentrated *in vacuo*. The residue was then purified through silica giving the titled compound (1.42 g, 52.9 % yield). The spectra matched those previously reported in the literature.[40]

**$^1$H NMR (400 MHz, cdcl$_3$) δ** 7.25 – 7.02 (m, 9H), 6.74 – 6.68 (m, 2H), 6.46 (d, *J* = 8.7 Hz, 2H), 2.46 (q, *J* = 7.4 Hz, 2H), 1.37 (s, 9H), 0.91 (t, *J* = 7.4 Hz, 3H).

**3-(4-(1-(4-hydroxyphenyl)-2-phenylbut-1-en-1-yl)phenoxy)propane-1,2-diol, (5-46)**

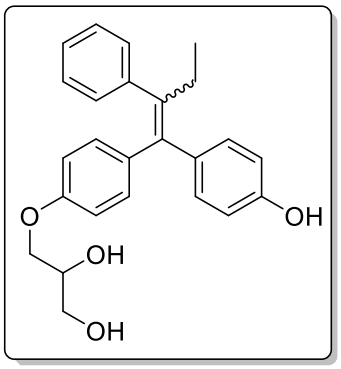


To a solution of diol **5-43** (1.6 g, 5.06 mmol) was added $NEt_3$ (0.706 mL, 5.06 mmol, 1 eq.) and glycidol (0.301 mL, 4.55 mmol, 0.9 eq.) in EtOH (24 mL) in a sealed flask and heated up to 80 degrees overnight. In the morning, the reaction mixture was cooled to room temperature and the solvent was removed in vacuo. The residue split between EtOAc (40 mL) and saturated ammonium chloride (40 mL), before the organic layer was dried over $MgSO_4$ and concentrated to dryness *in vacuo*. The residue was purified by flash column chromatography giving the titled compound as a thick colourless oil (735 mg, 37.2 % yield).

**$^{1}$H NMR (400 MHz, cd$_3$od) δ** 7.19 – 7.06 (m, 1H), 7.04 (d, *J* = 8.4 Hz, 1H), 6.96 (t, *J* = 5.7 Hz, 1H), 6.82 – 6.74 (m, 1H), 6.67 (d, *J* = 8.5 Hz, 1H), 6.62 – 6.55 (m, 1H), 6.42 (d, *J* = 8.5 Hz, 1H), 4.13 – 3.80 (m, 1H), 3.79 – 3.53 (m, 1H), 2.49 (p, *J* = 7.5 Hz, 1H), 0.92 (t, *J* = 7.4 Hz, 1H).

**$^{13}$C NMR (101 MHz, cd$_3$od) δ** 159.14, 158.29, 157.25, 156.36, 144.11, 144.10, 141.99, 141.80, 139.74, 139.71, 137.87, 137.50, 136.34, 135.98, 133.02, 133.00, 131.57, 130.89, 130.87, 128.84, 126.94, 115.84, 115.18, 115.09, 114.35, 71.84, 71.76, 70.34, 70.08, 64.21, 64.14, 29.89, 29.85, 13.94. ** due to the fact that the double bond is a 1:1 mixture of cis and trans isomers, and also the fact that the glycidol used was racemic, there are more carbons than expected. This is due to diastereomers.**

**4-(1-(4-((2,2-dimethyl-1,3-dioxolan-4-yl)methoxy)phenyl)-2-phenylbut-1-en-1-yl)phenol, (5-49)**

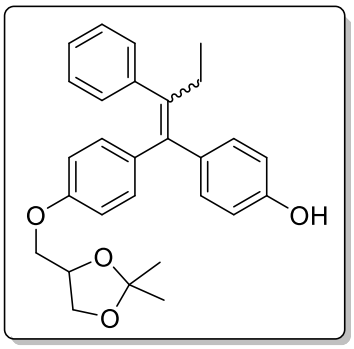


To a solution of **5-46** (106 mg, 0.271 mmol) was added to a flask under $N_2$ and dissolved in acetone (3 mL) at room temperature where *p*-TSA (7.7 mg, 0.040 mmol, 0.15 eq.) and 2,2-dimethoxypropane (66 µL, 542 mmol, 2 eq.) was added at 50 degrees and left to react for 5 hours. Once all the starting material had disappeared by TLC, the reaction mixture was cooled to rt where it was diluted with 10% $NaHCO_3$ (2 mL) and EtOAc (6 mL), the phases were separated, and the aqueous layer was extracted with EtOAc (2 x 6 mL), the organic layers were combined and dried over $MgSO_4$, before being concentrated *in vacuo*. The residue was then purified through silica giving the titled compound (102 mgs, 87 % yield) as a colourless oil.

**$^{1}$H NMR (400 MHz, cdcl3) δ** 7.19 – 7.04 (m, 7H), 6.92 – 6.83 (m, 1H), 6.82 – 6.69 (m, 3H), 6.56 – 6.52 (m, 1H), 6.48 – 6.44 (m, 1H), 4.96 (s, 0.5H), 4.70 (s, 0.5H), 4.54 – 3.77 (m, 5H), 2.52 – 2.42 (m, 2H), 1.49 – 1.34 (m, 6H), 0.92 (t, J = 7.4 Hz, 3H).

**$^{13}$C NMR (101 MHz, cdcl$_3$) δ** 157.20, 156.37, 154.22, 153.41, 142.53, 141.20, 141.16, 137.63, 137.61, 136.69, 136.33, 136.23, 135.89, 132.09, 131.92, 130.76, 130.59, 129.67, 127.83, 127.81, 125.92, 114.93, 114.23, 114.04, 113.29, 109.79, 109.69, 74.03, 73.98, 68.71, 68.42, 66.89, 66.80, 29.01, 29.00, 26.79, 26.73, 25.37, 25.34, 13.59.

** due to the fact that the double bond is a 1:1 mixture of cis and trans isomers, and also the fact that the glycidol used was racemic, there are more carbons than expected. This is due to diastereomers.

**IR (film):** 3400, 2920, 2851, 1722, 1673, 1598, 1496, 1273 $cm^{-1}$

**HRMS (ESI):** m/z (M+H) calculated for $C_{28}H_{30}O_4$: 430.2144; found: 430.2143.

**1-(4-(benzyloxy)-3-methoxyphenyl)-2-(4-(1-(4-((2,2-dimethyl-1,3-dioxolan-4-yl)methoxy)phenyl)-2-phenylbut-1-en-1-yl)phenoxy)ethan-1-one, (5-50)**

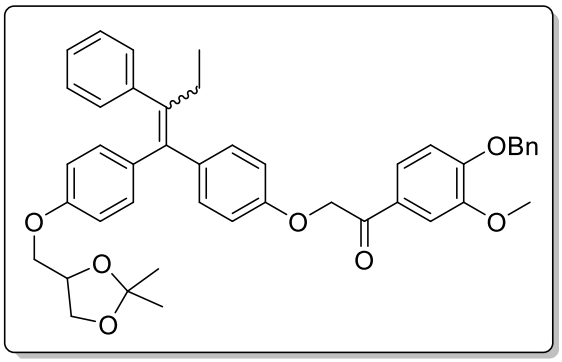


To a stirred solution of **5-49** (500 mg, 1.16 mmol, 1 eq.) in acetone (15 mL) was added $K_2CO_3$ (321 mg, 2.32 mmol, 2 eq.) added followed by alpha bromo ketone **5-8a** (582 mg, 1.74 mmol, 1.5 eq.) where it was left to stir overnight at room temperature. The following morning, the solvent was removed *in vacuo*, where it was then diluted with EtOAc (50 mL) and water (30 mL). The phases were separated, and the aqueous layer was extracted with EtOAc (2 x 20 mL), the organic layers were combined and dried over $MgSO_4$, before being concentrated *in vacuo*. The residue was then purified through silica giving the titled compound (737 mg, 92.7 % yield) as a colourless oil.

**$^1$H NMR (400 MHz, cdcl$_3$) δ** 7.61 – 7.27 (m, 7H), 7.19 – 6.84 (m, 10H), 6.78 – 6.71 (m, 2H), 6.59 – 6.50 (m, 2H), 5.30 – 5.05 (m, 4H), 4.53 – 4.34 (m, 1H), 4.22 – 4.02 (m, 1H), 3.99 – 3.86 (m, 5jH), 3.85 – 3.74 (m, 1H), 2.46 (q, J = 7.5 Hz, 2H), 1.49 – 1.34 (m, 6H), 0.91 (td, *J* = 7.3, 1.0 Hz, 3H).

**$^{13}$C NMR (101 MHz, cdcl$_3$) δ** 193.25, 193.20, 157.39, 156.98, 156.55, 156.15, 153.18, 153.05, 149.91, 149.82, 142.62, 142.58, 141.53, 141.48, 137.66, 137.23, 136.76, 136.73, 136.26, 136.23, 132.10, 132.07, 130.78, 130.75, 129.80, 128.86, 128.84, 128.32, 128.30, 128.13, 128.12, 127.98, 127.31, 127.30, 126.09, 122.75, 122.68, 114.53, 114.20, 113.79, 113.45, 112.38, 112.32, 110.94, 110.91, 109.88, 109.78, 74.17, 74.12, 70.98, 70.95, 70.91, 70.78, 68.89, 68.60, 67.06, 66.97, 56.27, 56.23, 29.19, 29.14, 26.98, 26.89, 25.52, 25.50, 13.74, 13.73.

** due to the fact that the double bond is a 1:1 mixture of cis and trans isomers, and also the fact that the glycidol used was racemic, there are more carbons than expected. This is due to diastereomers.**

**UPLC-MS**: 685.9 (M+H)

**1-(4-(benzyloxy)-3-methoxyphenyl)-2-(4-(1-(4-(2,3-dihydroxypropoxy)phenyl)-2-phenylbut-1-en-1-yl)phenoxy)ethan-1-one, (5-51)**

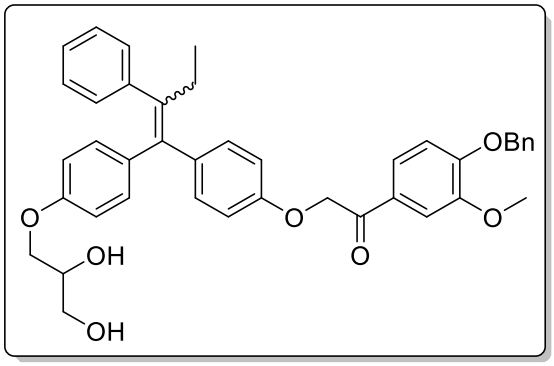


To a stirred solution of **5-50** above (634 mg, 1.09 mmol) was dissolved in 6:1 THF:water (20 mL) where 2M HCl (2 mL) was added at room temperature. The reaction was followed by TLC and upon consumption of all the SM, was quenched with 10% $NaHCO_3$ (10 mL). The reaction mixture was diluted with EtOAc and the phases were separated, the aqueous phase was extracted with EtOAc (5 mL) and chloroform (5 mL). The combined organic extracts were dried over $MgSO_4$, before being concentrated *in vacuo*. The residue was then purified through silica (MeOH/DCM) giving the titled compound (527 mg, 89 % yield) as a colourless oil.

**$^1$H NMR (400 MHz, cdcl$_3$) δ** 7.61 – 7.30 (m, 7H), 7.19 – 7.05 (m, 7H), 6.95 – 6.85 (m, 3H), 6.79 – 6.72 (m, 2H), 6.59 – 6.51 (m, 2H), 5.26 – 5.02 (m, 4H), 4.23 – 3.53 (m, 8H), 2.50 – 2.40 (m, 2H), 0.91 (td, *J* = 7.3, 1.1 Hz, 3H).

**2-(4-(1-(4-(2-(4-(benzyloxy)-3-methoxyphenyl)-2-oxoethoxy)phenyl)-2-phenylbut-1-en-1-yl)phenoxy)acetaldehyde, (5-52)**

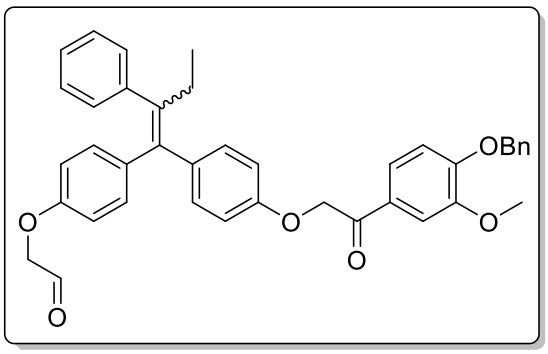


To a stirred solution of diol above (250 mg, 0.388 mmol) in DCM (7 mL) was added $NaIO_4$ (249 mgs, 1.16 mmol, 3 eq.) in water (2 mL) at room temperature. The reaction was stirred vigorously for 3 hours where most of the starting material had been consumed. It was diluted with brine (4 mL) before the phases were separated. The organic phase was dried ($MgSO_4$), and the solvent was removed *in vacuo*, before being purified by flash column chromatography giving the titled compound as a colourless oil (155 mgs, 63 % yield).

**$^1$H NMR (400 MHz, cdcl$_3$) δ** 9.88 (br s, 0.5H), 9.77 (br s, 0.5H), 7.62 – 7.28 (m, 7H), 7.20 – 7.05 (m, 7H), 6.94 – 6.84 (m, 3H), 6.81 – 6.70 (m, 2H), 6.60 – 6.49 (m, 2H), 5.33 – 4.98 (m, 4H), 3.93 (d, *J* = 14.5 Hz, 4H), 2.51 – 2.38 (m, 2H), 0.92 (dt, *J* = 8.5, 4.2 Hz, 3H).

**1-(4-(benzyloxy)-3-methoxyphenyl)-2-(4-(1-(4-(2-(dimethylamino)ethoxy)phenyl)-2-phenylbut-1-en-1-yl)phenoxy)ethan-1-one (5-54)**

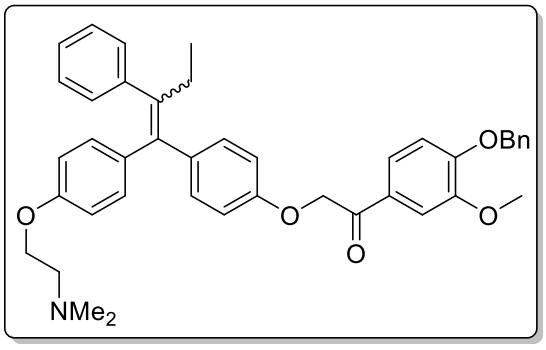


To a stirred solution of **5-52** (143 mg, 0.233 mmol, 1 eq.) in THF (5 mL) under $N_2$ was added a 2M solution of dimethylamine in THF (0.175 mL, 0.350 mmol, 1.5 eq.) at room temperature, followed by $Na(AcO)_3BH$ (75 mg, 0.700 mmol, 3 eq.) portionwise. The reaction was left to react for 5 hours, at which point no SM was visible by TLC. The reaction mixture was then diluted with brine (3 mL) and EtOAc (10 mL) and the phases were separated after stirring for 15 minutes. The aqueous phase was extracted with EtOAc (2 x 10 mL) and chloroform (1 x 10 mL), the organic extracts were combined, dried ($MgSO_4$) and the solvent removed *in vacuo*. The residue was purified by flash column chromatography (DCM/MeOH – 0-15 %) giving the titled compound as a thick oil (93 mgs, 62 % yield)

**$^1$H NMR (400 MHz, cdcl$_3$) δ** 7.62 – 7.55 (m, 1H), 7.55 – 7.48 (m, 1H), 7.46 – 7.28 (m, 5H), 7.21 – 7.06 (m, 7H), 6.94 – 6.81 (m, 3H), 6.78 – 6.71 (m, 2H), 6.59 – 6.45 (m, 2H), 5.24 (s, 1H), 5.22 (s, 2H), 5.06 (s, 1H), 4.26 (t, *J* = 5.1 Hz, 1H), 4.11 – 4.07 (m, 1H), 3.95 (s, 1.5H), 3.91 (s, 1.5H), 3.11 (dt, *J* = 36.9, 4.3 Hz, 2H), 2.63 (s, 3H), 2.57 (s, 3H), 2.46 (q, *J* = 6.7 Hz, 2H), 0.91 (td, *J* = 7.4, 1.8 Hz, 3H).

**2-(4-(1-(4-(2-(dimethylamino)ethoxy)phenyl)-2-phenylbut-1-en-1-yl)phenoxy)-1-(4-hydroxy-3-methoxyphenyl)ethan-1-one, (5-2)**

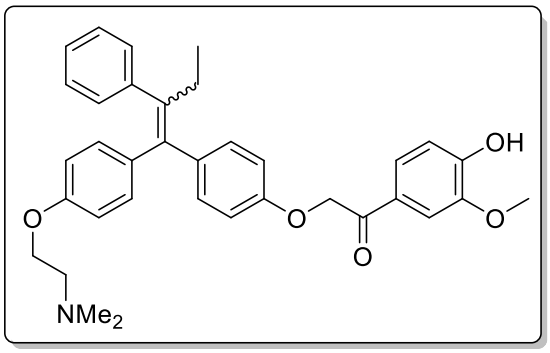


To a stirred solution of **5-54** (94 mg, 0.146 mmol) in degassed 10% MeOH/EtOAc (12 mL) was added Pd/C (9 mg) at room temperature. The $N_2$ atmosphere was replaced with a $H_2$ atmosphere in 3 cycles with a balloon of $H_2$ and vacuum. The reaction was followed by TLC and as the SM had been consumed, the atmosphere was replaced with $N_2$ and left to purge for 5 minutes. The reaction mixture was filtered through celite and the solvent removed *in vacuo*. The residue was purified by flash column chromatography (DCM/MeOH – gradient) giving the titled compound as a thick oil (74 mg, 92 % yield)

**$^1$H NMR (400 MHz, cdcl$_3$) δ** 7.65 – 7.58 (m, 1H), 7.55 – 7.50 (m, 1H), 7.17 – 7.05 (m, 7H), 7.00 – 6.86 (m, 3H), 6.79 – 6.71 (m, 2H), 6.59 – 6.51 (m, 2H), 5.23 (s, 1H), 5.07 (s, 1H), 4.14 (t, *J* = 5.6 Hz, 1H), 4.01 – 3.93 (m, 4H), 2.86 (t, *J* = 5.6 Hz, 1H), 2.77 (t, *J* = 5.4 Hz, 1H), 2.50 – 2.40 (m, 5H), 2.38 (s, 3H), 0.91 (td, *J* = 7.4, 2.0 Hz, 3H).

A 1:1 mixture of cis and trans isomers of **5-51** were separated following optimisation of the reverse phase HPLC conditions on an analytical scale, and then transferring this to a preparative scale. In total, approximately 250 mg were injected into the HPLC, with a total recovery of 94 mg for the first peak, and 110 mg for the second. This gave isomerically pure compounds as described below.

**(*Z*)-1-(4-(benzyloxy)-3-methoxyphenyl)-2-(4-(1-(4-(2,3-dihydroxypropoxy)phenyl)-2-phenylbut-1-en-1-yl)phenoxy)ethan-1-one, - Peak 1, (*Z*)-5-51**

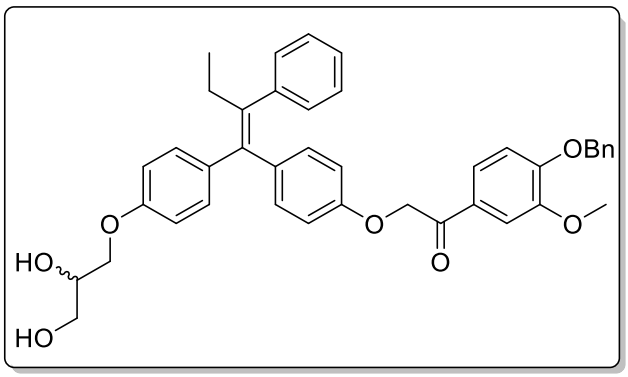


**$^{1}$H NMR (400 MHz, cdcl$_3$) δ** 7.55 – 7.45 (m, 2H), 7.45 – 7.28 (m, 5H), 7.19 – 7.11 (m, 4H), 7.11 – 7.02 (m, 3H), 6.93 – 6.81 (m, 3H), 6.79 – 6.70 (m, 2H), 6.63 – 6.52 (m, 2H), 5.22 (s, 2H), 5.06 (s, 2H), 4.10 – 4.03 (m, 3H), 3.91 (s, 3H), 3.88 – 3.69 (m, 2H), 2.46 (q, *J* = 7.4 Hz, 2H), 0.91 (t, *J* = 7.4 Hz, 3H).

**$^{13}$C NMR (101 MHz, cdcl$_3$) δ** 193.16, 157.14, 156.00, 152.98, 149.67, 142.41, 141.46, 137.48, 136.73, 136.61, 136.07, 131.97, 130.68, 129.66, 128.71, 128.18, 127.20, 126.01, 122.57, 114.12, 113.69, 112.19, 110.74, 70.81, 70.55, 70.44, 69.08, 63.69, 56.08, 29.70, 29.07, 13.61.

**(*E*)-1-(4-(benzyloxy)-3-methoxyphenyl)-2-(4-(1-(4-(2,3-dihydroxypropoxy)phenyl)-2-phenylbut-1-en-1-yl)phenoxy)ethan-1-one, - Peak 2, (*E*)-5-51**

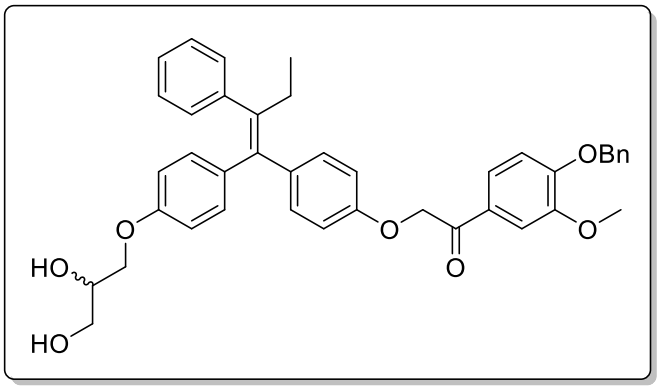


**$^{1}$H NMR (400 MHz, cdcl$_3$) δ** 7.63 – 7.52 (m, 2H), 7.47 – 7.28 (m, 5H), 7.19 – 7.04 (m, 7H), 6.91 (dd, *J* = 8.6, 6.3 Hz, 3H), 6.81 – 6.71 (m, 2H), 6.59 – 6.47 (m, 2H), 5.24 (s, 2H), 5.22 (s, 2H), 3.99 (dt, *J* = 8.0, 4.0 Hz, 1H), 3.94 (s, 3H), 3.91 – 3.80 (m, 2H), 3.70 (ddd, *J* = 16.9, 11.4, 4.4 Hz, 2H), 2.48 (q, *J* = 7.4 Hz, 2H), 0.92 (t, *J* = 7.4 Hz, 3H).

**$^{13}$C NMR (101 MHz, cdcl$_3$) δ** 193.26, 156.95, 156.36, 153.16, 149.86, 142.55, 141.55, 137.56, 137.16, 136.41, 136.17, 132.10, 130.74, 129.76, 128.82, 128.29, 128.03, 127.96, 127.29, 126.09, 122.72, 114.52, 113.43, 112.35, 110.88, 70.94, 70.81, 70.41, 68.97, 63.71, 56.22, 29.12, 13.71.

**(*Z*)-1-(4-(benzyloxy)-3-methoxyphenyl)-2-(4-(1-(4-(2-(dimethylamino)ethoxy)phenyl)-2-phenylbut-1-en-1-yl)phenoxy)ethan-1-one, - Peak 1, (*Z*)-5-53**

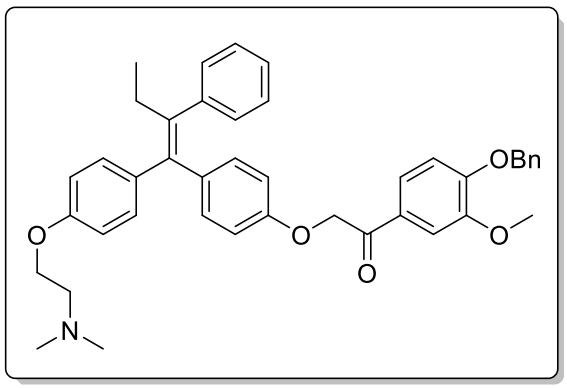


To a stirred solution of **(*Z*)-5-51** (93.7 mg, 0.1453 mmol) in THF:water 2:1 (2 mL) was added $NaIO_4$ (46.6 mg, 0.217 mmol, 1.5 eq.) at room temperature. The reaction was stirred for 3 hours where most of the starting material had been consumed. It was diluted with EtOAc (5 mL) before the phases were separated, and the aqueous phase extracted with EtOAc (3 x 5 mL). The organic phase was dried ($MgSO_4$), and the solvent was removed *in vacuo*. The residue was used without any further purification.

To a stirred solution of the crude aldehyde from the unpurified crude reaction mixture in THF (3 mL) under $N_2$ was added a 2M solution of dimethylamine in THF (110 µL, 0.218 mmol, 1.5 eq.) at room temperature, followed by $NaHBH_3$ (92 mg, 0.436 mmol, 3 eq.) portionwise. The reaction was left to react for 5 hours, at which point no SM was visible by TLC. The reaction mixture was then diluted with brine (2 mL) and EtOAc (3 mL), the phases were separated after stirring for 15 minutes. The aqueous phase was extracted with EtOAc (3 x 5 mL) and chloroform (1 x 5 mL), the organic extracts were combined, dried ($MgSO_4$) and the solvent removed *in vacuo*. The residue was purified by flash column chromatography (DCM/MeOH – gradient) giving the titled compound as a thick oil (75 mg, 80 % yield).

**$^1$H NMR (400 MHz, cdcl3)** δ 7.56 – 7.47 (m, 2H), 7.46 – 7.28 (m, 5H), 7.20 – 7.05 (m, 7H), 6.87 (d, J = 8.5 Hz, 3H), 6.80 – 6.70 (m, 2H), 6.60 – 6.51 (m, 2H), 5.22 (s, 2H), 5.06 (s, 2H), 4.20 (t, J = 5.3 Hz, 2H), 3.91 (s, 3H), 2.98 (t, J = 5.2 Hz, 2H), 2.57 – 2.41 (m, 8H), 0.92 (t, J = 7.4 Hz, 3H).

**$^{13}$C NMR (101 MHz, cdcl3) δ** 193.18, 157.12, 156.13, 153.05, 149.79, 142.55, 141.52, 137.62, 136.73, 136.70, 136.20, 132.08, 130.76, 129.77, 128.82, 128.28, 128.08, 127.96, 127.28, 126.08, 122.66, 114.18, 113.77, 112.30, 110.87, 70.92, 70.74, 64.91, 57.46, 56.20, 44.90, 29.16, 13.71.

**(*E*)-1-(4-(benzyloxy)-3-methoxyphenyl)-2-(4-(1-(4-(2-(dimethylamino)ethoxy)phenyl)-2-phenylbut-1-en-1-yl)phenoxy)ethan-1-one, - Peak 2, (*E*)-5-53**

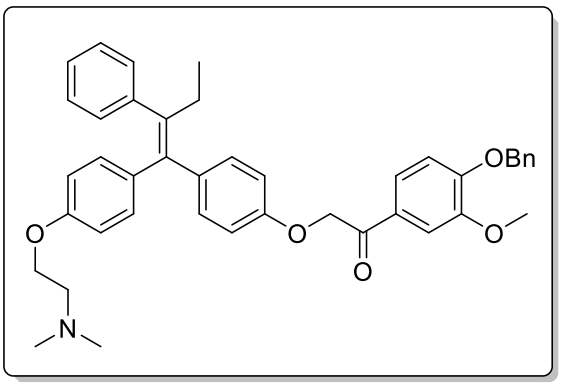


To a stirred solution of **(*E*)-5-51** (109.4 mg, 0.1696 mmol) in THF:water 2:1 (2 mL) was added $NaIO_4$ (54.4 mg, 0.255 mmol, 1.5 eq.) at room temperature. The reaction was stirred for 3 hours where most of the starting material had been consumed. It was diluted with EtOAc (5 mL) before the phases were separated, and the aqueous phase extracted with EtOAc (3 x 5 mL). The organic phase was dried ($MgSO_4$), and the solvent was removed *in vacuo*. The residue was used without any further purification.

To a stirred solution of the crude aldehyde from the unpurified crude reaction mixture in THF (3 mL) under $N_2$ was added a 2M solution of dimethylamine in THF (127 µL, 0.254 mmol, 1.5 eq.) at room temperature, followed by $NaHBH_3$ (107.8 mg, 0.508 mmol, 3 eq.) portionwise. The reaction was left to react for 5 hours, at which point no SM was visible by TLC. The reaction mixture was then diluted with brine (2 mL) and EtOAc (3 mL), the phases were separated after stirring for 15 minutes. The aqueous phase was extracted with EtOAc (3 x 5 mL) and chloroform (1 x 5 mL), the organic extracts were combined, dried ($MgSO_4$) and the solvent removed *in vacuo*. The residue was purified by flash column chromatography (DCM/MeOH – gradient) giving the titled compound as a thick oil (83 mg, 76 % yield).

**$^1$H NMR (400 MHz, cdcl3) δ** 7.62 – 7.56 (m, 2H), 7.47 – 7.28 (m, 5H), 7.20 – 7.03 (m, 7H), 6.91 (t, J = 8.5 Hz, 3H), 6.76 (d, J = 8.7 Hz, 2H), 6.53 (d, J = 8.7 Hz, 2H), 5.24 (s, 2H), 5.22 (s, 2H), 4.05 (t, J = 5.3 Hz, 2H), 3.94 (s, 3H), 2.91 (t, J = 5.2 Hz, 2H), 2.46 (s, 6H), 0.91 (t, J = 7.4 Hz, 3H).

**$^{13}$C NMR (101 MHz, cdcl3) δ** 193.21, 156.95, 156.19, 153.14, 149.86, 142.54, 141.48, 137.58, 137.17, 136.29, 136.18, 132.07, 130.73, 129.75, 128.81, 128.28, 128.06, 127.95, 127.28, 126.07, 122.71, 114.50, 113.41, 112.35, 110.88, 70.93, 70.84, 64.46, 57.21, 56.22, 44.65, 29.10, 13.70.

**(Z)-2-(4-(1-(4-(2-(dimethylamino)ethoxy)phenyl)-2-phenylbut-1-en-1-yl)phenoxy)-1-(4-hydroxy-3-methoxyphenyl)ethan-1-one, - Peak 1, (*Z*)-5-3**

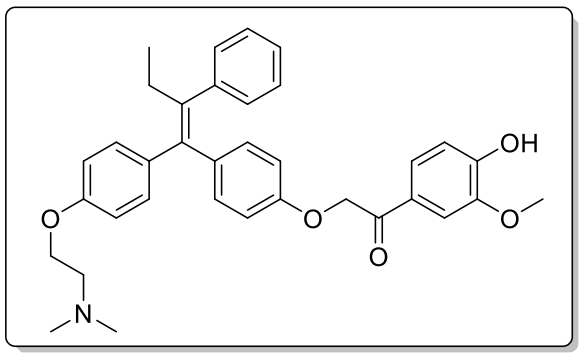


To a stirred solution of **(*Z*)-5-53** (50 mg, 0.078 mmol) in degassed 10% MeOH/EtOAc was added Pd/C (5 mgs, 10% wt.) at room temperature. The $N_2$ atmosphere was replaced with a $H_2$ atmosphere in 3 cycles with a balloon of $H_2$ and vacuum. The reaction was followed by TLC and as the SM had been consumed, the atmosphere was replaced with $N_2$ and left to purge for 5 minutes. The reaction mixture was filtered through celite and the solvent removed *in vacuo*. The residue was purified by flash column chromatography (DCM/MeOH – gradient) giving the titled compound as a thick oil (36.1 mg, 84% yield).

**$^1$H NMR (400 MHz, cdcl3) δ** 7.65 – 7.51 (m, 1H), 7.19 – 7.05 (m, 2H), 6.97 – 6.84 (m, 1H), 6.78 – 6.69 (m, 1H), 6.56 – 6.44 (m, 1H), 5.23 (s, 1H), 3.96 (t, J = 5.7 Hz, 1H), 3.92 (s, 1H), 2.72 (t, J = 5.7 Hz, 1H), 2.46 (q, J = 7.4 Hz, 1H), 2.34 (s, 2H), 0.91 (t, J = 7.4 Hz, 1H).

**$^{13}$C NMR (101 MHz, cdcl3) δ** 193.12, 157.00, 156.66, 151.76, 147.35, 142.65, 141.36, 137.73, 137.26, 135.99, 132.03, 130.77, 129.81, 127.95, 127.35, 126.05, 123.56, 114.53, 114.50, 113.44, 110.34, 70.85, 65.38, 58.04, 56.19, 45.62, 29.13, 13.74.

**(*E*)-2-(4-(1-(4-(2-(dimethylamino)ethoxy)phenyl)-2-phenylbut-1-en-1-yl)phenoxy)-1-(4-hydroxy-3-methoxyphenyl)ethan-1-one, Peak 1, (*E*)-5-3**

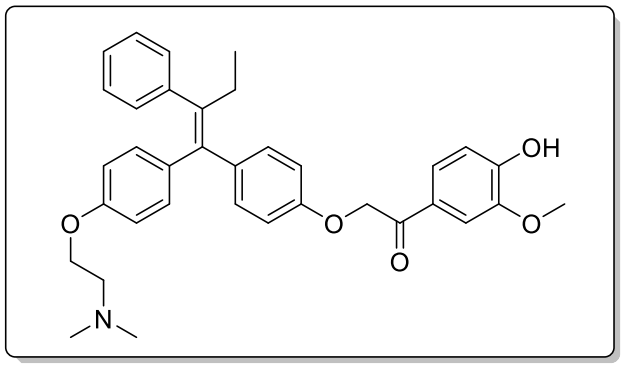


To a stirred solution of **(*E*)-5-53** (50 mg, 0.078 mmol) in degassed 10% MeOH/EtOAc was added Pd/C (5 mg, 10% wt.) at room temperature. The $N_2$ atmosphere was replaced with a $H_2$ atmosphere in 3 cycles with a balloon of $H_2$ and vacuum. The reaction was followed by TLC and as the SM had been consumed, the atmosphere was replaced with $N_2$ and left to purge for 5 minutes. The reaction mixture was filtered through celite and the

solvent removed *in vacuo*. The residue was purified by flash column chromatography (DCM/MeOH – gradient) giving the titled compound as a thick oil (37.7 mg, 92% yield)

**1H NMR (400 MHz, cdcl3) δ** 7.54 – 7.47 (m, 1H), 7.18 – 7.04 (m, 7H), 6.96 – 6.82 (m, 4H), 6.79 – 6.70 (m, 2H), 6.61 – 6.48 (m, 2H), 5.07 (s, 2H), 4.11 (t, J = 5.7 Hz, 2H), 3.91 (s, 3H), 2.81 (t, J = 5.7 Hz, 2H), 2.46 (q, J = 7.4 Hz, 2H), 2.39 (s, 6H), 0.91 (t, J = 7.4 Hz, 3H).

# Methods - Biological assays

## Cell culture

HEK293T and LS174T cells were purchased from the ATCC and cultured in DMEM supplemented with L-glutamine and 10% fetal bovine serum (Life Technologies) at 37ºC and 5% CO2. Mouse embryonic fibroblasts were harvested from 14 day-old embryos. Briefly, pregnant females were sacrificed 14 days after plug formation, uteri were removed, and embryos were dissected: heads and fetal livers were discarded. The rest was minced and digested with trypsin and grown in 10-cm plates with aforementioned supplemented DMEM.

## Luciferase assay

HEK293T cells were seeded in 24-well plates and transfected with plasmids encoding 12xCAGA-Firefly_Luc and Tk-Renilla_Luc (75 and 10 ng per well, respectively), using polyethylenimine (Polysciences) as transfection reagent. After 7h, medium was replaced for starvation medium (DMEM + 0.05% FBS). The next day, cells were treated with compounds from a 10 mM stock solution in DMSO, diluted between 103 and 108 times (as indicated), as well as 5 ng/ml recombinant human TGFB1. Luciferase activity was measured 16h later using the Dual Luciferase Assay kit (Promega): media were aspirated and cells were lysed in 200 µl passive lysis buffer (kit) for 20 minutes. Bioluminescence was measured in a Berthold Lumat LB6507 luminometer (18 µl reagents, 10 seconds measurements).

## Mice and mouse tumour organoids

All experiments with mouse models were performed in the Batlle lab and approved by the Animal Care and Use Committee of Barcelona Science Park (CEEA-PCB) and the Catalan government. Mice are maintained in specific-pathogen-free (SPF) facility with a 12-hour light-dark cycle and fed with standard diet and water ad lib. All mice were closely monitored for animal welfare.

UbC-CreERT2 (B6.Cg-Tg(UBC-cre/ERT2)1Ejb/2J; Stock 008085) and Rosa26mTmG (B6.129(Cg)-Gt(ROSA)26Sortm4 (ACTB-tdTomato,-EGFP)Luo/J; Stock 007676) mice were described before.[41][42]

The latter allele allowed us to detect recombination by the shift from tdTomato to EGFP expression upon Cre activation with Z-4-OHT. These mice were used to derive MEFs (see above).

Mouse tumour organoids (MTOs) are derived from genetic mice and cultured as described in Tauriello 2018. Briefly, organoids are tumour epithelial cells grown in a 3D matrix where they adopt an organotypic architecture, typically as spheroids with a lumen. In this way, cells retaining a somewhat normal polarity (which means that the outside surface, inside/luminal surface and cell-cell contacts are individually specialized for their tasks), that is more physiological than in conventional 2D cell culture. As they were derived from the same strain of mice as the hosts that were used for tumour implantation (see below), these are not rejected by the mouse's immune system. Moreover, these organoids are capable of recreating a complex tumour architecture that recapitulates human cancers, including the recruitment of a rich and pro-tumorigenic (i.e. TGF-β rich) stroma; such a sophisticated system to transplant humanlike tumours, and study liver metastasis, was not previously described.

## Mouse injections and treatments

For TGF-β inhibitor studies, C57BL/6J animals were purchased from Janvier at 6 weeks of age and injected at 7-8 weeks. For transplantation of MTOs into the liver, cells were trypsinized (digesting the matrix and disaggregating organoids into single cells), counted and 300,000 cells were injected in HBSS (Hank's Balanced Salt Solution, Lonza) into the spleen, thus delivering the cells directly into the portal vein that connects the intestine to the liver. MTOs expressing a luciferase reporter were measured by bioluminescence imaging, using retroorbital injection of 50 µl 15 mg/ml D-luciferin potassium salt (Resem BV). Photons per second from the region spanning thorax/abdomen were quantified and normalized to the measure at the day of injection.

Treatment with compounds occurred by gavage (tube feeding) with a suspension of between 4 and 120 mg/ml in a 1% sodium carboxymethylcellulose (Sigma), 0.4% sodium dodecyl sulfate (Sigma), 0.085% polyvinylpyrrolidone, 0.05% antifoam-A (Sigma) in milli-Q water. Mice were treated twice a day with 150 µl for 14 days or until endpoint. Liver tumours (LiMs) were counted by eye on fixed livers.

For the assessment of toxicity, intestines, skin samples, hearts, thoracic skeletons and limbs were

fixed in 10% formalin, phosphate buffered (Sigma). Soft tissues were embedded in paraffin blocks, sectioned and stained with haematoxylin & eosin. Bones were first decalcified for 2 weeks before embedding, sectioning and staining. An experienced pathology (Neus Prats) analysed tissues for histopathological abnormalities. The macroscopically obvious pectus excavatum phenotype (caved in sternum) was found to associate to defects in the sternocostal cartilage areas (between sternum bones and ribs). Furthermore, the cartilage ossification zone at the ends of the long bones was analysed for defects in the hypertrophic zone.

## LigF enzymatic assays

For in vitro fluorescence assays, purified LigF was diluted to 15 µg/ml in 20 mM Tris-HCl (pH 7.5), 1 mM glutathione and 30 µM MUAV model compound was added. Reactions were performed in a 96-well solid polystyrene plate (Corning) and measured with a top-well plate reader (BioTek FL600 fluorometer) at 360 exitation, 485 emission and sensitivity 100.

For assays in cell culture, cells were stably transduced to express LigF by lentiviral infection with pLenti PGK puro vector and packaging plasmids pCAG-RTR2, pCAG-VSVG and pCAG-KGP1R. After selection with 1 µg/ml puromycin (InvivoGen), infected cells were seeded into 24-well plates, and 4-methylumbelliferone acetovanillone (MUAV) was added. At time points after addition, culture medium was taken for measurements of 4-MU fluorescence as described above.

## LC-MS/MS analysis of LigF reactions

For in vitro enzymatic assays with guaymoxifen (5-3), the compound was diluted from a 30 mM stock solution in DMSO to 50 µM in 20 mM Tris-HCl (pH 7.5), 1 mM glutathione and 15 µg/ml LigF was added. Reaction samples, as well as a sample before enzyme addition and putative product Z-4-OHT were diluted 2:3 in MeOH and 2 µl was injected onto a BioBasic C18 column (5 µm, 2.1x150 mm, Thermo; using a Thermo EC Finnigan Mod Micro AS autosamples and Thermo EC Quarternary pump, Finnigan Mod. Surveyor MS chromatograph) with a water-MeOH gradient (60-90% MeOH in 30 min; 90-100% in 5 min; 100 µl/min flow rate). LC-MS coupling was performed with the Advion Triversa Nanomate (Advion BioSciences, Ithaca, NY, USA) as the nanoESI source performing nanoelectrospray through chip technology. The Nanomate was attached to an LTQ-FT Ultra mass spectrometer and

operated at a spray voltage of 1.7 kV and a delivery pressure of 0.5 psi in positive mode. In a LTQ-FT Ultra (Thermo Scientif) mass spectrometer, analyses were performed using 40V capillary voltage and 120V tube lens voltage. MS was operated in a data-dependent acquisition (DDA) mode and in selected reaction monitoring (SRM) mode. Survey MS scans were acquired in the FT with the resolution (defined at 400 m/z) set to 100,000. Up to six of the most intense ions per scan were fragmented and detected in the linear ion trap. The ion count target value was 1,000,000 for the survey scan and 50,000 for the MS/MS scan. Target ions already selected for MS/MS were dynamically excluded for 30 s. For SRM, maximum injective was set to 400 ms and 2 microscans average.

Data are represented as XIC (extracted ion chromatogram) peak areas of parallel reaction monitoring (PRM) transitions, using QuanBrowser (Xcalibur software 2.0SR2). In figure XX, all peak areas were combined and the relative peak area is plotted.

## Cellular co-culture assays

MEF recombination: MTOs transduced with pLenti PGK-LigF (puro) or with an equivalent empty vector were trypsinized and single cells added onto Ub-creERT2; R26-mTmG MEFs grown in 12-well plates. The next day, either Z-4-OHT or guaymoxifen was added in concentrations ranging from 1000 to 1 nM. Two days later, cells were trypsinized and analysed by flow cytometry for TdTomato/EGFP fluorescence (Gallios, Beckman Coulter). Fluorescence was analysed on viable cells in 2 dimensions and scored as percentages in the 4 quadrants. EGFP positive quadrants (Q2 and Q4, with or without TdTomato) were considered recombined and the fraction of the total was calculated. Data are the average (+SD) from two independent experiments.

Wnt-OFF reporter: HEK293T cells transduced with pLenti PGK-LigF (puro) or with an equivalent empty vector were co-plated with LS174T-NTCF4-ERT2 (LS-NE) cells (described in Whissel 2014 Nat Cell Biol), in a ratio of 1/10 in 6-well plates. Co-cultures were treated with DMSO, 1 µM Z-4-OHT or guaymoxifen 1 or 10 µM. After 16h, cells were lysed in trizol for RNA extraction (PureLink RNA Mini Kit, Life Technologies) and cDNA preparation (High Capacity cDNA RT kit, Applied Biosysytems). Stem cell gene ASCL2 (repressed by 4-OHT-mediated Wnt-OFF; Hs_00270888_S1), differentiation gene KRT20 (activated by 4-OHT-mediated Wnt-OFF; Hs_00300643_m1) and housekeeping gene PPIA

(Hs_99999904_m1) were analysed by RT-qPCR using Taqman probes (Applied Biosystems) on a StepOnePlus Real-Time PCR system (Applied Biosystems). Data were normalized to DMSO controls. Data are the average of technical replicates (+SD) from a single experiment.

[1] G. R. Fulmer, A. J. M. Miller, N. H. Sherden, H. E. Gottlieb, A. Nudelman, B. M. Stoltz, J. E. Bercaw, K. I. Goldberg, *Organometallics* **2010**, *29*, 2176–2179.

[2] U. Mundla, Sreenivasa Reddy (Eli Lilly and company), *A Pyridin Quinolin Substituted Pyrrolo[1, 2-B] Pyrazole Monohydrate as a TGF- Beta Inhibitor*, **2007**.

[3] E. C. Taylor, N. F. Haley, R. J. Clemens, *J. Am. Chem. Soc.* **1981**, *103*, 7743–7752.

[4] K. De, J. Legros, B. Crousse, D. Bonnet-Delpon, *J. Org. Chem.* **2009**, *74*, 6260–6265.

[5] J. S. Sawyer, D. W. Beight, P. Ciapetti, T. V Decollo, A. G. Godfrey, T. Goodson, D. K. Herron, H. Y. Li, J. Liao, W. T. Mcmillen, et al., *Novel Pyrole Derivatives As Pharmaceutical Agents*, **2002**.

[6] I. S. Cho, L. Gong, J. M. Muchowski, *J. Org. Chem.* **1991**, *56*, 7288–7291.

[7] H.-Y. Li, W. T. McMillen, C. R. Heap, D. J. McCann, L. Yan, R. M. Campbell, S. R. Mundla, C.-H. R. King, E. a Dierks, B. D. Anderson, et al., *J. Med. Chem.* **2008**, *51*, 2302–6.

[8] C. Miesch, T. Emrick, *J. Colloid Interface Sci.* **2014**, *425*, 152–8.

[9] E. Fuglseth, T. Anthonsen, B. H. Hoff, *Tetrahedron: Asymmetry* **2006**, *17*, 1290–1295.

[10] D. A. Weinstein, M. H. Gold, *Holzforschung* **1979**, *33*, 134–135.

[11] E. Masai, Y. Katayama, S. Kubota, S. Kawai, M. Yamasaki, N. Morohoshi, *FEBS Lett.* **1993**, *323*, 135–40.

[12] T. Kerl, F. Berger, H.-G. Schmalz, *Chemistry* **2016**, *22*, 2935–8.

[13] Y. Li, Y. Zhou, Q. Shi, K. Ding, R. Noyori, C. A. Sandoval, *Adv. Synth. Catal.* **2011**, *353*, 495–500.

[14] J. Barberá, R. Iglesias, J. L. Serrano, T. Sierra, M. R. de la Fuente, B. Palacios, M. A. Pérez-Jubindo, J. T. Vázquez, *J. Am. Chem. Soc.* **1998**, *120*, 2908–2918.

[15] A. Solladié-Cavallo, M.-C. Simon-Wermeister, D. Farkhani, *Helv. Chim. Acta* **1991**, *74*, 390–396.

[16] J. Geraint, *Anti-Inflammatory 1-Phenyl-2-Aminoethanol Derivatives, Pharmaceutical Compositions Thereof for Topical Use, and Processes of Their Manufacture.*, **1979**, 79300893.9.

[17] D. Brenna, M. Benaglia, R. Porta, S. Fernandes, A. J. Burke, *European J. Org. Chem.* **2017**, *2017*, 39–44.

[18] T. N. T. Nguyen, N. O. Thiel, F. Pape, J. F. Teichert, *Org. Lett.* **2016**, *18*, 2455–2458.

[19] R. S. Givens, K. Stensrud, P. G. Conrad, A. L. Yousef, C. Perera, S. N. Senadheera, D. Heger, J. Wirz, *Can. J. Chem.* **2011**, *89*, 364–384.

[20] S. Sakuraba, H. Takahashi, H. Takeda, K. Achiwa, *Chem. Pharm. Bull.* **1995**, *43*, 738–747.

[21] K. E. McCarthy, S. A. Miller, B. L. Chenard, T. W. Butler, M. L. Dumont, J. Z. Stemple, *J. Label. Compd. Radiopharm.* **1997**, *39*, 973–985.

[22] J. Teske, B. Plietker, *Org. Lett.* **2018**, *20*, 2257–2260.

[23] B. Rammurthy, P. Swamy, M. Naresh, K. Srujana, C. Durgaiah, G. Krishna Sai, N. Narender, *New J. Chem.* **2017**, *41*, 3710–3714.

[24] M. Weitman, L. Lerman, S. Cohen, A. Nudelman, D. T. Major, H. E. Gottlieb, *Tetrahedron* **2010**, *66*, 1465–1471.

[25] S. Kandil, A. D. Westwell, C. McGuigan, *Bioorg. Med. Chem. Lett.* **2016**, *26*, 2000–2004.

[26] Y. Sri Ranganath, V. Harinadha Babu, G. Sandeep, R. Parameshwar, *J. Chem. Pharm. Res.* **2011**, *3*, 62–68.

[27] Q. Zhang, X. Peng, M. Grilley, J. Y. Takemoto, C.-W. T. Chang, *Green Chem.* **2015**, *17*, 1918–1925.

[28] M. Akazawa, K. Uchida, J. J. D. de Jong, J. Areephong, M. Stuart, G. Caroli, W. R. Browne, B. L. Feringa, *Org. Biomol. Chem.* **2008**, *6*, 1544.

[29] M. Krause, X. Ligneau, H. Stark, M. Garbarg, J. C. Schwartz, W. Schunack, *J. Med. Chem.* **1998**, *41*, 4171–6.

[30] B. Schmidt, M. Riemer, U. Schilde, *European J. Org. Chem.* **2015**, *2015*, 7602–7611.

[31] P. E. Tessier, A. J. Penwell, F. E. S. Souza, A. G. Fallis, *Org. Lett.* **2003**, *5*, 2989–2992.

[32] X. Tan, L. Kong, H. Dai, X. Cheng, F. Liu, C. Tschierske, *Chemistry* **2013**, *19*, 16303–13.

[33] H. Gao, H. Cheng, Z. Yang, M. Prehm, X. Cheng, C. Tschierske, *J. Mater. Chem. C* **2015**, *3*, 1301–1308.

[34] J. Dansereau, S. Gautreau, A. Gagnon, *ChemistrySelect* **2017**, *2*, 2593–2599.

[35] X. Wang, M. Nakajima, E. Serrano, R. Martin, *J. Am. Chem. Soc.* **2016**, *138*, 15531–15534.

[36] L.-M. Zhao, H.-S. Jin, J. Liu, T. C. Skaar, J. Ipe, W. Lv, D. A. Flockhart, M. Cushman, *Bioorg. Med. Chem.* **2016**, *24*, 5400–5409.

[37] V. N. Korotchenko, A. V. Shastin, V. G. Nenajdenko, E. S. Balenkova, *J. Chem. Soc. Perkin Trans. 1* **2002**, *2*, 883–887.

[38] M. Shimizu, C. Nakamaki, K. Shimono, M. Schelper, T. Kurahashi, T. Hiyama, *J. Am. Chem. Soc.* **2005**, *127*, 12506–12507.

[39] D. D. Yu, B. M. Forman, *J. Org. Chem.* **2003**, *68*, 9489–91.

[40] L.-G. Milroy, B. Koning, D. S. V. Scheppingen, N. G. L. Jager, J. H. Beijnen, J. Koek, L. Brunsveld, *Bioorg. Med. Chem. Lett.* **2018**, *28*, 1352–1356.

[41] Y. Ruzankina, C. Pinzon-Guzman, A. Asare, T. Ong, L. Pontano, G. Cotsarelis, V. P. Zediak, M. Velez, A. Bhandoola, E. J. Brown, *Cell Stem Cell* **2007**, *1*, 113–126.

[42] M. D. Muzumdar, B. Tasic, K. Miyamichi, L. Li, L. Luo, *genesis* **2007**, *45*, 593–605.

# Chapter 8

# Selected Spectra

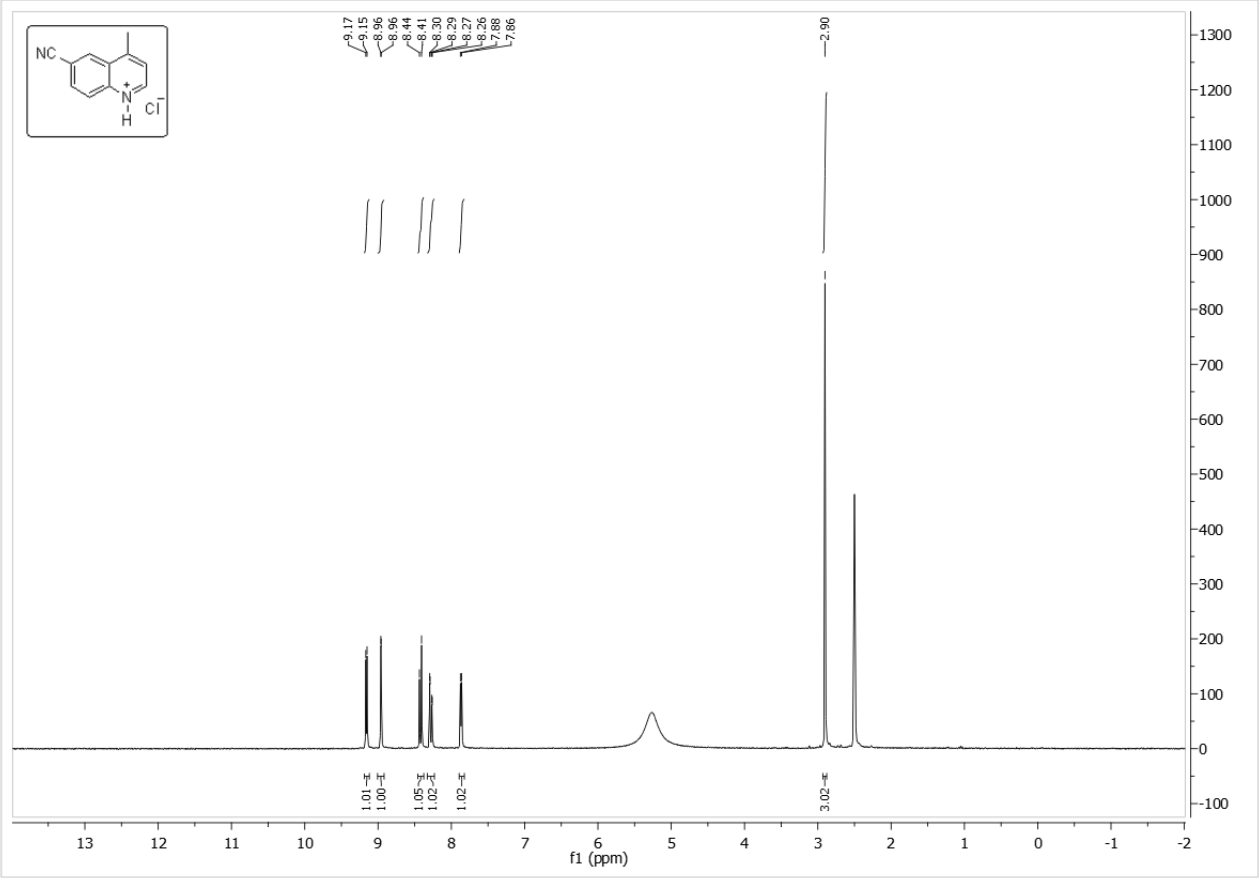
NC
N
H
Cl
9.17
9.15
8.96
8.96
8.44
8.41
8.30
8.29
8.27
8.26
7.88
7.86
2.90
1.01
1.00
1.05
1.02
1.02
3.02
f1 (ppm)

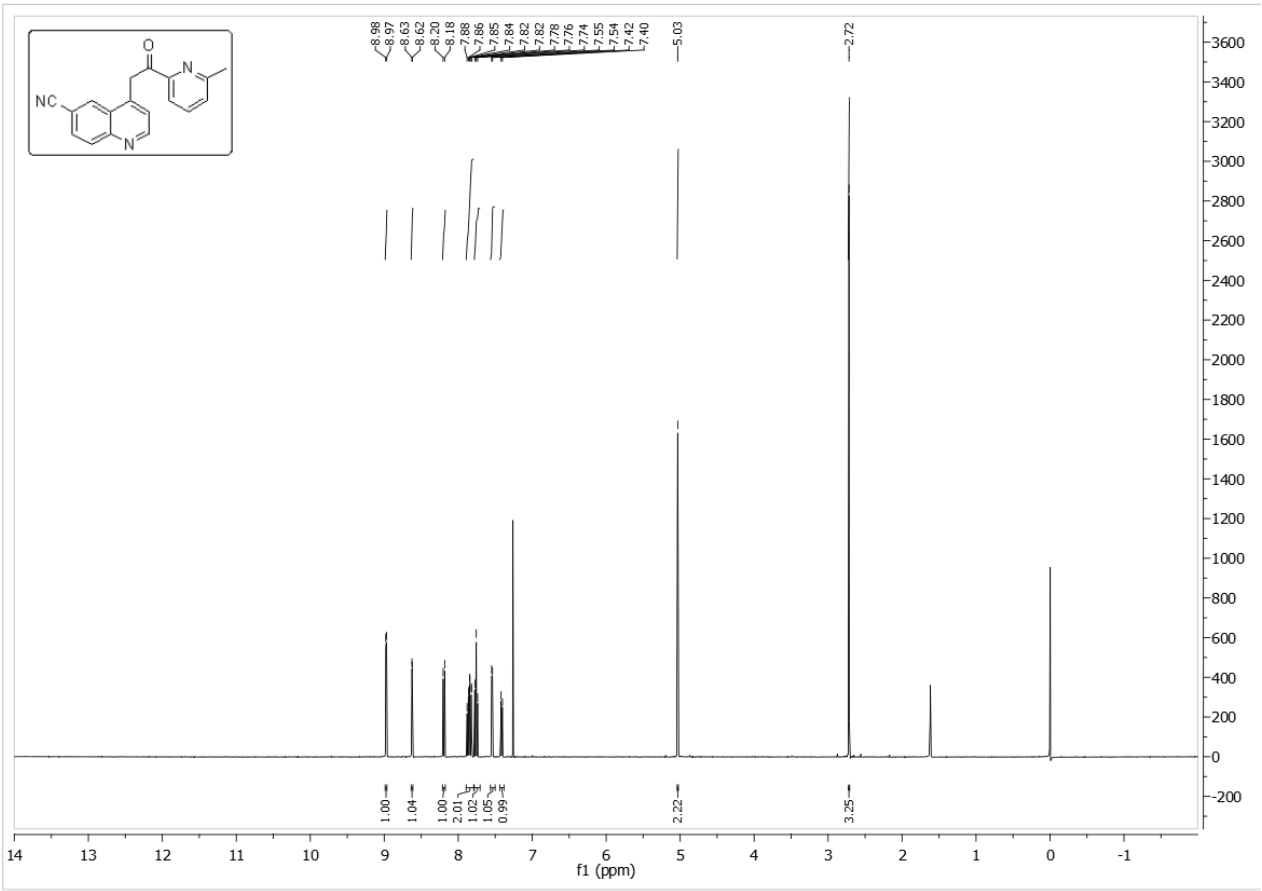
8.98
8.97
8.63
8.62
8.20
8.18
7.88
7.86
7.85
7.84
7.82
7.82
7.78
7.76
7.74
7.55
7.54
7.42
7.40
5.03
2.72
1.00
1.04
1.00
2.01
1.02
1.05
0.99
2.22
3.25
f1 (ppm)

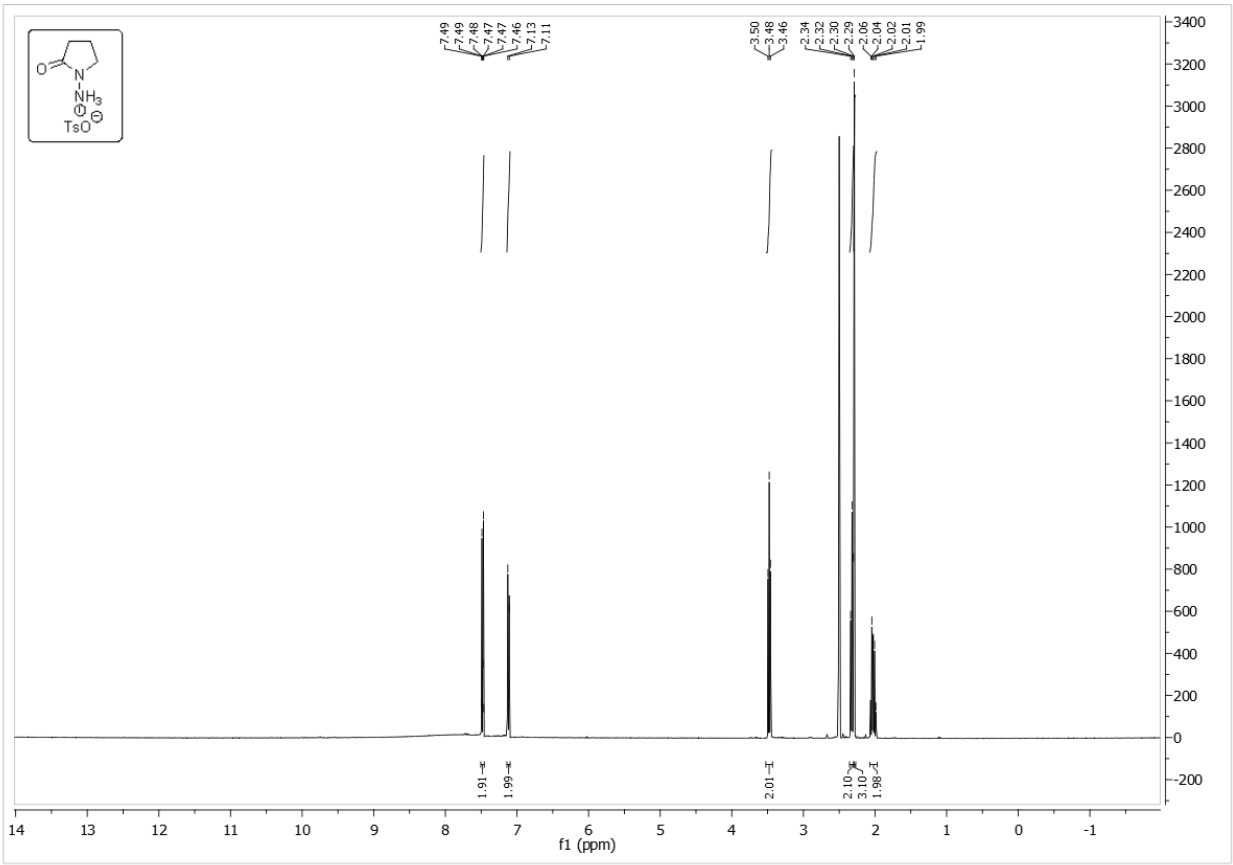
7.49
7.49
7.48
7.47
7.47
7.46
7.13
7.11
3.50
3.48
3.46
2.34
2.32
2.30
2.29
2.06
2.04
2.02
2.01
1.99
1.91
1.99
2.01
2.10
3.10
1.98
f1 (ppm)

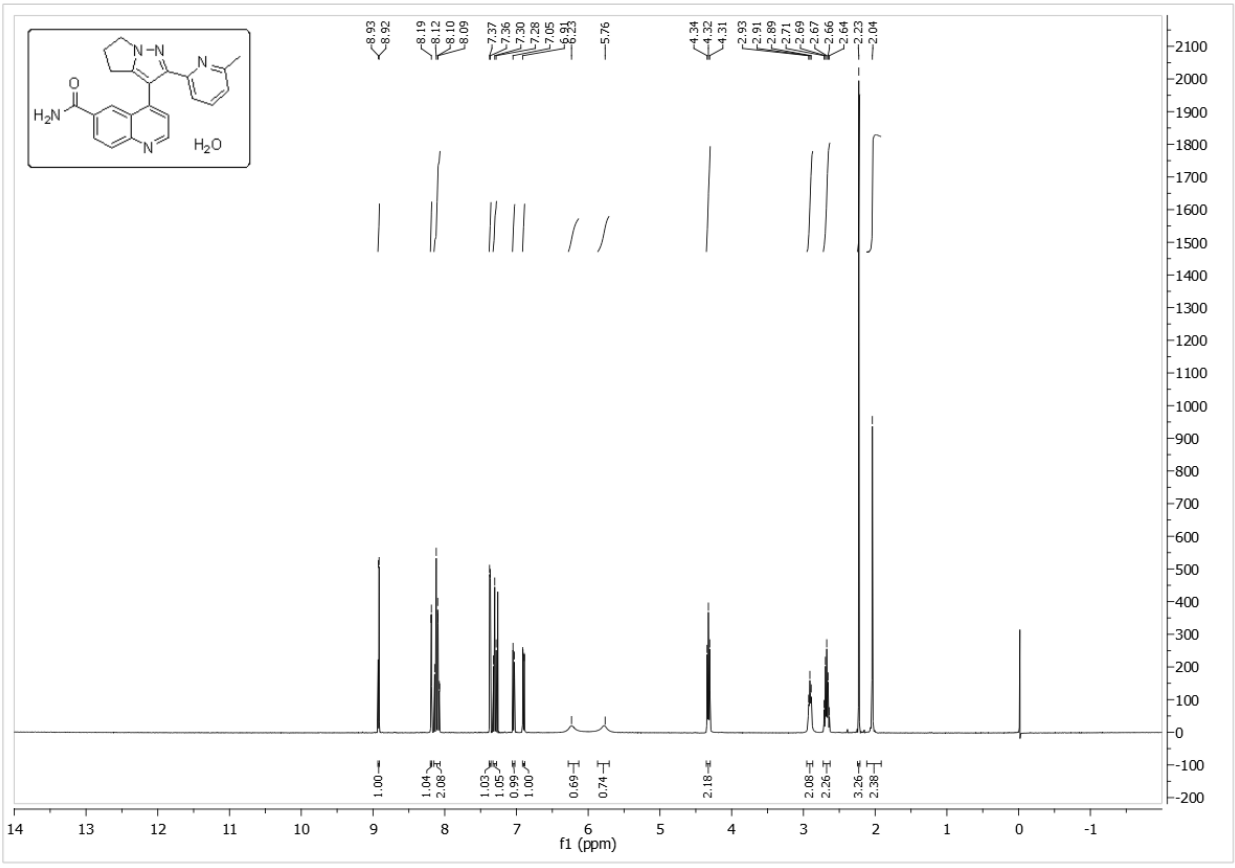
8.93
8.92
8.19
8.12
8.10
8.09
7.37
7.36
7.30
7.28
7.05
6.91
6.23
5.76
4.34
4.32
4.31
2.93
2.91
2.89
2.71
2.69
2.67
2.66
2.64
2.23
2.04
1.00
1.04
2.08
1.03
1.05
0.99
1.00
0.69
0.74
2.18
2.08
2.26
3.26
2.38
f1 (ppm)

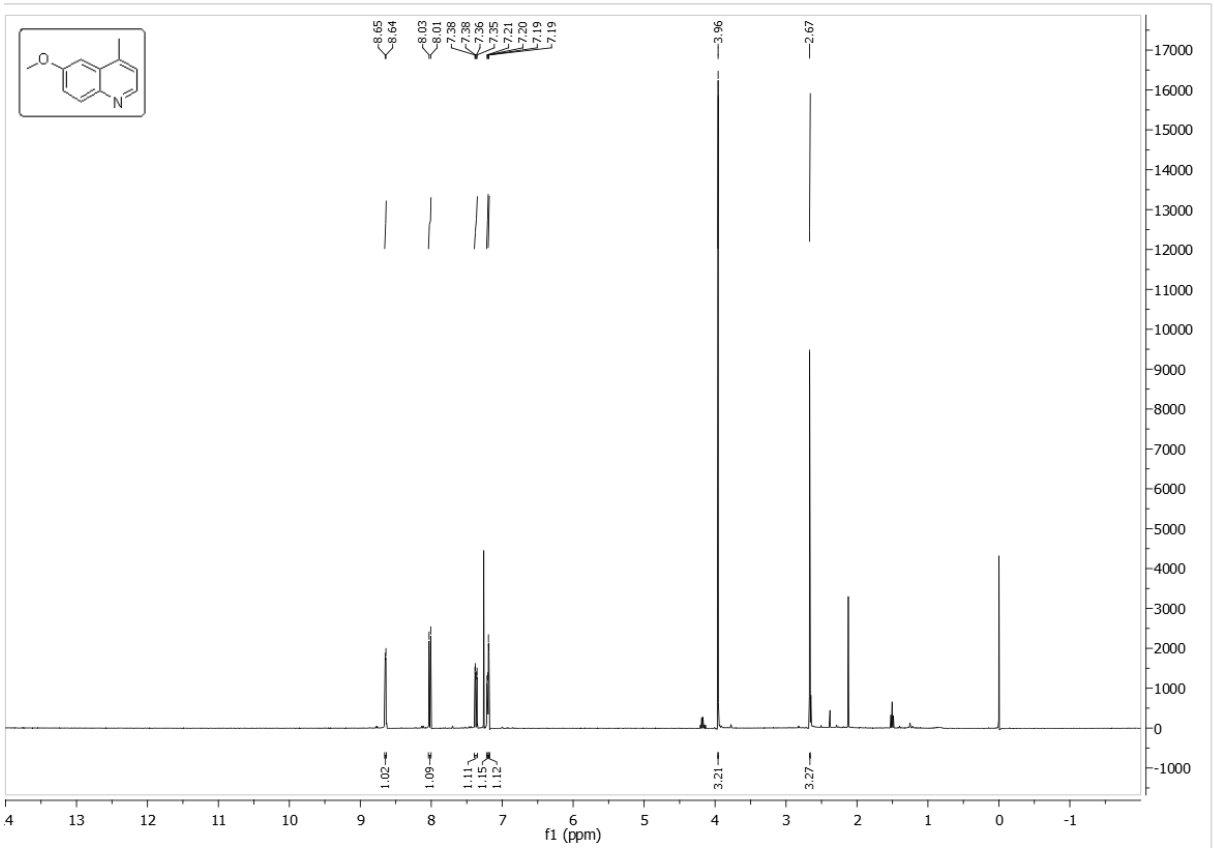
8.65
8.64
8.03
8.01
7.38
7.36
7.35
7.21
7.20
7.19
7.19
3.96
2.67
1.02
1.09
1.11
1.15
1.12
3.21
3.27
f1 (ppm)

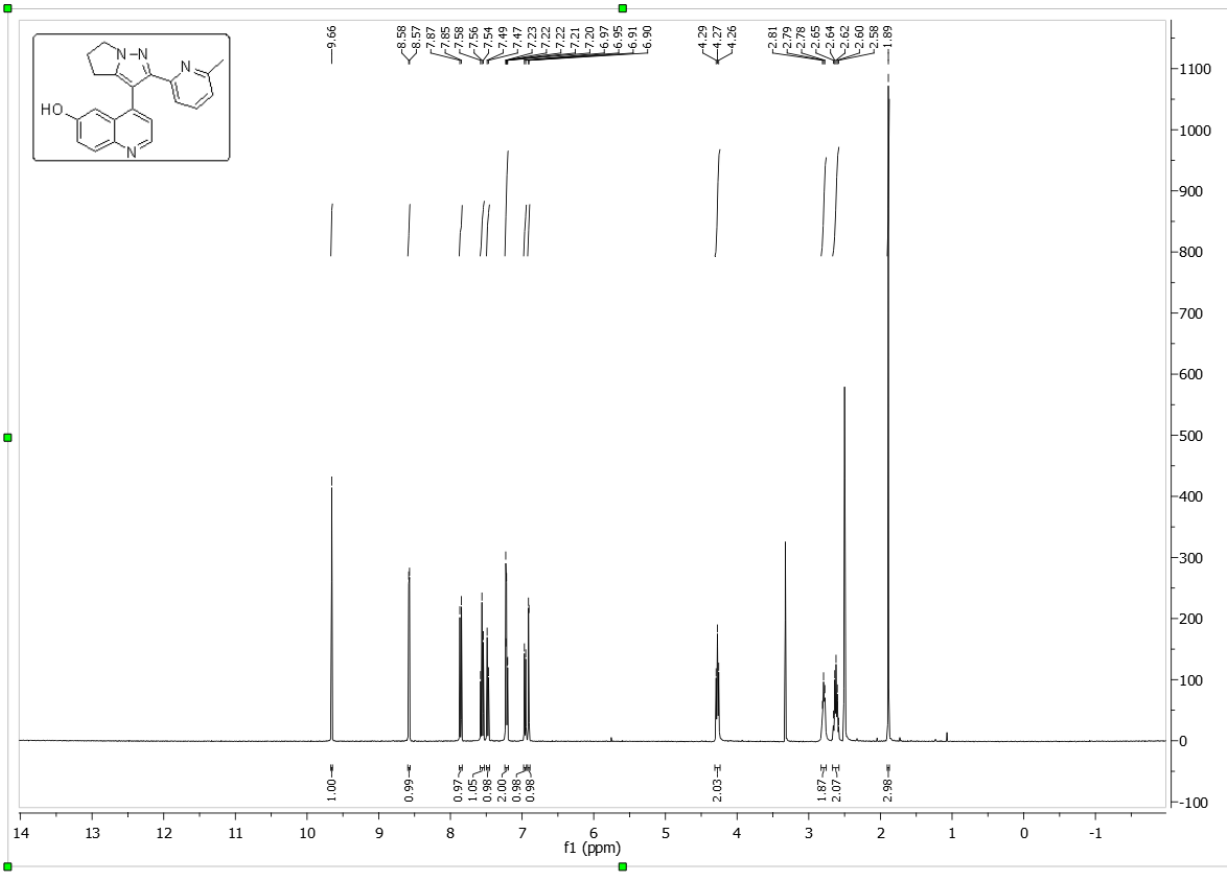
HO
N
N
9.66
8.58
8.57
7.87
7.85
7.58
7.56
7.54
7.49
7.47
7.23
7.22
7.22
7.21
7.20
6.97
6.95
6.91
6.90
4.29
4.27
4.26
2.81
2.79
2.78
2.65
2.64
2.62
2.60
2.58
1.89
1.00
0.99
0.97
1.05
0.98
2.00
0.98
0.98
2.03
1.87
2.07
2.98
f1 (ppm)

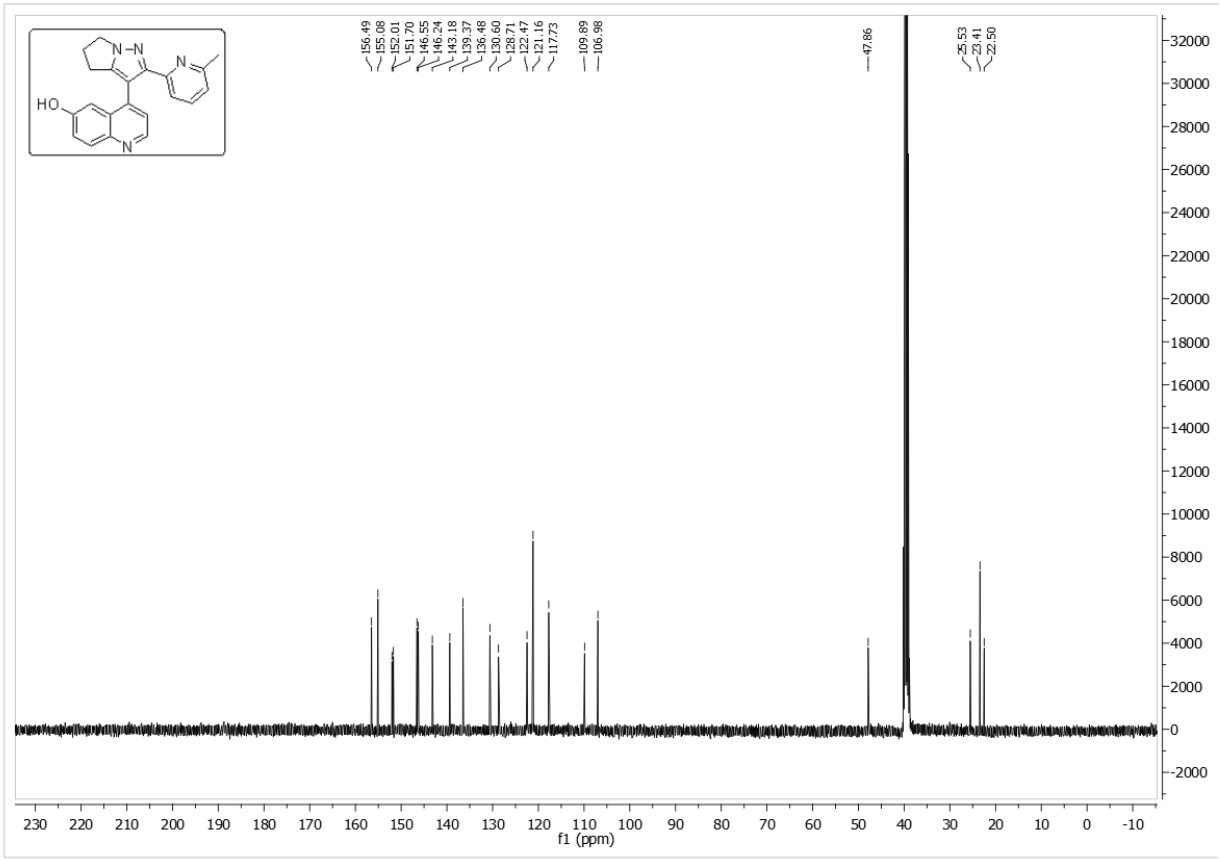
156.49
155.08
152.01
151.70
146.55
146.24
143.18
139.37
136.48
130.60
128.71
122.47
121.16
117.73
109.89
106.98
47.86
25.53
23.41
22.50
HO
N
N
N
f1 (ppm)

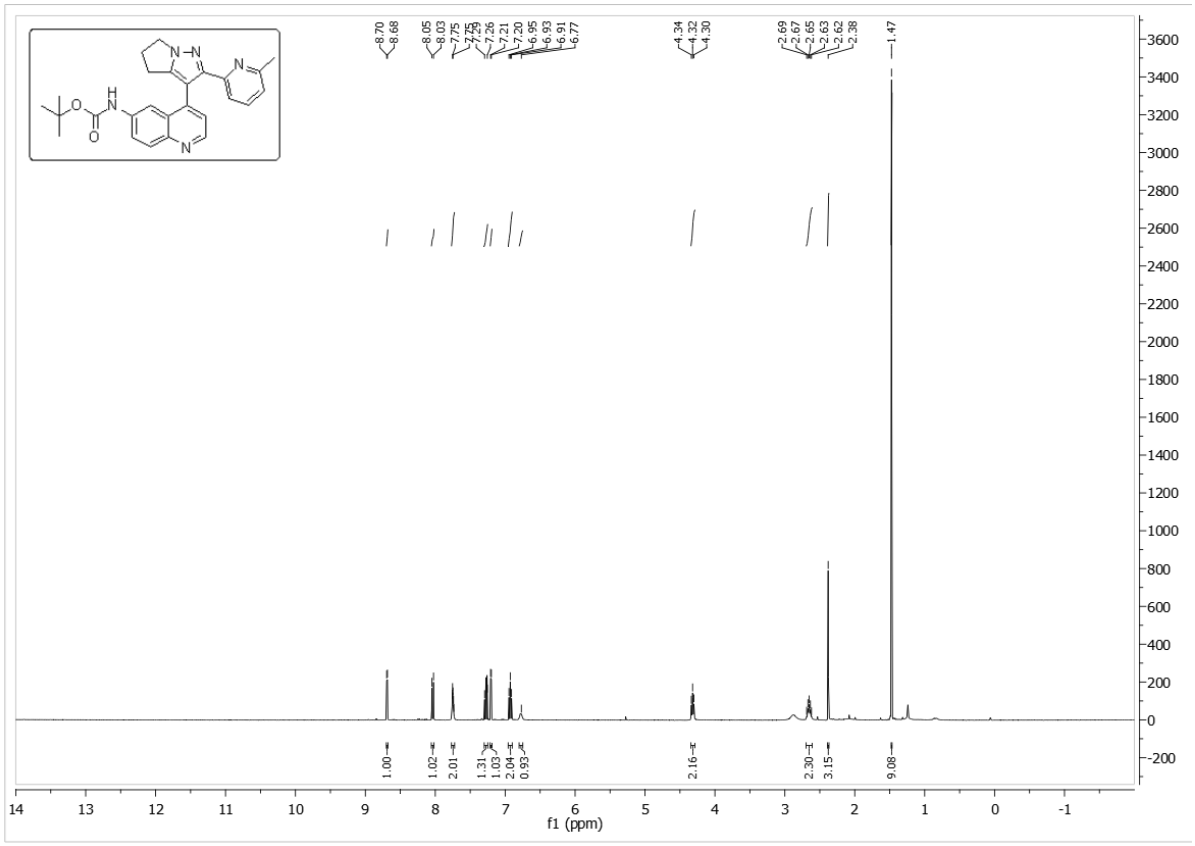
8.70
8.68
8.05
8.03
7.75
7.73
7.29
7.26
7.21
7.20
6.95
6.93
6.91
6.77
4.34
4.32
4.30
2.69
2.67
2.65
2.63
2.62
2.38
1.47
1.00
1.02
2.01
1.31
1.03
2.04
0.93
2.16
2.30
3.15
9.08
O
O
H
N
N
N
f1 (ppm)

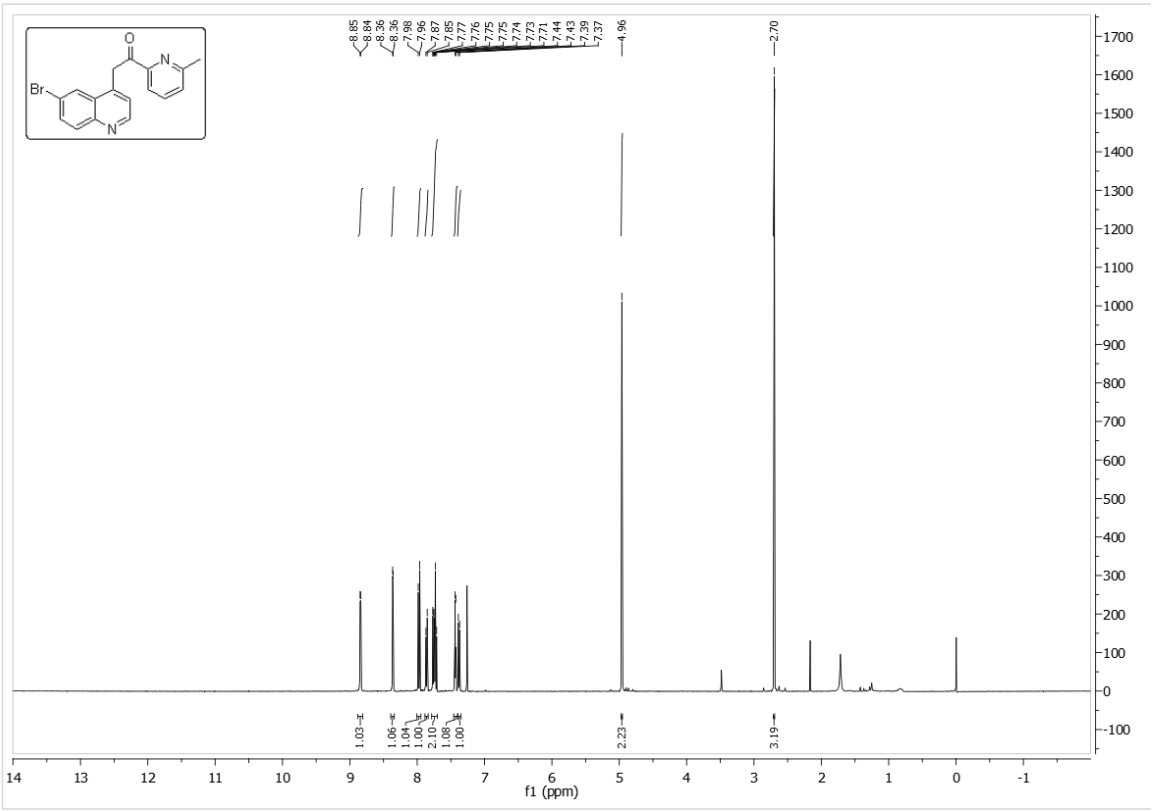
8.85
8.84
8.36
8.36
7.98
7.96
7.87
7.85
7.77
7.76
7.75
7.75
7.74
7.73
7.71
7.44
7.43
7.39
7.37
4.96
2.70
1.03
1.06
1.04
1.10
2.19
1.08
1.00
2.23
3.19
f1 (ppm)

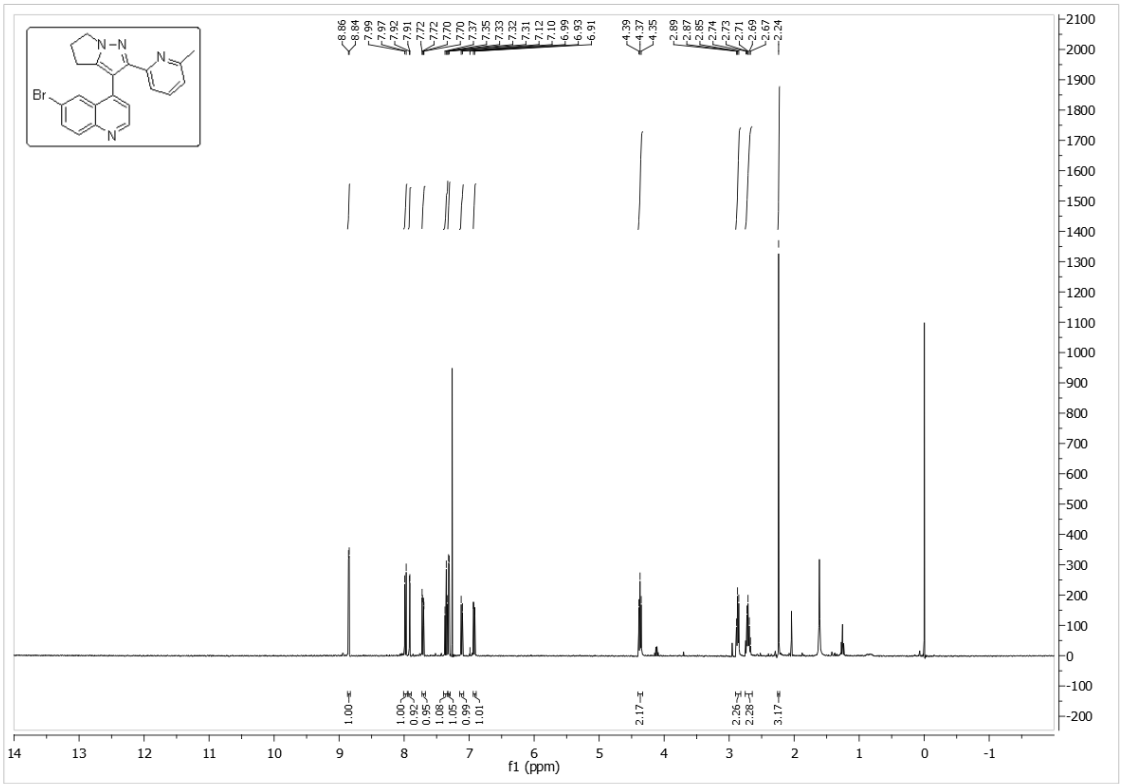
8.86
8.84
7.99
7.97
7.92
7.91
7.72
7.72
7.70
7.70
7.37
7.35
7.33
7.32
7.31
7.12
7.10
6.99
6.93
6.91
4.39
4.37
4.35
2.89
2.87
2.85
2.74
2.73
2.71
2.69
2.67
2.24
1.00
1.00
0.92
0.95
1.08
1.05
0.99
1.01
2.17
2.26
2.28
3.17
f1 (ppm)

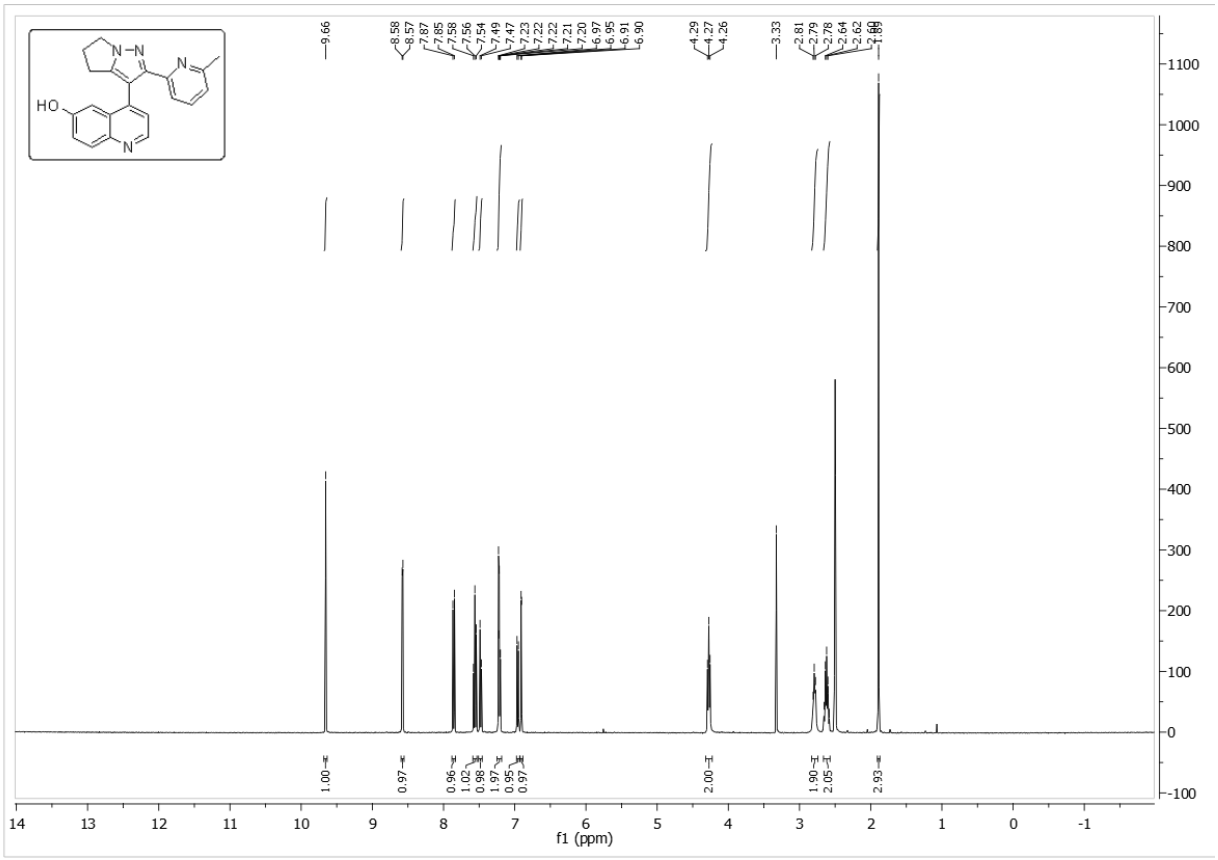
9.66
8.58
8.57
7.87
7.85
7.58
7.56
7.54
7.49
7.47
7.23
7.22
7.21
7.20
6.97
6.95
6.91
6.90
4.29
4.27
4.26
3.33
2.81
2.79
2.78
2.64
2.62
1.89
1.00
0.97
0.96
1.02
0.98
1.97
0.95
0.97
2.00
1.90
2.05
2.93
f1 (ppm)

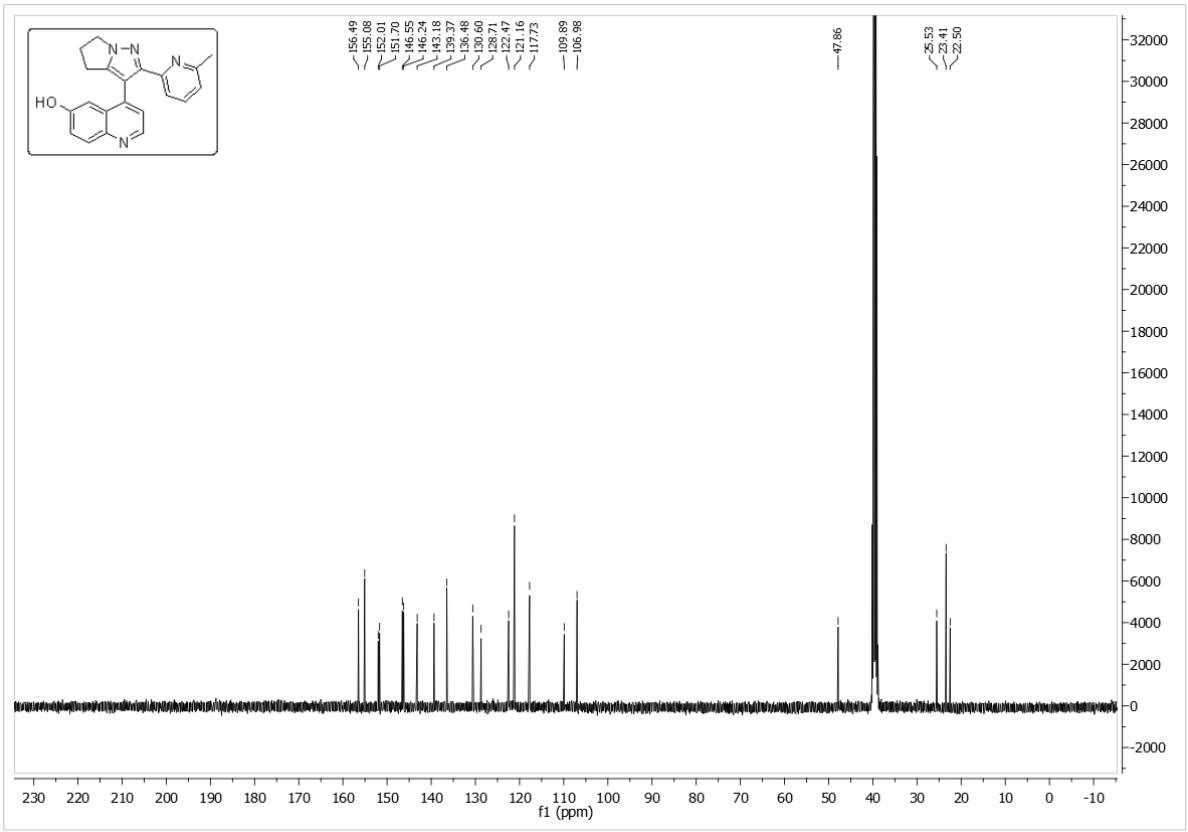
156.49
155.08
152.01
151.70
146.55
146.24
143.18
139.37
136.48
130.60
128.71
122.47
121.16
117.73
109.89
106.98
47.86
25.53
23.41
22.50
f1 (ppm)

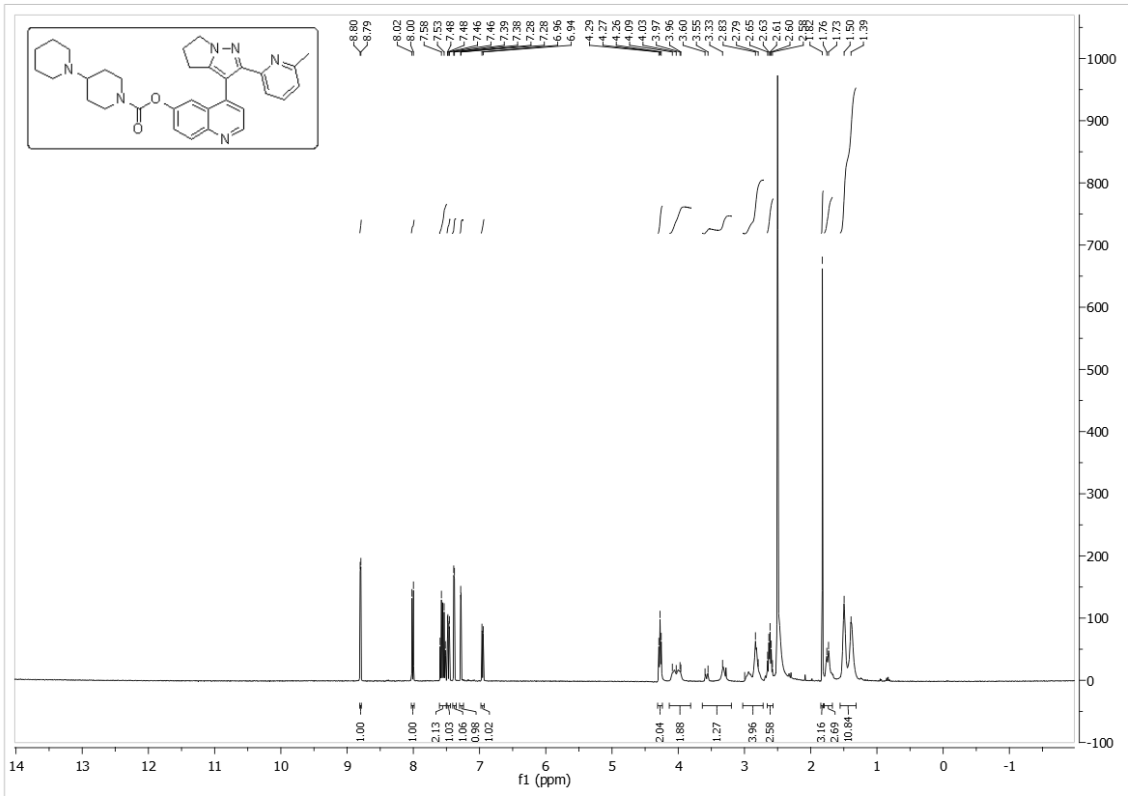
8.80
8.79
8.02
8.00
7.58
7.53
7.48
7.48
7.46
7.46
7.39
7.38
7.28
7.28
6.96
6.94
4.29
4.27
4.26
4.09
4.03
3.97
3.96
3.60
3.55
3.33
2.83
2.79
2.65
2.63
2.61
2.60
1.82
1.76
1.73
1.50
1.39
1.00
1.00
2.13
1.03
1.06
0.98
1.02
2.04
1.88
1.27
3.96
2.58
3.16
2.69
10.84
f1 (ppm)

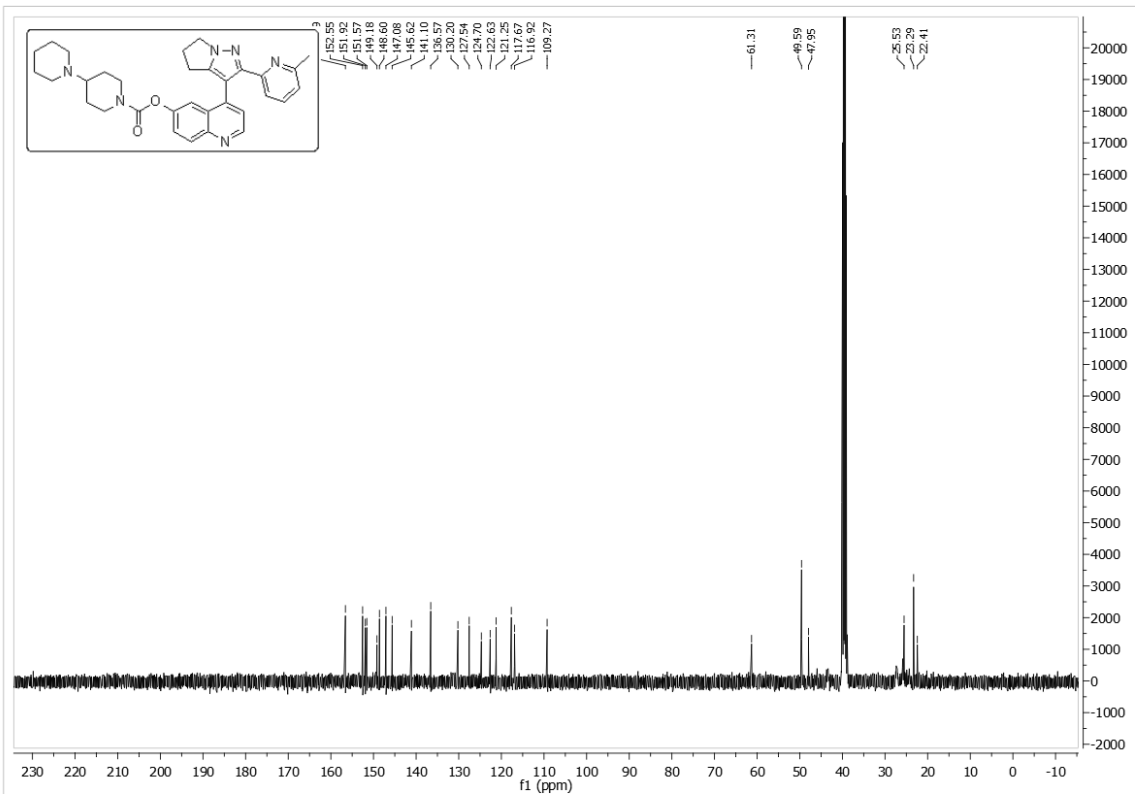
152.55
151.92
151.57
149.18
148.60
147.08
145.62
141.10
136.57
130.20
127.54
124.70
122.63
121.25
117.67
116.92
109.27
61.31
49.59
47.95
25.53
23.29
22.41
f1 (ppm)

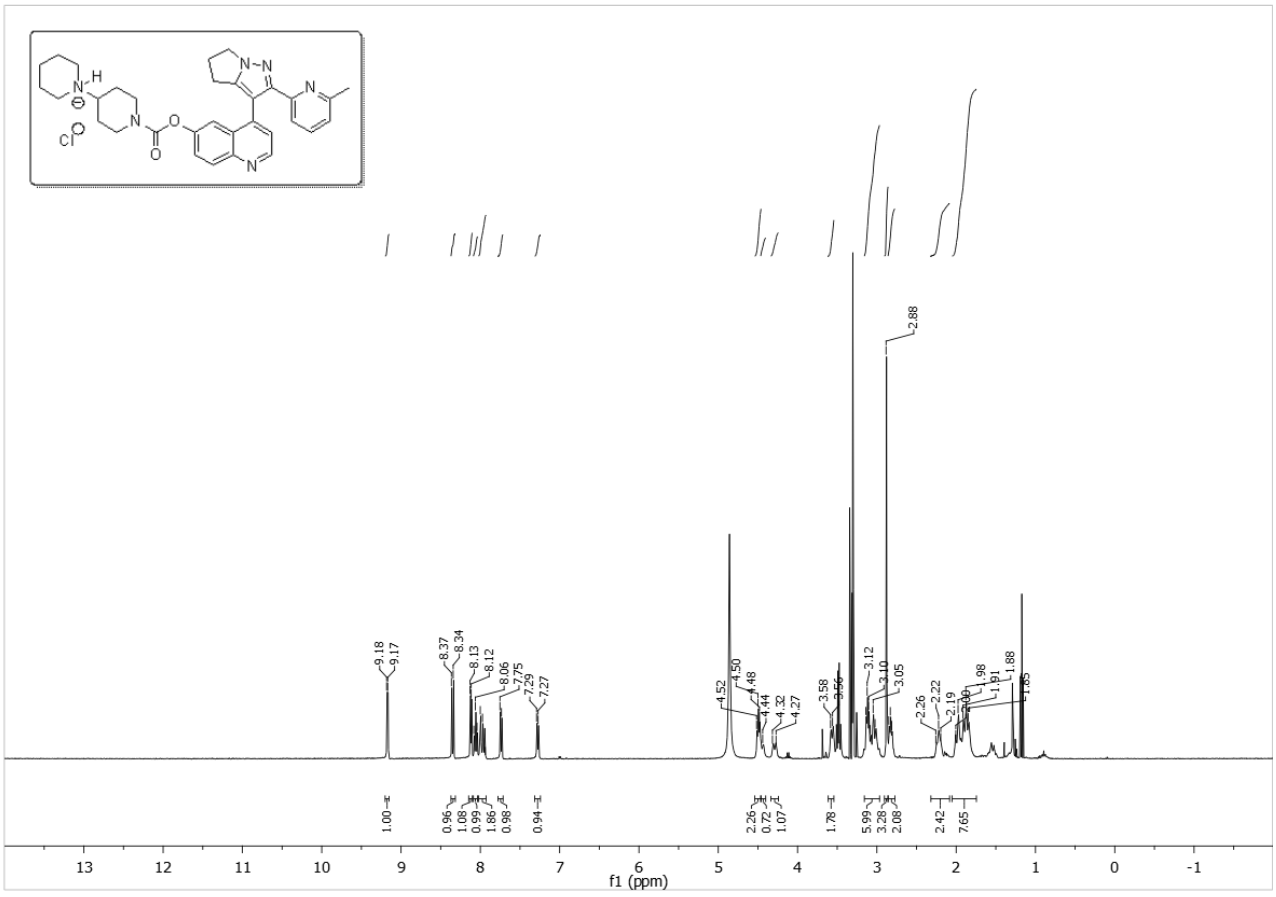
9.18
9.17
8.37
8.34
8.13
8.12
8.06
7.75
7.29
7.27
4.52
4.50
4.48
4.44
4.32
4.27
3.58
3.56
3.12
3.10
3.05
2.88
2.26
2.22
2.19
1.98
1.91
1.88
1.85
1.00
0.96
1.08
0.99
1.86
0.98
0.94
2.26
0.72
1.07
1.78
5.99
3.28
2.08
2.42
7.65
f1 (ppm)

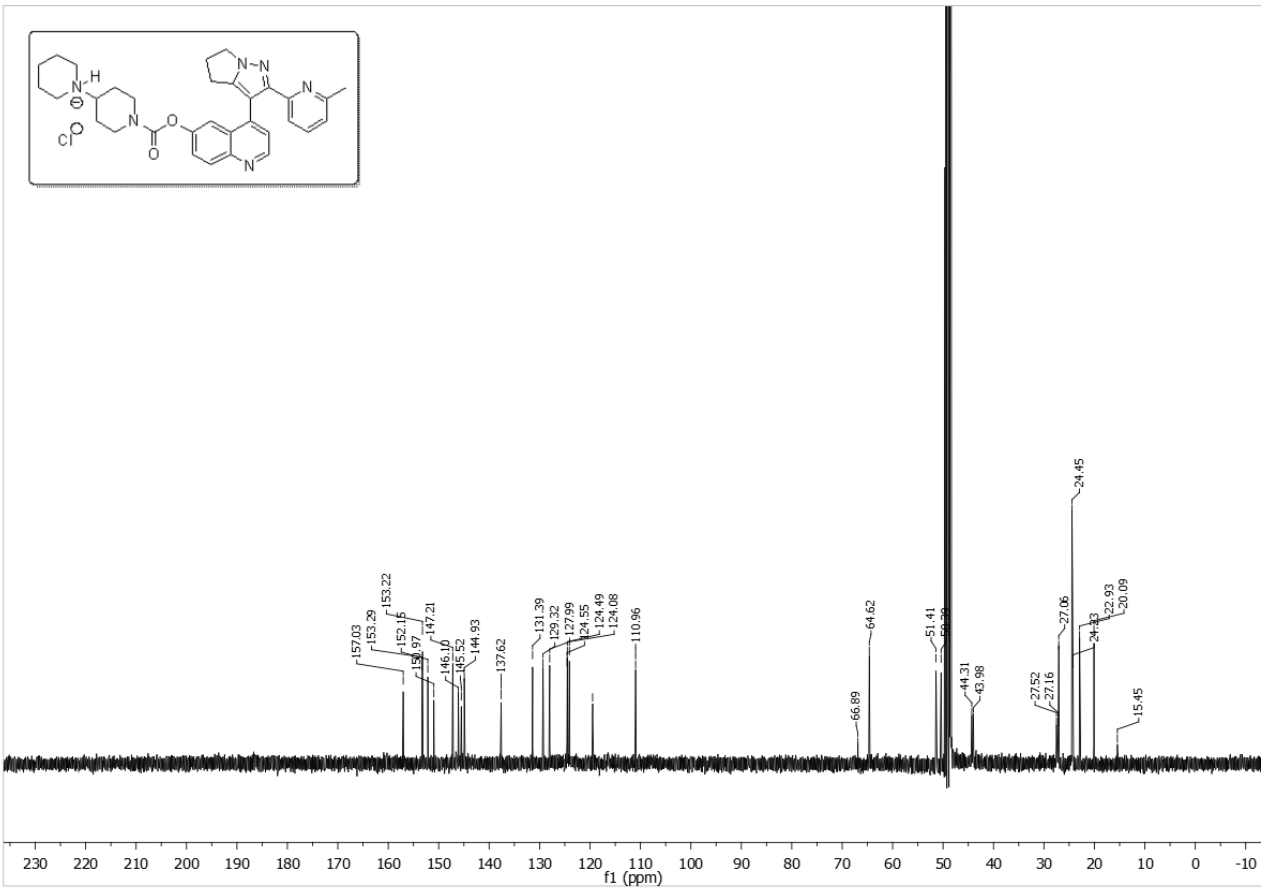
157.03
153.29
153.22
152.15
150.97
147.21
146.10
145.52
144.93
137.62
131.39
129.32
127.99
124.55
124.49
124.08
110.96
66.89
64.62
51.41
44.31
43.98
27.52
27.16
27.06
24.45
24.13
22.93
20.09
15.45
f1 (ppm)

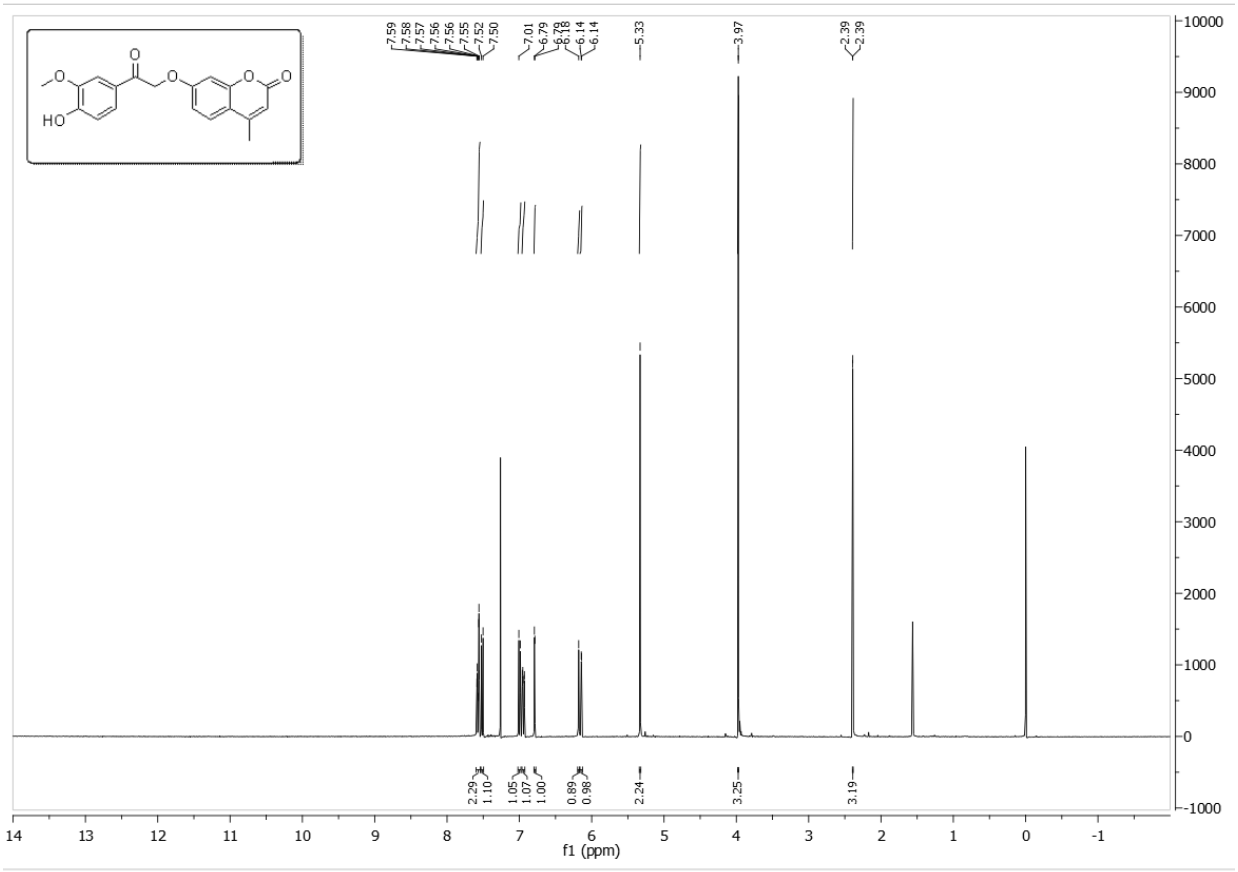
7.59
7.58
7.57
7.56
7.56
7.55
7.52
7.50
7.01
6.79
6.18
6.14
6.14
5.33
3.97
2.39
2.39
HO
O
O
O
O
O
2.29
1.10
1.05
1.07
1.00
0.89
0.98
2.24
3.25
3.19
f1 (ppm)

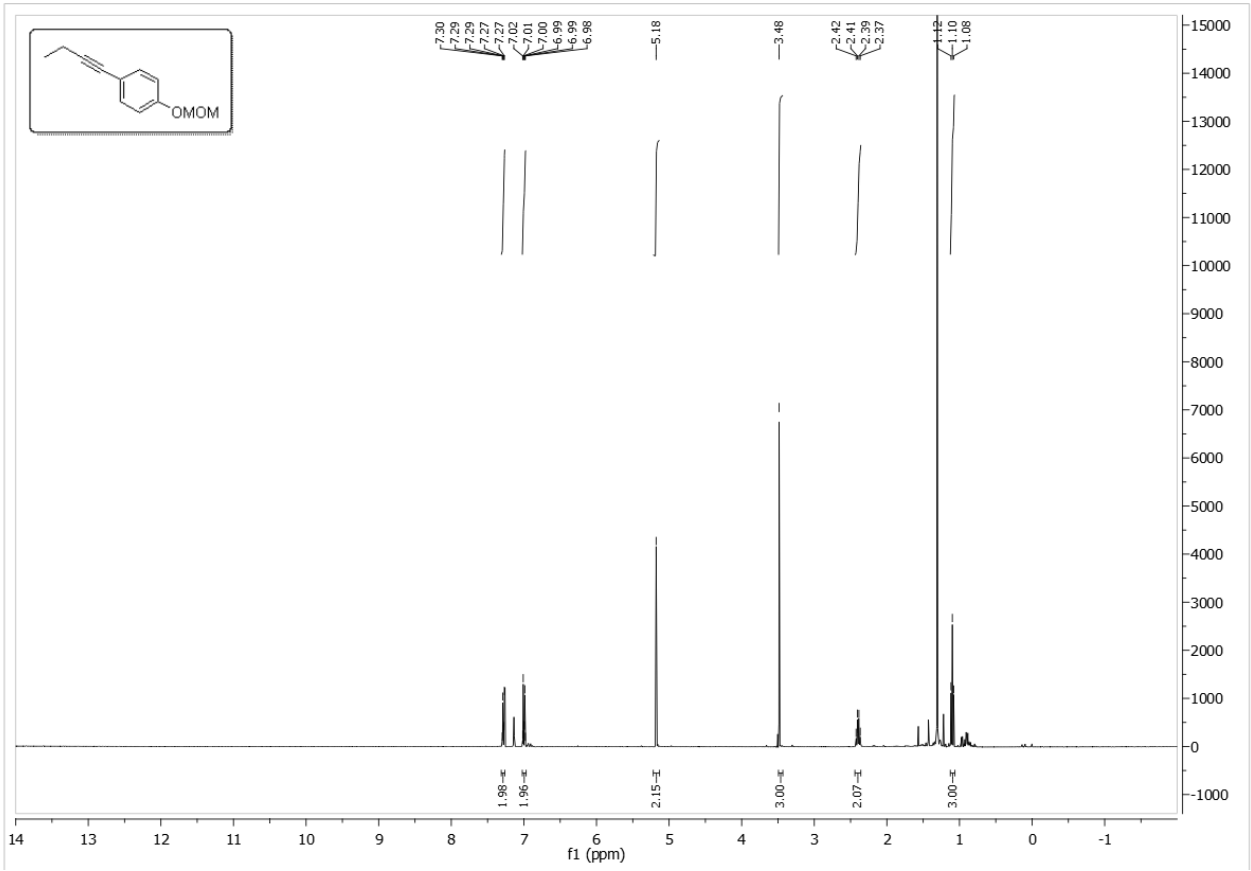
7.30
7.29
7.29
7.27
7.27
7.27
7.02
7.01
7.00
6.99
6.99
6.98
5.18
3.48
2.42
2.41
2.39
2.37
1.12
1.10
1.08
OMOM
1.98
1.96
2.15
3.00
2.07
3.00
f1 (ppm)

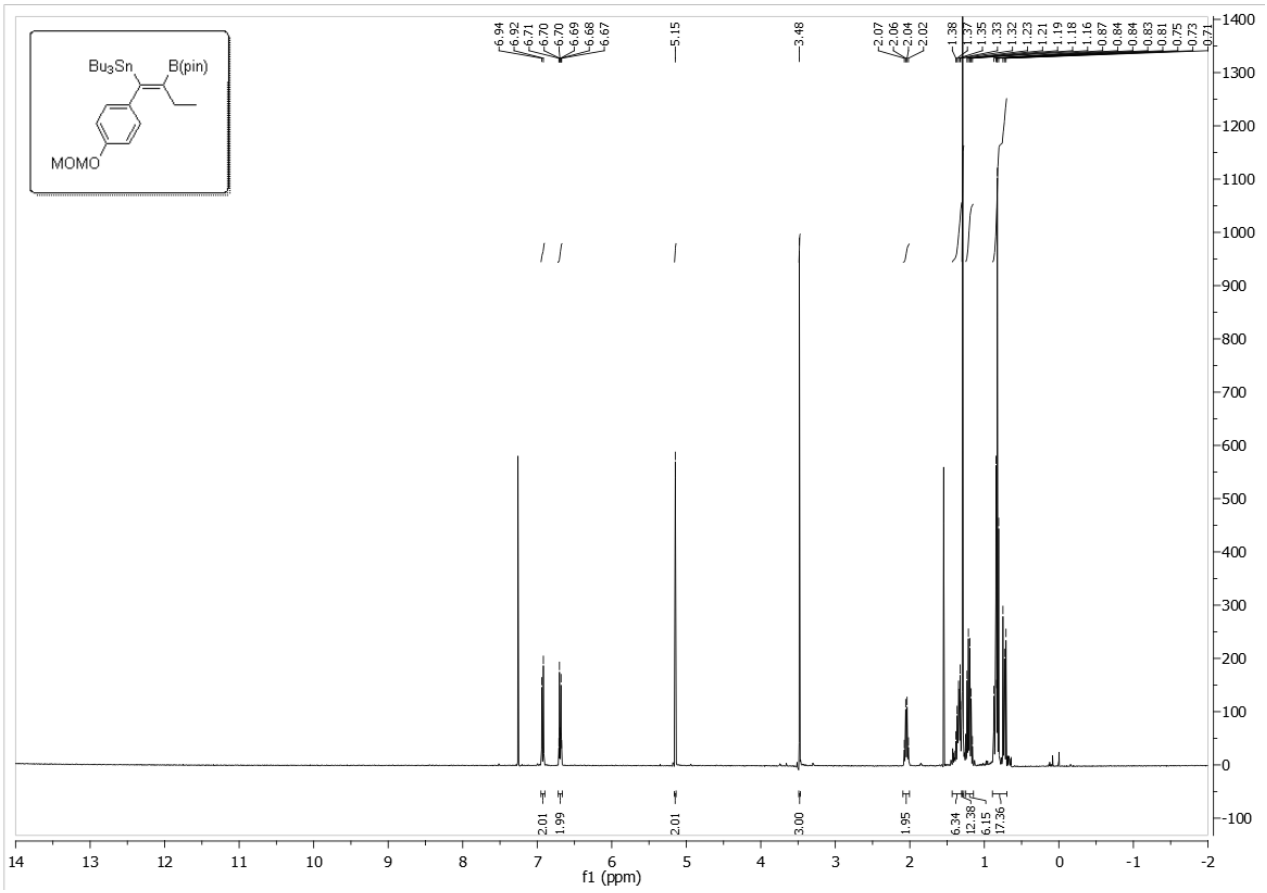
Bu3Sn
B(pin)
MOMO
f1 (ppm)

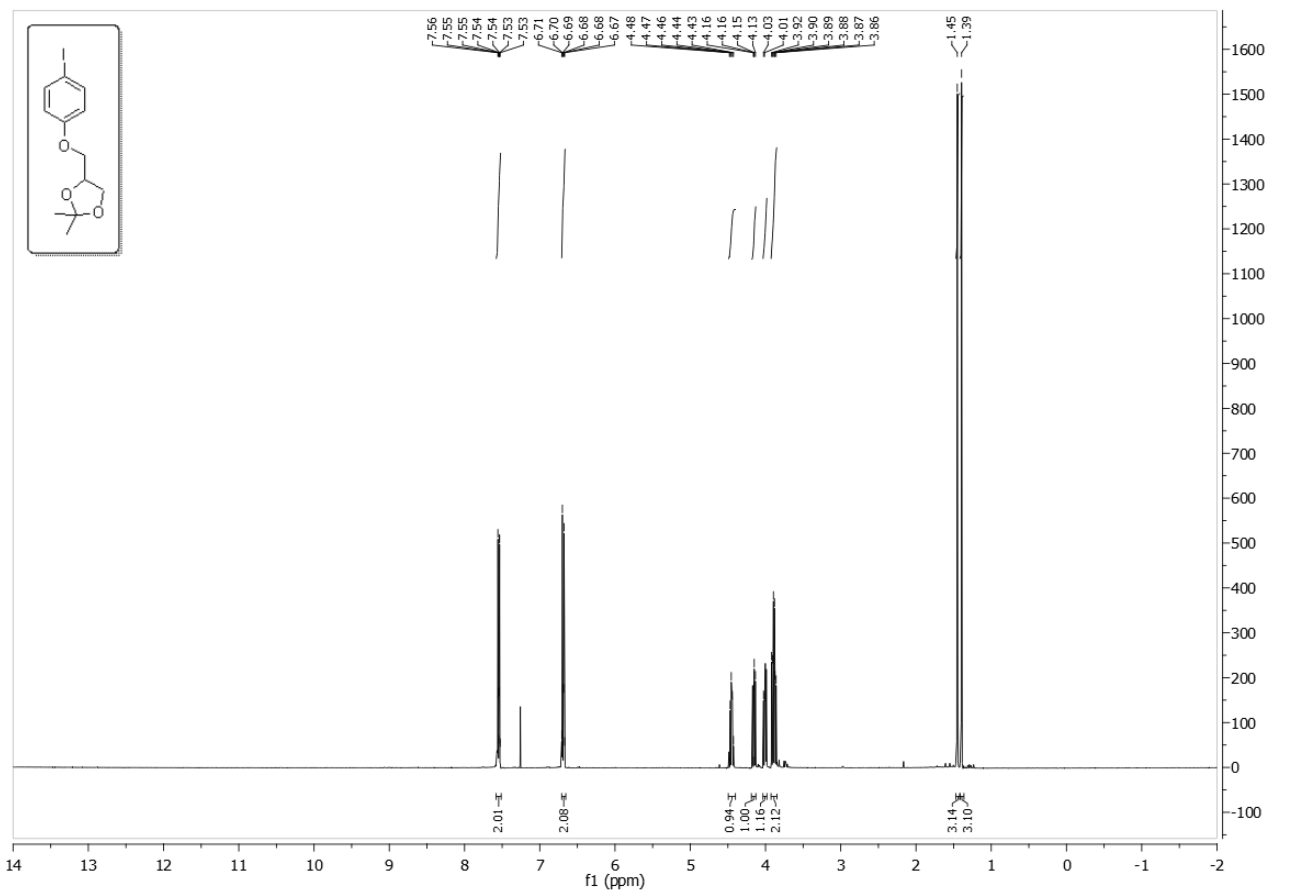
f1 (ppm)

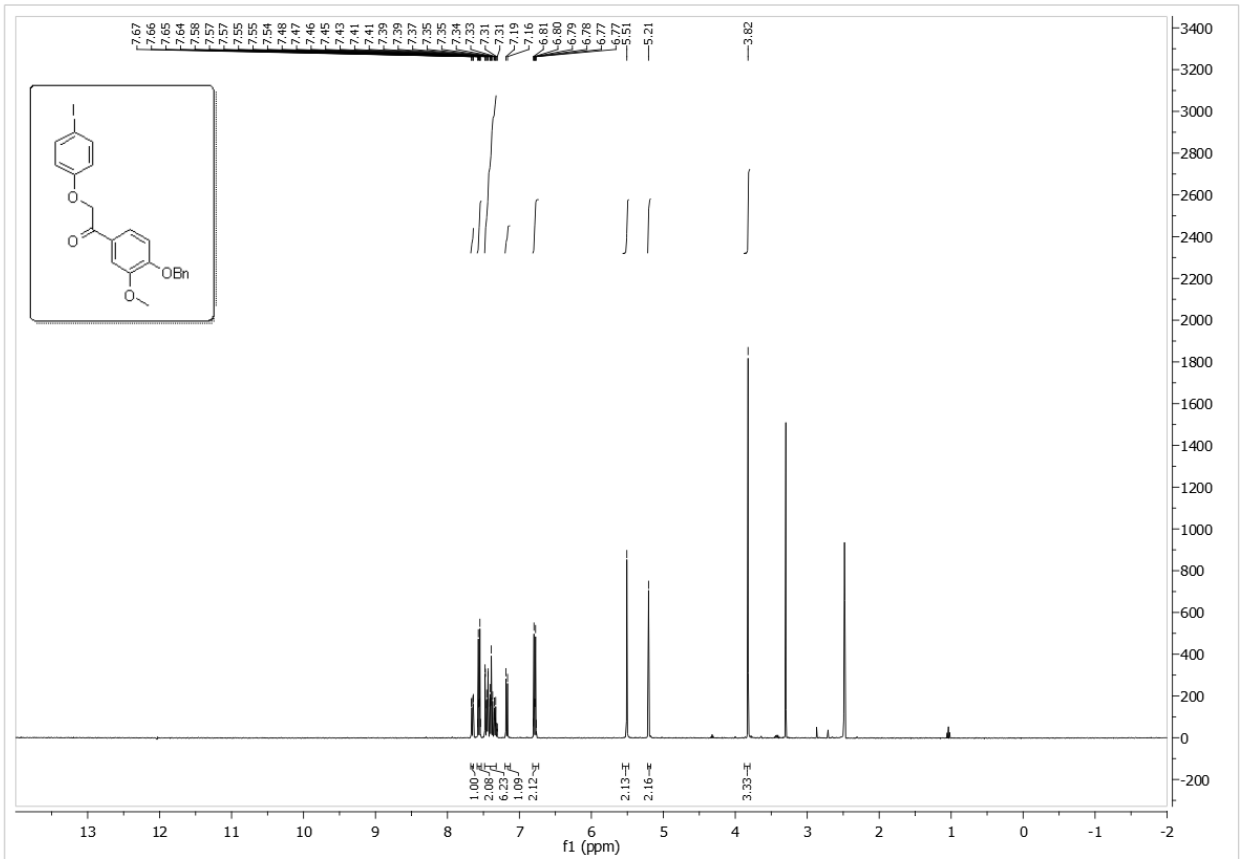
7.67
7.66
7.65
7.64
7.58
7.57
7.57
7.55
7.55
7.54
7.48
7.47
7.46
7.45
7.43
7.41
7.41
7.39
7.39
7.37
7.35
7.35
7.34
7.33
7.31
7.31
7.19
7.16
6.81
6.80
6.79
6.78
6.77
6.77
5.51
5.21
3.82
I
O
O
OBn
O
1.00
2.08
6.23
1.09
2.12
2.13
2.16
3.33
f1 (ppm)

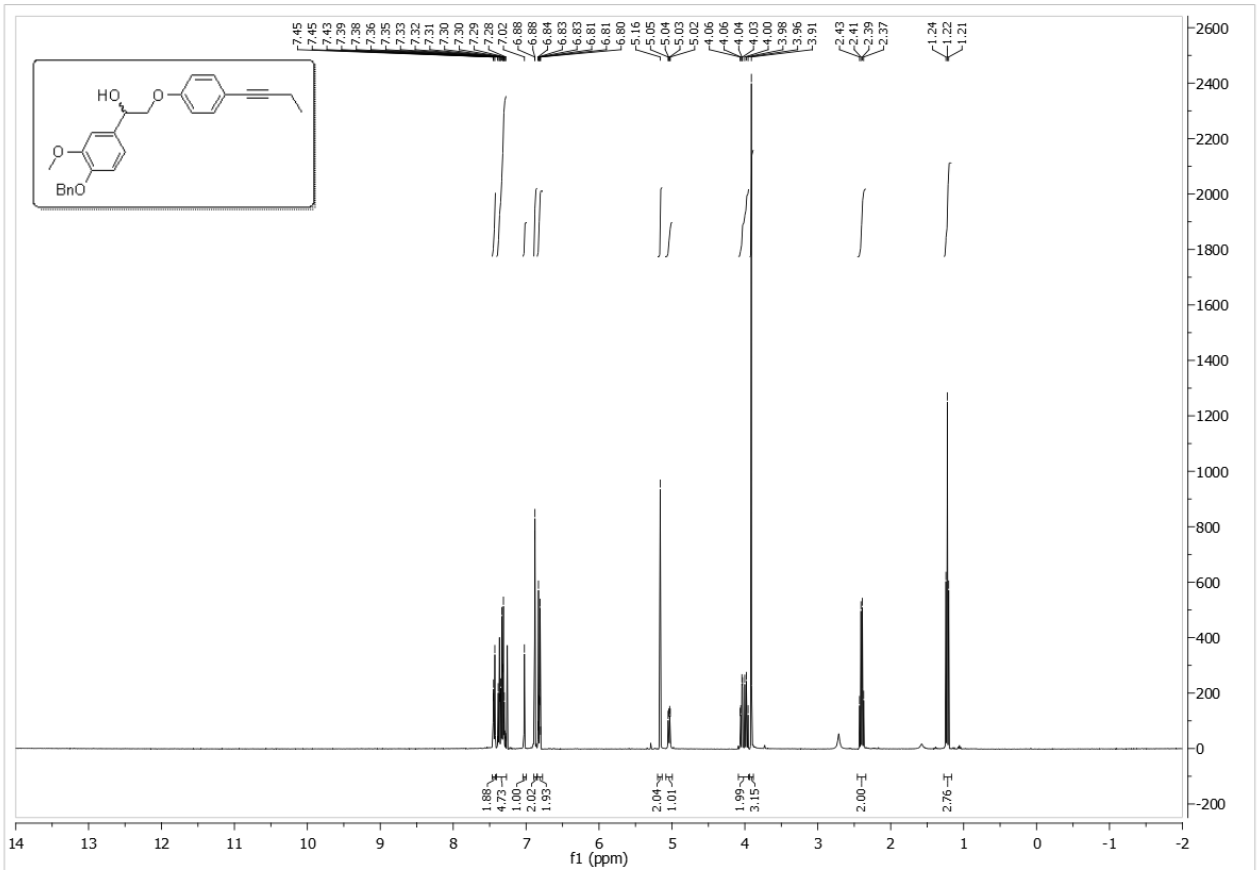
7.45
7.45
7.43
7.39
7.38
7.36
7.35
7.33
7.32
7.31
7.30
7.30
7.29
7.28
7.02
6.88
6.88
6.84
6.83
6.83
6.81
6.81
6.80
5.16
5.05
5.04
5.03
5.02
4.06
4.06
4.04
4.03
4.00
3.98
3.96
3.91
2.43
2.41
2.39
2.37
1.24
1.22
1.21
HO
O
O
BnO
1.88
4.73
1.00
2.02
1.93
2.04
1.01
1.99
3.15
2.00
2.76
f1 (ppm)

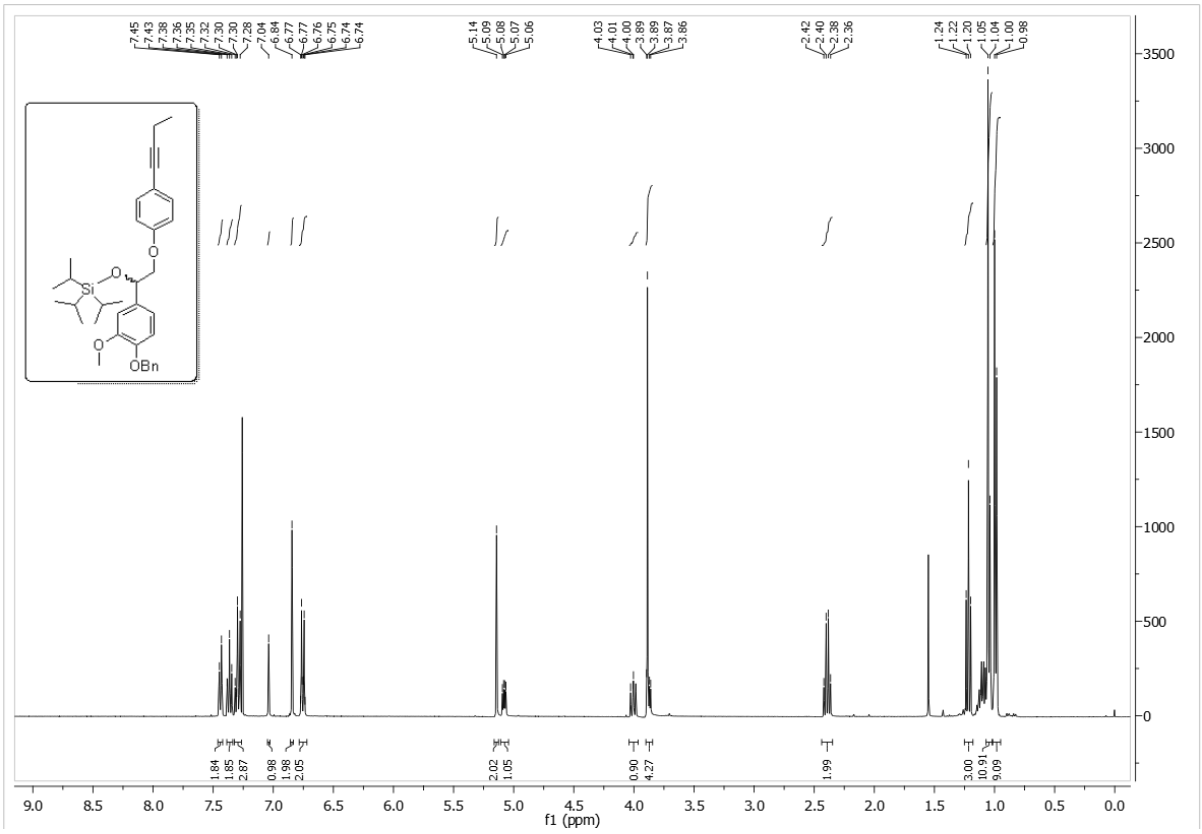
7.45
7.43
7.38
7.36
7.35
7.32
7.30
7.30
7.28
7.04
6.84
6.77
6.77
6.76
6.75
6.74
6.74
5.14
5.09
5.08
5.07
5.06
4.03
4.01
4.00
3.89
3.89
3.87
3.86
2.42
2.40
2.38
2.36
1.24
1.22
1.20
1.05
1.04
1.00
0.98
OBn
1.84
1.85
2.87
0.98
1.98
2.05
2.02
1.05
0.90
4.27
1.99
3.00
10.91
9.09
f1 (ppm)

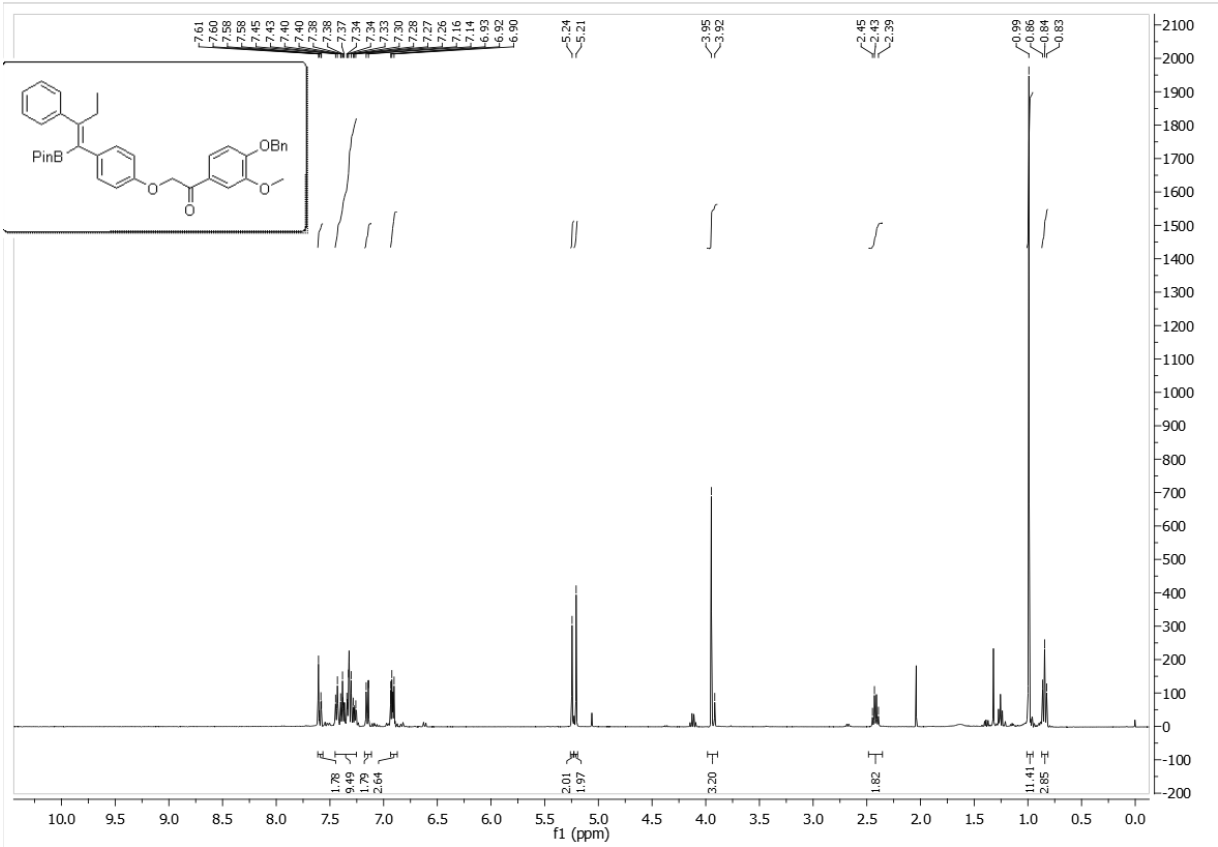
7.61
7.60
7.58
7.58
7.45
7.43
7.40
7.40
7.38
7.38
7.37
7.34
7.34
7.33
7.30
7.28
7.27
7.26
7.16
7.14
6.93
6.92
6.90
5.24
5.21
3.95
3.92
2.45
2.43
2.39
0.99
0.86
0.84
0.83
PinB
OBn
1.78
9.49
1.79
2.64
2.01
1.97
3.20
1.82
11.41
2.85
f1 (ppm)

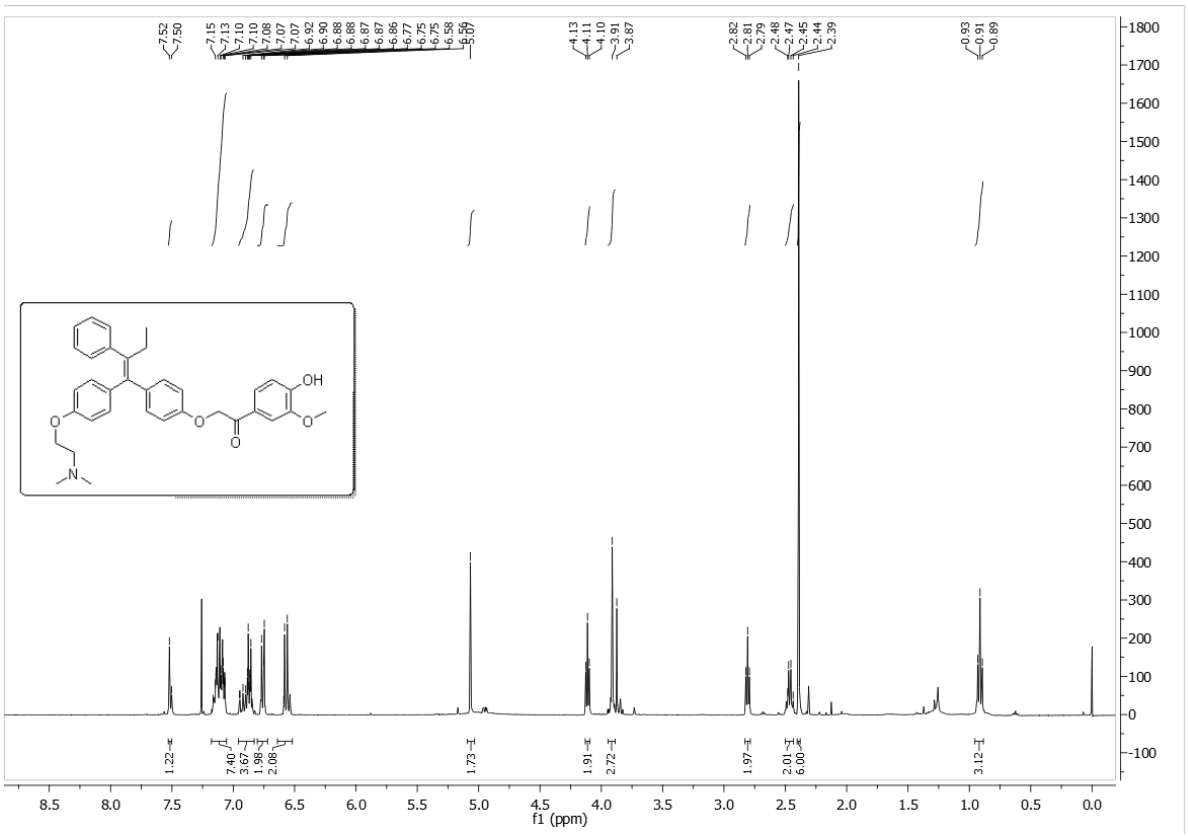
7.52
7.50
7.15
7.13
7.10
7.10
7.08
7.07
7.07
6.92
6.90
6.88
6.88
6.87
6.87
6.86
6.77
6.75
6.75
6.58
6.56
5.07
4.13
4.11
4.10
3.91
3.87
2.82
2.81
2.79
2.48
2.47
2.45
2.44
2.39
0.93
0.91
0.89
OH
O
O
O
O
N
1.22
7.40
3.67
1.98
2.08
1.73
1.91
2.72
1.97
2.01
6.00
3.12
f1 (ppm)

# Chapter 9

# List of Structures

# List of structures

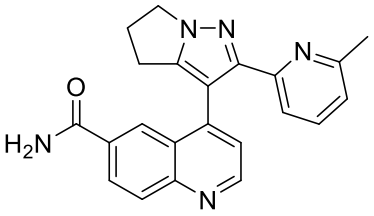

**1-1**

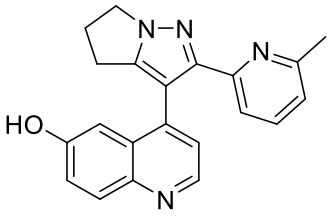

**1-2**

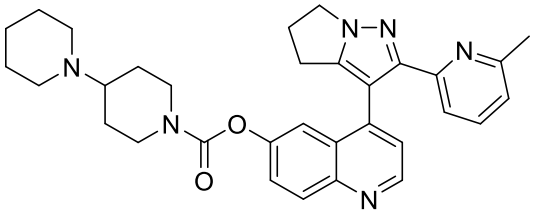

**1-3**

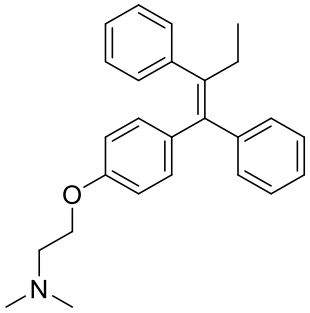

**1-4**

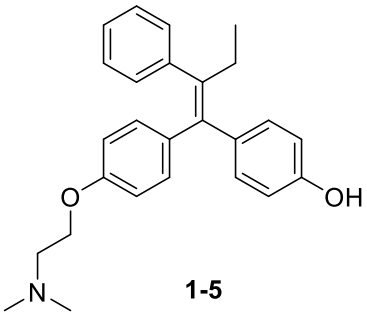

**1-5**

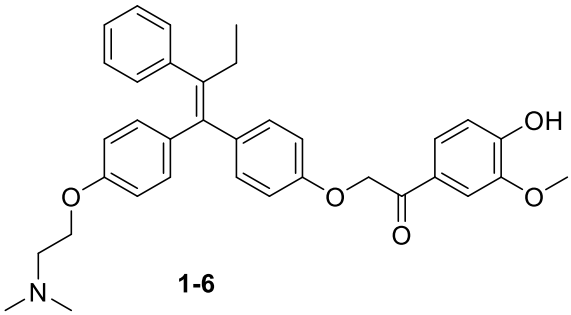

**1-6**

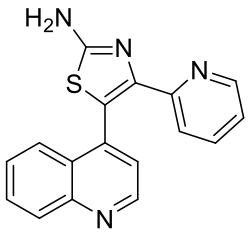

**2-1**

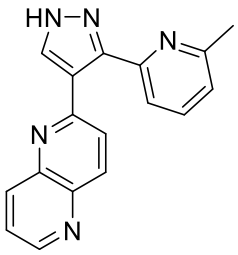

**2-2**

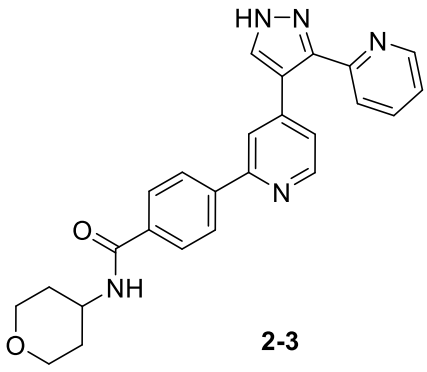

**2-3**

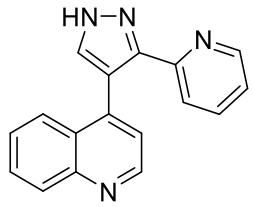

**2-4**

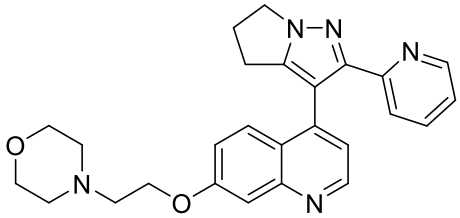

**2-5**

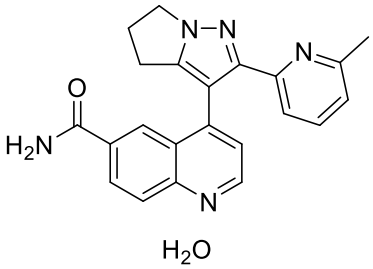

**2-6**

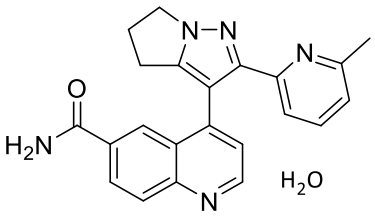

**3-1**

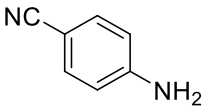

**3-2**

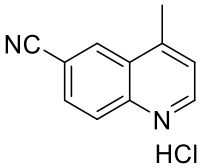

**3-3**

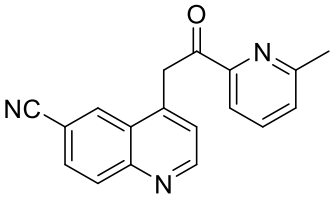

**3-4**

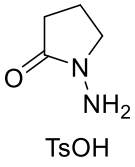

**3-5**

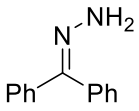

**3-6**

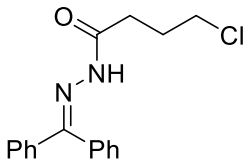

**3-7**

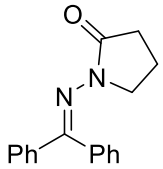

**3-8**

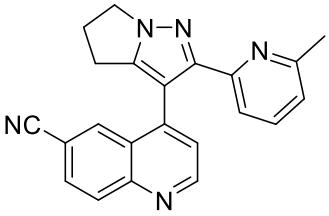

**3-9**

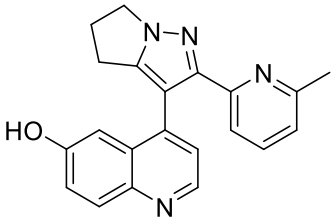

**3-10**

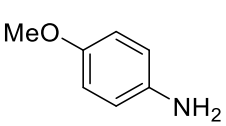

**3-11**

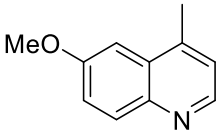

**3-12**

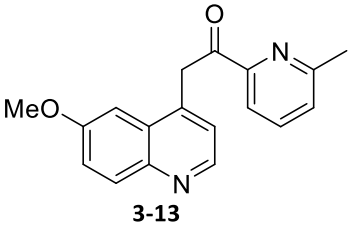

**3-13**

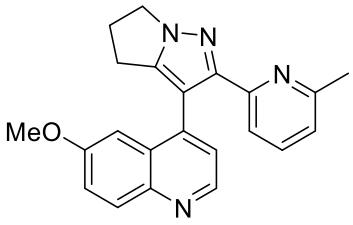

**3-14**

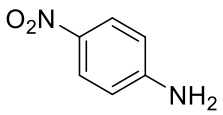

**3-15**

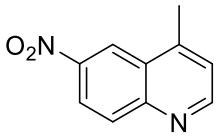

**3-16**

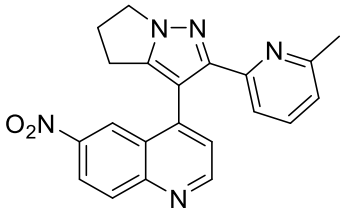

**3-17**

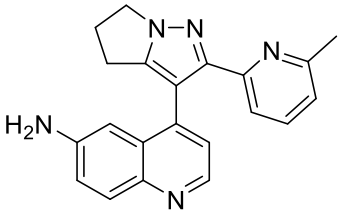

**3-18**

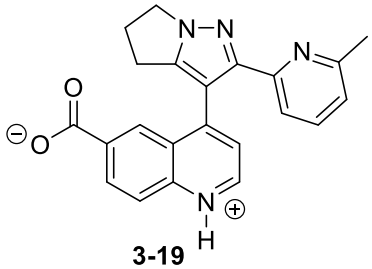

**3-19**

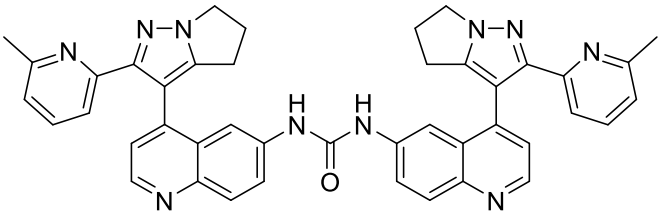

**3-20**

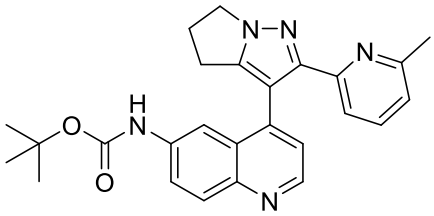

**3-21**

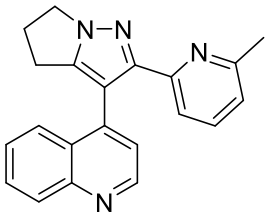

**3-22**

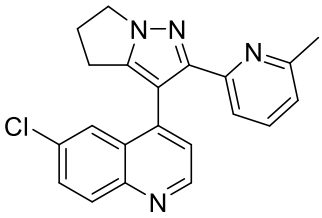

**3-23**

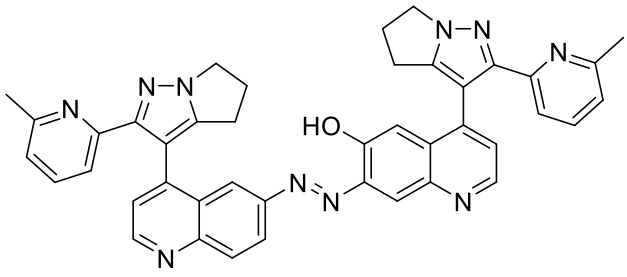

**3-24**

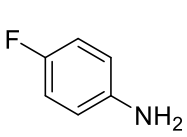

**3-25**

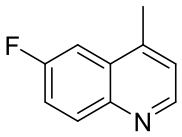

**3-26**

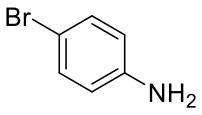

**3-27**

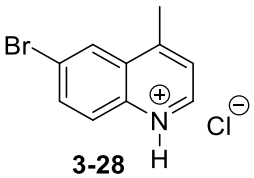

**3-28**

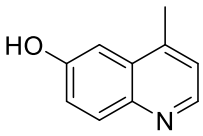

**3-29**

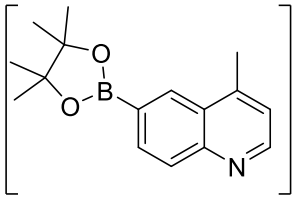

**3-30**

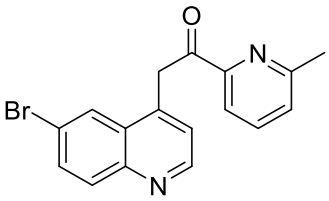

**3-31**

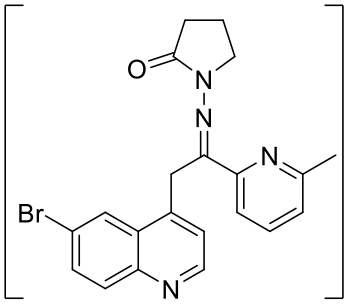

**3-32**

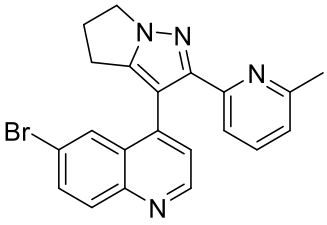

**3-33**

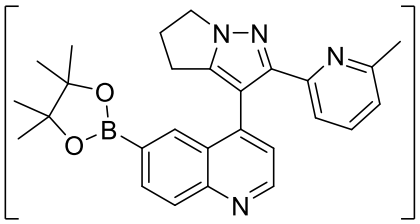

**3-34**

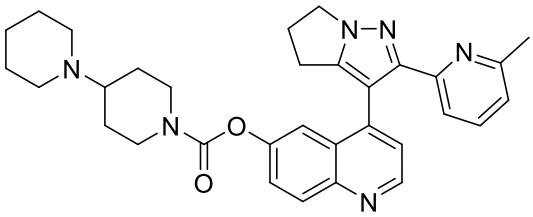

**3-35**

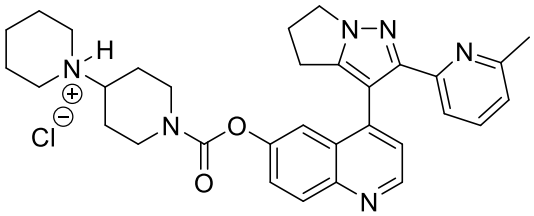

**3-36**

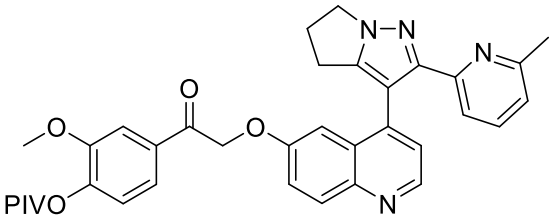

**3-37**

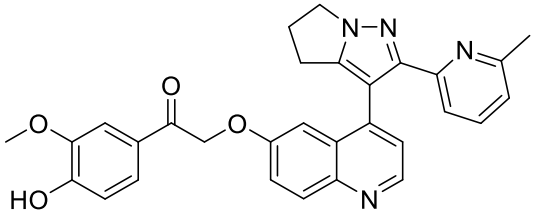

**3-38**

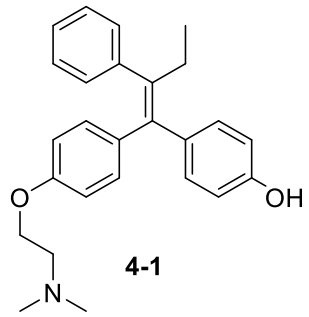


**4-1**

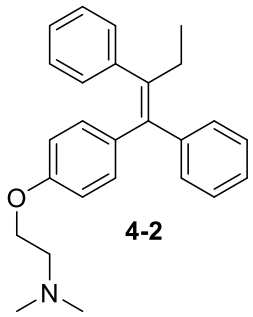


**4-2**

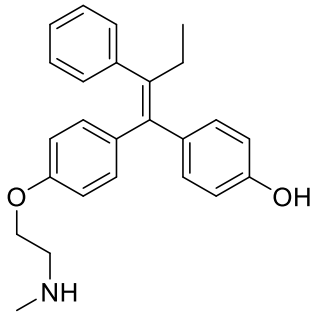


**4-3**

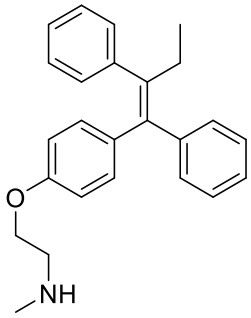


**4-4**

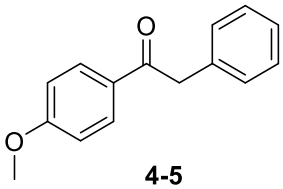


**4-5**

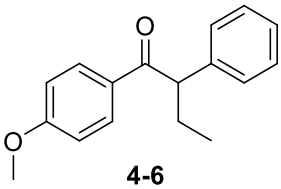


**4-6**

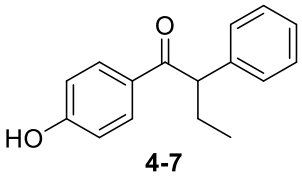


**4-7**

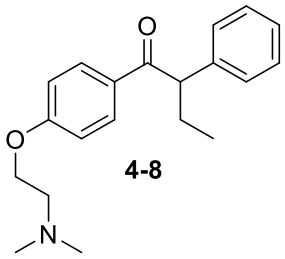


**4-8**

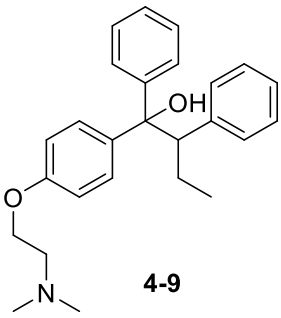


**4-9**

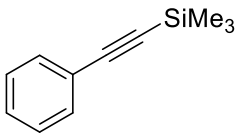


**4-10**

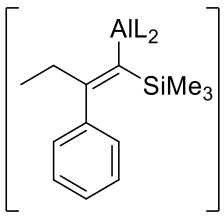


**4-11**

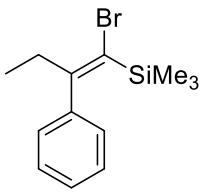


**4-12**

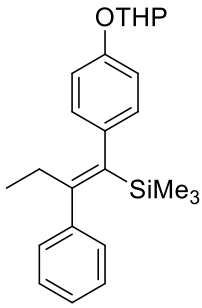


**4-13**

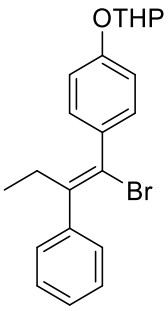


**4-14**

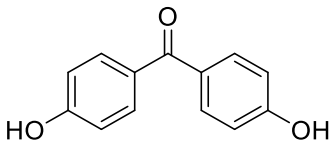


**4-15**

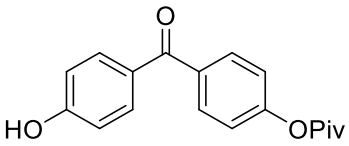


**4-16**

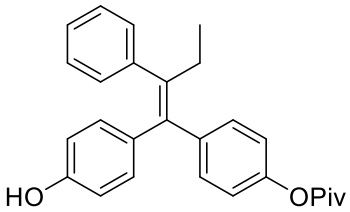


**4-17**

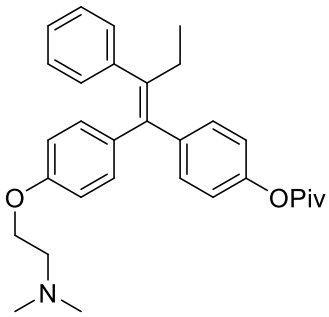


**4-18**

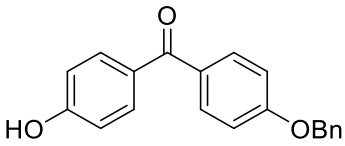


**4-19**

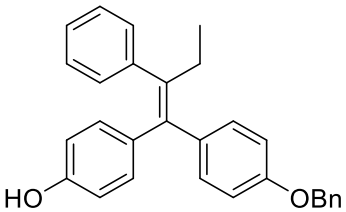


4:1 E:Z

**4-20**

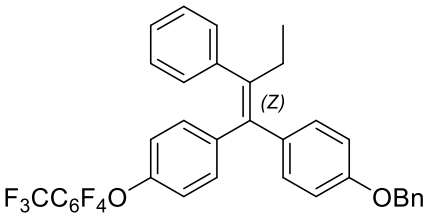


**4-21**

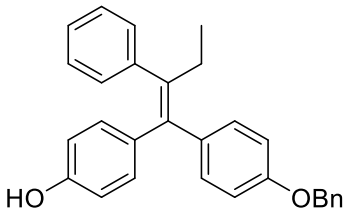


**4-22**

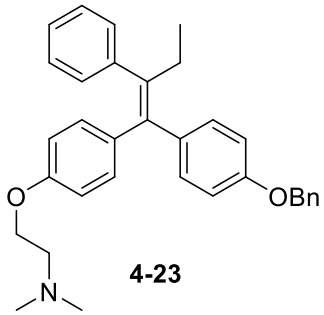


**4-23**

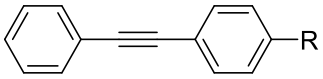


**4-24**

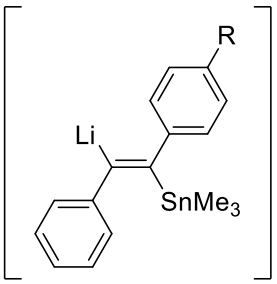


**4-25**

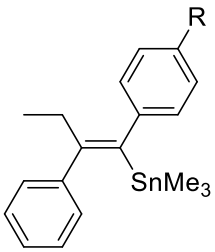


**4-26**

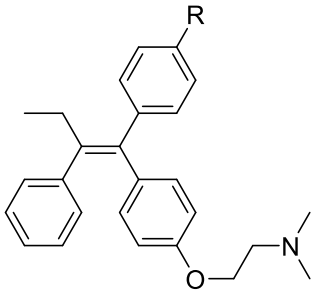


**4-27 R=OMOM**
**4-1 R=OH**

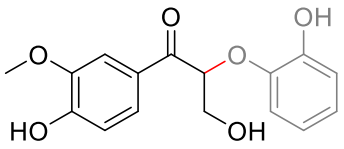


**5-1**

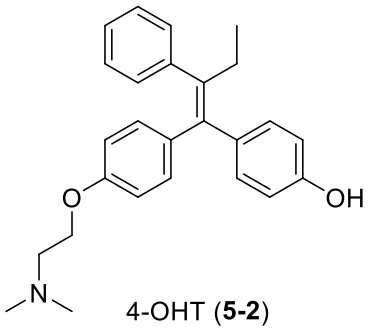


4-OHT (**5-2**)

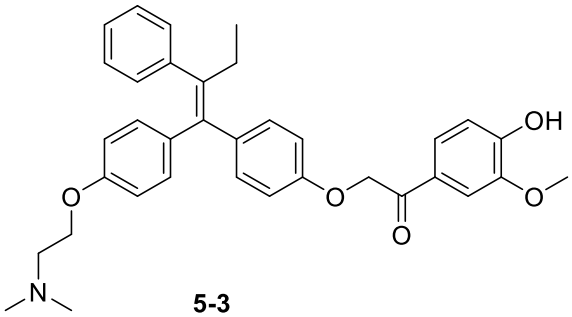


**5-3**

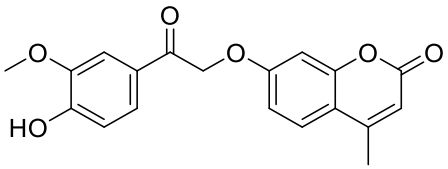


**5-4a**

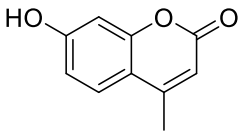


**5-5** (4-MU)

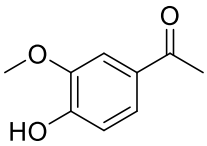


**5-6**

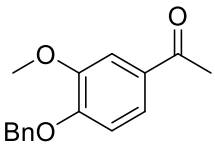


**5-7a**

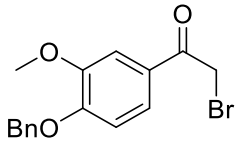


**5-8a**

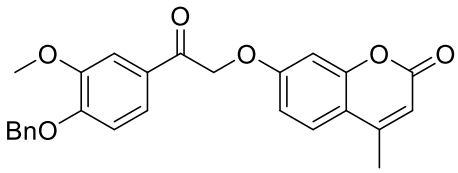


**5-4b**

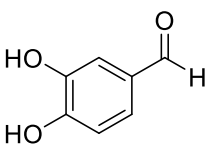


**5-9**

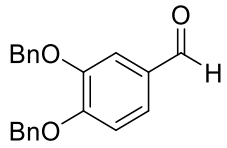


**5-10**

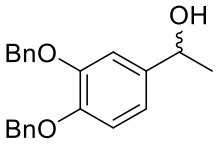


**5-11**

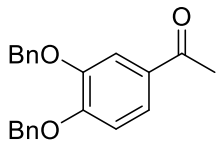


**5-7e**

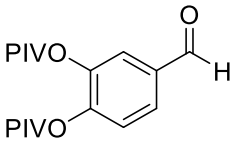


**5-12**

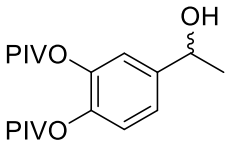


**5-13**

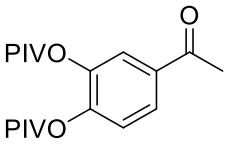


**5-7f**

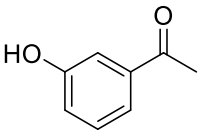


**5-14**

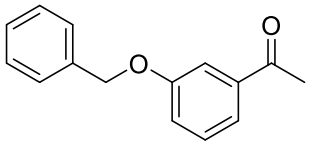


**5-7g**

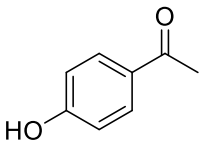


**5-15**

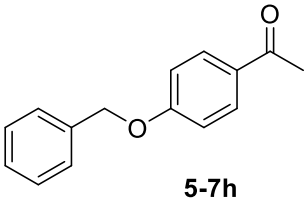


**5-7h**

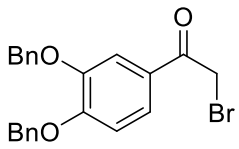


**5-8e**

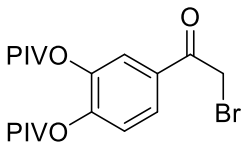


**5-8f**

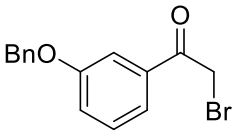


**5-8g**

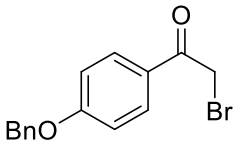


**5-8h**

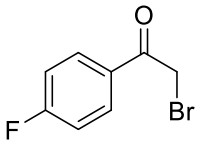


**5-8i**

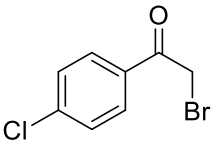


**5-8j**

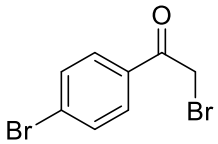


**5-8k**

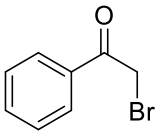


**5-8l**

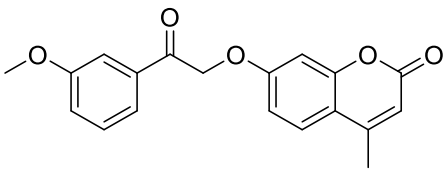


**5-4c**

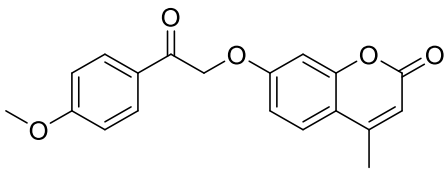


**5-4d**

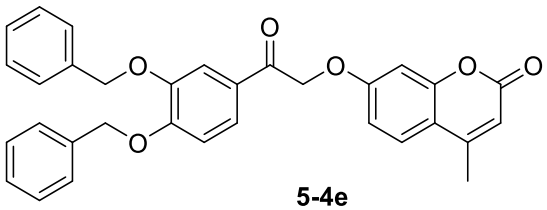


**5-4e**

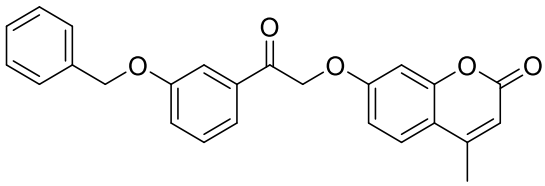


**5-4g**

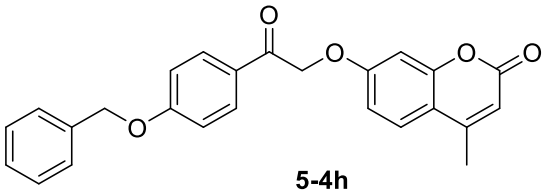


**5-4h**

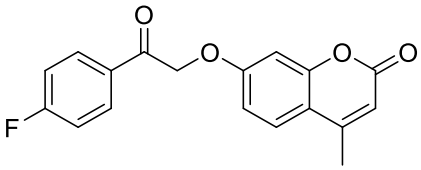


**5-4i**

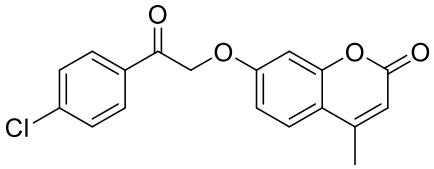

**5-4j**

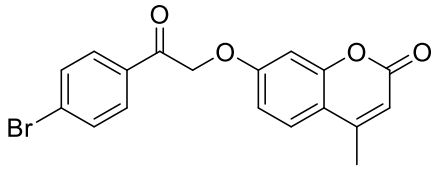

**5-4k**

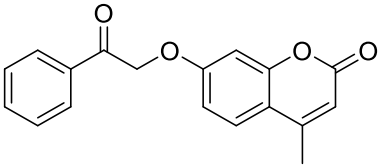

**5-4l**

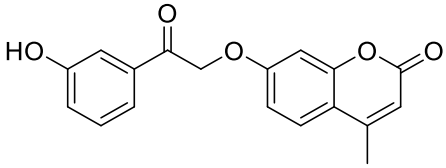

**5-4m**

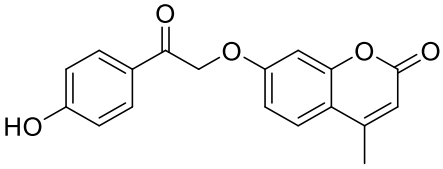

**5-4n**

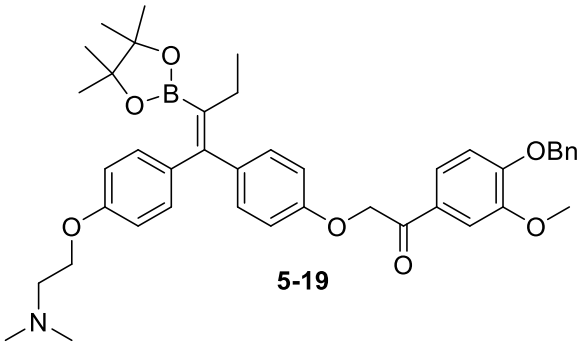

**5-19**

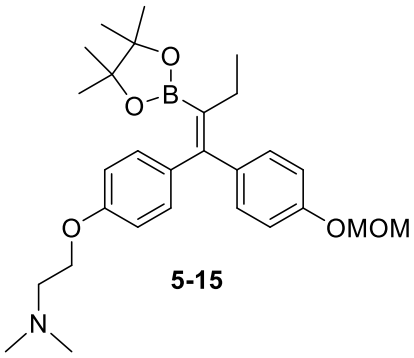

**5-15**

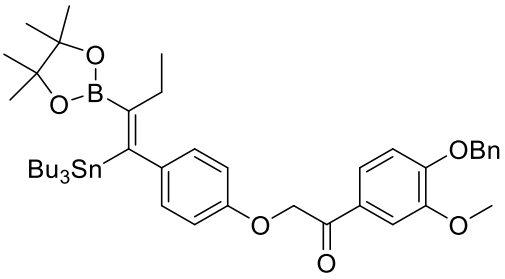

**5-18**

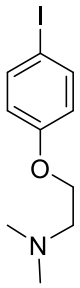

**5-16**

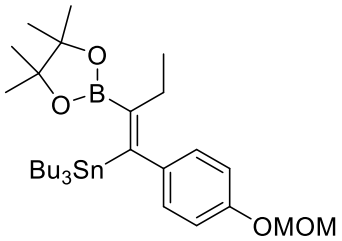

**5-14**

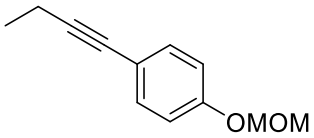

**5-13**

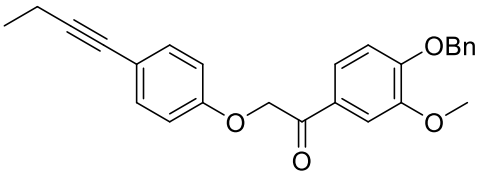

**5-17**

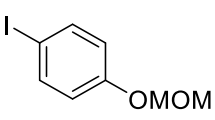

**5-20**

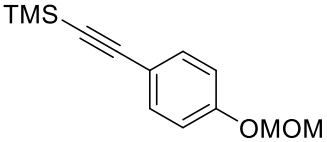

**5-21**

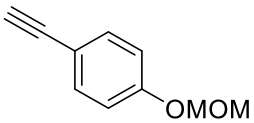

**5-22**

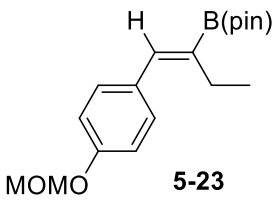


**5-23**

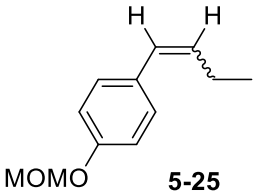


**5-25**

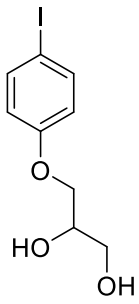


**5-27**

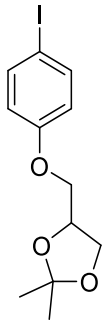


**5-26**

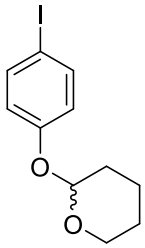


**5-28**

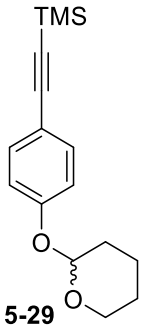


**5-29**

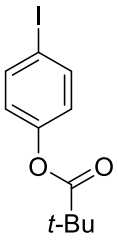


**5-30**

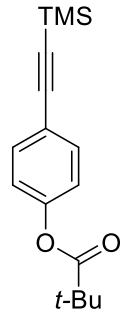


**5-31**

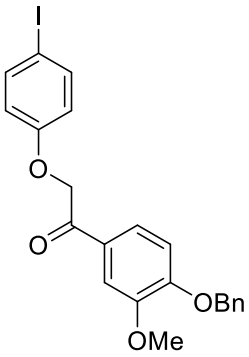


**5-32**

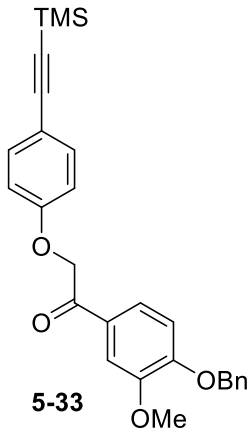


**5-33**

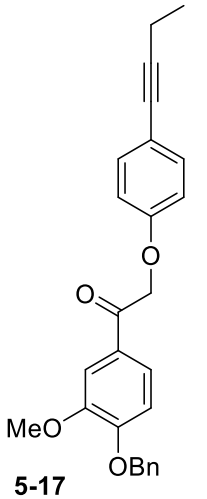


**5-17**

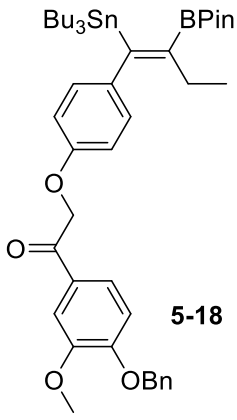


**5-18**

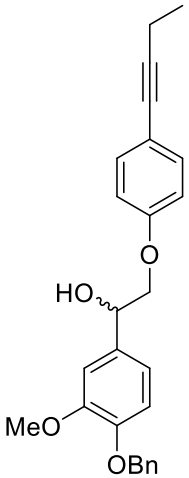


**5-34**

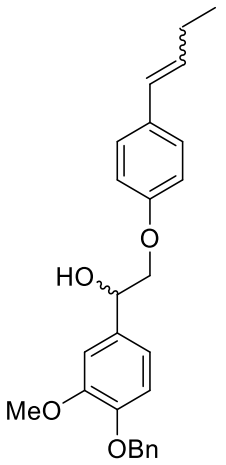


**5-35**

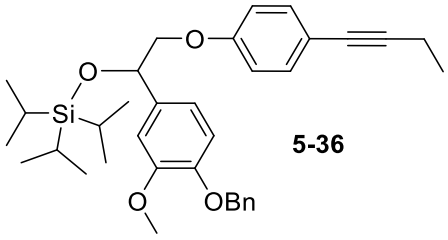


**5-36**

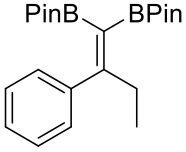


**5-37**

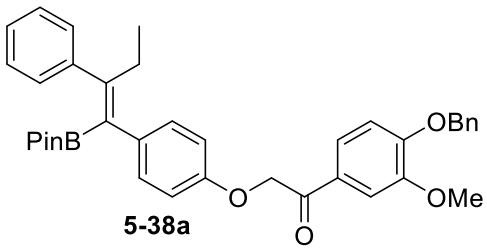


**5-38a**

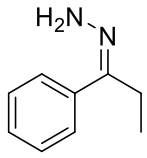


**5-40**

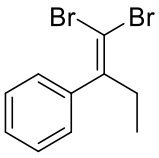


**5-41**

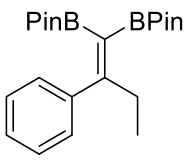


**5-37**

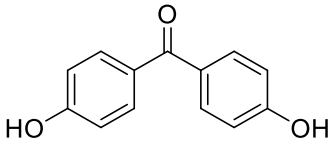


**5-41**

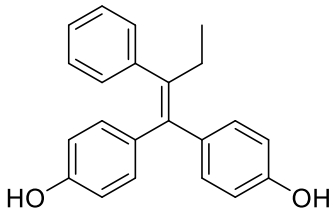


**5-43**

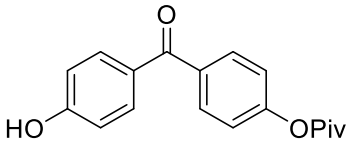


**5-44**

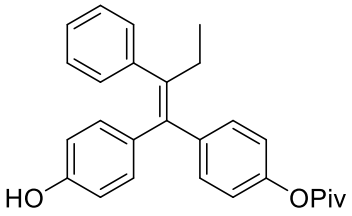


**5-45**

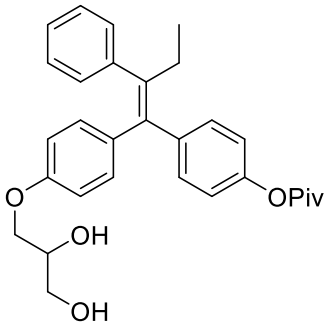


**5-46**

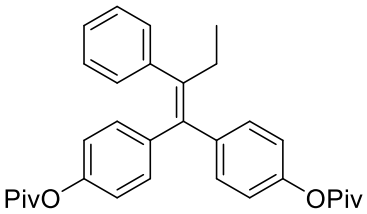


**5-47**

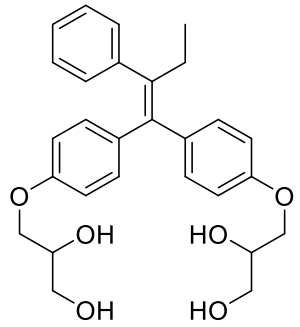


**5-48**

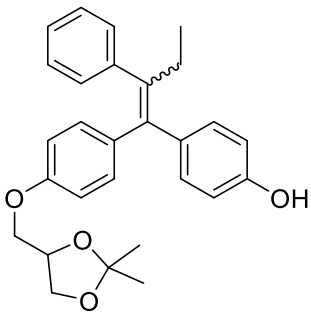


**5-49**

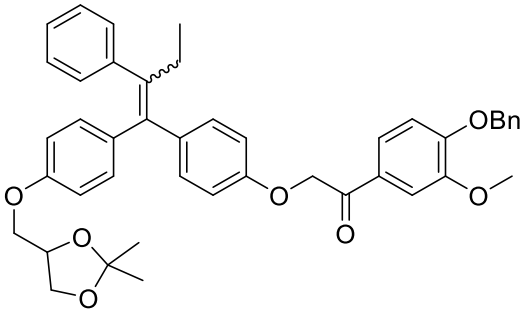


**5-50**

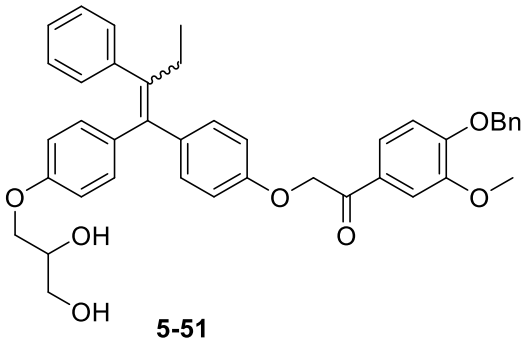


**5-51**

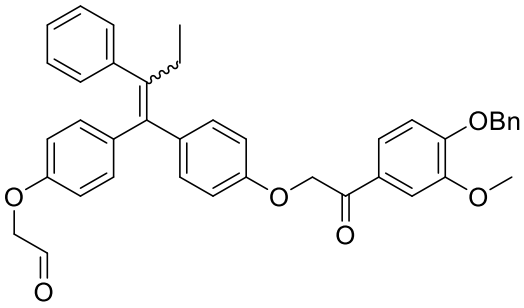


**5-52**

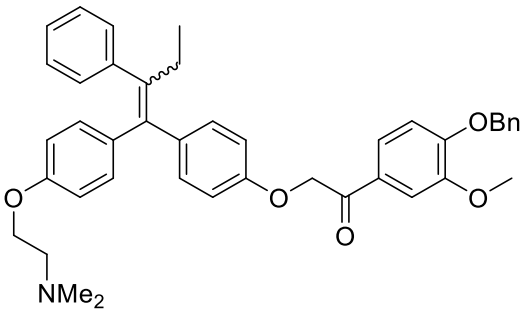


**5-53**